Practical Approximate Analysis of Beams and Frames
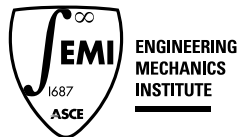
Nabil Fares, Ph.D.

ASCE

EMI ENGINEERING MECHANICS INSTITUTE

Practical Approximate Analysis of Beams and Frames

Nabil Fares, Ph.D.

ASCE

EMI
ENGINEERING
MECHANICS
INSTITUTE
ASCE

Lecture Notes in Mechanics

Aristotle and Archytas defined mechanics as the *"organization of thought towards solving perplexing problems that are useful to humanity."* In the spirit Aristotle and Archytas, Lecture Notes in Mechanics (LNMech) transcends the traditional division of mechanics and provides a forum for presenting state-of-the-art research that tackles the range of complex issues facing society today.

LNMech provides for the rapid dissemination of comprehensive treatments of current developments in mechanics, serving as a repository and reference for innovation in mechanics, across all relevant application domains.

LNMech publishes original contributions, including monographs, extended surveys, and collected papers from workshops and conferences. All LNMech volumes are peer reviewed, available in print and online through ASCE, and indexed by the major scientific indexing and abstracting services.

Contents

This page intentionally left blank

Preface

The aim of this book is to present a new approach to approximately analyze beams and frames. The new approach has the following desirable features:

- The approach is relatively short and simple, robust with good accuracy and is practically applicable to realistic problems. Some former students who have learned these methods have reported that, in the workplace, they have been able to complete an accurate approximate analysis of a structure in the time it took their colleagues to enter a description of the structure into a computer model.

- The approach is naturally amenable to parametric studies and results presenting summaries and ranges of behavior covering a wide range of situations are pervasive throughout the book. This builds a knowledge base that a practitioner can use to anticipate the range of possible results that may be encountered with a new structure.

- The approach has strong visual components, especially in the emphasis on consistent semi-quantitative sketching of deformed structures. These sketches are especially useful as repositories and enhancements to experience. The reason is that: i) There is a synergy between such sketches and moment diagrams which are essential for design so that experience in one translates into improvements in the other. ii) Both deeper insight and more experience with the analysis of beam and frame structures allows the user to be more accurate or to add more details in the sketches of the deformed shapes. Having drawn such improved sketches, the user then remembers and consolidates both insight and experience. iii) Comparisons between the sketches of the deformed structures and moment diagrams allows inconsistencies to be detected and hence, reduces potential manual errors.

- The approach generally localizes all dimensional quantities in one or a few factors so that the main parameters to be estimated are the relevant relative stiffnesses. This non-dimensionalization also generally leads to having all calculated non-dimensional quantities lying between negative and positive one. Both of these effects reduce the likelihood of manual error because the range of possible values become

rather limited and because one of the main sources of error is usually in dimensional calculations and unit conversions. Extensive experience and practice with the method and with typical relative stiffnesses also eventually leads to results being recalled, due to the limited range of common non-dimensional results, rather than calculated which further enhances the speed and accuracy of the user.

• In addition to moment diagrams, the approach also addresses how to estimate deflections, influence lines and moments of inertia.

• The approach identifies a possible framework for the non-destructive evaluation of framed structures. A specific experimental method based on that framework is proposed and analyzed.

• The approach sheds light on the limits of applicability of the widely used lumped-mass model for the dynamical analysis of structures. The implications are presented and discussed.

For all the above reasons, we recommend this book to both students and practitioners. However, we note that the proposed new approximate approach must be complemented with other material in order to constitute a good second course in structural analysis. For example, a good second course would include the approximate approach in this book, the direct stiffness method, training on the use of some structural analysis software and, if time permits, exposure to one or two other advanced structural analysis topics.

Finally, the main objective of this book is to provide students and practitioners of structural mechanics with a new analysis approach that complements the use of software but provides a critical role for the structural engineer. That role is necessarily at a higher conceptual level and must cater to the strengths of humans which is the recognition of patterns, preferably visible ones. The author hopes that this work would encourage others to refine and extend this approach or its essence to other areas of structural engineering and indeed to most other topics where software is displacing much of the skills that were previously provided by people.

Dedication

This book is dedicated to Professor Jim Rice who taught me to 'figure the answer and then do the calculation' and to my wife Maha who supported and encouraged me to complete this book.

This page intentionally left blank

Chapter 1

Approximate Analysis of Beams and Frames with No Sidesway

1.1   Introduction to Sketching

Throughout this book, we will be concerned with sketching the deformations of beams and frames. Such sketches, when qualitatively precise, illustrate the behavior of structures in a visually rich and informative way. For example, such sketches may be directly related to bending moment diagrams which are a basis for design. By qualitatively precise sketches, we mean that we will be mostly concerned with: i) getting the right sign of the curvature at each point which implies ii) approximately identifying the location of each inflection point which are locations of zero curvature and hence zero moment, iii) getting the right sign of the slopes at the ends of members and iv) getting the right sign of the displacements. In general, we will greatly exaggerate the magnitude of the displacements and place minor emphasis on the details of the deformed shape beyond the above concerns.

To start our sketching program, we will observe the deformation of a real but very slender beam. Specifically, we will consider the deformations of a long slender straw shown in figures 1.1a–d. As long as the material is linear elastic, the shape of that slender straw will be representative of any beam under similar loading conditions but the straw will have relatively very large deformations. While sketching the deformation of a beam, we will talk of displacement, slope and curvature. For a horizontal beam, positive displacement will be up, positive slope will correspond to a counter-clockwise rotation from the horizontal and the convention for positive and negative curvature is shown in figure 1.2.

(a) applied moment—fixed

(b) applied moment—pinned

(c) applied moment—spring

(d) applied moment—fixed then sheared
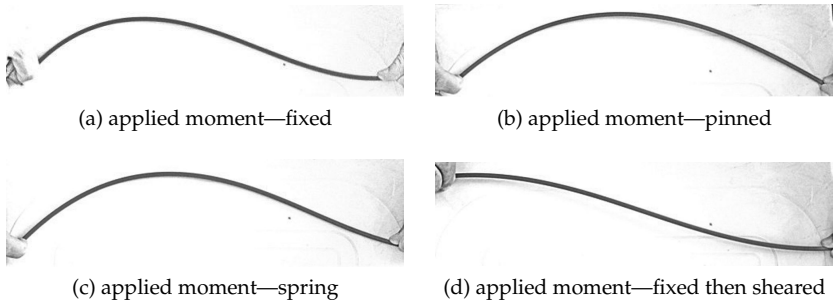
Figure 1.1. Loading of a simple slender beam.

| positive curvature | negative curvature |
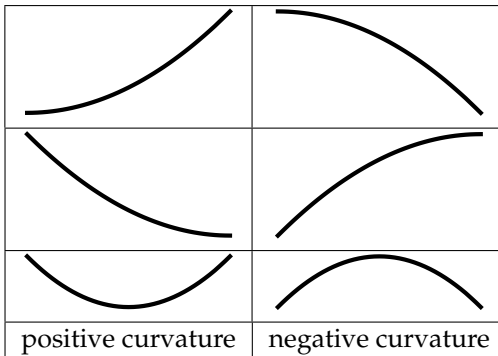
Figure 1.2. Convention for positive and negative curvatures.

Let's start by sketching figure 1.1a in a way that is consistent with our objectives. First we draw small straight line "stubs" at each end of the beam as shown in figure 1.3a. At the left end, we draw a stub with a positive slope and zero displacement while at the right end we draw a stub with zero slope and zero displacement. Next, we notice that the curvature near the left end is negative while the curvature at the right is positive with the inflection point (*ie.* zero curvature) somewhat closer to the right end. Based on calculations for the case shown in figure 1.1a, the inflection point is calculated to be at one third the length from the right end. Therefore, starting with the left stub, we draw a curve with negative curvature and, starting with the right stub, we draw a curve

(a) Place slope stubs at the ends

(b) Lightly sketch the curvatures starting from the ends

(c) Smoothly join the curves from each end noting the inflection points
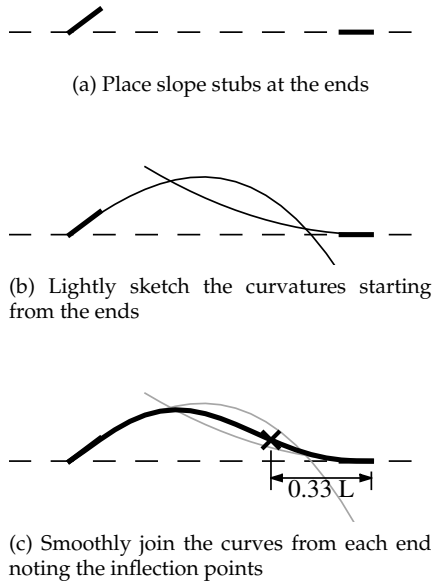
Figure 1.3. Steps in sketching the deformed shape of beam 1.1a.

with a positive curvature. We draw the left and right curves so that they meet closer to the right end as shown in figure 1.1b. Finally, we smoothly join the two curves while trying to make the location of zero curvature to appear about one third the length from the right end as shown in figure 1.1c. In general, these are the 3 steps in drawing a beam or column when there is no chord rotation. Specifically, we draw stubs at the ends, lightly sketch curves with the right curvatures at different locations and finally join the curves into one smooth curve.

We sketch the beams in figures 1.1b and 1.1c in the same way. In figure 1.1b, there is zero curvature at the right end so that the curve on the right is initially straight with the result shown in figure 1.4 and 1.5. Based on calculations, we know that the rotation on the right is half the rotation on the left and we must take care to approximately reproduce that feature in sketching figure 1.4. In figure 1.1c, the intention is to provide some resistance in-between fully fixed with zero rotation and no resistance as in figure 1.1b. The result is that the location of zero curvature occurs between zero and one third the length from the right end and the rotation on the right side is between zero and half the rotation of the left end.

(a) Place slope stubs at the ends

(b) Lightly sketch the curvatures
starting from the ends

(c) Smoothly join the curves from
each end noting the inflection
points
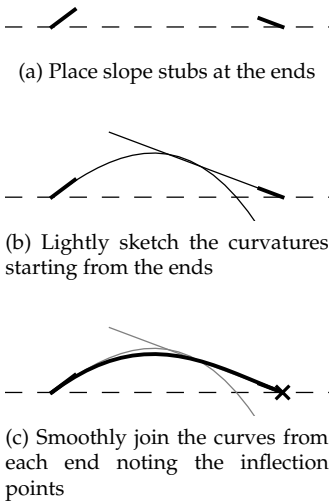
Figure 1.4. Sketching the deformed
shape of beam 1.1b.

(a) Place slope stubs at the ends

(b) Lightly sketch the curvatures
starting from the ends

(c) Smoothly join the curves from
each end noting the inflection
points
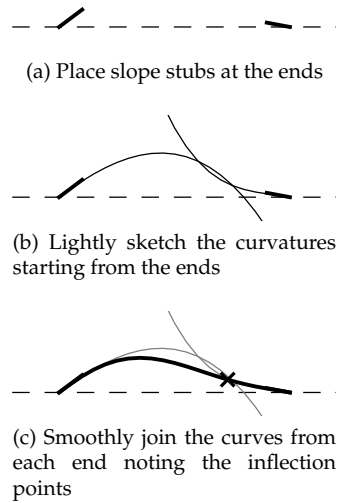
Figure 1.5. Sketching the deformed
shape of beam 1.1c.

1.2 Passive Members in Continuous Beams and Frames

How does sketching the deformation and bending moment of single members help us in doing the same for assemblies of such members such as beams and frames? To explain, we will first define a passive part of a structure to be that part, if any, that has no loads applied and that has no sidesway in any of its members. Neglecting axial deformations, a loaded beam or column connected to a passive part of a structure at a node will experience the equivalent of a linear rotary spring at that node as illustrated in figure 1.6. In that figure, we see the effect of the passive structures on member AB being reduced to two rotary springs at the ends. The behavior of the loaded member can then be sketched and analyzed by knowing the behavior of a single loaded member (beam or column) with hinges and rotary springs at each end.

After considering the behavior of the loaded member, we consider the members in the passive structures (*eg.* the members to the left and right of member AB in figure 1.6). We observe that every member of a
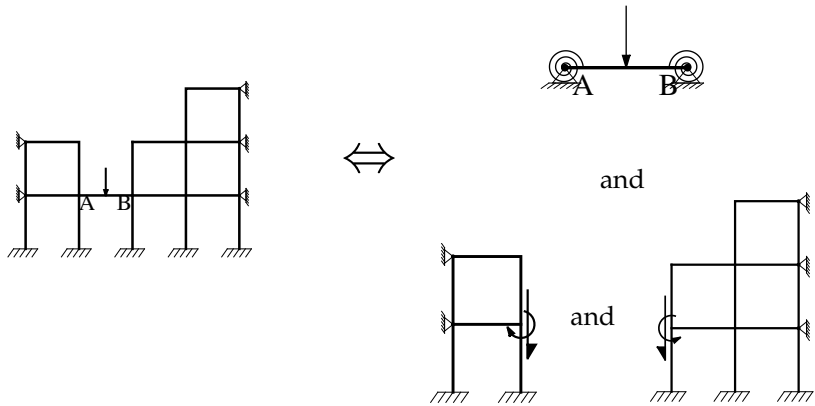
Figure 1.6. Deconstructing a structure into active member and passive parts.

passive structure will behave approximately similar to a beam or column that is hinged on both sides, with a moment applied at one end and a rotary spring at the other as shown in the isolated members BC, BE and CF of figure 1.7. We can think of the effect of the loaded member as propagating from the member outwards in both directions with the nearer beams and columns being loaded first (see figure 1.7). We first analyze the loaded member with the ends having rotational springs and obtain the moments at either end (*eg.* the end moments in member AB in figure 1.6). The end moments that are thus obtained are then distributed onto the connected members in a way that is similar but not the same as the moment distribution method (see discussion below). Each beam and column in a passive part of the structure may be considered as being hinged on both sides with an applied moment obtained from distributing a moment at the end closest to the loaded member and with a rotary spring at the other end. Such a member is then analyzed and the moment at the spring end is obtained. This moment is then again distributed to its attached members. In this way, the whole structure may be sketched and analyzed member by member by simply knowing the behavior of a single loaded beam with rotary springs at each hinged end (*eg.* member AB in figure 1.6) and by knowing the behavior of an unloaded hinged beam with one end loaded by a moment and the other end having a rotary spring (*eg.* the isolated members BC, BE and CF of figure 1.7).

The approach is mildly complicated by having loops (*ie.* box formed by two beams and two columns). Practically, this will not matter because, as we will see, the bending moments and the deformations decrease rapidly as we move farther away from the loaded member.
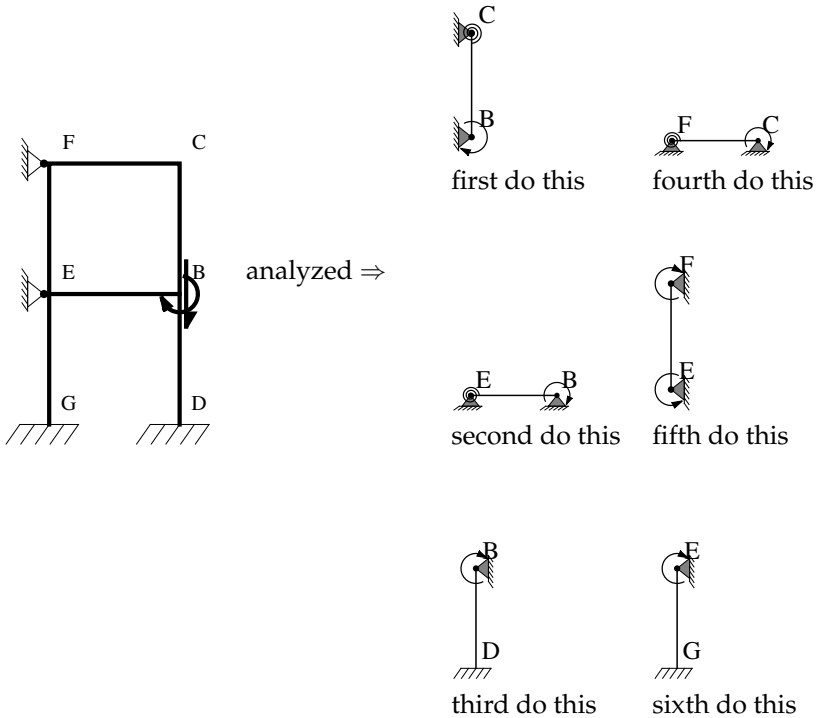
Figure 1.7. Decomposing a passive structure into successive members to be analyzed.

However, the last member in a loop (*eg.* member EF in figure 1.7) may be treated as a hinged beam or column with applied moments at each end obtained from the influence of the previous members that are closer to the loaded beam. Sketching the deformation and bending moment of such a case is elementary. There is some ambiguity in which member in a loop is to be analyzed last but this can be simply determined by considering the member in the loop with the smallest end moments to be the last. This member can be determined by experience or by choosing between two alternatives. Alternatively, this last member may be arbitrarily chosen. The important point to notice in analyzing a passive structure is that, at each step, we analyze one member with fully specified conditions before passing to the next. There is no iteration and each member is considered once before moving to the next member.

For the above approach of analyzing a loaded member connected to a passive structure, we need i) to determine or estimate the stiffnesses of the associated rotary springs, ii) to determine or estimate the

end moments at the ends of loaded members attached to passive structures and iii) to quantitatively analyze a hinged member with an applied moment at one end and a rotary spring at the other (see for example figures 1.10). This will allow us to completely specify then analyze each member of a passive structure. In the next section, we will address the third point which is the analysis of the member shown in figure 1.11. In the sections after that we will also address how to analyze various types of loaded beams with rotational springs at each end. In this section, we will address the question of how to handle the first point which is the estimation of the stiffness of rotary springs representing the behavior of passive structures.

The first point is how to estimate the value of an equivalent rotary spring representing the behavior of a passive structure attached at the end of a member. Here, we use the classic concept of stiffness and note that in the absence of sidesway, the rotational stiffness at a node is the sum of the rotational stiffnesses of the connected members. For example, in figure 1.8a, the stiffness of the rotary spring at node B is the stiffness of member 1 for the case shown in figure 1.10f (*ie.* fixed end). In figure 1.8b, we have to add the effect of the stiffnesses of members 1 and 2 and in figure 1.8c we also have to add the effect of member 3 where that member has the stiffness shown in figure 1.10a (*ie.* hinged end). In each of those cases, we can come up with a value of 'k' so that $k \times 4EI/L$ gives the stiffness of the rotary spring at end B by solving for 'k' in the equation shown above the spring. Note that 'E,' 'I,' and 'L' are the Young's modulus, moment of inertia and length of member AB. The value of 'k' is the ratio of the rotational stiffness of the connected members relative to the rotational stiffness of the active member (*eg.* member AB in figures 1.8) when that member has its far end fixed. For example, if members 1, 2, 3 and AB in figures 1.8 have the same Young's modulus, moment of inertia and length then the value of 'k' is 1, 2 and 2.75 in figures 1.8a, 1.8b and 1.8c respectively. From now on, we will refer to 'k' as the k-value, rotary stiffness factor or stiffness factor of the rotary spring at a node. Typical rotary stiffness factors in structures are in the range of 0.75 to 3. We may also consider the stiffness factors of 0 and ∞ as being the special cases of a hinged and fixed end respectively.

In the cases of figure 1.8, the stiffnesses of the connected members can be exactly determined. In a more general case, such as in figure 1.9, the rotational stiffness of one or more members connected to the active member (*ie.* member AB) may not be available exactly. However, since all members are passive (this includes loops or box configurations), the rotational stiffness of any attached member whose Young's modulus is E, moment of inertia is I and length is L will be between 3 to $4EI/L$ where 3
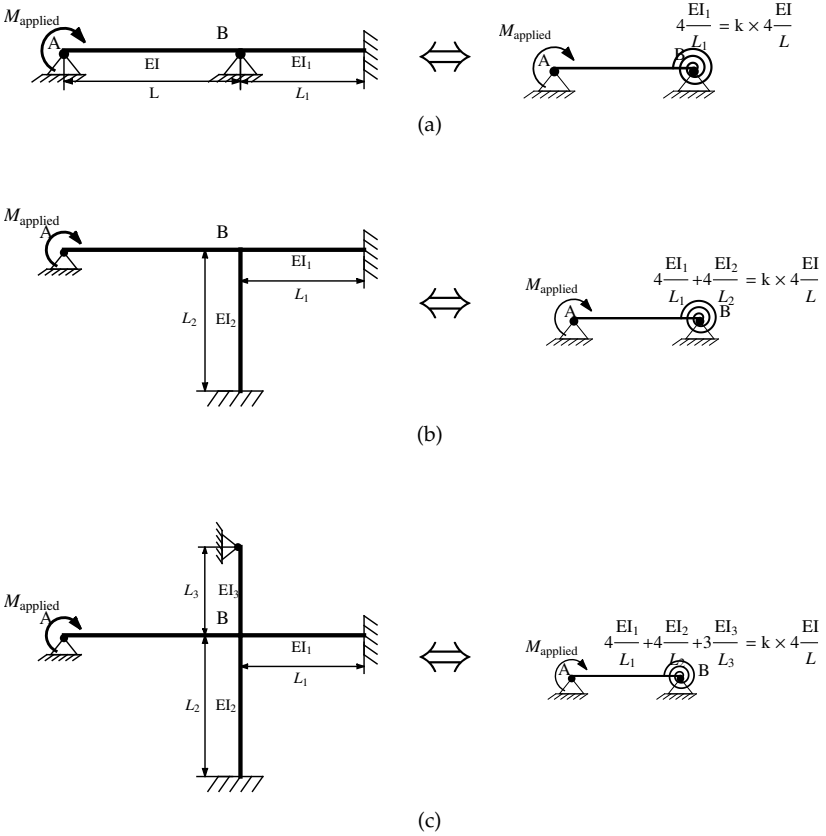
Figure 1.8. Determining the exact stiffness in special cases.
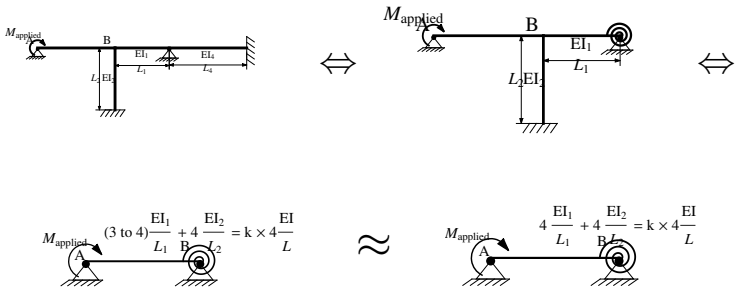
Figure 1.9. Estimating the rotational stiffness at node B for member AB.
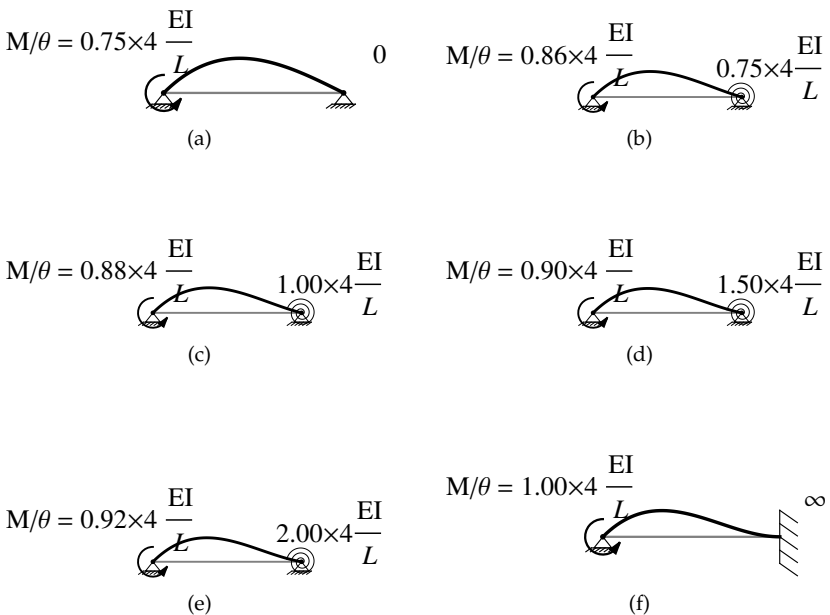
Figure 1.10. Effective bending stiffness at one end of a beam when a spring is at the other end.

is for a hinged end and 4 is a for a fixed end as shown in figures 1.10a–f. At this point, we could determine the exact rotational stiffness of a member attached to a rotational spring as shown for some selected cases in figures 1.10, but instead, we can get a good estimate by simply using a value of $4EI/L$ for any such member. This will, of course, usually overestimate the stiffness contribution of that member. This procedure is illustrated in figure 1.9 where the contribution of member 1 to the rotational stiffness at B is estimated as $4(EI_1/L_1)$. In the next section, the analysis will indicate that such an estimate leads to a maximum error of less than 4% for the transmitted moment relative to the applied moment at the other end (*eg.* error in moment at B relative to moment at A of member AB in figure 1.9) and less than 2.5% for the distance of the inflection point from the rotational spring relative to the length of the beam (*eg.* the distance of the inflection point from node B in member AB relative to the total length of AB of figure 1.9). Experience with using such an estimate along with other associated approximations indicates that the overall analysis of a structure using this method will give results that are within 5 to 10% of the exact results in terms of bending moments

except for moments that are small compared to the maximum moment in the structure (*ie.* moments that are less than about 5% of the maximum).

The second point that was needed to analyze all members in a passive structure is to determine the end moment at the loaded ends of the members in a passive structure. This is again done using the idea of stiffness or of relative stiffness as is done in the classic method of moment distribution. The difference is that the active member is removed from the joint and its presence is indicated by the moment transmitted from the active member to that point. For example, the moment at B on the passive structure BCDEFG in figure 1.7 will be distributed on members BC, BE and BD with no contribution of the stiffness of member AB (see figure 1.5). Again, we encounter the problem of not having available the exact rotational stiffness of one or more members connected to the active member. This will again be handled by replacing the rotational stiffness of a connected member which is between 3 to $4EI/L$ by $4EI/L$. The maximum error on the distributed bending moment that is incurred in such a procedure will be less than 7.2%. This maximum error can be determined as follows:

Assume there is a node with several attached members where each member has a possibly different rotational stiffness. Consider any member in that group and call it member 1. We now apply a unit moment on the node. The moment that is distributed to member 1 will be $(k_1/(k_1 + k_{rest})$ where k_1 is the rotational stiffness of member 1 and k_{rest} is the combined rotational stiffnesses of the rest of the members. We now consider the maximum error incurred if we overestimate the rotational stiffness of member 1 or of any of the other members by a factor of up to $(4/3)$ (*ie.* the difference of rotational stiffness between a hinged and fixed far end). The result of such an optimization gives a maximum error relative to the applied unit moment of 7.2%. Since member 1 was chosen as any member in the group, this is then the maximum error that may be incurred by any member due to distributing a moment over the atached members. In practice, the error is much smaller than 7.2% because the worst case occurs only when one member has a maximum overestimation (*ie.* from hinged to fixed) while all the other members have no overestimation in their stiffness (*ie.* all other members have hinged far-ends).

We note that if we want to obtain better estimates in our analysis, we simply have to use better estimates of the rotational stiffness of connected members. If we use the exact rotational stiffnesses we will get exact results, which, with the use of extensive tables or formulas may be done by propagating the rotational stiffness from the supports back to the loaded member. However, such a process can be quite long and error prone. The rotational stiffnesses indicated in figures 1.10 illustrates a short table of results while the appendices give more extensive tables

as well as exact formulas. In practice, using the results of figure 1.10a, 1.10c and 1.10f and roughly estimating values in between those cases for any given member gives negligible errors in the bending moments as compared to exact results for most cases.

In summary, we have described the concept of an active member connected to passive parts of a structure. The active member may be analyzed by considering the member with its applied loads and with rotational springs at its ends. We obtain the moments at the spring ends and then distribute them over the attached members. Subsequently, each member in a passive part of the structure may be analyzed by considering a member with one end having a hinge and an applied moment equal to its distributed moment while at the other end having a hinge with a rotary spring. The moment at this rotary spring is again distributed to its attached members to eventually analyze the whole structure.

We have described how to distribute a moment onto the attached members and how to estimate the stiffness of the rotary springs involved in this process. In the next section, we will study the behavior of a member with a hinge and an applied moment at one end and a hinge with a rotary spring at the other and in subsequent sections we will describe how to analyze a member with applied loads and with rotational springs at both ends. This will then allow us to analyze any (single) active member connected to a passive structure and by using the principle of superposition to analyze any beam or frame that has no sidesway.

1.3   Beam with a Moment Applied at One End and Resisting at the Other

In the last section, we found that the analysis of a member with a hinge and an applied moment at one end and a hinge with a rotary spring at the other (see figure 1.11) is basic to the approximate analysis of beams and frames with no sidesway. In this section, we will fully analyze this member.

In the following discussions, when referring to the beam shown in figure 1.11, we will call the end where the moment is applied the near end and the other the far end. What then are the analysis results that are of interest and why? Referring to figure 1.11, the results of interest are as follows:

i) The ratio of the far-end bending moment to the near end bending moment which is called the carry-over-factor for moments: We need this to determine the moment at the far end once the moment at the near
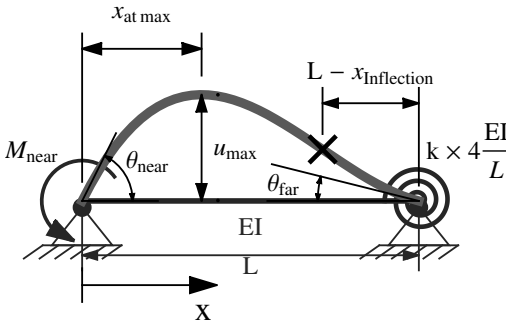
Figure 1.11. Beam with moment at near end and rotary spring at far end.

end has been obtained. This result is then essential in obtaining good quantitative approximations for bending moment diagrams in the passive parts of a structure as described in the previous section.

Table 1.1 shows values of $-M_{\text{far}}/M_{\text{near}}$ which are always zero or positive because, intuitively, the applied moment is resisted in the opposite sense at the rotary spring. This ratio of moments increases monotonically from 0 (hinged) to 0.5 (fixed) as seen in figure 1.12. In case we need to determine it precisely, $-M_{\text{far}}/M_{\text{near}} = 2k/(3+4k)$ where 'k' is the stiffness factor of the rotary spring. The carry-over factor for moments has the value of 0.5 for a fixed end and corresponds to the usual value of the carry over factor used in moment distribution. From the point of view of moment distribution, the approximation method described in the previous section avoids iterations by using more accurate "carry over factors." In practice, we only need to memorize a few "carry-over-factors" such as

Table 1.1. Hinged Beam with Applied Moment at One End and Rotary Spring at Other

k	$-\dfrac{M_{\text{far}}}{M_{\text{near}}}$	$\dfrac{M_{\text{near}}}{\theta_{\text{near}}4EI/L}$	$-\dfrac{\theta_{\text{far}}}{\theta_{\text{near}}}$	$1-\dfrac{x_{\text{infl}}}{L}$	$\dfrac{x_{\text{at max}}}{L}$	$\dfrac{u_{\text{max}}}{\theta_{\text{near}}L}$
0.000	0.000	0.750	0.500	0.000	0.423	0.192
0.500	0.200	0.833	0.333	0.167	0.392	0.176
0.750	0.250	0.857	0.286	0.200	0.384	0.172
1.000	0.286	0.875	0.250	0.222	0.377	0.168
1.500	0.333	0.900	0.200	0.250	0.368	0.164
2.000	0.364	0.917	0.167	0.267	0.362	0.161
3.000	0.400	0.938	0.125	0.286	0.355	0.158
4.000	0.421	0.950	0.100	0.296	0.350	0.156
∞	0.500	1.000	0.000	0.333	0.333	0.148

Figure 1.12. Plots of inflection point location and carry-over-moment.

those at $k = 0, 1, 3$ and ∞ and interpolate (or roughly estimate) values of the "carry-over-factors" in between. Alternatively, we may use the exact formula that was specified above.

ii) The rotary stiffness at the near end: We need this to distribute an applied moment at a node to the attached members in proportion to their stiffness. We may also need this if we want to more accurately determine the effective stiffness of a member in a passive part of the structure. The normalized stiffness factor varies between 0.75 for a hinged end to 1 for a fixed end with most of the variation occuring between $k = 0$ and $k = 1$. In practice, taking this stiffness factor to be 0.75 for a hinge and 1 otherwise gives a good approximation for most applications. In case we need an exact expression, the rotary stiffness factor at the near end is given by $(3 + 4k)/(4 + 4k)$ where 'k' is the stiffness factor at the far end.

iii) The ratio of the far end to the near end rotation: This is useful in sketching the deformed shape of beams and frames. This result is also essential in obtaining quantitative but approximate influence lines for indeterminate frames and beams. The negative of the ratio of rotations $-\theta_{\text{far}}/\theta_{\text{near}}$ varies between 0 for a fixed end to 0.5 for a hinged end and has the exact formula $1/(2 + 2k)$. We note that even for a flexible passive structure (eg. $k = 0.75$), the rotation at the far end is below 0.3 the rotation at the near end. This rotation is then imposed on all connected members at that end which then sets the scale for the deformations in those attached members. For
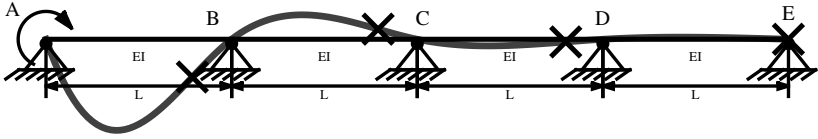
Figure 1.13. Illustration of the decrease in deformation in a continuous beam based on exact analysis.

example, if we have a continuous beam as shown in figure 1.13, then the maximum deformation in member BC is less than 0.3 times the maximum deformation in member AB. Similarly, the maximum deformation in member CD is less than about $0.3 \times 0.3 = 0.09$ the maximum in AB. This indicates that there is approximately a geometric progression for the decrease in deformations as the member gets farther away from the active one. This rapid decrease in deformations is even more pronounced in a frame than in a beam. The reason is that in a frame, the effective rotary stiffness factor 'k' at a node due to the combined resistance of all the attached members will generally be larger than 1 and the decrease in deformation as we go farther from the loaded member will then be even faster. In addition, the moment transmitted in a member of a frame will usually be distributed on more than one member at the node due to the attached columns which again further decreases the deformations in subsequent members.

iv) The location of the inflection point: This is useful in sketching the deformed shape of beams and frames because it identifies the location where the beam changes curvature. Note that the crosses ($\times$) in figure 1.13 indicate the locations of inflection points. The location of the inflection point may be inferred from the end moments (or vice-versa) because the bending moment diagram is linear and passes through zero at the inflection point. The relation between bending moment and inflection point location measured from the left is given by:

$$1 - \frac{x_{\text{inflection}}}{L} = \frac{\left|\frac{M_{\text{far}}}{M_{\text{near}}}\right|}{1 + \left|\frac{M_{\text{far}}}{M_{\text{near}}}\right|} \qquad (1.1a)$$

$$\Leftrightarrow \quad \left|\frac{M_{\text{far}}}{M_{\text{near}}}\right| = \frac{1 - x_{\text{inflection}}/L}{x_{\text{inflection}}/L} \qquad (1.1b)$$
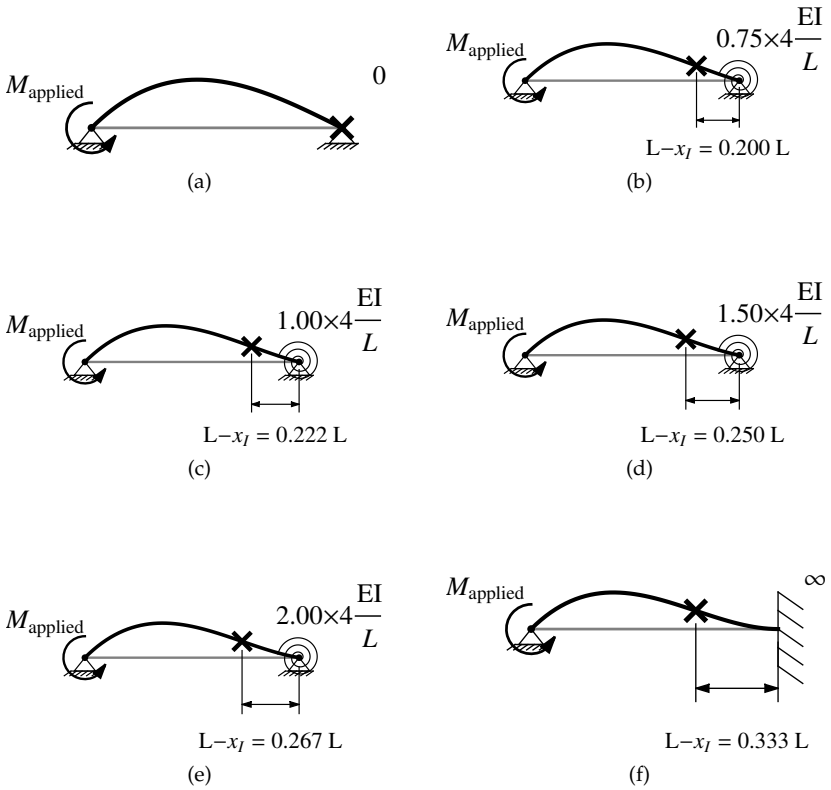
Figure 1.14. Inflection points marked with $\times$ as the rotary spring stiffness increases (a) to (f).

The distance of the inflection point from the far end varies from 0 for a hinged end to 1/3 for a fixed end. Most of the change occurs between $k = 0$ and $k = 1$ with relatively slow variation after $k = 1$. This result is plotted in figure 1.12 and illustrated in figure 1.14 where the the inflection point seems to jump left between $k = 0$ and $k = 0.75$ but then the movement is barely discernible between $k = 0.75$ and $k \to \infty$. If needed, the exact expression for the location of the inflection point is given by:

$$1 - \frac{x_{\text{inflection}}}{L} = \frac{2k}{3 + 6k} \qquad (1.2a)$$

$$\Rightarrow \qquad \left| \frac{M_{\text{far}}}{M_{\text{near}}} \right| = \frac{2k}{3 + 4k} \qquad (1.2b)$$

The above exact results are simple enough but the practitioner is expected to memorize a few values from table 1.1 and use those values with interpolation between them rather than use the exact formula each time. With practice, the use of those values becomes simple and automatic.

v) The location at which the deflection is maximum: This is mildly useful in sketching in the sense of knowing the general location where the maximum occurs. In particular, we will not be sufficiently careful in sketching deformations to require an accurate location for the maximum. However, this location becomes important when sketching influence lines for indeterminate structures because it indicates the location of maximum influence in the member. The location of the maximum deflection always occurs closer to the near end and its distance to the near end monotonically decreases from about 0.42 for a hinged end to 1/3 (*ie.* becomes closer to the near end) for a fixed far end.

vi) The magnitude of the maximum deflection: This will generally be mostly neglected in sketching deformations since, for clarity, we will generally greatly exaggerate the deformations. However, this result is essential in approximating the influence lines of an indeterminate structure. This maximum varies from about $0.19 \times \theta_{\text{near}} L$ for a hinged far end and decreases monotonically to about $0.15 \times \theta_{\text{near}} L$ for a fixed end.

Aside from the above results, we note that since there are no loads on the member then the shear force in the member is constant, the bending moment is linear, the slope varies parabolically and the displacement is a cubic function. In particular, the shear force is then given by:

$$V = \frac{(|M_{\text{near}}| + |M_{\text{far}}|)}{L} \tag{1.3}$$

The above result always applies when there are no forces applied on the member (except possibly at the ends) and we will repeatedly use it for columns when studying sidesway in frames.

1.4   Example: Continuous Beam with Moment Applied at Only One Node

In the first example, we consider the continuous beam shown in figure 1.15 with a unit clockwise moment applied at node C. We will be concerned with sketching the exaggerated deformed shape of the beam
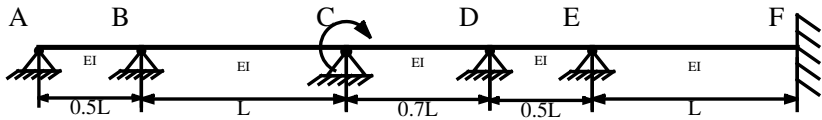
Figure 1.15. A continuous beam with an applied unit clockwise moment at point C.

with particular attention to identify the location of the inflection points. Next we will draw an approximate bending moment diagram with the moments approximately calculated and indicated on that figure.

To sketch the continuous beam, we start with the node where the external moment is applied which is node C. We choose a rotation at that node (*eg.* about $60°$) in the same sense (*ie.* clockwise) as the applied moment and we draw a short straight line to indicate that rotation (see figure 1.15 at node C). That short straight line extends at both sides of node C because the slope must be continuous at any point where there is no internal hinge. The exact magnitude of the rotation at C does not matter because we are only interested in indicating the shape of the deformations.

Next we indicate a rotation at node B using a straight line segment in the opposite sense and at some fraction of the rotation at node C (see figure 1.16 node B). The rotation at B is determined by considering member BC and viewing member AB as equivalent to a rotary spring at B as shown in figure 1.17a. From the previous section, we know that the ratio of rotations at B relative to C will be less than 0.5. For a quick sketch, we can take the rotation at B to be one quarter to one third that of C. Alternatively, for a more precise sketch, we calculate the k-value for the rotary spring at node B in member BC to get a k-value of 1.5. This k-value is obtained by the ratio of rotary stiffness of an isolated member AB as shown in figure 1.17b divided by the ratio of $(EI/L)_{BC}$ of member BC.
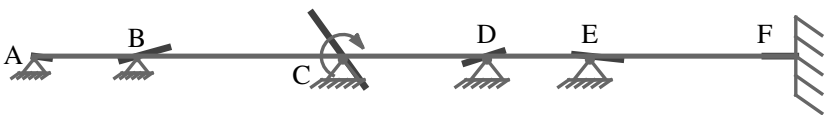
Figure 1.16. Straight line extensions placed at each node.

$k = 0.75 \dfrac{1/(0.5\,L)}{1/L} = 1.5$

(a)

$k = 0$

(b)

$k \approx 1 \dfrac{1/(0.5\,L)}{1/(0.7\,L)} \approx 1.4$

(c)

$k = 1 \dfrac{1/(1\,L)}{1/(0.5\,L)} = 0.5$

(d)

$k = \infty$

(e)
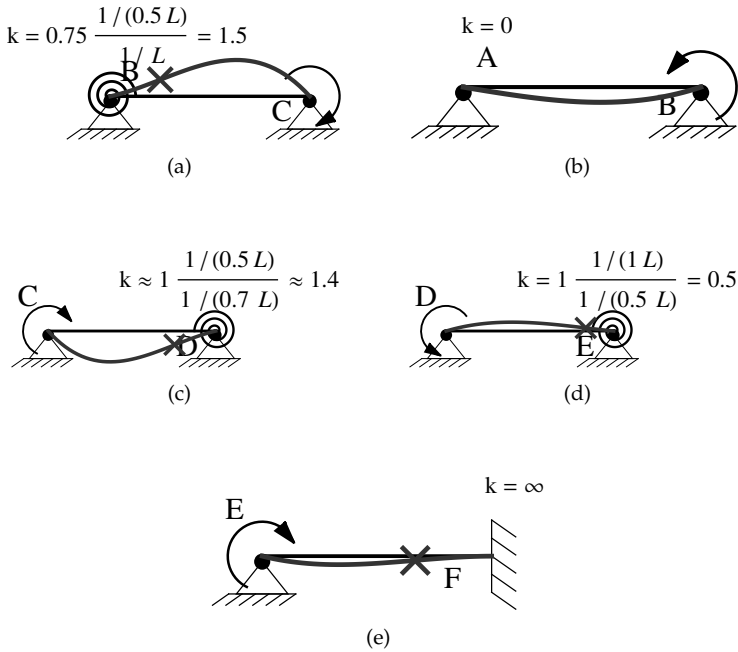
Figure 1.17. Isolated members of the continuous beam shown in figure 1.15.

This more precise calculation gives a ratio of angles of 0.25 (see table 1.1) which for a rotation at C of 60° means a rotation of 15° at node B. Of course, such precision in manual sketching is impractical and unnecessary for our purposes.

To complete the rotational indications for the left side, we consider member AB as shown in figure 1.17. For that member, the rotation at node A is known to be −0.5 that of node B and we indicate that by a short straight line at node A as shown in figure 1.16 at node A. This process is then repeated for members CD then DE and EF. Member EF has a fixed end and so there is no rotation at node F and we indicate this by a short straight line at node F.

After sketching the short line segments shown in figure 1.16, we now connect the lines using the procedures indicated in figure 1.3, 1.4 and 1.5 as applicable. We also place an "×" to highlight the location of inflection points. These are obtained from the tables based on the values of the rotary spring k-values illustrated in figure 1.17. The result is shown in figure 1.18. Note that the inflection point between CD would be estimated to be at $0.17L$ from point D based on the discussion above;
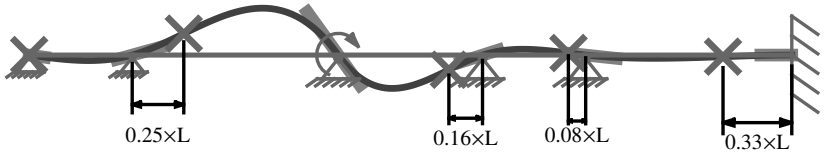
Figure 1.18. Sketch of the deformed shape with inflection point locations.

however, the exact result of about $0.16L$ is shown in the figure. All other obtained values are the same as the exact result to within the accuracy shown in the figure (*ie.* 2 digits after the decimal). This difference is quite acceptable for an approximate method.

Now, we focus our attention on sketching the bending moment diagram. Since there are no loads on the members, the bending moment diagrams of each member will be a straight line. Hence, we only need to calculate the values at the ends of those segments. To determine those values, we start again with node C. The unit applied moment at node C will be resisted by both members BC and CD at their ends as shown in figure 1.19. The fraction of the applied unit moment distributed to the members (*ie.* M_{CD} and M_{CB}) is obtained in proportion to their relative stiffness. This gives $M_{CB} \approx (EI/L)/\big((EI/L) + (EI/(0.7L))\big) \approx 0.41$ and $M_{CD} \approx (EI/(0.7L))/\big((EI/L) + (EI/(0.7L))\big) \approx 0.59$. To get a better approximation, we must use better estimates for the stiffnesses of members BC and CD at C. The exact results are shown in figure 1.20 which agree with the simple estimates to 2 significant digits.

Once the distributed moments at C are calculated, we proceed member by member away from node C. The bending moment at the other
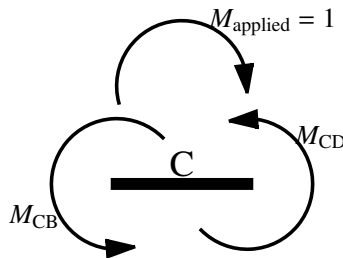
Figure 1.19. A continuous beam with an applied unit clockwise moment at point C.
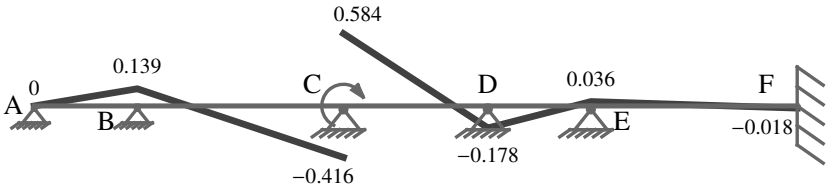
Figure 1.20. The bending moment diagram for the continuous beam of figure 1.15.

end of each member may either be determined by using the location of the inflection point or by referring back to the tables. As an example of using the tables, we consider calculating the moment at B of member BC. For that member, we have a k-value of 1.5 which from the tables gives a "carry-over-moment" of 0.333; therefore, the moment at B will be $M_{\text{CB}} \times 0.333 \approx 0.416 \times 0.333 \approx 0.139$. The moments in all the other members may be calculated similarly or by using similar triangles while knowing the approximate location of the inflection point. The final result is shown in figure 1.20.

1.5   Outline of Approximate Method for Analyzing Structures with No Sidesway

As the previous example shows, we can approximately analyze beams and frames with no sidesway and with moments applied only at nodes. This is done by the following steps:

i) Distribute the applied moment onto the connected members according to their effective stiffness. Each of those effective stiffnesses may be estimated by using table 1.1 as a guide. In any case, the error in using a rough estimate for the stiffness (*ie.* EI/L of each member) will be less than 7.2% as discussed previously.

ii) Consider each member in turn starting with the members connected to the node with the applied moment. Model that member as a hinged beam with an applied moment at one end and a rotary spring at the other. By roughly estimating the stiffness of the rotary spring, we can well approximate the inflection point and the end moments.

iii) The end moments at the rotary springs are considered as applied moments on the nodes which are then distributed to their other connected members using the same procedure as step (i). These three

steps are then repeated until the whole structure is completed without requiring iteration.

iv) In case of a loop, the last member in a loop will have specified moments at both ends. Its deformed shape may easily be sketched and the bending moment is a straight line connecting the two end moments.

Applied moments at multiple nodes is handled through superposition. This means we analyze each applied moment when acting alone on the structure and then we sum up the responses. We note that since the effect of an applied moment decreases rapidly away from the point of application (eg. figure 1.13), the moment at any node may be evaluated by considering the superposition of the effects of only "nearby" applied moments. This gives good approximate results when all the applied moments have comparable magnitudes. Further discussions and shortcuts on how to analyze combined loads is discussed in a later section.

To proceed further, we must consider the response of loaded members. As indicated in the section on passive members, a single loaded member in a structure with no sidesway may be handled by isolating the member and placing rotary springs of appropriate stiffness at each end. Therefore, to analyze beams and frames with no sidesway and with only one loaded member we do the following:

i) Analyze the loaded member with appropriate rotary springs at each end. In particular, calculate the end moments at the rotary springs.

ii) Use the calculated moments at the ends of the loaded member as if they were external moments applied on the rest of the members connected at those ends. At that point, the rest of the structure on the left and right of the loaded member can then be analyzed using the four steps detailed above.

Beams or frames with more than one loaded member may be analyzed by superposition. This means we analyze one loaded member when acting alone on the structure and then we sum up the responses due to all the loaded members. Again, since the effect of applied moments decreases rapidly away from the point of application, the moment at any node may be evaluated by considering the superposition of the effects of only "nearby" loaded member when end moments of each loaded member acting separately are comparable to end moments of other loaded members acting separately.

Therefore, to be able to analyze any beam and frame with no sidesway, we still need to know the response of a loaded beam with rotary springs at each hinged end. We will consider only two special cases:

i) a uniformly loaded beam and ii) a concentrated or point force any-
where on the beam. The point force solution may be approximately used
to analyze most other loading cases, especially at members other the the
one being loaded.

1.6   Beam with a Uniform Load

A beam with a uniform load is a special type of load but it is a type that
is often encountered in applications. We first consider three special end
conditions for a uniformly loaded beam as shown in figure 1.21. We will
refer to these cases as simply supported or hinged-hinged beam for fig-
ure 1.21a, fixed-fixed beam for figure 1.21b and hinged-fixed beam for
figure 1.21c. The deformations and bending moment diagrams associ-
ated with the special end conditions are shown in figure 1.22 and 1.23
respectively. Of course, the case of fixed-hinged beam will be a mirror
image of case figure 1.21c because we will assume that the members are
homogeneous and prismatic (*ie.* same properties and same cross-section
along the length). Because of that symmetry, the response for mirror im-
age supports will be mirror image responses (*eg.* mirror image deforma-
tions and moment diagrams).
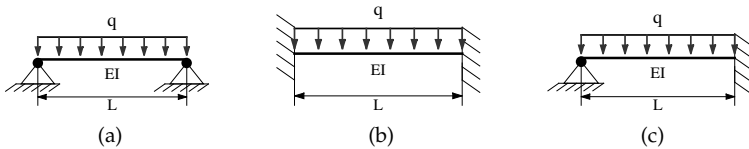
Figure 1.21. Three special cases for the end conditions of a uniformly loaded
beam.

Figure 1.22. Deformations of the special cases for the end conditions of a uni-
formly loaded beam.

The simply supported beam in figure 1.21a has deformations with
no inflection points and its curvature is always positive as seen in
figure 1.22a. Consequently, its bending moment diagram is always pos-
itive and its shape is as shown in figure 1.23a. This bending moment

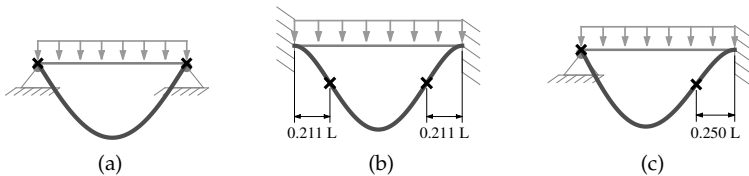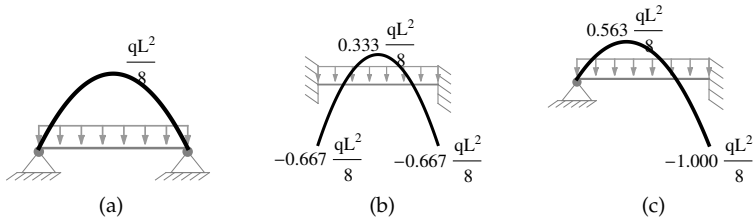**Figure 1.23.** Moment diagrams of the special cases for the end conditions of a uniformly loaded beam.
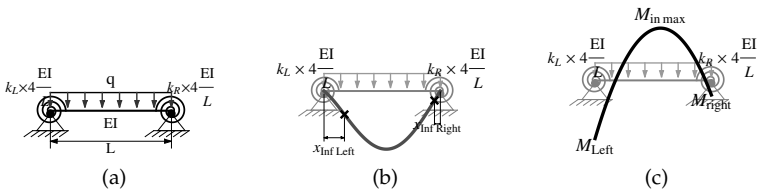
Figure 1.24. Uniformly loaded beam attached to passive structures on both sides.

reaches a maximum value of $qL^2/8$ where 'q' is the magnitude of the uniform load and 'L' is the length of the beam. By considering the general case shown in figure 1.24a, we find that this is the maximum positive moment that can occur in any uniformly loaded beam that is attached to passive structures on both ends. Consequently, in tabulations and plots of bending moments of a uniformly loaded beam, we will always present those results as ratios of that maximum moment (*ie.* we normalize by that maximum). This normalization is also useful in manual calculations because i) all the dimensional values are centralized in one place and thus we only need to do a careful dimensional calculation once and ii) we only need to remember a few non-dimensional values between 0 and 1 to get an acceptable approximation of most beams and frames with no sidesway.

The fixed-fixed beam in figure 1.21b has deformations with two inflections points and zero slopes or rotations at each end as seen in figure 1.22b. Its bending moment diagram is as shown in figure 1.23b where the negative moment at the ends is twice the positive in the middle. The sum of the absolute values of the positive moment in the middle and negative moment at an end equals $qL^2/8$. This is always true whenever the rotary spring stiffnesses at the ends are the same including the limit of infinite stiffness of the fixed-fixed ends. The reason is that we can view the symmetric end conditions as a superposition of the
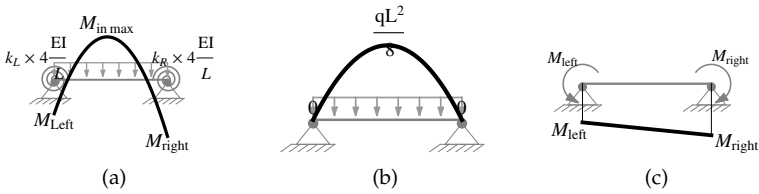
Figure 1.25. Superposition of moment diagrams for uniformly loaded beam.

hinged-hinged case (simply supported) and applied end-moments as shown in figure 1.25. Thus when the end moments are the same then we are superposing a uniform bending moment with the bending moment of a simply supported case and thus, for the symmetric case, we get a downward vertical translation of the simply supported case.

The hinged-fixed beam in figure 1.21c has deformations with one inflection point and zero slope or rotation at the fixed end as seen in figure 1.22c. Its bending moment diagram is as shown in figure 1.23c where the negative moment reaches a value of $qL^2/8$. By considering the general case shown in figure 1.24a, we find that this is the maximum negative moment that can occur in any uniformly loaded beam that is attached to passive structures on both ends. Thus the maximum positive moment occurs in the hinged-hinged case and the maximum negative moment occurs in the hinged-fixed case. Also using the general case in figure 1.24a, we find that the distance of '$0.25L$' of the inflection point from the fixed end is the farthest that an inflection point can occur in a uniformly loaded beam attached to passive structures on both ends.

Having considered some special cases, we now consider the general case shown in figure 1.24. A representative sketch of the deformed shape and the bending moment diagram are shown in figures 1.24b and 1.24c. In order to sketch the deformed shape, we need to i) identify the approximate location of the inflection points and mark those by an '$\times$,' ii) roughly indicate the relative rotations of the left versus the right end and iii) roughly indicate the right location of the maximum deflection. Of these three requirements, only the inflection points need to be numerically indicated since their location will be the basis for calculating the approximate values of the bending moment diagram. We now discuss each of these three requirements separately.

First we consider the locations of the inflection points. In general, there are two inflection points in a uniformly loaded beam that is attached to passive structures on both ends. The distance of an inflection point from the nearest end increases as the stiffness factor of that end increases. For example, if $k_R = 0$ then the left inflection point is at $x = 0$

when $k_L = 0$ (*ie.* a hinge at the left end) and increases monotonically with 'k_L' to reach a value of $0.25L$ when $k_L \to \infty$. The location of an inflection point divided by the length of the beam (*ie.* normalized location) depends only on the spring stiffness factors 'k_L' and 'k_R' (see figure 1.24). To get some insight on this dependence, we draw a contour plot of the location of the inflection point on the left versus the two stiffness factors (see figure 1.26). We notice that the location of the left inflection point is rather insensitive of the stiffness factor on the right (*ie.* 'k_R'). Therefore, we consider obtaining a simple expression for the location of the inflection points as a function of the stiffness factor near the end that it occurs. This will allow us to avoid extensive tables for the inflection point as a function of two variables which are the two stiffness factors. This approximate expression will be presented and discussed next.

$x_{\text{infl left}}/L$
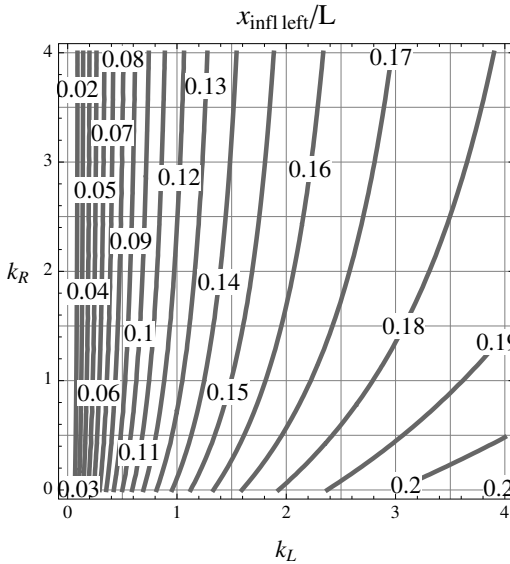
Figure 1.26. Contour plot of the location of the left inflection point versus end stiffnesses.

To get an approximate location for the inflection point at an end as a function of the spring stiffness factor near that end, we calculate the locations of the inflection points when both stiffness factors are the same, curve fit the results using a simple rational expression and round to get
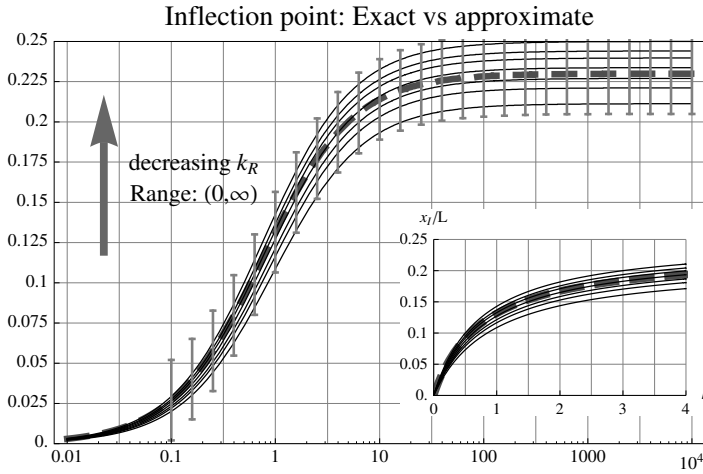
Figure 1.27. Comparsion of inflection point location between exact (solid thin lines) and approximate (dashed thick line).

simple numbers. The result is:

$$x_{I\text{left}}/L \approx \frac{0.92k_L}{3 + 4k_L} \tag{1.4a}$$

$$1 - x_{I\text{right}}/L \approx \frac{0.92k_R}{3 + 4k_R} \tag{1.4b}$$

We compare the result of the approximate expression with the exact one as shown in figure 1.27. That figure also shows error bars that are $\pm 2.5\%$ of the beam length away from the approximate results. If we do an optimization to determine the exact maximum and minimum errors, we get an error between about -2.34% when $k_L \approx 1.76$ and $k_R \to \infty$, and 2% when $k_L \to \infty$ and $k_R = 0$. Note that this is a percentage error which is relative to the length of the beam while the relative error relative to the location would be higher because we are sometimes dealing with small numbers; specifically, the true relative errors are about -38% when $k_L \to 0$ and $k_R \to \infty$ and 8% when $k_L \to \infty$ and $k_R = 0$. For the purposes of sketching and obtaining the bending moment diagram, it is the error relative to the length that is relevant. For example, when we are indicating the location of the inflection point on a sketch of the beam, the visual perception will be

relative to the length of the beam. In that regards, $\pm 2.5\%$ would be barely discernible and about the thickness of the line drawn. Moreover, in a manual sketch small features will be perceived relative to the length of the beam and, in particular, the error in a manual indication of the inflection points will usually exceed an error of $\pm 2.5\%$ relative to the length.

The second point to be addressed in relation to sketching is to give guidelines on how to sketch the relative rotations at the ends of a uniformly loaded beam. We note that we want to be consistent but not much precise in this matter because we only want to do a 'rough' manual sketch of the deformations. Also, unlike the location of the inflection points, the effect of end rotations do not enter into the calculations of the approximate bending moment diagram which is the basis for design. The first guide related to end rotations is that, of course, the rotation at a stiffer end will be lower than at the other end and that the slopes will be the same when both ends have the same stiffness. To further guide our sketching of end rotations or slopes, plots of the normalized end slopes and of the relative end slopes are shown in figure 1.28. By considering figure 1.28a, we note that the rotation at one end becomes progressively less sensitive to the stiffness at the other end as its own stiffness increases. By considering figure 1.28b, we note that the ratio of minimum to maximum slope varies between about 30% to about 90% for a difference in stiffness factors between 0.5 and 4. From this result, we recommend that for manual sketches, the figure should show the slope at the stiffer end to be from about half to about the same as that of the other end with half being associated with a larger difference in stiffness factors; the exception is when one end is fixed which always requires that end to be shown with zero slope.
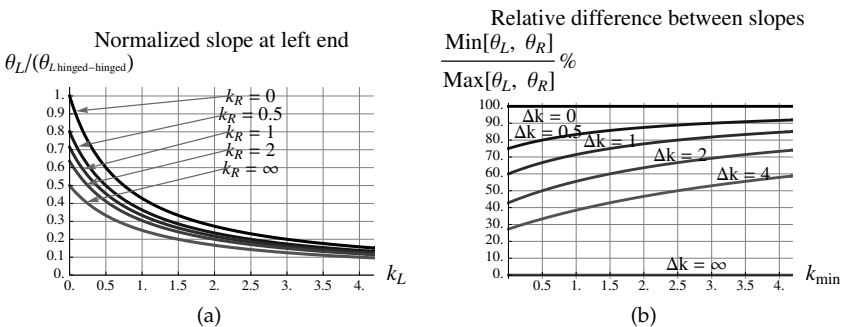

Figure 1.28. Slopes and relative slopes at the ends of a uniformly loaded beam.
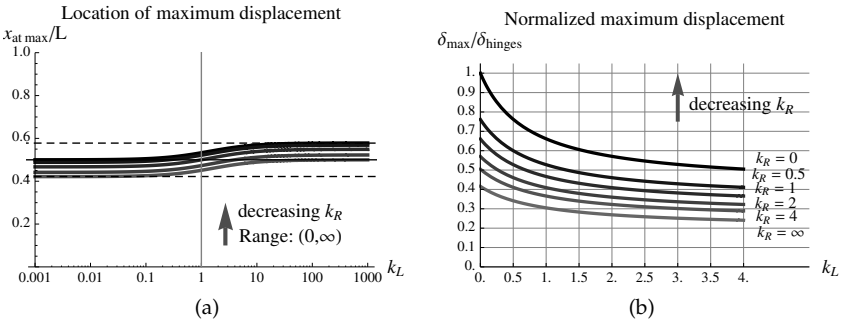
Figure 1.29. Location and magnitude of the maximum displacement in a uniformly loaded beam.

The third and final point to be addressed in relation to sketching the deformed shape is to show a sketch with the location of the maximum displacement occuring at approximately the right location. For that purpose, we plot the location of the maximum displacement for a wide range of combinations of stiffness factors as shown in figure 1.29a. We notice that this location remains relatively close to the middle. If we optimize the location of the maximum displacement over all values of (positive) stiffness factors, we obtain that the maximum should occur at the middle with a maximum offset of about $\pm 7.85\%$. As a guide to sketching, we then should aim at showing the maximum to occur somewhere near the middle with a slight bias if any (*eg.* about 5%) to appear nearer to the more flexible side. Of course, in 'rough' sketches, this bias will barely be noticed but, for the careful viewer, this would indicate that the figure was done by a knowledgeable analyst.

The approximate sketching of the bending moment diagram relies on correctly identifying the location of inflection points. Once the inflection points have been determined, the maximum moment inside the beam and the moments at the ends may be determined by statics. The process of doing this is illustated in figure 1.30. Any uniformly loaded beam with spring-hinged ends may be viewed as a simply supported beam between the inflection points with two end pieces on the left and right. The reason is that the bending moment at inflection points is zero and therefore these locations may be viewed as having hinged supports on top of the remaining parts of the beam. The simply supported beam and each of the ends may then be simply analyzed to obtain the maximum internal bending moment and the end moments. These are
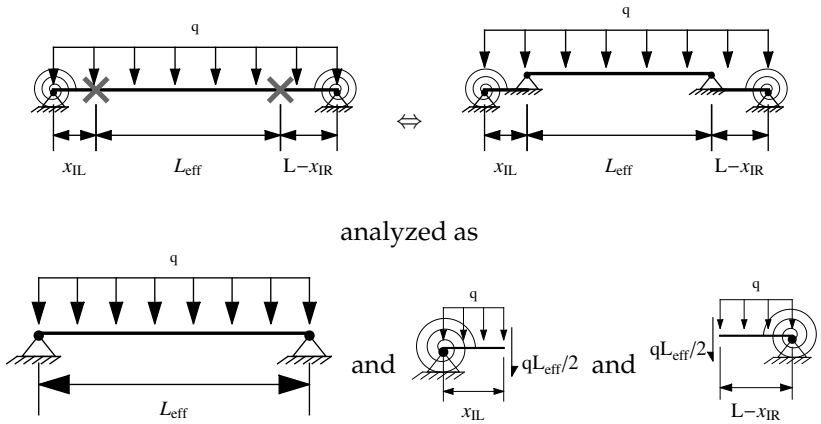
Figure 1.30. Obtaining moment diagram by knowing the location of the inflection points.

given by:

$$M_{\text{in max}} = \frac{qL_{\text{effective}}^2}{8} \tag{1.5a}$$

$$M_{\text{left}} = \frac{qL_{\text{effective}}}{2} \times x_{\text{IL}} + \frac{qx_{\text{IL}}^2}{2} = \frac{qx_{\text{IL}}\left(L_{\text{eff}} + x_{\text{IL}}\right)}{2} \tag{1.5b}$$

$$M_{\text{right}} = \frac{qL_{\text{effective}}}{2} \times (L - x_{\text{IR}}) + \frac{q\left(L - x_{\text{IR}}\right)^2}{2}$$
$$= \frac{q\left(L - x_{\text{IR}}\right)\left(L_{\text{eff}} + L - x_{\text{IR}}\right)}{2} \tag{1.5c}$$

In addition to the above, we also deduce that the location of the maximum internal bending moment is at the center of the effective simply supported beam between the inflection points (*ie.* at $(x_{\text{IL}} + x_{\text{IR}})/2$). Finally, we can sketch the bending moment diagram. This diagram must be a parabola because, from elementary mechanics of materials, the second derivative of the moment is a constant equal to the uniform distributed load. In addition, this parabola has a negative curvature and must pass through the inflection points which are locations where the bending moment is zero. Finally, after drawing such a parabola, we can mark the maximum internal bending moment and end moments from the values calculated using formulas 1.5a to 1.5c).
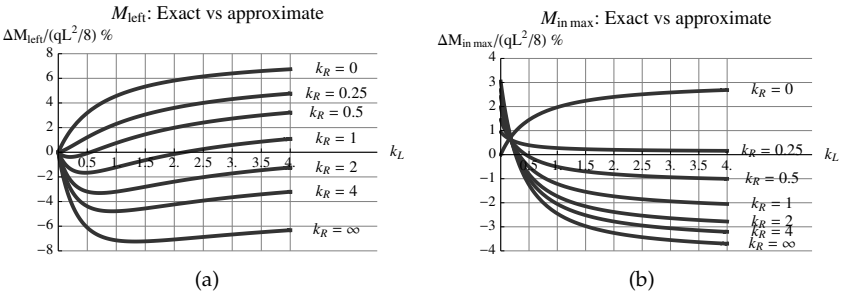
Figure 1.31. Error between bending moments obtained from exact versus approximate location of inflection points.

Of course, the errors in the calculated bending moments are related to the errors in the approximate locations of the inflection points. If we use formula 1.4a and 1.4b to estimate the location of inflection points and we plot the error at the left end (right is analogous) and at the inner maximum bending moment then we get the results shown in figure 1.31. Note that those percent errors are relative to the maximum moment in a simply supported beam. For the left end moment (right end is equivalent), by optimizing the difference between the approximate and exact results, we find that the maximum error is between -7.23% which occurs when $k_L \approx 1.33$ and $k_R \to \infty$ and 8% which occurs when $k_L \to \infty$ and $k_R = 0$. Alternatively, we can characterize the relative error by constraining the smallest (absolute) value of the left end moment. Specifically, if the approximately calculated left end moment is (in absolute value) greater than $0.2\ qL^2/8$ then the maximum relative error is between -8% which occurs when $k_L \to \infty$ and $k_R = 0$ and 31.7% which occurs when $k_L \approx 0.295$ and $k_R \to \infty$.

For the inner maximum moment, by optimizing the difference between the approximate and exact results, we find that the maximum error relative to $qL^2/8$ is between -4.17% which occurs when $k_L \to \infty$ and $k_R \to \infty$ and 3.04% which occurs when $k_L \to \infty$ and $k_R = 0$ (or vice versa). Alternatively, we can characterize the relative error of the inner maximum moment. Specifically, the relative error of the inner maximum moment is between about -6.77% which occurs when $k_L \approx 1.32$ and $k_R \to \infty$ and about 5.39% which occurs when $k_L \to \infty$ and $k_R = 0$. The approximate expression for the inner maximum moment has generally lower percent error than the one for the end moment because its value never goes below about $0.33\ qL^2/8$ while the end moments can reach zero. In any case, these results show that this approximate analysis

gives sufficient accuracy for preliminary design or to check the output of computer calculations.

In sketching the bending moment diagram, it is useful to be consistent and 'roughly' accurate in showing the location of the maximum internal moment. For that purpose, we can estimate the location from the location of the inflection points as previously indicated. Alternatively, we sketch the location of maximum internal moment (figure 1.32) and note that the maximum always occurs within $\pm 12.5\%$ of the beam length from the center and always occurs closer to the more flexible side. Figure 1.32 also shows the relative magnitude of the maximum internal bending moment for a wide range of end conditions which will be later useful in studying multiple loadings. From figure 1.32, we suggest as a guide to manual sketching that the location of the maximum should be shown somewhere near the middle with a slight bias if any (*eg.* about 5%) to appear nearer to the more flexible side. Of course, in 'rough' sketches, this bias will barely be noticed but, for the careful viewer, this would again indicate that the figure was done by a knowledgeable analyst.
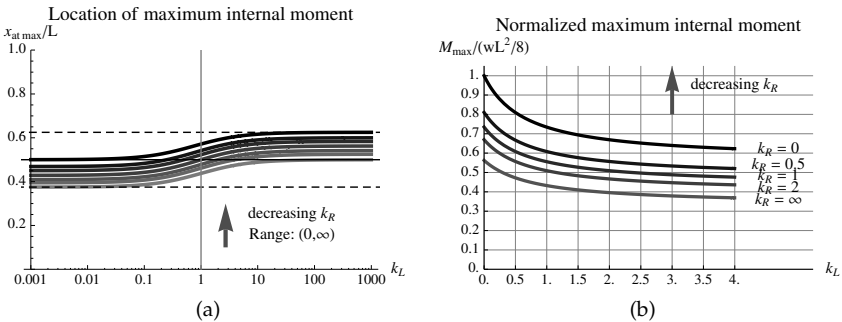
Figure 1.32. Location of the maximum moment.

The above discussions presented extensive details of how to sketch the deformed shapes and the bending moment diagrams of a uniformly loaded beam that is attached to passive structures at both ends. This discussion involved features in the sketching and approximations that are much more accurate than has previously been presented in the literature. To gain some practice and insight, we present and discuss a range of results for the uniformly loaded beam.

We begin by considering the case of symmetry where the passive structures at both ends provide about the same resistance to deformations. This is indicated by having $k_L = k_R = k$ in table 1.2. Some of the interesting results for this case include:

Table 1.2. Uniformly Loaded Beam: Symmetric Spring Resistance.

k	x_{Infl}/L at left	$1 - x_{\text{Inf}}/L$ at right	$-M_{\text{left}}/\frac{qL^2}{8}$	$-M_{\text{right}}/\frac{qL^2}{8}$	$M_{\text{in max}}/\frac{qL^2}{8}$
0.000	0.000	0.000	0.000	0.000	1.000
0.500	0.092	0.092	0.333	0.333	0.667
0.750	0.113	0.113	0.400	0.400	0.600
1.000	0.127	0.127	0.444	0.444	0.556
1.500	0.146	0.146	0.500	0.500	0.500
2.000	0.158	0.158	0.533	0.533	0.467
3.000	0.173	0.173	0.571	0.571	0.429
4.000	0.181	0.181	0.593	0.593	0.407
∞	0.211	0.211	0.667	0.667	0.333

i) $k = 0$ (simply supported): This gives the largest possible positive moment for a uniformly loaded beam attached to passive structures at both ends.

ii) $k \to \infty$ (fixed-fixed): The negative moments at the ends are twice those at the middle. Also, the inflection points are the farthest into the beam of any symmetric case and occur at a distance of about $0.21L$ from each end.

iii) $k = 1$: This is the value we would use to approximate any non-terminal span (*ie.* not occuring at either end) of a continuous beam of equal spans. In this case, the internal maximum moment is about 0.56 that of the simply supported case and the negative moments at the ends are about 0.44. Also, inflection points are at a distance of about $0.13L$ from the ends.

iv) $k = 1.5$: At this value, the negative and positive moments are equal in absolute values. If we minimize the maximum absolute value of bending moments in a uniformly loaded beam for any uniformly loaded beam attached to passive supports then we get this case. For a material whose yield in tension is the same as in compression (*eg.* steel), this constitutes the end supports that would allow the largest uniform load to be supported before failure.

Three examples of symmetric cases for the exact deformations and exact bending moment diagrams are shown in figures 1.33 and 1.34
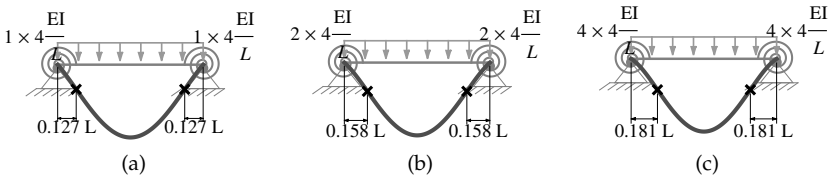
Figure 1.33. Deformed shape of selected cases of unifomly loaded beam with symmetric supports.

respectively. We note that the negative curvature part of the deformation is barely discernible and thus the importance of indicating (*eg.* in the figures with an '×') the location of the inflection points. Aside from the magnitude of the deformations and the location of the inflection points, the deformation shapes for the symmetric cases are about the same over a wide range of stiffness factors. They all look somewhat like parabolas with relatively short pieces at each end having slight negative curvatures.

The moment diagrams shown in figure 1.34 all have the same shape but with a vertical downward shift that increases with the stiffness factor 'k.' Of course, this causes the bending moments to intersect the zero line at different locations which coincide with the location of the inflection points.
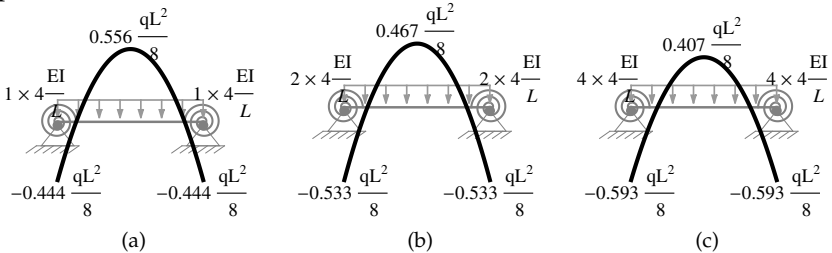
Figure 1.34. Moment diagrams of selected cases of uniformly loaded beam with symmetric supports.

In comparison with the symmetric case, we first present a few cases where the ends have unequal stiffness factors but neither end is a hinge or a fixed end (see figures 1.35 and 1.36). From figure 1.35, we notice that, aside from the location of inflection points, the shapes are still similar to those of the symmetric cases. In particular, in manual sketches, they would be indistinguishable. Therefore, we only need to learn how to manually sketch one prototypical shape when neither end is a hinge or a fixed end.

Figure 1.35. Deformed shape of selected cases of uniformly loaded beam with non-symmetric supports.

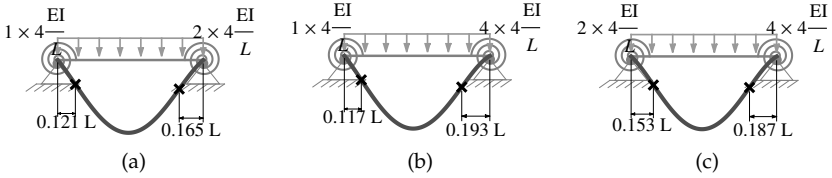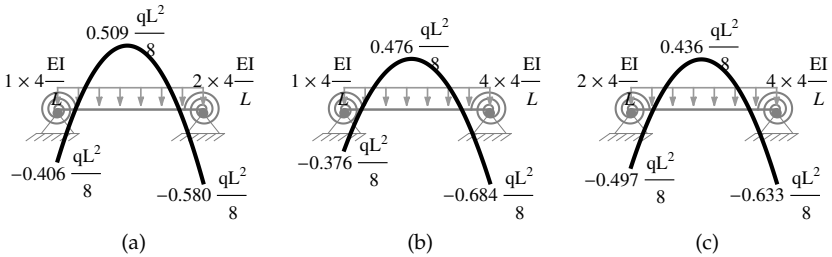**Figure 1.36.** Moment diagrams of selected cases of uniformly loaded beam with non-symmetric supports.

The bending moment diagrams (figures 1.36) for the unsymmetric case differ from those of the symmetric ones only by their unequal values at the ends. As noted before and indicated in figure 1.32a, the location of the maximum does not move much from the middle of the beam. Therefore, as a guide to manual sketching, we suggest first marking the location of the negative moments at the ends and the positive maximum internal moment somewhere near the middle and then drawing an inverted parabola that passes through those points. Also, as much as possible in a manual sketch, the location of zero bending moment should coincide with those of the inflection points.

After considering cases of the uniformly loaded beam where the end conditions are neither a hinge nor a fixed end, we now consider each of those possibilites. The cases where each end is either a hinge or a fixed end have been discussed and are shown in figures 1.22 and 1.23 for the deformed shape and bending moment diagrams respectively. The deformed shape of the simply supported case looks similar to the cases shown in figures 1.33 and 1.35 except that there are no inflection points. The new feature in the deformed shape only occurs at a fixed end; in that case, there is a clear negative curvature portion and the slope is zero at the fixed end. Those features can be manually drawn using a

Table 1.3. Uniformly Loaded Beam: One End Hinged.

k	x_{Infl}/L at left	$1 - x_{\text{Inf}}/L$ at right	$-M_{\text{left}}/\frac{qL^2}{8}$	$-M_{\text{right}}/\frac{qL^2}{8}$	$M_{\text{in max}}/\frac{qL^2}{8}$
0.000	0.000	0.000	0.000	0.000	1.000
0.500	0.000	0.100	0.000	0.400	0.810
0.750	0.000	0.125	0.000	0.500	0.766
1.000	0.000	0.143	0.000	0.571	0.735
1.500	0.000	0.167	0.000	0.667	0.694
2.000	0.000	0.182	0.000	0.727	0.669
3.000	0.000	0.200	0.000	0.800	0.640
4.000	0.000	0.211	0.000	0.842	0.623
∞	0.000	0.250	0.000	1.000	0.563

technique similar to the one outlined in the introduction and illustrated in figure 1.3. Based on extensive viewing of exact test cases, we note that a clear negative curvature portion of the curve near a rotary spring support only gradually occurs as the stiffness factor increases beyond about 10 to 20. Such a stiffness factor is very high and may be practically considered as equivalent to a fixed end. Finally, the bending moment diagrams for these special cases are similar to those shown in figures 1.34 and 1.36 except that the end with the hinge has zero moment and may be manually sketched in the same way.

We now consider the case where one end is a hinge and the other is connected to a passive structure. This is indicated by having $k_L = 0$ and $k_R = k$ in table 1.3. Some of the interesting results for this case include:

i) $k = 0$ (simply supported): This was discussed previously.

ii) $k \to \infty$ (hinged-fixed): This gives the maximum negative moment that can occur in any uniformly loaded beam that is attached to passive structures on both ends. Interestingly, that maxium equals (in absolute value) the maximum possible positive moment. In addition, this case also gives the largest distance that an inflection point can move away from an end in a uniformly loaded beam attached to passive structures at both ends. That distance is at $0.25L$ from the fixed end.

iii) $k = 1$: This is the value we would use to approximate a hinged endspan of a continuous beam of equal spans. In this case, the normalized internal maximum moment is about 0.74 that of the simply supported case and the normalized negative moments at the spring-end is about

0.57. Also, the inflection point is at a distance of about $0.14L$ from the spring end.

iv) $k \approx 1.641$ (not shown): At this value, the normalized negative and positive moments are both equal to about 0.686 in absolute value. If we minimize the maximum absolute value of bending moments in a uniformly loaded beam for any uniformly loaded beam attached to a hinge at one end and a passive support at the other, then we get this case. For a material whose yield in tension is the same as in compression (*eg.* steel), this constitutes the end support at the right with a hinged left end support that would allow the largest uniform load to be supported before failure.

Three examples of hinged-spring cases of table 1.3 for the exact deformations and exact bending moment diagrams are shown in figures 1.37 and 1.38 respectively. We note that the deformations look similar to those of the symmetric cases except that there is no negative curvature at the hinged end which is indicated by putting a '×' at the hinge. Again, we must indicate the location of the inflection point which may be approximately calculated using formulas 1.4 or exactly obtained from table 1.3.
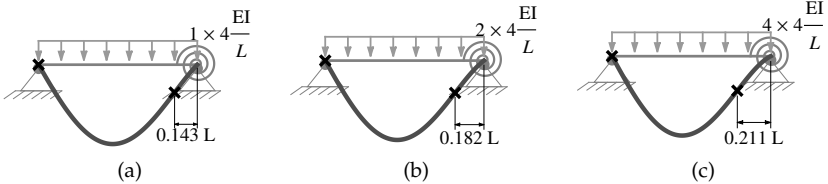

Figure 1.37. Deformed shape of selected cases of uniformly loaded beam with hinge-spring supports.
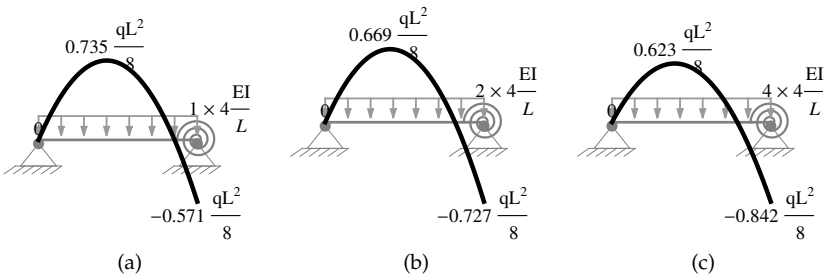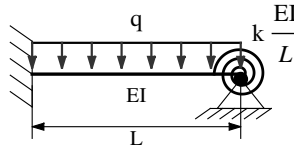

Figure 1.38. Moment diagrams of selected cases of uniformly loaded beam with hinge-spring supports.

Table 1.4. Uniformly Loaded Beam: One End Fixed.

k	x_{Infl}/L at left	$1 - x_{\text{Inf}}/L$ at right	$-M_{\text{left}}/\frac{qL^2}{8}$	$-M_{\text{right}}/\frac{qL^2}{8}$	$M_{\text{in max}}/\frac{qL^2}{8}$
0.000	0.250	0.000	1.000	0.000	0.563
0.500	0.240	0.073	0.889	0.222	0.472
0.750	0.236	0.094	0.857	0.286	0.449
1.000	0.234	0.109	0.833	0.333	0.432
1.500	0.230	0.130	0.800	0.400	0.410
2.000	0.227	0.144	0.778	0.444	0.396
3.000	0.223	0.161	0.750	0.500	0.379
4.000	0.221	0.171	0.733	0.533	0.369
∞	0.211	0.211	0.667	0.667	0.333

The moment diagrams shown in figure 1.38 all have the same shape except for the magnitudes of the maximum and minimum. These can be manually sketched as discussed before for the symmetric case or the hinged-fixed case.

Finally, we now consider the case where one end is fixed and the other is connected to a passive structure. This is indicated by having $k_L \to \infty$ and $k_R = k$ in table 1.4. Some of the interesting results for this case include:

i) $k = 0$ (fixed-hinged): This is the mirror image of the hinged-fixed case which was discussed before.

ii) $k \to \infty$ (fixed-fixed): This gives the fixed-fixed case. This gives the lowest, in absolute value, bending moment at the fixed end. If we minimize the maximum absolute value of bending moments in a uniformly loaded beam for any uniformly loaded beam attached to a fixed end at one end and a passive support at the other then we get this case. For a material whose yield in tension is the same as in compression (*eg.* steel), this constitutes the end support at the right with a fixed left end support that would allow the largest uniform load to be supported before failure.

iii) $k = 1$: This is the value we would use to approximate a fixed end-span of a continuous beam of equal spans. In this case, the internal maximum moment is about 0.43 that of the simply supported case and the similarly normalized negative moments at the ends are about 0.83

at the fixed end and 0.33 at the spring end. Also, the inflection points are at a distance of about $0.23L$ from the fixed end and $0.11L$ from the spring end.

iv) $k \approx 1.573$ (not shown): At this value, the negative moment at the spring end equals the maximum positive moment with a normalized bending moment of about 0.408 in absolute value. Of course, the highest moment in absolute value is still the moment at the fixed end which in this case equals a normalized value of about 0.796.

Three examples of fixed-spring cases of table 1.4 for the exact deformations and exact bending moment diagrams are shown in figures 1.39 and 1.40 respectively. We note that the deformations look similar to those of the fixed-hinged case except that there is an inflection point near the hinge-spring end. Again, we must indicate the location of the inflection points which may be approximately calculated using formulas 1.4 or exactly obtained from table 1.4.

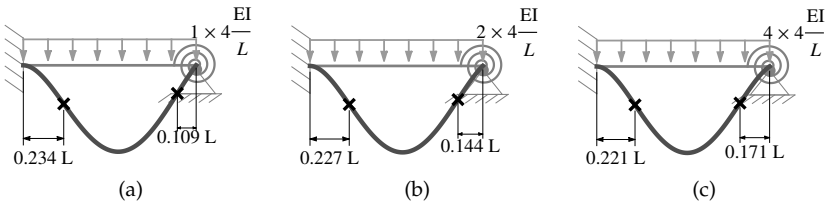**Figure 1.39.** Deformed shape of selected cases of uniformly loaded beam with fixed-spring supports.
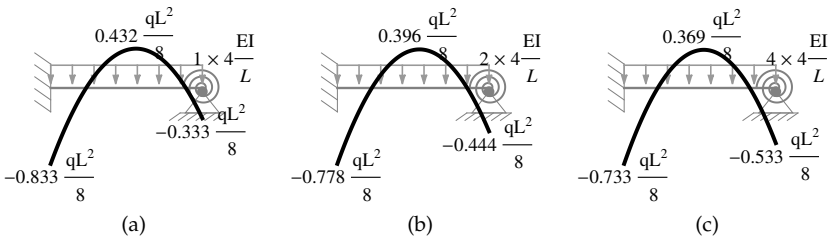

Figure 1.40. Moment diagrams of selected cases of uniformly loaded beam with fixed-spring supports.

The moment diagrams shown in figure 1.40 all have the same shape as the fixed-hinge case except for the magnitudes of the maximum and minimum. These can all be manually sketched as discussed before.

1.7 Example: Uniform Load

As an example of applying the methods developed so far, we consider the structure shown in figure 1.41. We have only one member loaded by a uniform load of magnitude one and all the members have length 5 units and the same moment of inertia 'EI.'
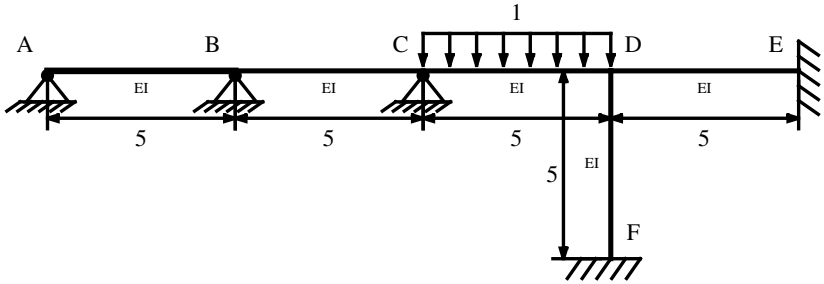

Figure 1.41. Example of a structure with no sidesway and one member uniformly loaded.

As a first step, we decompose the structure into components (figure 1.42). We start with member CD (figure 1.42c). The stiffness factor on the right is exactly 2 because the resistance on that side is provided by two similar members that are fixed on the far end. The stiffness factor on the left is somewhere between 0.75 and 1 (exactly about 0.86), but, for simplicity, we take it to be equal to 1. Using formulas 1.4, we calculate the approximate location of the inflection points, sketch the deformed shape and indicate the approximate location of the inflection points with '×.' Next we turn to the members left of member CD (figures 1.42b then 1.42a). These are handled using the techniques discussed for a member loaded with an end moment and connected to a passive structure at the other end. Finally, we consider the members to the right of member CD and again they are handled similar to those of the members to the left.

If we compare the approximate and exact locations (figure 1.43) of inflection points we find good agreement. The largest error occurs at the inflection point in member CD near node C (9% of the beam length) and we attribute this error more to the approximate estimation of the stiffness factor at C where we used a round number of 1 instead of some number between 0.75 and 1 (*eg.* the mean 0.88). If we had used a stiffness factor at C of 0.88 then the error would have been about 6% of the beam's length.
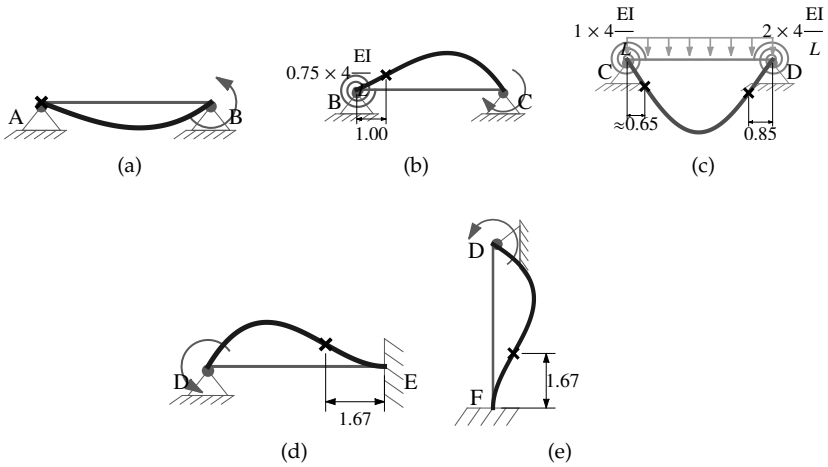
Figure 1.42. Decomposition of structure shown in figure 1.41 with deformed shapes.
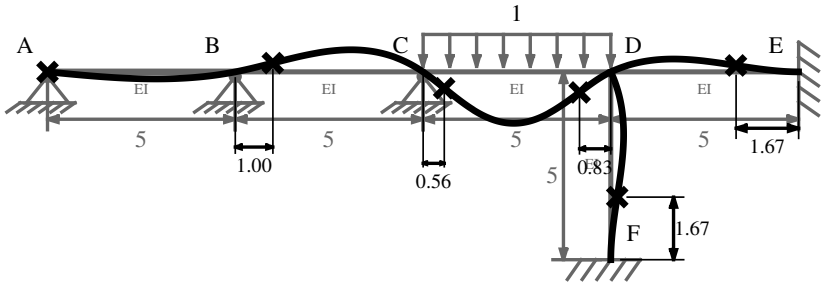
Figure 1.43. Exact shape of the deformed structure of figure 1.41.

Having obtained the approximate location of the inflection points, we then get the bending moments for the uniformly loaded beam using formulas 1.5 and for the end-moment loaded beams using formulas 1.1. The results are shown in figure 1.44. We note the care in passing the location of zero bending moment through the inflection points in each of the members.

If we compare the approximate and exact values (figure 1.45) of maximum and minimum bending moments, we again find good agreement. The largest error again occurs at node C (about 18% relative error). If we
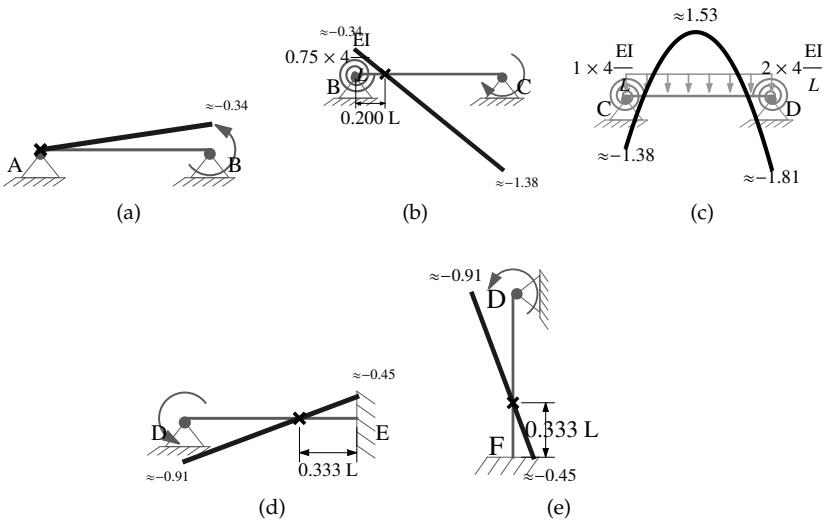
Figure 1.44. Decomposition of structure shown in figure 1.41 with moment diagrams.
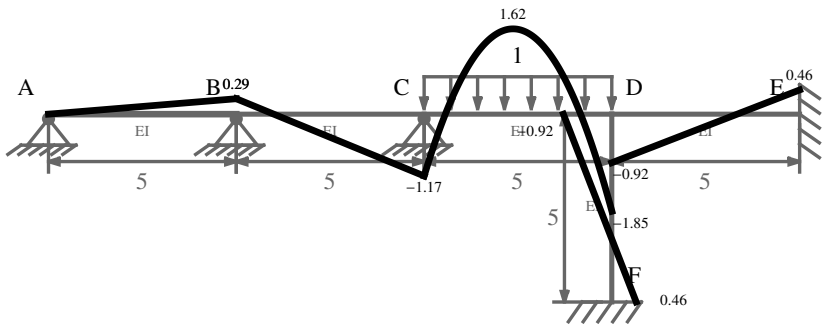
Figure 1.45. Exact shape of the moment diagram of figure 1.41.

had used a stiffness factor at C of 0.88 then the relative error would have been about 10%. We note that the relative error in the maximum positive and negative moments at the left and right ends which occur in member CD are only about -5.5%, 17.9% and -2.2% respectively.

Finally, we note that there is no need to sketch each of the members separately as shown in figures 1.42 and 1.44. We simply first sketch the deformed shape while being aware of the process implied by figure 1.42

and then do the same (on a separate sketch) for the bending moment diagram. With practice, this process becomes quick so that we only need one or two minutes (with the aid of a calculator) to sketch an approximate deformed shape and bending moment diagram for figure 1.41 which include approximate values for inflection points and bending moments that are indicated on the sketches. This level is relatively quickly attained if the practioner becomes familiar with the results (including numerical values) shown in figures 1.33 to 1.40.

1.8   Beam with a Point Force

Loading a beam with a point force is another special type of loading that is often encountered in applications. Similar to the uniformly loaded beam we will, in general, have two stiffness factors on each side parameterizing the resistance of the attached passive structures. Unlike the uniformly loaded beam, we have a third parameter which is the location of the point force. This third parameter will make the analysis slightly more complex than that of the uniform load.

To start, we will again consider three special end conditions for a centrally loaded beam as shown in figure 1.46. These cases are the simply supported or hinged-hinged beam for figure 1.46a, fixed-fixed beam for figure 1.46b and hinged-fixed beam for figure 1.46c. The deformations and bending moment diagrams associated with the special end conditions are shown in figure 1.47 and 1.48 respectively. Of course, the case of fixed-hinged beam will be a mirror image of the case shown in figure 1.46c because we will assume that the members are homogeneous and prismatic (*ie.* same properties and same cross-section along the length) and because the point force is centrally located. In such cases, the response for mirror image supports will be mirror image responses (*eg.* mirror image deformations and mirror image moment diagrams).

The simply supported beam in figure 1.46a has deformations with no inflection points and its curvature is always positive as seen in
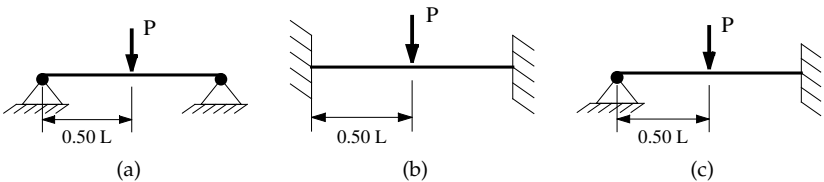

Figure 1.46. Three special cases for the end conditions of a a beam with a central point force.
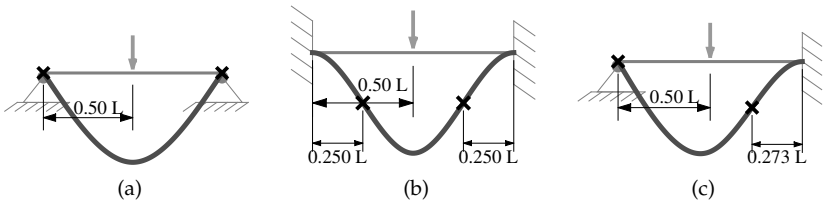
Figure 1.47. Deformations of the special cases for the end conditions of a centrally applied point force.

figure 1.46a. This deformed shape when normalized is nearly identical to that of a simply supported beam with a uniform load; the maximum difference in the normalized shapes is only about 2.6% and is negligible in a manual sketch. Corresponding to the deformed shape, the bending moment diagram is always positive and its shape is as shown in figure 1.48a. This bending moment reaches a maximum value of $PL/4$ where 'P' is the magnitude of the point force and 'L' is the length of the beam. By considering the general case shown in figure 1.52a, we find that this is the maximum positive moment that can occur in any beam that is attached to passive structures on both ends and loaded with a point force that may be located anywhere on the beam. Consequently, in tabulations and plots of bending moments of a uniformly loaded beam, we will always present those results as ratios of that maximum moment (*ie.* we will normalize by that maximum). This normalization is also useful in manual calculations because i) all the dimensional values are centralized in one place and thus we only need to do a careful dimensional calculation once and ii) we only need to remember a few non-dimensional values between 0 and 1 to do an acceptable approximate analysis of most beams and frames with no sidesway.
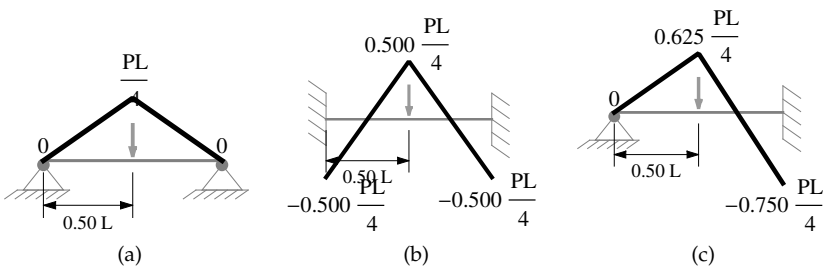

Figure 1.48. Moment diagrams of the special cases for the end conditions of a centrally applied point force.

The fixed-fixed beam in figure 1.46b has deformations with two in-flections points and zero slopes or rotations at each end as seen in fig-ure 1.47b. Again this deformed shape is similar to the equivalent uni-formly loaded beam but is slightly sharper in shape with a maximum difference in the normalized shapes of only 6.25%; this is again negligible in a manual sketch. Corresponding to the deformed shape, the bending moment diagram is as shown in figure 1.48b where the negative moment at the ends is the same as the positive one in the middle; this is to be con-trasted with a uniformly loaded beam where the negative moments at the ends are twice the positive moment in the middle. The sum of the absolute values of the positive moment in the middle and negative mo-ment at an end equals '$PL/4$.' This is always true for central loading and whenever the rotary spring stiffnesses at the ends are the same including the limit of infinite stiffness of the fixed-fixed ends. The reason is that we can view the symmetric end conditions as a superposition of the hinged-hinged case (simply supported) and of applied equal end-moments as shown in figure 1.53. Thus when the end moments are the same, then we are superposing a uniform bending moment with the bending mo-ment of a simply supported case. This then implies that any symmetric support case will have a bending moment diagram that is a downward vertical translation of the bending moment diagram of the simply sup-ported case.

The hinged-fixed beam in figure 1.46c has deformations with one inflection point and zero slope or rotation at the fixed end as seen in figure 1.47c. Again this deformed shape is similar to the equivalent uni-formly loaded beam but is slightly sharper with a maximum difference in the normalized shapes of only 7.8%; this is again negligible in a manual sketch. Its bending moment diagram is as shown in figure 1.48c where the negative moment reaches a value of $0.75PL/4$. By considering the general case shown in figure 1.52a, we find that this is not the maxi-mum negative moment that can occur in a beam that is attached to pas-sive structures on both ends and having a point force somewhere along its span. That maximum does occurs for a hinged-fixed case but with the location of the point force being at about $0.423L$ distance from the fixed end (ie. $0.577L$ distance from the hinged end). The corresponding maximum negative moment is about $0.77PL/4$. Also using the general case in figure 1.52a, we find that the maximum distance of an inflection point from its nearest end also occurs for the hinge-fixed case and has a value of one-third the beam length ($\approx 0.333L$). This case occurs in the limit as the point force approaches but does not reach the hinged end. We note that this limiting case is then equivalent to that of a beam with an infinitesimal moment applied at one end and a fixed end at the other.
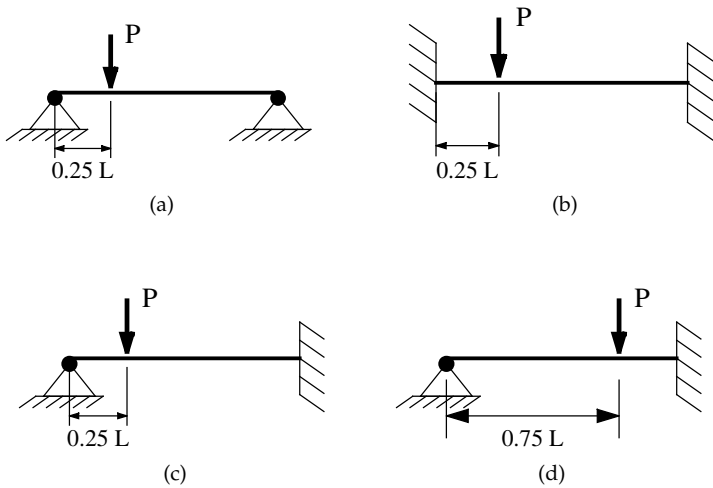
Figure 1.49. Four special cases for the end conditions of a beam with a non-central point force.

Having considered centrally loaded cases with special end conditions, we now consider similar special end conditions but with non-centrally loaded cases as shown in figure 1.49. These are the simply supported beam with a load at a quarter the length from one support shown in figure 1.49a, the fixed-fixed beam with a load at a quarter the length from one support shown in figure 1.49b and the hinged-fixed beam with a load at a quarter and at three-quarters the length from the hinged end as shown figures 1.49c and 1.49d respectively.

What is interesting about the deformations in figure 1.50 is that they all look similar to the corresponding cases of figure 1.46 except for a relatively slight shift of the location of maximum deformation in the direction of the point force. Of course, the inflection points are still to the left and to the right of the point force, even when the point force gets very close to an end.

The bending moment diagrams corresponding to figures 1.49 are shown in figures 1.51. As with the other cases, the maximum positive moment always occurs at the location of the point force. This can be simply understood from the relations between loading, shear force and bending moment. The slope of the bending moment is the shear force and the slope of the shear force is the distributed load at a point which is zero except at the reactions and the location of the point force. Therefore, the shear force diagram is piecewise constant and 'jumps' by the value 'P' which is the magnitude of the point force and at the location
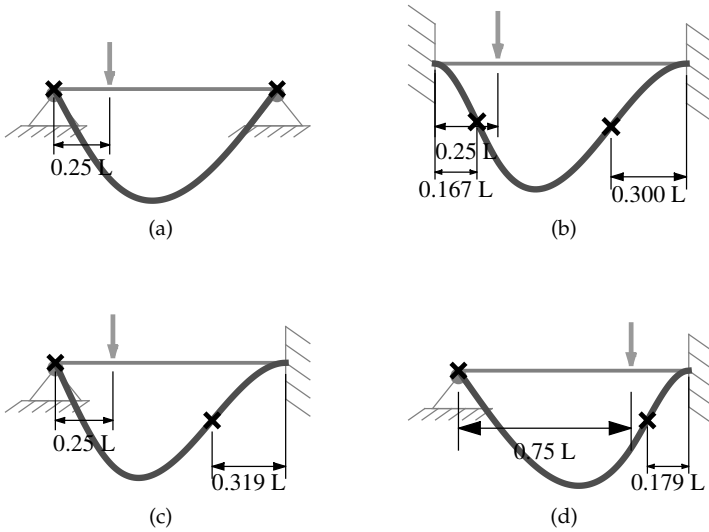
Figure 1.50. Deformations for the figure 1.49 having non-centrally applied point forces.

of the point force. This then gives the moment diagram as a piecewise linear and continuous plot which must then reach a maximum at the point force.

The maximum positive moment in the simply supported case, such as in figure 1.51a, has a simple relation equal to

$$(1 - (x_F / L))(x_F / L) PL = \hat{d}_{F \text{ Right}} \hat{d}_{F \text{ Left}} PL$$

where 'x_F' is the distance of the point force from the left end, 'L' is the length of the beam, 'P' is the magnitude of the point force and '$\hat{d}_{F \text{ Right}}$' and '$\hat{d}_{F \text{ Left}}$' are the normalized distances from the point force to the right and left ends respectively. The normalization of the distances are with respect to the length of the beam. From this expression for the bending moment, we can deduce that the maximum occurs when the point force is in the middle of the beam. More generally, the maximum positive moment always occurs at the middle of a beam when the end support conditions are symmetric. This last observation includes the limit of fixed-fixed end conditions shown in figure 1.51b. By contrast, the largest (in absolute value) negative moment for the symmetric case never occurs when the point force is at the middle of the beam but always occurs when the point force is some distance between '$L/3 \approx 0.333L$' and $\approx 0.423L$ from
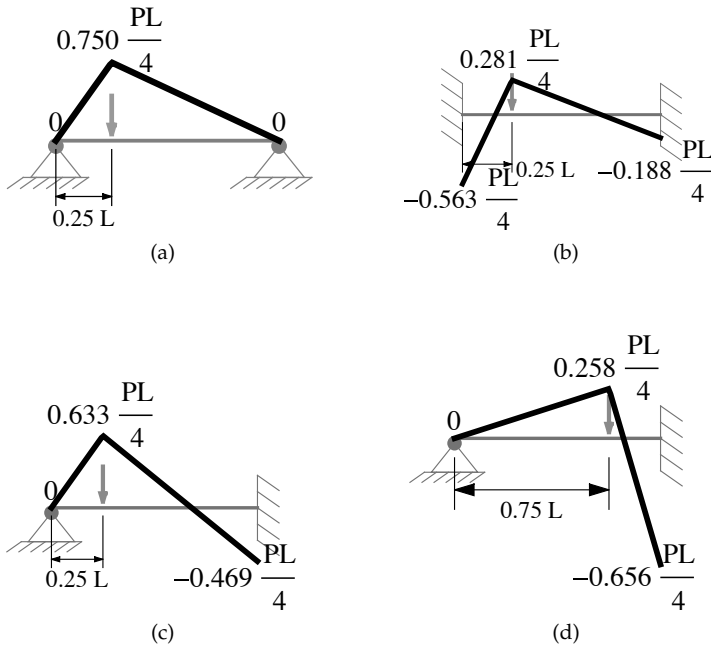
Figure 1.51. Moment diagrams for the figure 1.49 having non-centrally applied point forces.

an end. These limits occur as the stiffness factor goes from the limit at infinity (*ie.* fixed-fixed) to the limit at close to zero respectively. We say almost hinged-hinged because the hinged-hinged case has zero moments at each end.

The hinged-fixed cases in figure 1.49c and d have non-symmetric end conditions with $x_F = 0.25L$ and $x_F = 0.75L$ respectively. Due to the non-symmetry of end conditions, their moment diagrams shown in figures 1.51c and 1.51d are not mirror images of each other. For the hinged-fixed case, the maximum positive moment over all values of 'x_F' (*ie.* location of the point force) occurs when the point force is at a distance of $\approx 0.366L$ from the hinged-end. We note that maximum positive moment when the point force is at $0.25L$ from the hinge is larger than when the point force is at the middle but smaller than when it is at $0.75L$. The largest value that the maximum positive moment can have in the hinge-fixed case is when the point force is at $\approx 0.366L$ from the hinged end and has a value of $\approx 0.696PL/4$. By comparison, the negative moment at the fixed end in both figures 1.51c and 1.51d is smaller (in absolute

value) than the corresponding one when the point force is at the middle. The largest value that the negative moment can have in the hinge-fixed case is when the point force is at $\approx 0.577L$ from the hinged end and has a value of $\approx 0.770PL/4$. This result is to be contrasted with the uniform loading case as follows. If we consider the total load on a uniformly loaded beam to be $P = qL$ then for the hinged-spring case, the largest positive moments are $\approx 0.281PL/4$ and $\approx 0.5PL/4$ respectively. The significantly larger values of $\approx 0.696PL/4$ and $\approx 0.770PL/4$ for the point force in both cases respectively is due to concentrating the load at a more influential point in the beam or, equivalently, due to the added flexibility in choosing the location of the point force.

Having considered some special cases, we now consider the general case shown in figure 1.52. A representative sketch of the deformed shape and the bending moment diagram are shown in figures 1.52b and c. As in the uniformly loaded case, in order to sketch the deformed shape, we need to i) identify the approximate location of the inflection points and mark those by an '×,' ii) roughly indicate the relative rotations of the left versus the right end and iii) roughly indicate the right location of the maximum deflection. Of these three requirements, only the inflection points need to be numerically indicated since their location will be the basis for calculating the approximate values of the bending moment diagram. We now discuss each of the three requirements separately.
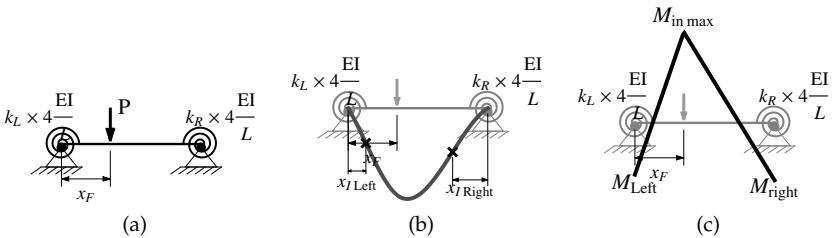

Figure 1.52. General point force on a beam attached to passive structures on both sides.

First we consider the locations of the inflection points. In general, there are two inflection points in a point force loaded beam that is attached to passive structures on both ends. These inflection points occur one on each side of the point force. The distance of an inflection point from its nearest end increases as the stiffness factor of that end increases and decreases as the point force approaches that end. For example, if $k_R = 0$ and the point force is at the center (ie. $x_F = 0.5L$) then the left inflection point is at $x = 0$ when $k_L = 0$ (ie. a hinge at the left end) and increases monotonically with 'k_L' to reach a value of $0.273L$

when $k_L \to \infty$. By considering the general case shown in figure 1.52a, we find that for any beam attached to passive structures on both ends and as the point force moves across the beam, the distance of an inflection point to its nearest end may not exceed one third the length of the beam (*ie.* $\approx 0.333L$). This limit case occurs for the hinged-fixed or fixed-hinged case when the point force approaches the hinged end. In terms of lower limit, the distance of an inflection point to its nearest end may be zero when the nearest end is a hinge. These two limits may be summarized by saying that the location of inflection points must always be outside the middle third of the beam.

The location of an inflection point divided by the length of the beam (*ie.* normalized location) depends only on the spring stiffness factors 'k_L' and 'k_R' and on the location of the point force (see figure 1.53). To get some insight, we draw contour plots of the location of the left inflection point versus the stiffness factors for various values of the coordinate 'x_F' (origin at left end) of the point force (see figures 1.54). We notice that the location of an inflection point is rather insensitive to the stiffness factor on the right (*ie.* 'k_R'). Therefore, we consider obtaining a simple expression for the location of the inflection points as a function of the stiffness factor near the end that it occurs multiplied by a function that only depends on the location of the point force 'x_F.' This reduces the dependence of the location of an inflection point from three to two parameters at the expense of using an approximate expression. This approximate expression will be presented and discussed next.

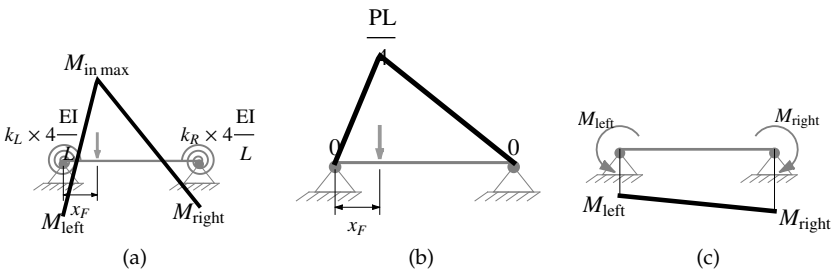**Figure 1.53.** Superposition of moment diagrams for a beam with a point force.

Relatively simple expressions for the approximate locations of the inflection points for the beam shown in figure 1.52b are as follows:

$$x_{I\,\text{Left}}/L \approx \frac{3k_L}{2+4k_L} \times \frac{\hat{x}_F}{1+\hat{x}_F} \tag{1.6a}$$

$$1 - x_{I\,\text{Right}}/L \approx \frac{3k_R}{2+4k_R} \times \frac{(1-\hat{x}_F)}{1+(1-\hat{x}_F)} \tag{1.6b}$$

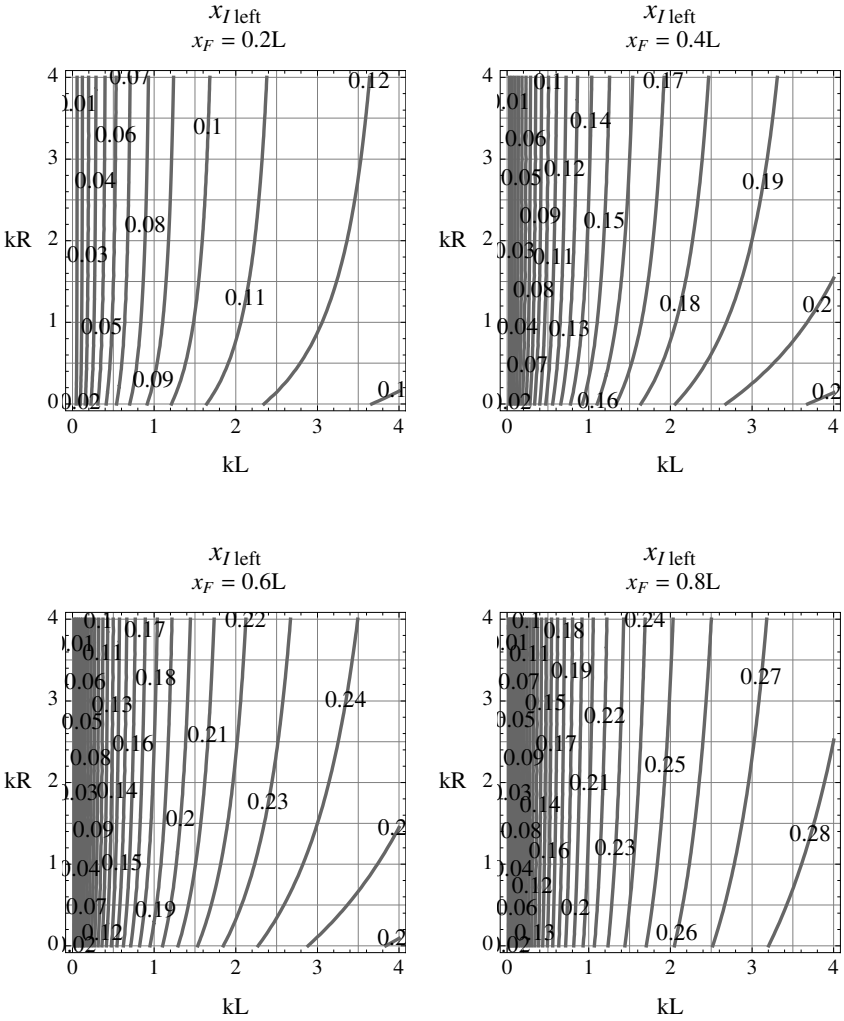**Figure 1.54.** Contour plot of the location of the inflection point versus end stiffnesses for various locations of the point force.

where:

$x_{I\,Left}$, $x_{I\,Right}$, k_L, k_R and x_F are illustrated in figures 1.52a and b.

L is the length of the beam

$\hat{x}_F = x_F/L$, which is the normalized coordinate of the point force

P is the magnitude of the point force

Inflection point: Exact vs approximate
$k_R = \{0, 0.25, 0.5, 1, 2, 4, \infty\}$
$x_F = \{0.1, 0.2, 0.3, 0.4, 0.5, 0.6, 0.7, 0.8, 0.9\}$
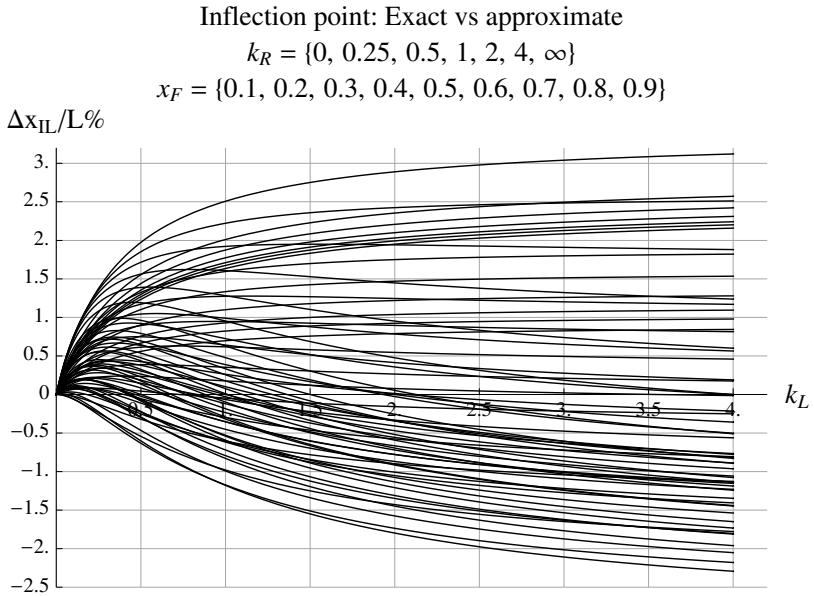

Figure 1.55. Comparsion of inflection point location between exact and approximate.

The results of the approximate expression 1.6a for the location of the left inflection point may be compared with the exact one and this is shown in figure 1.55. In that figure, each possible pairs of values of k_R and x_F where k_R is selected from the first list and x_F is selected from the second list generate one curve. All these curves lie between -2.5% and 3.5%. If we do an optimization to determine the maximum possible difference between the approximate and the exact value for all values of stiffness factors and for all locations of the point force, we get that the maximum error is between about -3.0% and 4.1% and occur for the cases of fixed-hinged with the location of the point force at $x_F = 0.302$ and of fixed-fixed with the location of the point force $x_F \to 1$. Note that this is a percentage error which is relative to the length of the beam while the relative error relative to the location would be higher because we are dealing with small numbers. For the purposes of sketching and obtaining the bending moment diagram, it is the error relative to the length that is relevant. For example, when we are indicating the location of the inflection point on a sketch of the beam, the visual perception will be relative to the length of the beam. In that regards, $\pm 4\%$ would be barely discernible. Moreover, in a manual sketch small features will be perceived

relative to the length of the beam and, in particular, the error in a manual indication of the inflection points may exceed an error of $\pm 4\%$ relative to the length.

The second point to be addressed in relation to sketching is to give guidelines on how to sketch the relative rotations at the ends of a uniformly loaded beam. We note that we want to be consistent but not much precise in this matter because we only want to do a 'rough' manual sketch of the deformations. Unlike the location of the inflection points, the effect of end rotations do not enter into the calculations of the approximate bending moment diagram which is the basis for design. The first obvious comment related to end rotations is that the rotation at an end decreases as its stiffness factor increases and the rotation increases as the point force gets closer to that end. For example, for symmetric end conditions, the end closer to the point force will have a larger slope while for a central point force, the end with the larger stiffness factor will have a lower slope. To further guide our sketching of end rotations, we consider the relative effects of the location of the point force versus the stiffness factors. The location 'x_F' at which the left and right end rotations are the same is given by $x_F = (1/2) + (k_R - k_L) / (2 (1 + k_L + k_R))$ and is plotted in figure 1.56. For example, figure 1.56 indicates that when $k_L = 2$ and $k_R \approx 1.17$ then $\hat{x}_F \approx 0.4$. In that case, if $\hat{x}_F > 0.4$ then the rotation on the right will be larger while if $\hat{x}_F < 0.4$ then the rotation on the left will be larger. From this result, we recommend that for manual sketches, an awareness of the tradeoff between stiffness and location of a point force should be clear in cases of symmetry but that in other cases the sketch should be mostly guided by the general shape. In addition, the case of a fixed end should always have a zero slope at its end. Finally, if a sketcher wants to show (or show-off) a refined knowledge in this case, then figure 1.56 would be useful.

The third and final point to be addressed in relation to sketching the deformed shape is where to show the maximum displacement so that it is 'roughly' in the right location. For that purpose, we plot the location of the maximum displacement for a wide range of combinations of stiffness factors and location of the point force as shown in figure 1.57a. We notice that this location remains relatively close to the middle. If we optimize the location of the maximum displacement over all values of (positive) stiffness factors, we obtain that the maximum should always occur in the middle third of the beam (*ie.* between about $0.333L$ and $0.667L$). To further guide our sketching of the location of maximum displacement, we consider how the location of the maximum displacement depends on the location of the point force and the stiffness factors. To that end we plot contours where the maximum displacement occurs at the center showing the tradeoff between the stiffness factors and the location of the
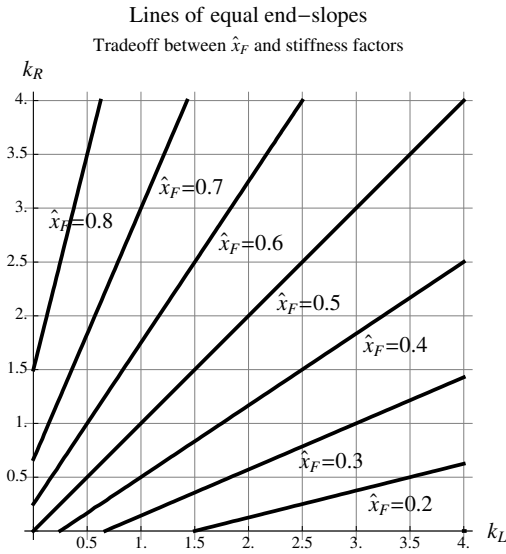
Lines of equal end−slopes

Tradeoff between $\hat{x}_F$ and stiffness factors

Figure 1.56. Values of normalized x_F at which the slopes at the ends are equal for a point force loaded beam.

point force in keeping the location of maximum displacement centered and this is shown in figure 1.57b. Of course, figure 1.57b shows that when the stiffness factors are equal (*ie.* $k_R = k_L$), then the location of the point force must be at the center so that the maximum displacement remains at the center. This result simply means that, for a symmetric configuration, the maximum displacement is at the center. For all cases, the contours shows boundaries such that if the force is to the right of the value indicated for the contour then the location of maximum displacement will be to the right of center and vice versa. From these results, we recommend that for manual sketches, the deformed shape should be mostly guided by the examples shown in this section while making sure that the maximum always occurs in the middle third of the beam. Finally, if a sketcher wants to show (or show-off) a refined knowledge in this case, then figure 1.57b would be useful.

The approximate sketching of the bending moment diagram relies on correctly identifying the location of inflection points. Once the inflection points have been determined, the maximum moment inside the beam and the moments at the ends may be determined by statics. The process of doing this is illustated in figure 1.58. Any point force loaded beam with spring-hinged ends may be viewed as a simply supported
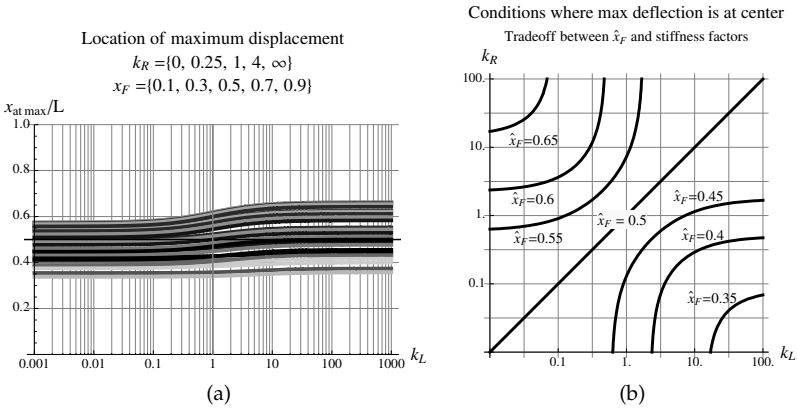
Figure 1.57. Location of the maximum displacement in a point force loaded beam. Notice the logarithmic scale in figure (b).
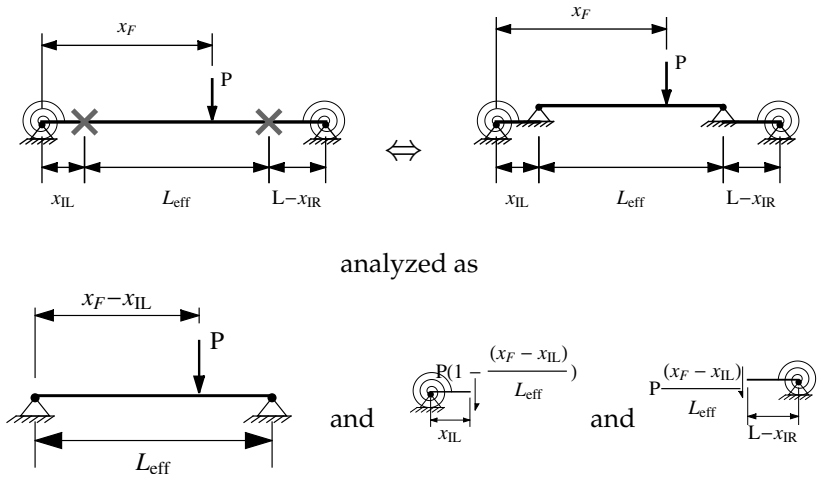

Figure 1.58. Obtaining moment diagram by knowing the location of the inflection points.

beam between the inflection points with two end pieces on the left and right. The reason is that the bending moment at inflection points is zero and therefore these locations may be viewed as having hinged supports on top of the remaining parts of the beam. The simply supported beam and each of the ends may then be simply analyzed to obtain the

maximum internal bending moment and the end moments while know-
ing that the maximum positive moment occurs at the location of the
point force. Referring to the notation shown in figure 1.58, the expres-
sions for the maximum positive moment and the end moments are then
given by:

$$
\begin{aligned}
M_{\text{in max}} &= \frac{P\left(x_F - x_{\text{IL}}\right)\left(L_{\text{eff}} - \left(x_F - x_{\text{IL}}\right)\right)}{L_{\text{eff}}} \\
&= \frac{P\left(x_F - x_{\text{IL}}\right)\left(x_{\text{IR}} - x_F\right)}{L_{\text{eff}}} \\
&= \hat{d}_{F\text{eff right}}\,\hat{d}_{F\text{eff left}}\,P L_{\text{eff}}
\end{aligned}
\tag{1.7a}
$$

$$
M_{\text{left}} = -\frac{P\left(x_{\text{IR}} - x_F\right) x_{\text{IL}}}{L_{\text{eff}}} = -\,\hat{d}_{F\text{eff right}}\,P x_{\text{IL}}
\tag{1.7b}
$$

$$
M_{\text{right}} = -\frac{P\left(x_F - x_{\text{IL}}\right)\left(L - x_{\text{IR}}\right)}{L_{\text{eff}}} = -\hat{d}_{F\text{eff left}}\,P\left(L - x_{\text{IR}}\right)
\tag{1.7c}
$$

where $M_{\text{in max}}$, M_{left} and M_{right} are the bending moments shown in
figure 1.53

P is the magnitude of the point force

L is the length of the beam

L_{eff} is the effective length of the beam which is illustrated in figure 1.58

$x_{\text{IL}}, x_{\text{IR}}$ are the left and right coordinates of the inflection points

x_F is the coordinate of the point force

$d_{F\text{eff right}} = x_{\text{IR}} - x_F$ is the distance from the point force to the right
inflection point

$d_{F\text{eff left}} = x_F - x_{\text{IL}}$ is the distance from the point force to the left in-
flection point

$\hat{d}_{F\text{eff right}} = d_{F\text{eff right}}/L_{\text{eff}}$ and $\hat{d}_{F\text{eff left}} = d_{F\text{eff left}}/L_{\text{eff}}$

Finally, using these critical values of the bending moment, we can
construct the bending moment diagram. This diagram must be two
straight line segments of different slopes meeting at the location of the
point force as in figure 1.52c. The reason is that the second derivative of
the bending moment which equals the distributed load is zero since there
is no distributed load to the left or to the right of the point force. This sec-
ond derivative is, from elementary mechanics, equal to the bending mo-
ment. Also, at the point force, the bending moment must be continuous

but has a discontinuity in slope equal to the discontinuity of the internal shear force. This discontinuity in shear, from equilibrium, must equal the magnitude of the point force. Finally, the straight line segments must pass through zero at the inflection points. Therefore, in a manual sketch, we choose a representative value for the maximum positive moment and draw straight lines going down to the left and right and passing through the corresponding left and right inflection points. We then mark the values of the maximum positive moment and the moments at each end as in figure 1.52c.

Of course, the errors in the calculated bending moments are related to the errors in the approximate locations of the inflection points. If we use formula 1.6a and 1.6b to estimate the location of inflection points and we plot the relative error at the left end (right is analogous) and at the inner maximum bending moment then we get the results shown in figures 1.59 and 1.60 respectively. Note that those percent errors are relative to the exact moments. For the left end moment (right end is
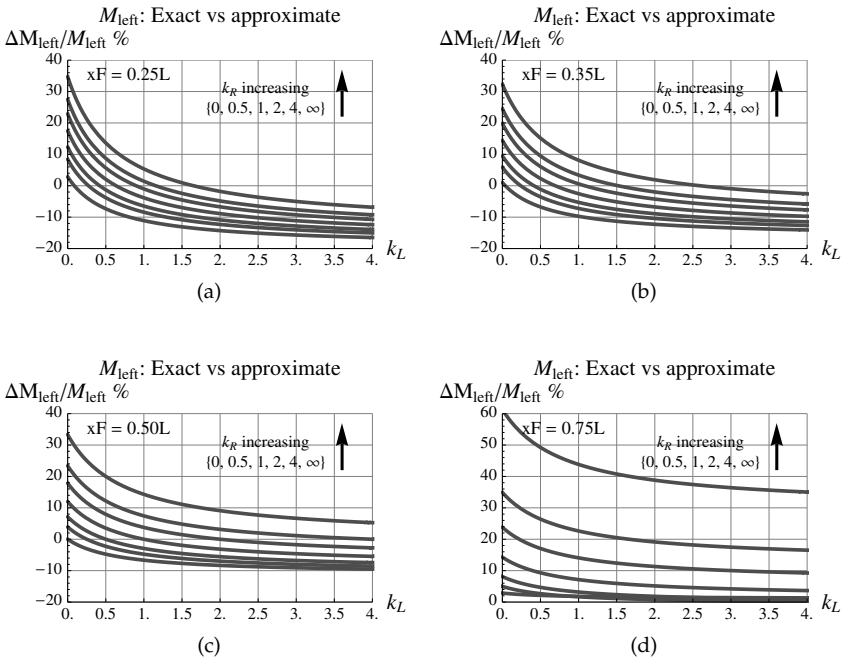

Figure 1.59. Error between left end bending moments obtained from exact versus approximate location of inflection points.
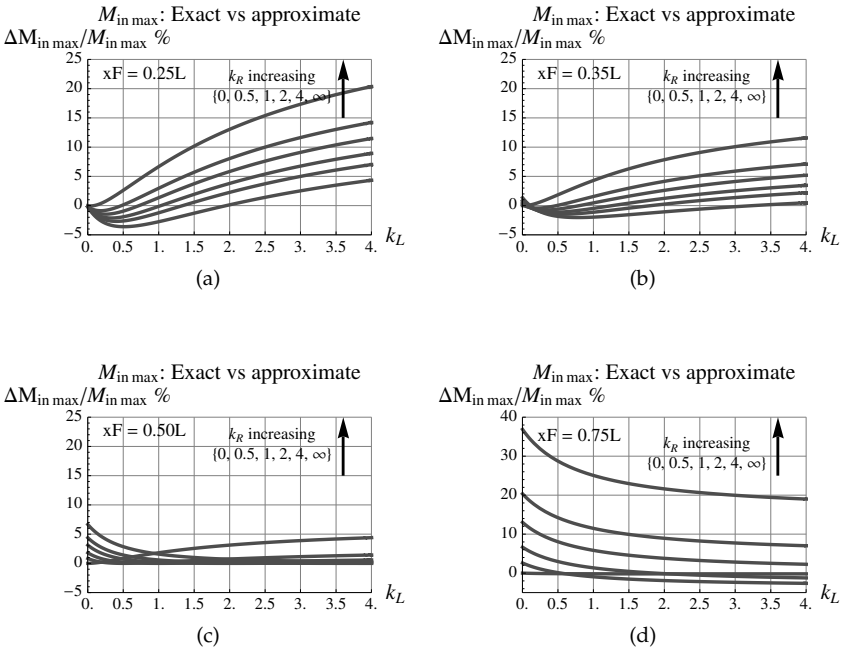
Figure 1.60. Error between maximum positive bending moments obtained from exact versus approximate location of inflection points.

equivalent), we can obtain bounds on the relative error by optimizing the relative difference between the approximate and exact results. By doing this, we find that if the approximately calculated end moment is greater or equal than $0.2PL/4$, for any stiffness factors at the ends and any location of the point force then the relative error is between -23.5% which occurs when $k_L \to \infty$, $k_R = 0$ and $x_F \approx 0.073L$ and 39.7% which occurs when $k_L \to \infty$, $k_R \to \infty$ and $x_F \approx 0.787L$. These relative errors decrease as the end moment gets larger or as the maximum stiffness factors at either end decreases. For example, if the stiffness factors at either end is less than 4 and the calculated approximate moment is greater or equal than $0.1PL/4$ (half the previous value) then the relative error is between -20.3% and 38.0%. Finally, the absolute error in the end moments is always between $-0.05PL/4$ which occurs when $k_L \to \infty$, $k_R \to \infty$ and $x_F \approx 0.785L$ and $0.12PL/4$ which occurs when $k_L \to \infty$, $k_R = 0$ and $x_F \approx 0.284L$.

For the inner maximum positive moment, by optimizing the difference between the approximate and exact results, we find that if the point force remains within the middle half (*ie.* between $0.25L$ and $0.75L$)

then the relative error is between -3.60% which occurs when $k_L \to \infty$, $k_R \approx 0.510L$ and $x_F = 0.75L$ and 36.9% which occurs when $k_L \to \infty$, $k_R = 0$ and $x_F = 0.25L$. The absolute error in the maximum positive moment is always (*ie.* for any stiffness factors and any location of the point force) between $-0.02PL/4$ and $0.1PL/4$.

Finally, we note that a more extensive inspection of the errors shows that for most cases, the actual relative errors are usually much less than the bounds given above. Figures 1.59 and 1.60 show that we can expect good accuracy within about $\pm10\%$ for a wide range of values of stiffness factors and point force locations and that the worst errors occur when either end has high stiffness or when we get too close to an end. In any case, the bounds for both the end moments and the maximum positive moments show that this approximate analysis gives sufficient accuracy for preliminary design or to check the output of computer calculations.

Based on the above discussions, we can sketch the moment diagram as two straight line segments meeting at the location of the point force and having a maximum positive moment at that location. The straight line segments must pass through zero at the location of the inflection points on either side. Finally, we annotate the plots by showing the values of the maximum positive moment and the values of the negative moments at the ends. Both the inflection points and the bending moments may be approximately calculated using the formulas presented.

One additional general point of interest related to the bending moment diagram is the following. If we are given a beam attached to passive structures on both ends as in figure 1.52, then where must we place the point force in order to maximize either the postive or the negative bending moment? Those locations of the point force would be the ones most critical in designing the beam. We will start by considering the critical location of the point force that gives the largest positive moment. In that case, figure 1.61 shows contours of the normalized critical locations. We start by noting that the largest positive moment always occurs at the location of the point force. Furthermore, the largest positive moment will always occur when the point force is closer to the more flexible side which is the one with the lower rotary stiffness factor. If both sides have the same stiffness then the critical location of the point force is at the center. Based on an optimization analysis of the critical location of the point force, we find that the smallest distance of the point force from the flexible support for all cases of passive supports is about $0.366L$. That smallest distance corresponds to the case of a hinge at the flexible side and a fixed end at the other. Therefore, to estimate the largest positive moment on a beam with passive supports, we must place the point force at a distance somewhere between $0.366L$ and $0.5L$ from the more flexible support. The simplest strategy is to place the point force at the
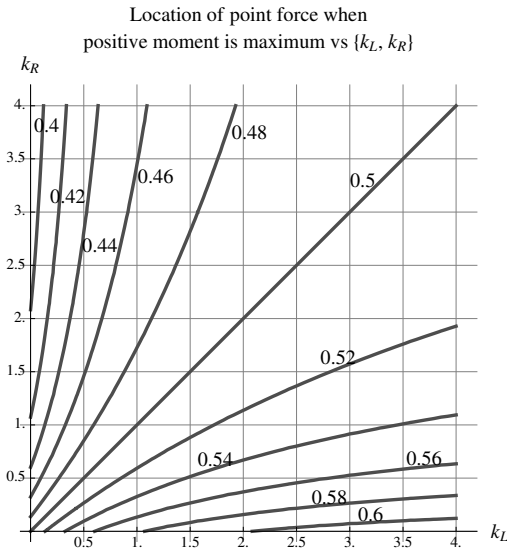
Figure 1.61. Contours of the normalized distance of a point force from the left end when the positive moment is maximum for fixed stiffness factors.

center when the supports are symmetric and at $0.43L$ (*ie.* midway between $0.366L$ and $0.5L$) from the flexible support otherwise. This simple strategy guarantees that the estimated critical location is within about $\pm 7\%$ the length of the beam from the exact critical location and that the corresponding maximum positive moment is always within about 4% of the exact one.

We now consider the largest negative moment for a moveable point force acting on a beam with specified passive supports. In that case, the largest possible negative moment will always occur at the stiffer support. Based on an optimization analysis of the critical location of the point force, we find that the point force must always be at a distance of between $0.333L$ to $0.423L$ from the stiffer support. Surprisingly, while the stiffness factor at an end affects the magnitude of the negative moment at that end, the location of the point force at which the largest negative moment occurs at that end (whether it is the overall maximum or not) is unaffected by its own stiffness factor. That critical location only depends on the stiffness factor of the opposing end. Therefore, we can plot the critical location of the point force that gives the largest negative moment at the left end as a function of the stiffness factor at the right end as shown in figure 1.62. As noted, the distance of the critical location of
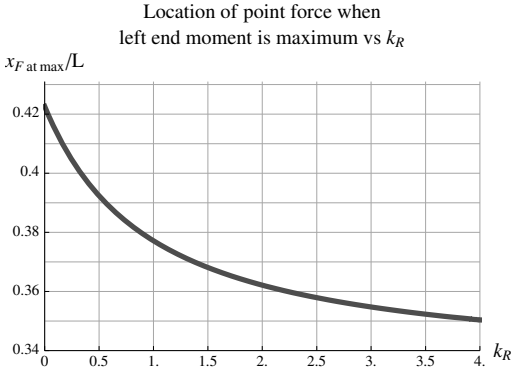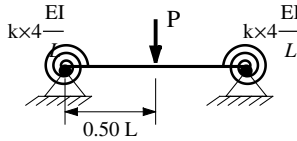
Location of point force when
left end moment is maximum vs k_R

$x_{F\,at\,max}/L$

Figure 1.62. Location of a point force when the left end negative moment is maximum as a function of the right-end stiffness factor.

the point force is always between $0.333L$ to $0.423L$. Based on figure 1.62, we also note that the distance between the critical location of a point force and the stiffer end decreases as the stiffness factor of the far end increases. The limits of $0.333L$ and $0.423L$ occur when the more flexible support is either a fixed end or a hinge respectively. Based on this discussion, we suggest that the simplest strategy to estimate the critical location of the point force is to always place the point force at a distance of $0.38L$ (*ie.* about midway between $0.333L$ and $0.423L$) from the stiffer support. This simple strategy guarantees that the estimated critical location is always within about $\pm 5\%$ the length of the beam from the exact critical location and that the corresponding maximum negative moment is always within about 1.5% of the exact one. Of course, when one of the supports is a hinge, we could choose to place the point force at the exact critical distance of about $0.423L$ from the other end.

To gain further insight with sketching the deformation and bending moment diagrams, we present and discuss a range of results for the point force loaded beam. We begin by considering the case of symmetry where the passive structures at both ends provide about the same resistance to deformations. This is indicated by having $k_L = k_R = k$ in tables 1.5 and 1.6. We start with the centrally loaded case of figure 1.5. Some interesting values of the stiffness factor 'k' include:
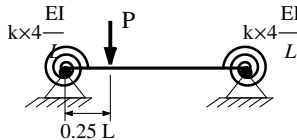
i) $k = 0$ (simply supported): This gives the largest possible positive moment for a point force loaded beam attached to passive structures at both ends.

Table 1.5. Point Force Loaded Beam: Symmetric Spring Resistance ($x_F = 0.5L$).

k	x_{Infl}/L at left	$1 - x_{Inf}/L$ at right	$-M_{left}/\frac{PL}{4}$	$-M_{right}/\frac{PL}{4}$	$M_{in\,max}/\frac{PL}{4}$
0.000	0.000	0.000	0.000	0.000	1.000
0.500	0.125	0.125	0.250	0.250	0.750
0.750	0.150	0.150	0.300	0.300	0.700
1.000	0.167	0.167	0.333	0.333	0.667
1.500	0.188	0.188	0.375	0.375	0.625
2.000	0.200	0.200	0.400	0.400	0.600
3.000	0.214	0.214	0.429	0.429	0.571
4.000	0.222	0.222	0.444	0.444	0.556
∞	0.250	0.250	0.500	0.500	0.500

Table 1.6. Point Force Loaded Beam: Symmetric Spring Resistance ($x_F = 0.25L$).

k	x_{Infl}/L at left	$1 - x_{Inf}/L$ at right	$-M_{left}/\frac{PL}{4}$	$-M_{right}/\frac{PL}{4}$	$M_{in\,max}/\frac{PL}{4}$
0.000	0.000	0.000	0.000	0.000	0.750
0.500	0.076	0.155	0.234	0.141	0.539
0.750	0.092	0.186	0.288	0.163	0.494
1.000	0.103	0.206	0.325	0.175	0.463
1.500	0.118	0.231	0.375	0.188	0.422
2.000	0.127	0.245	0.407	0.193	0.396
3.000	0.137	0.262	0.446	0.196	0.366
4.000	0.144	0.271	0.470	0.197	0.348
∞	0.167	0.300	0.563	0.188	0.281

ii) $k \to \infty$ (fixed-fixed): The negative moments at the ends are equal to the positive one at the middle. If we minimize the maximum absolute value of bending moments in a central point force loaded beam for any beam attached to passive supports and loaded with a point force in the middle then we get this case. For a material whose yield in tension is the same as in compression (*eg.* steel), this constitutes the end supports that would allow the largest central point force to be supported before

failure. Also, for this fixed-fixed case, the inflection points are the far-thest into the beam of any centrally loaded symmetric case and occur at a distance of 0.25L from each end.

iii) $k = 1$: This is the value we would use to approximate any non-terminal span (*ie*. not occuring at either end) of a continuous beam of equal spans. In this case, the internal maximum moment is about 0.67 that of the simply supported case and the negative moments at the ends are about 0.33. Also, inflection points are at a distance of about $0.17L$ from the ends.

Next we consider the symmetric case but the point force is at $0.25L$ from the left end (table 1.6). Some interesting values of the stiffness factor 'k' include:

i) $k = 0$ (simply supported): The maximum positive moment is $0.75PL/4$.

ii) $k \to \infty$ (fixed-fixed): The inflection points are at $0.167L$ and $0.3L$ from the left and right ends respectively. The maximum positive moment is $0.281PL/4$ while the negative end moments are $0.563PL/4$ and $0.188PL/4$. The negative moment at the left end is the largest value for any symmetric case when the load location is at $0.25L$. However, the maximum negative moment at the right has the largest value when $k \approx 3.95$ and has a value $0.197PL/4$.

iii) $k = 1$: This is the value we would use to approximate any non-terminal span (*ie*. not occuring at either end) of a continuous beam of equal spans. In this case, the internal maximum moment is about $0.463PL/4$ while the negative end moments are $0.325PL/4$ and $0.175PL/4$. Also, inflection points are at a distance of about $0.103L$ and $0.206L$ from the left and right ends respectively.

Three examples of symmetric cases for the exact deformations and exact bending moment diagrams are shown in figures 1.63 and 1.64 re-spectively. We note that the negative curvature part of the deformation is barely discernible and thus the importance of indicating (*eg*. with an '×') the location of the inflection points. Note that the there are always two inflection points, one to the left and one to the right of the location of the point force and that is true no matter how close the point force ap-proaches an end as long as that end has positive resistance (*ie*. anything other than a hinge). Aside from the magnitude of the deformations and the location of the inflection points, the deformation shapes for the sym-metric cases are about the same over a wide range of stiffness factors except for a slight but visible increase in the negative curvature parts at
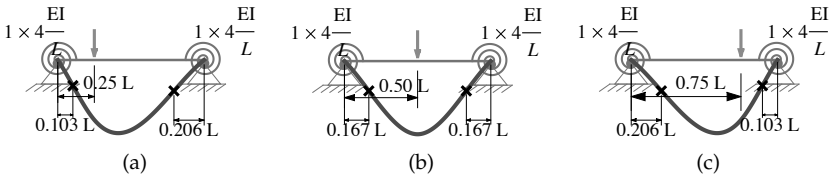
Figure 1.63. Deformed shape of selected cases of unifomly loaded beam with symmetric supports.
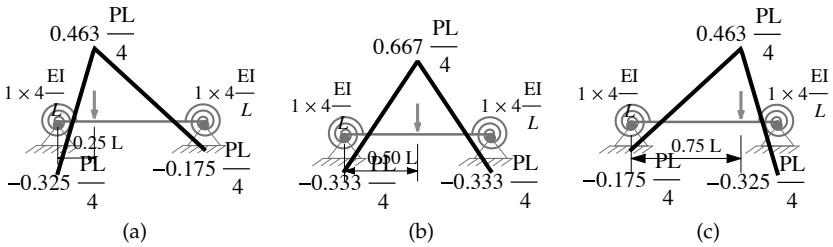

Figure 1.64. Moment diagrams of selected cases of uniformly loaded beam with symmetric supports.

each end. They all look somewhat like parabolas with a short slightly negative curvature parts at each end. As the point force moves closer to one or the other end, we get an asymmetry that shifts the maximum displacement slightly towards the side of the point force as seen in figures 1.63a and c. However, as noted in the discussions on the location of the maximum displacement, this remains relatively close to the middle and, in general, does not coincide with the location of the point force.

The moment diagrams shown in figure 1.64 all have the same shape that is tilted left or right so that the maximum positive moment always occurs under the point force. The moment diagrams for the point force is easier to draw than the one for a uniform load because it always consists of two straight line segments meeting at the location of the point force and passing through the inflection points on either side.

In comparison with the symmetric resistance case, we present three cases where the ends have unequal stiffness factors but neither end is a hinge or a fixed end (see figures 1.65). From figures 1.65, we notice that, aside from the location of inflection points, the shapes are still similar to those of the symmetric cases except for a slightly more noticeable negative curvature at the stiffer end. In particular, in manual sketches, they would be appear almost the same. Therefore, we only need to learn how to manually sketch one prototypical shape where neither end is a hinge
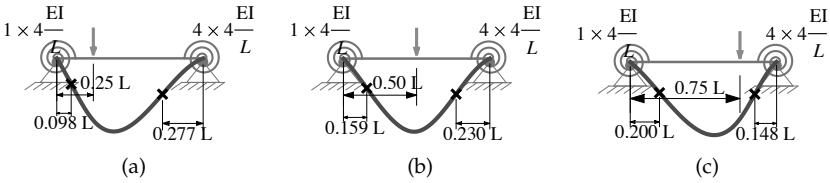
Figure 1.65. Deformed shape of selected cases of point force loaded beam with non-symmetric supports.

or a fixed end. The effect of the point force in the non-symmetric case is similar to that of the symmetric case with figures 1.65a and c being typical.

The bending moment diagrams (figures 1.66) for the unsymmetric case are similar to those of the symmetric ones. As with the symmetric case, the maximum positive moment is always at the location of the point force. The procedure for manually sketching the moment diagrams of the non-symmetric cases is identical to that of the symmetric ones.
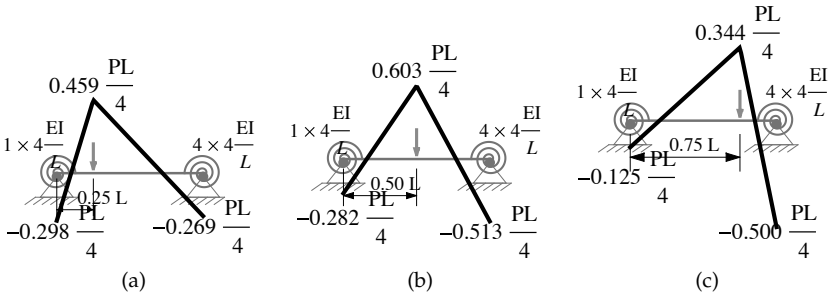
Figure 1.66. Moment diagrams of selected cases of point force loaded beam with non-symmetric supports.

The special case when one end is a hinge is next considered and the deformations and bending moment diagrams are shown in figures 1.67 and 1.68 respectively. Aside from having no inflection point on the side of the free hinge, the shapes, if manually sketched would appear similar to the cases discussed above. For that reason, we will place a small '×' at the hinge in that case to distinguish it from the other cases. Note that in figures 1.67, the location of the right inflection point only varies from about $0.11L$ to $0.21L$ as the point force moves from a distance of $0.25L$ to $0.75L$ from the right support. As discussed previously, the inflection point remains close to its nearest end and can never exceed a distance of about $0.333L$ from its nearest end even if the point force is almost at the opposite end (*ie.* in figures 1.67, this would be almost at the left end).
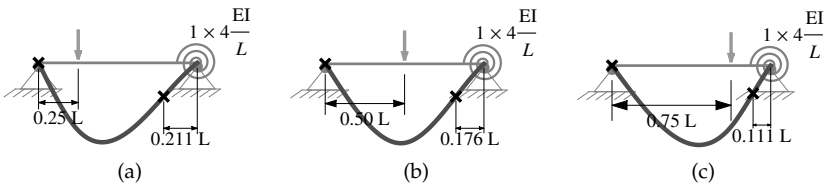
Figure 1.67. Deformed shape of selected cases of point force loaded beam with hinge-spring supports.

We show the bending moment diagrams of figures 1.67 in figures 1.68. These figures indicate that the special case of one end being a hinge can only be distinguished from other cases by having a zero moment at the hinged end. The rest of the procedure for sketching the moment diagram remains the same as seen in figures 1.68.
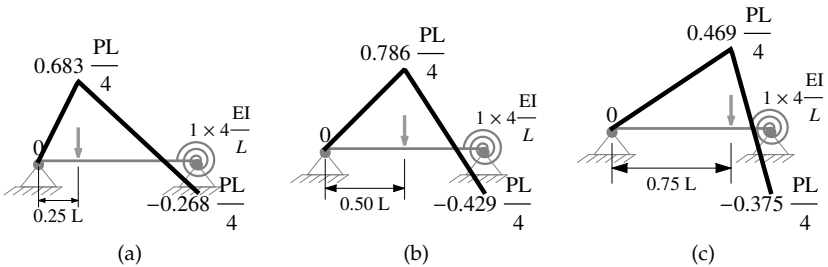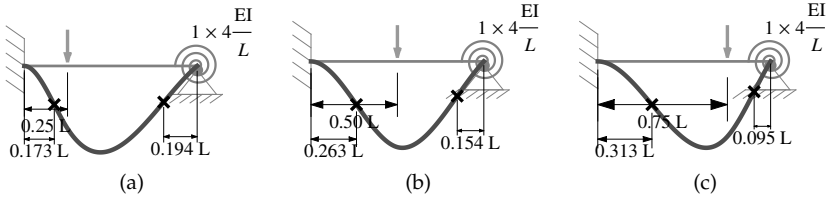

Figure 1.68. Moment diagrams of selected cases of point force loaded beam with hinge-spring supports.

The special case when one end is fixed is next considered and the deformations and bending moment diagrams are shown in figures 1.69 and 1.70 respectively. Aside from having zero slope and a more noticeable negative curvature near the fixed end, the shapes, if manually sketched would appear similar to the cases discussed above. Note that again in figures 1.69, the location of either inflection point varies within a relatively narrow range as the point force moves from a distance of $0.25L$ to $0.75L$ from the either support. As discussed previously, the inflection point remains close to its nearest end and can never exceed a distance of about $0.333L$ from its nearest end even if the point force is almost at the opposite end.

Figure 1.69. Deformed shape of selected cases of point force loaded beam with fixed-spring supports.
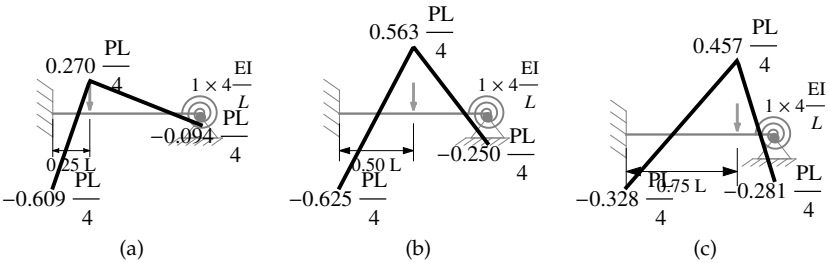

Figure 1.70. Moment diagrams of selected cases of point force loaded beam with fixed-spring supports.

Concerning the bending moment diagrams of figures 1.69 shown in figures 1.70, the special case of one end being fixed is similar to the general unsymmetric cases discussed in figures. Therefore, these cases can be sketched in a manner similar to the previous cases.

1.9   Example: Point Force

As an example of applying the methods related to the point force, we consider the structure shown in figure 1.71. We have only one member loaded by a point force load of magnitude one and located at 1.75 units from point C with all the members having length 5 units and the same moment of inertia 'EI.'

As a first step, we decompose the structure into components (figure 1.72). We start with member CD (figure 1.72c). The stiffness factor on the right is exactly 2 because the resistance on that side is provided by two similar members that are fixed on the far end. The stiffness factor on the left is somewhere between 0.75 and 1 (exactly about 0.86), but, for simplicity, we take it to be equal to 1. Using formulas 1.6, we calculate the approximate location of the inflection points, sketch the
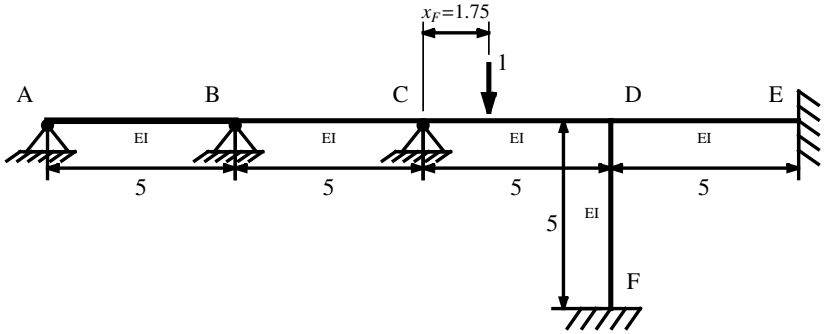
Figure 1.71. Example of a structure with no sidesway and one member point force loaded.
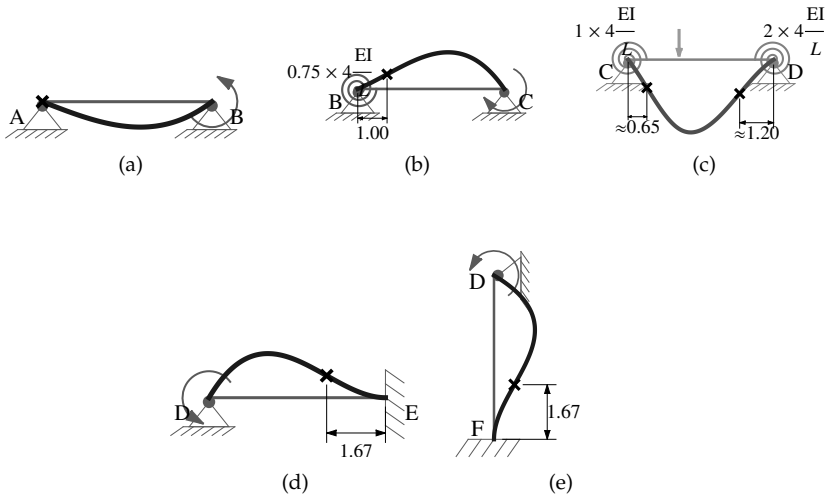

Figure 1.72. Decomposition of structure shown in figure 1.71 with deformed shapes.

deformed shape and indicate the approximate location of the inflection points with '×.' Next we turn to the members left of member CD (figures 1.72b then 1.72a). These are handled using the techniques discussed for a member loaded with an end moment and connected to a passive structure at the other end. Finally, we consider the members to the right of member CD and again they are handled similar to those of the members to the left.
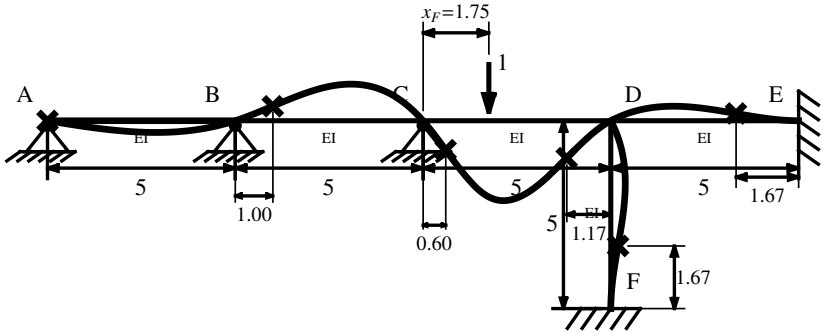
Figure 1.73. Exact shape of the deformed structure of figure 1.71.

If we compare the approximate and exact locations (figure 1.73) of inflection points we find good agreement. The largest error occurs at the inflection point in member CD near node C (0.9% of the beam length) and we attribute this error more to the approximate estimation of the stiffness factor at C where we used a round number of 1 instead of some number between 0.75 and 1 (*eg.* the mean 0.88). If we had used a stiffness factor at C of 0.88 then the error would have been about 0.3% of the beam's length.

Having obtained the approximate location of the inflection points, we then get the bending moments for the point force loaded beam using formulas 1.7 and for the end-moment loaded beams using formulas 1.1. The results are shown in figure 1.74. We note the care in passing the location of zero bending moment through the inflection points in each of the members.

If we compare the approximate and exact values (figure 1.75) of maximum and minimum bending moments, we again find good agreement. The largest error again occurs at node C. We note that the relative error in the maximum positive and negative moments at the left and right ends which occur in member CD are only about 2.7%, -10.3% and 2.4% respectively.

Finally, we note that there is no need to sketch each of the members separately as shown in figures 1.72 and 1.74. We simply first sketch the deformed shape while being aware of the process implied by figure 1.72 and then do the same (on a separate sketch) for the bending moment diagram. With practice, this process becomes quick so that we only need one or two minutes (with the aid of a calculator) to sketch an approximate deformed shape and bending moment diagram for figure 1.71 which
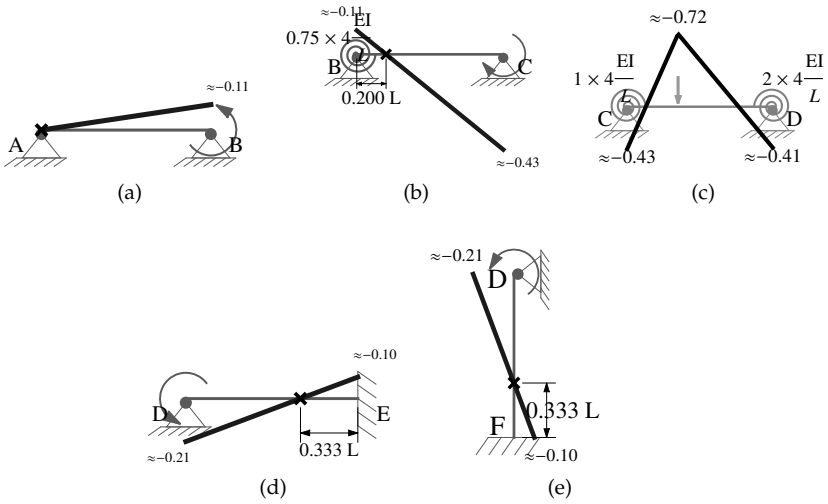
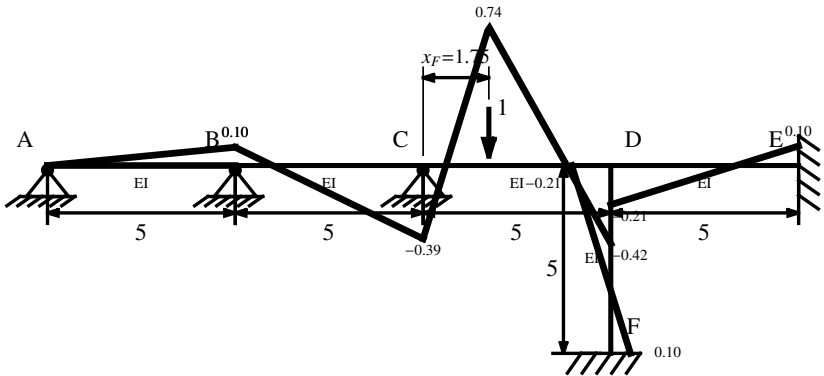**Figure 1.74.** Decomposition of structure shown in figure 1.71 with moment diagrams.

Figure 1.75. Exact shape of the moment diagram of figure 1.71.

include approximate values for inflection points and bending moments that are indicated on the sketches. This level is relatively quickly attained if the practioner becomes familiar with the results (including numerical values) shown in figures 1.63 to 1.70.

1.10   Comments and Examples on Multiple Loads

If we load a structure so that there is only one loaded member or node, the magnitude of the response of a particular member in the structure decreases rapidly as that member gets farther from the loaded member or node (see figure 1.13 and related discussion). The influence of the load is highest on the loaded member or node, then on the members directly attached to either end of the loaded member or node then on the members directly attached to those members and so on. The reason for the rapid decrease is primarily due to the carry over factor for moments which is always less than half and usually around a third; as the member gets farther from the loaded node or member, these carry over factors are multiplied by each other and lead to a geometric type of decrease. The decrease may also be due to the distribution of an applied moment at a node over the attached members. This reduces the applied moment because each connected member gets a fraction of the applied moment; of course, this last effect is not present if we have a continuous beam supported on rollers or hinges.

For linear analysis, we may superpose the response of single loads to obtain the effect of simultaneously applied multiple loads as illustrated in figure 1.77. Because of linear superposition and because of the rapidly decreasing response when we load only a single member or node, the interaction of multiple loads of comparable magnitude is significant only when the loaded members or nodes are separated by at most one member. In other cases, the deformations, bending moments or any response of a member may be approximately evaluated as being only due to the nearest loaded member; members that may happen to be at equal distances from two or more loads will generally have negligible values compared to the other members. Therefore, we will consider only two example cases, one with the loaded members separated by one member and one with the loaded members being adjacent.

Before proceeding with the examples in obtaining the bending moment diagrams, we note the following basic observation in summing moment diagrams:

- The sum of the plots of two straight line segments is a straight line segment. Therefore, when we add two straight line segments, it is sufficient to sum the value at the ends of the segments.

- If we sum a piecewise straight line with a straight line segment, we will obtain a piecewise straight line segment whose discontinuities are at the same locations as the original one. Therefore, it is sufficient to

sum values at each discontinuity point of the original straight line segment.

- If we sum a parabolic segment with a straight line segment, we will obtain a parabolic segment. The location of the maximum of the resulting parabolic segment may be different than the original one. However, for the purpose of approximate analysis, we will assume that the location is about the same. Therefore, it is sufficient to sum the value at the ends of the segments and at the location of the maximum of the original parabolic segment.

If other cases are encountered then it is helpful to sketch the bending moment diagrams of each load case and estimate the location and values of the maxima and minima from those sketches.

We now consider an example of the case of two loaded members separated by one other member as shown in figure 1.76. There is a distributed load whose net force is $1 \times 5 = 5$ units and a point force of 4 units. To obtain the bending moment diagram, we will use superposition as illustrated in figure 1.77. We will obtain the bending moment diagrams for the distributed load and the point force load acting separately and add the separate values at each point to obtain their combined bending moment diagram.
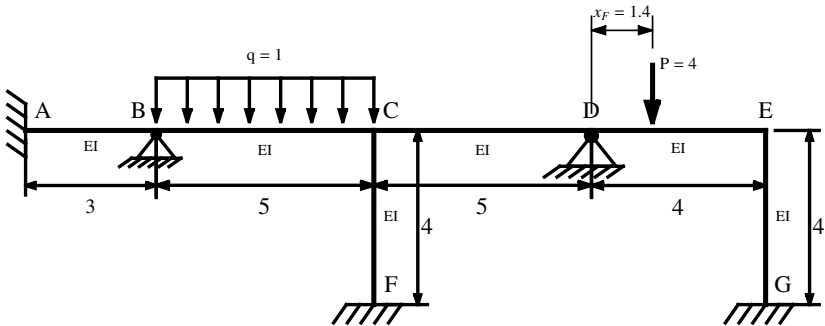

Figure 1.76. Multiple loads of comparable magnitude (total load) separated by one member.

First, we consider the structure loaded only with the distributed load and, to approximately analyze it, we decompose the structure as shown in figure 1.78. We start with member BC (figure 1.78b). The stiffness factor on the left and right are approximately $(EI/3)/(EI/5) \approx 1.67$ and $\approx (EI/4 + EI/5)/(EI/5) = 2.25$ respectively. Using formulas 1.4, we
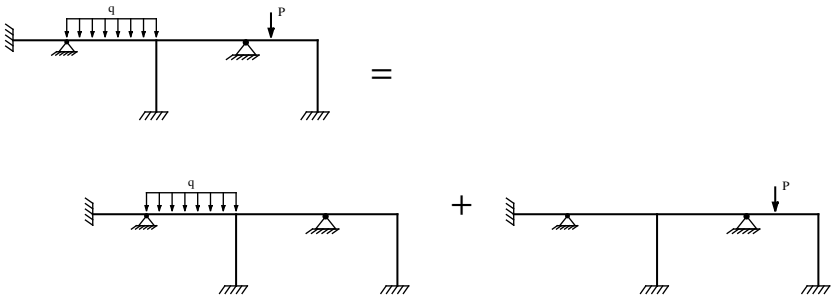
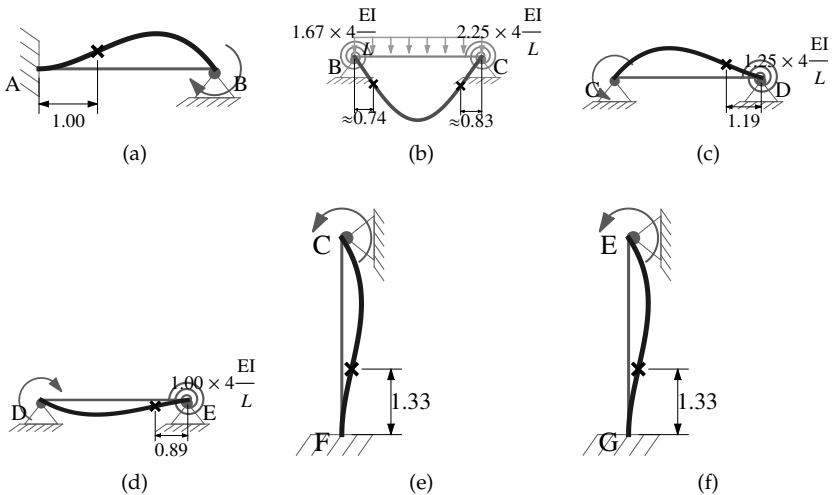**Figure 1.77.** Superposition of multiple loads as the sum of separate single loads.

Figure 1.78. Decomposition of structure shown in figure 1.76 with deformed shapes when we only apply the distributed load.

calculate the approximate location of the inflection points, sketch the deformed shape and indicate the approximate location of the inflection points with '×.' Next we turn to the members to the left (figure 1.78a) and right of member BC (figures 1.78c, d, e and f). These are all handled using the techniques discussed for a member loaded with an end moment and connected to a passive structure at the other end. Note that the approximate location of all inflection points are indicated on the sketch of the deformed structures. After we have obtained the approximate location of the inflection points, we then get the bending moments for the uniformly loaded beam using formulas 1.5 and for the end-moment loaded

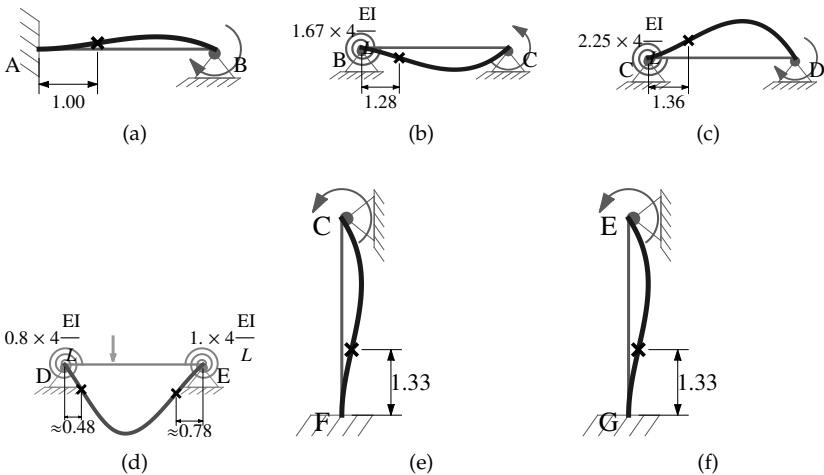beams using formulas 1.1. The corresponding exact results are given in one of the bending moment diagrams shown in the bottom left moment diagram of figure 1.80. For comparison, if we consider the approximate results for member BC then we get the following key values from left to right as -1.55, 1.47 and -1.76 versus -1.56, 1.48 and -1.74 as shown in figure 1.80 bottom left on member BC. This is excellent agreement for an approximate analysis.

Next we consider the structure loaded only with the point force load and, to approximately analyze it, we decompose the structure as shown in figure 1.79. We start with member DE (figure 1.79d). The stiffness factor on the left and right are $\approx (EI/4)/(EI/5) = 0.8$ and $(EI/4)/(EI/4) = 1$ respectively. Using formulas 1.6, we calculate the approximate location of the inflection points, sketch the deformed shape and indicate the approximate location of the inflection points with '×.' Next we turn to the members to the left (figure 1.79a, b, c and e) and right of member DE (figures 1.78f). These are all handled using the techniques discussed for a member loaded with an end moment and connected to a passive structure at the other end. Note that the approximate location of all inflection points are indicated on the sketch of the deformed structures. After we have obtained the approximate location of the inflection points, we then get the bending moments for the uniformly loaded beam using formulas 1.7 and for the end-moment loaded beams using formulas 1.1. The corresponding exact results are given in one of the bending

Figure 1.79. Decomposition of structure shown in figure 1.76 with deformed shapes when we only apply the point force load.
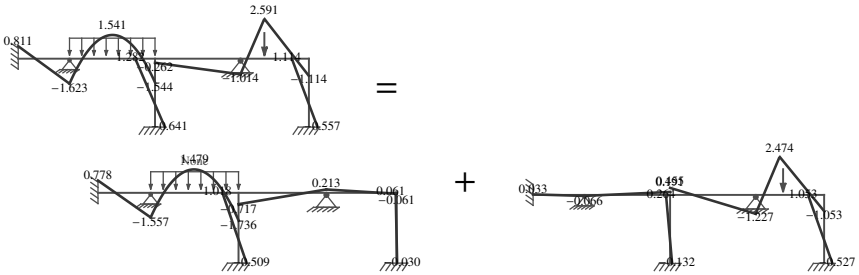
Figure 1.80. Exact shape of the moment diagram of figure 1.76 and when each of the loads is applied separately.

moment diagrams shown in figure 1.80. For comparison, if we consider the approximate results for member DE then we get the following key values from left to right as −1.28, 2.44 and −1.04 versus −1.23, 2.47 and −1.05 as shown in the bottom right moment diagram of figure 1.80 on member DE. This is again excellent agreement for an approximate analysis.

Finally, we take the sum of the bending moment diagrams to get the top moment diagram in figure 1.80. By following the guidelines described above for summing moment diagrams, we get for member BC the following key values from left to right as −1.62, 1.54 and −1.55 versus −1.6, 1.54 and −1.54 as shown in the top moment diagram of figure 1.80 on member BC. The corresponding comparison for member DE is approximately −1.04, 2.54 and −1.11 versus −1.01, 2.59 and −1.14 as shown in the top moment diagram of figure 1.18 on member DE. The combined moment diagram again gives excellent agreement for an approximate analysis.

If we need to sketch the deformed shape for the combined loading of figure 1.76, then we will use the moment diagram (figure 1.80 top moment diagram) as a guide. The location of inflection points may be approximated from visually estimating the location of the zero moments in the bending moment diagram. In particular, since the bending moment in member CD is always negative, it has no inflection points and has a negative curvature that increases to the right. The resulting deformed shape is shown in figure 1.81.

The deformed shape of figure 1.81 represents an example of a structure subject to combined loading where the loaded members are separated by one other member. This deformed shape may vary in character as we change the relative total load of the uniform load versus the point force load. As an illustration of this, we present the deformed shape for
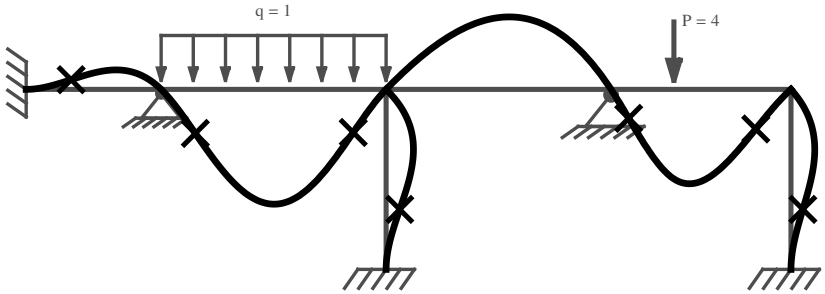
Figure 1.81. Exact deformed shape for the loading of figure 1.76.
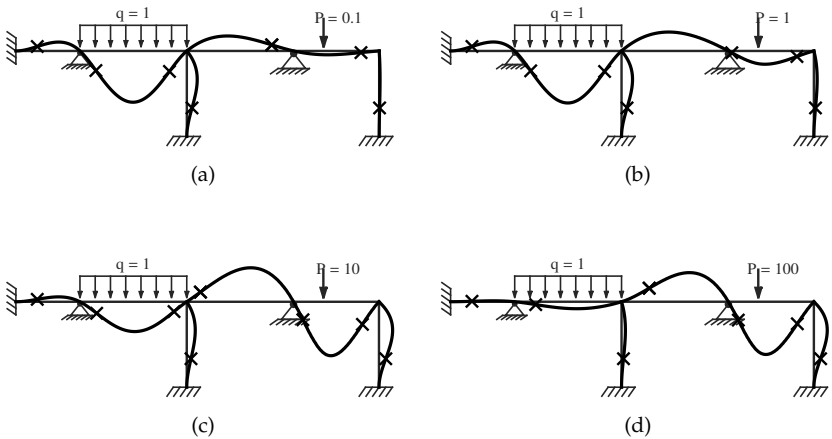

Figure 1.82. Examples of exact deformed shapes for the structure of figure 1.76 but with different magnitudes of the point force load.

four different load cases of the structure shown in figures 1.82. When the magnitude of the point force is relatively small then the distributed load dominates and we get only one inflection point on the member with the point force load and one inflection point in the intermediate member between them (see figure 1.82a). When the point force magnitude becomes comparable to that of the uniform load, we get the case shown in figure 1.82b which is similar to that of figure 1.81. As the point force magnitude increases further, we get an inflection point in the intermediate member between the loaded members as shown in figure 1.82c; this inflection point is closer to the uniform loaded member which is in con-

trast with the case of figure 1.82a. If we further increase the magnitude of the point force then the right side inflection point of the uniformly loaded member will disappear as shown in figure 1.82d.

Having considered the case where there is one member separating the loaded members, we now consider an example of the case of two loaded members that are adjacent as shown in figure 1.83. There is a distributed load whose net force is $1 \times 5 = 5$ units and a variable point force magnitude denoted by P. Since the bending moment diagram may be directly obtained once the inflection point locations have been identified, we will only present the deformed shape including an indication of the location of all inflection points.
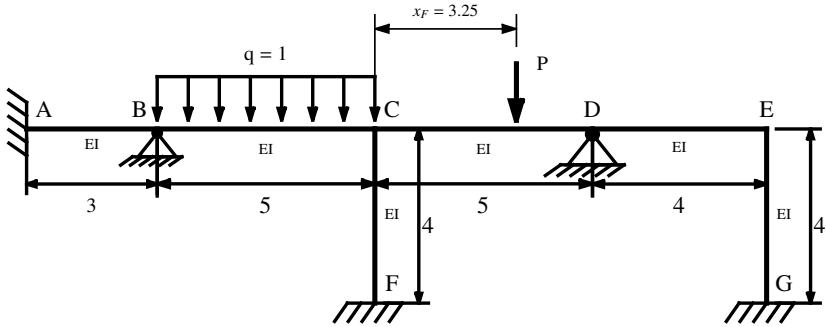
Figure 1.83. An example of multiple loads that are adjacent.

In figures 1.84, we present the deformed shape for four different load cases of the structure shown in figures 1.83. When the magnitude of the point force is relatively small then the distributed load dominates and we get only one inflection point on the member with the point force load as shown in figure 1.84a. In that figure we also note that the member with the point force load moves up counter to the direction of the point force and this occurs because of the overwhelming influence of the neighboring distributed load. When the point force magnitude becomes comparable to that of the uniform load, we get the cases shown in figure 1.84b and c. In both those cases, each of the loaded members have two inflection points but either the uniform load or the point force load have a larger influence as shown in figure 1.84b and figure 1.84c respectively. The load with the greater influence (*ie.* higher bending moment at the common end point) will cause the other member to move up on some portion of its span that is adjacent to the other loaded member. Finally, as the point force magnitude further increases, it will dominate
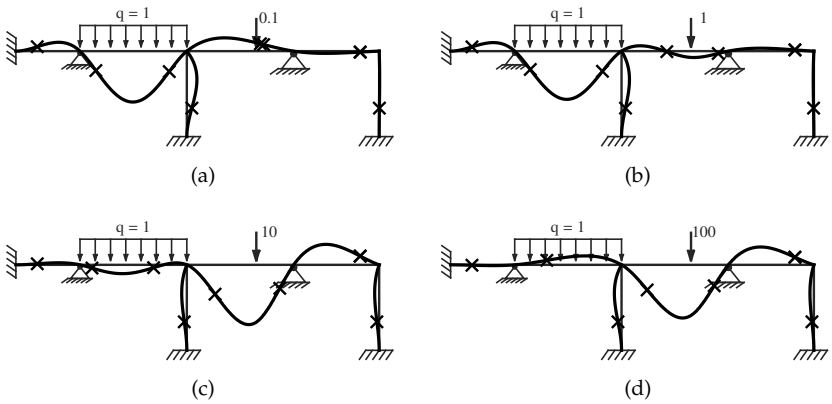
Figure 1.84. Examples of exact deformed shapes for the structure of figure 1.83 with different magnitudes of the point force load.

the uniformly loaded member and we get only one inflection point in that member as shown in figure 1.84d.

Finally, we consider the case of symmetry where both the structure and loading are symmetric relative to a center line as for example shown in figures 1.85 and 1.86. For the purposes of approximate analysis, we note that we only need the conditions of symmetry to apply locally because, as previously discussed, the influence of loading and constraints decreases rapidly with distance. This observation greatly increases the scope of applicability of the case of symmetry. Similar to the general case,
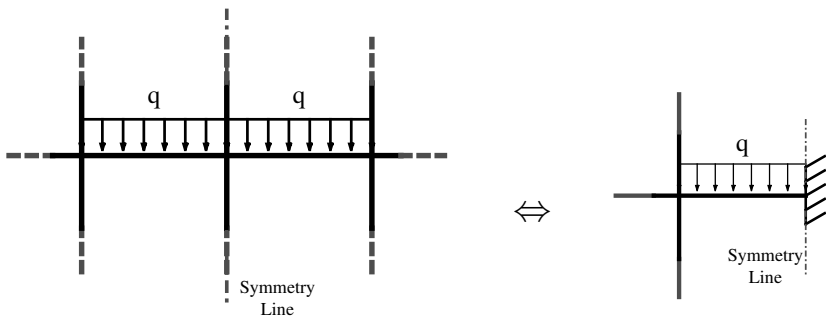
Figure 1.85. Example of a symmetric structure and loading where the members attached to the line of symmetry are loaded.
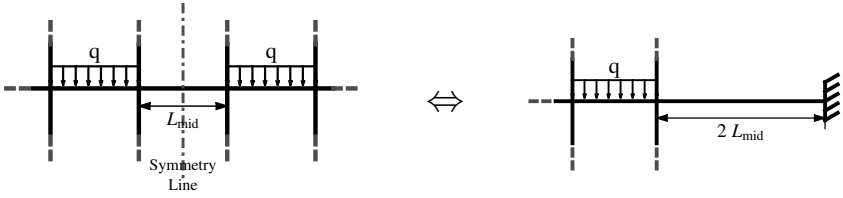
Figure 1.86. Example of a symmetric structure and loading where the centerline passes through a middle unloaded member.

we need only consider cases where the loaded members are either adjacent as in figure 1.85 or separated by one other member as in figure 1.86. Each of these cases will be discussed next.

First we consider the case when the structure is symmetric and the loaded members are adjacent (*eg.* figure 1.85). In that case, the common end cannot rotate right or left otherwise it violates the symmetry of the response which must also be symmetric in linear analysis. Therefore, that common end is equivalent to a fixed end for each side of the symmetric structure as shown in figure 1.85. By analyzing either half of the structure with the fixed end, we can analyze the structure with less effort than otherwise.

Second we consider the cases when the structure is symmetric and the loaded members are separated by one other unloaded member as shown in figure 1.86. In that case, the rotation of the left end of the central member must be equal and opposite to the right end. From elementary analysis, the apparent stiffness of that member relative to either connected half of the structure is equivalent to attaching a similar member but with twice the length and with a fixed support at the far end as shown in figure 1.86. By analyzing either half of the structure with the equivalent member, we can analyze the structure with less effort than otherwise. If the middle member is loaded, we can use superposition to analyze the case without the middle member unloaded and then with only the middle member loaded.

1.11   Beam with Two or More Internal Hinges

In this section, we will discuss the effect of an internal hinge on the analysis of continuous beams or frames. In a figure, an internal hinge is indicated by a hollow circle along the span of a member and corresponds to an internal constraint that requires the bending moment to be zero at that

location. While it is admissible to apply a point force at an internal hinge we must be careful when specifying an applied point or concentrated moment. When applying such a moment, we must specify whether that moment is actually applied on the member to the left or to the right of the internal hinge. In fact, it is admissible to apply two point moments, one to the left and one to the right of the internal hinge and this kind of loading has an important application in the study of influence lines.

We start by considering the case of three or more internal hinges in a bending member. Such members are always statically unstable if we apply any load on their span irrespective of the end conditions or supports. The reason is that a bending member must satisfy two boundary conditions associated with the bending deformations at each end. These conditions may be of the support (*eg.* no rotation), of the loading type (*eg.* applied end moment) or of a combination of both. Two of those boundary conditions must directly or indirectly constrain the rigid body motion of the member. This then leaves only two 'free' equations to satisfy other constraints. With three or more internal hinges, we have more constraints than can be met by a bending member. Therefore, any member with three or more internal hinges may be removed from the structure as being structurally irrelevant.

From the above, we deduce that we only need to consider the case of one or two internal hinges. We start with the case of a bending member with two internal hinges and we wil divide the discussion into two parts: i) when the member is acting as part of a passive structure as shown in figure 1.87 and ii) when the member is attached on both ends to passive structures while being loaded over its span. By considering these two cases, we can then use the methods developed previously to do an approximate analysis for any structure containing one or more members each having two internal hinges.

To study the member having two internal hinges as part of a passive structure, we consider it under the conditions shown in figure 1.87. The figure shows an applied rotation at one end and a rotary spring at
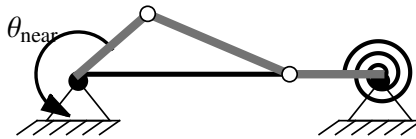

Figure 1.87. A beam with two internal hinges considered as part of a passive structure.

the other. Such a member has zero stiffness at the near end (*ie*. the end where the rotation is applied) and its deformation is indicated by the solid gray line shown in figure 1.87. Each piece of that beam remains rigid during deformation with the first two pieces rotating rigidly while the third piece which is attached to the rotary spring remains immobile. The shear force and the bending moments are uniformly zero across the member and the deformations may be calculated from a pure consideration of kinematics or geometry. These results are true as long as the stiffness of the rotary spring shown in figure 1.87 is nonzero. When it is zero, then the member is statically unstable and kinematically indeterminate. Finally, we note that the deformations indicated in figure 1.87 are appropriate only for small deformations while large deformations are shown in figure 1.87. These large deformations are shown for clarity but the reader must imagine all deformations to be small in order for the small deformations theory of bending of straight members to be applicable.

Based on the above discussion, if a member with two internal hinges is part of a passive structure, then its stiffness contribution at a connection is zero and it cannot transmit a moment across its span. More generally, when a member with two internal hinges is part of a structure and has no load applied on its span then it is structurally irrelevant and may be omitted for the purposes of analysis as illustrated in figure 1.88. For design purposes, a member with two internal hinges may be used to structurally isolate the effects of loading one part of a structure from another.
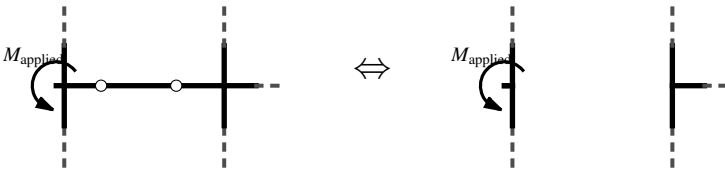

Figure 1.88. A two-hinged beam has zero bending stiffness and cannot transmit a moment across its span.

We now consider the case when a member with two internal hinges is attached on both ends to passive structures while being loaded over its span. Such a member is statically determinate which means that the largest and smallest bending moments within the span and the end moments may be determined from free body diagrams and statics. Once the end moments have been determined, the rest of the passive structure

may be approximately analyzed using the developed procedures. If either end of a beam with two internal hinges is attached to a hinge with no rotary stiffness then the beam is statically unstable and thus structurally irrelevant. Such a beam must be free of any loading and may again be omitted for the purposes of analysis.

The placement of internal hinges in a beam is usually by design but may also be encountered in structural integrity assessments of partially failed structures. If the internal hinges in a beam are to be introduced by design then it is natural to ask where should we place them. The answer depends on the type of loading that is applied on the span. If we consider the case of a uniform load, then the lowest bending moment in absolute value (*ie.* positive or negative) is obtained when the internal hinges are at $\left(2 \pm \sqrt{2}\right) L/4 \approx (0.146, 0.854)L$ and has a value of $qL^2/16$. This optimal placement of the internal hinges is independent of the stiffness of the passive structures attached to the ends of the beam because a beam with two internal hinges is statically determinate. Of course, the passive structures must provide non-zero stiffness at both ends to avoid loading a statically unstable beam. If the beam was without internal hinges then this optimal location of internal hinges correspond to the location of the inflection points when the stiffness factors on the beam at both ends equals 1.5.

If we consider a pont force loading that may occur anywhere on the span, then the lowest bending moment in absolute value in a beam with two internal hinges is obtained when the internal hinges are at $(1/4, 3/4)L$ and has a value of $PL/8$. This optimal placement of the internal hinges is independent of the stiffness of the passive structures attached to the ends of the beam because a beam with two internal hinges is statically determinate. Again, the passive structures must provide non-zero stiffness at both ends to avoid loading a statically unstable beam. If the beam was without internal hinges then this optimal location of internal hinges correspond to the location of the inflection points when the point force is at the middle of the beam and the stiffness factors on the beam at both ends are indefinitely large (*ie.* $k \to \infty$) which correspond to fixed supports.

If we want to avoid the worst placement of two internal hinges in a beam then the following results apply. For uniform loading or for point force loading, the worst conditions in terms of getting the largest possible positive bending moment occurs when we place one internal hinge at the left end and the other at the right end so as to effectively produce a simply supported beam. This produces a maximum positive bending moment of $qL^2/8$ and $PL/4$ for the uniform load and point force load respectively. However, the worst conditions for the largest possible negative bending moment or of the largest poosible absolute value of the

bending moment occurs when we place both internal hinges infinitesimally or very close to each other and infinitesimally or very close to either end of the beam. This produces a maximum negative bending moment of $qL^2/2$ and PL for the uniform load and point force load respectively. These values are four times larger than the corresponding ones for maximum positive moment and they correspond to the values obtained for a cantilever which is a member supported on only one side.

How did the two internal hinges produce an effect equivalent to a cantilever? When two internal hinges occur in a beam, the part of the beam in between the internal hinges acts like a link providing zero vertical stiffness and zero rotary stiffness to either of its attached ends. If we make a very small link of this kind and place it near one end of the beam, then that end will be structurally isolated from the rest of the beam since it cannot affect the other side either through vertical or through rotary resistance. The part of the beam from the internal hinges to the other support then effectively becomes a cantilever and we get the largest possible bending moments for the loading cases considered. We note that placing two internal hinges very close to each other appears to be geometrically similar to having one internal hinge. However, the effect of two very close internal hinges is structurally different than one internal hinge. The reason is that we can transmit shear across one internal hinge but not across a link member formed between two internal hinges. Both the vertical and rotational isolation are needed to get the conditions of a cantilever which produce the largest bending moment under the considered types of loading. Of course, the distance between two internal hinges cannot be infinitesimal but must be constrained by physical and geometric considerations. However, the optimization result for the largest negative moments provides a bound or limit which when approached leads to severe bending moments on a loaded beam.

Having considered the general behavior of a loaded beam with two internal hinges attached to passive structures on each end, we will discuss how to sketch the deformed shape and the bending moment diagram of such a member. Such knowledge is needed to sketch the deformed shape and bending moment diagrams of a whole structure containing one or more members of this type.

We start by considering a beam with two internal hinges loaded by a uniform load and attached to passive structures on both ends. Examples of such deformations for various locations of the internal hinges are shown in figure 1.89. The behavior of each piece of the beam from one end to the nearest internal hinge is that of a uniformly loaded cantilever but with flexible support. Such a cantilever will have an initial rotation at the support and a negative cuvature throughout its span. The
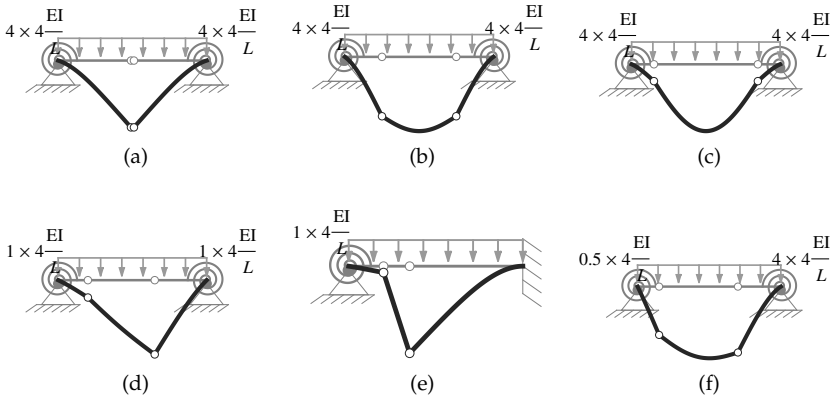
Figure 1.89. Examples of the deformations of a beam with two internal hinges loaded by a uniform load and attached to passive structures on both ends.

tip deflection of such a cantilever $\left(qL^4(1 + k)/8kEI\right)$ where 'q' is the distributed load, 'E' is Young's modulus, 'I' is the moment of inertia, 'L' is the length of the cantilever and 'k' is the rotary spring stiffness factor at the supported end. The important point to note is that the deflection is proportional to the fourth power of the length of the beam so that if the length doubles, the deflection increases by a factor of 16. This observation explains the relative deflections of the internal hinges shown in figures 1.89d, e and f where the relative deflection at the internal hinges changes rapidly with the ratio of their respective lengths. Finally, the middle portion of the beam deflects like a simply supported beam but whose supports are subsequently moved to match the deflection of the internal hinges. For the same length and under a uniform load, the maximum deflection of a simply supported beam is 9.6 times less than that of a cantilever of comparable length but with fixed support. That is why the separation between the hinges must be relatively large compared to either of the end pieces in order for the deflection of the middle portion to appear significant as demonstrated by the examples in figures 1.89b, c, d, e and f. When the length of the middle piece is less or equal to the length of at least one end piece of the beam and when the stiffness factor at the support of that end piece is less or equal to 2, then its deformation is relatively insignificant and the middle piece appears almost like a straight line as illustrated in figures 1.89d and e.

The bending moment diagrams of a loaded beam with two internal hinges loaded by a uniform load and attached to passive structures on both ends is always a parabola passing through each of the internal
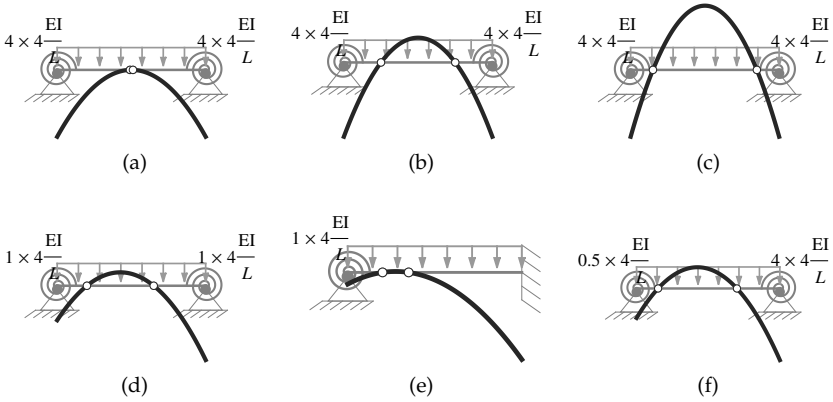
Figure 1.90. Bending moment diagrams of the beams shown in figure 1.89.

hinges. The value of this parabola at the end points and at the middle support may be determined from statics. Its functional form is given by $(q/2)(x - x_{HL})(x - x_{HR})$ where 'q' is the magnitude of the uniform load, 'x' is the coordinate of any point from the left end and 'x_{HL}' and 'x_{HR}' are the coordinates of the left and right internal hinges respectively. The maximum positive moment always occurs at the midpoint between the internal hinges and has a value of $q(x_{HR} - x_{HL})^2/8$. As examples, the bending moment diagrams corresponding to the cases shown in figure 1.89 are shown in figure 1.90.

We now consider a beam with two internal hinges loaded by a point force load and attached to passive structures on both ends. Examples of such deformations for various locations of the internal hinges and various locations of the point force are shown in figure 1.91. When the point force is applied at a location between a support and its nearest internal hinge then that piece will behave like a cantilever but with flexible support, the middle piece will rotate rigidly while the other end piece will remain immobile as for example in figures 1.91a, b and c. When the point force is in the middle piece (*ie.* on the span between the internal hinges) then the middle piece will behave like a simply supported beam subject to that point force but whose supports are subsequently moved to match the deflection of the internal hinges. In that case, both end pieces will behave like cantilevers with flexible supports and a point force applied at their edges. Again, the maximum deflection of a simply supported beam is generally much less than that of a cantilever of comparable length but with fixed support. That is why the separation between the internal hinges must be relatively large compared to either of the end pieces

in order for the deflection of the middle portion to appear significant as demonstrated by the examples in figures 1.91d, e and f. In some cases, the relative deformation of the middle piece might be so small that it appears almost like a straight line.
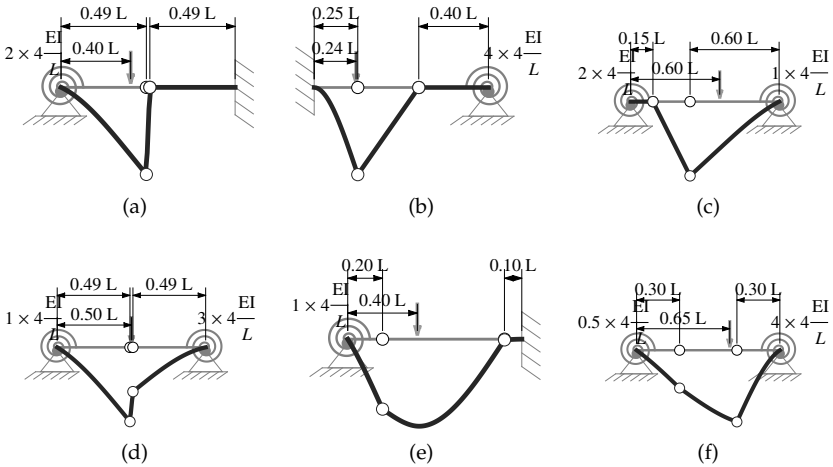

Figure 1.91. Examples of the deformations of a beam with two internal hinges loaded by a uniform load and attached to passive structures on both ends.

The shape of the bending moment diagrams of a loaded beam with two internal hinges loaded by a point force load and attached to passive structures on both ends depends on the location of the point force. When the point force is on either end piece (*ie.* piece of the member from an end to its nearest internal hinge) then the moment diagram is a straight line varying from a maximum at the end of the end pieces that is loaded to a value of zero at the location of the point force; the rest of the beam from the point force to the other end has a bending moment diagram which is identically zero. Examples of this are shown in figures 1.92a, b and c. When the point force is in the middle piece of the beam then the bending moment diagram has the shape of a broken straight line with a maximum at the location of the point force and passing through zero at the internal hinges. Examples of this are shown in figures 1.92d, e and f. The maximum positive moment always occurs at the location of the point force and has a value of $P\left(x_F - x_{HL}\right)\left(x_{HR} - x_F\right)/\left(x_{HR} - x_{HL}\right)$ where 'P' is the magnitude of the point force, 'x_F' is the coordinate of the point force and 'x_{HL}' and 'x_{HR}' are the coordinates of the left and right internal hinges respectively.
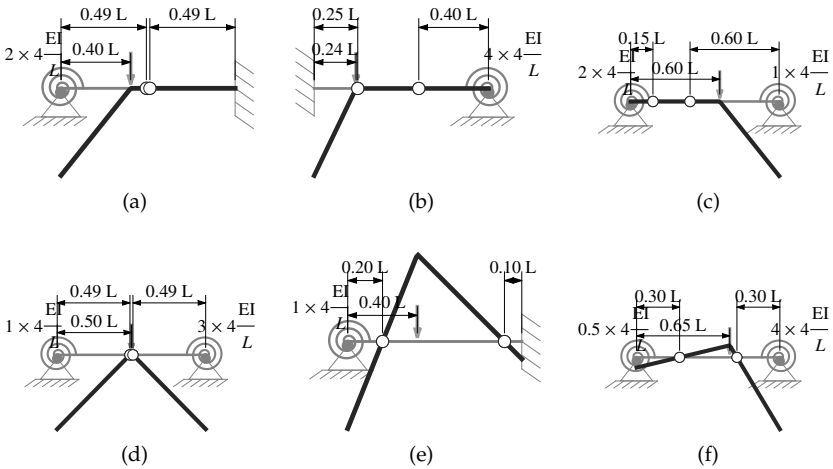
Figure 1.92. Bending moment diagrams of the beams shown in figure 1.91.

1.12   Beam with One Internal Hinge, a Moment Applied at One End and Resisting at the Other

In this section, we will discuss the effect of one internal hinge in a beam on the analysis of continuous beams or frames. As before, we will divide the discussion into two parts: i) when the member is acting as part of a passive structure as shown in figure 1.93 and ii) when the member is attached on both ends to passive structures while being loaded over its span. By considering these two cases, we can then use the methods developed previously to do an approximate analysis for any structure containing one or more members each having one internal hinge.

To study the member having one internal hinges as part of a passive structure, we consider it under the conditions shown in figure 1.93. The figure shows an internal hinge at a distance 'x_H' from the near end, an applied moment M_{near} at the near (or left) end and a rotary spring with stiffness factor 'k' at the other. This beam is statically determinate in that the reactions, shear force and bending moments can all be determined by using only statics. Using statics, we can determine the carry-over factor for moments which is given by:

$$-M_{\text{far}}/M_{\text{near}} = (L - x_H)/x_H \tag{1.8}$$

Note that the carry-over factor for moments is independent of the stiffness factor 'k' or of any deformational properties of the beam such as
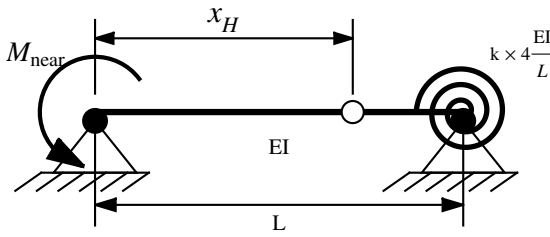
Figure 1.93. A beam with one internal hinge considered as part of a passive structure.

Young's modulus. This carry-over factor may also be determined by using similar triangles while knowing that the moment diagram is a straight line that must pass through the location of the internal hinge and whose value at the near end is M_{near}. The resulting formula for carry-over factor is peculiar in that it has 'x_H' as a denominator and this may take the value zero. This means that the carry-over factor tends to infinity as the internal hinge approaches the near end. If that happens, then any moment applied at the near end will be infinitely magnified at the far end. The reason this happens is as follows. Consider that we apply a moment M_{near} at the near end. Using a free body diagram of the piece of the beam from the near end to the internal hinge, we can determine that the applied moment must be balanced by a shear force multiplied by the length of that piece which is 'x_H.' As 'x_H' decreases and the applied moment remains fixed then the shear force must increase indefinitely so that the product of the shear times 'x_H' remains equal to M_{near}. This indefinitely increasing shear force acts like an applied force at the tip of a cantilever on the remaining piece of the member and hence the moment at the rotary spring must be the product of an indefinitely increasing shear force multiplied by '$L - x_H$.' This gives an indefinitely large resisting moment at the spring end. Of course, there are physical and geometrical limitations to this effect but it is still possible to get highly magnified resisting moments at the far end by placing the internal hinge very close to the near end. Note that this effect does not exist if the the internal hinge is exactly at the near end because the applied moment will then be applied at a continous beam with no internal hinges as shown in figure 1.11 and such a beam always has a carry-over factor less than 0.5.

In addition to the carry over factor, we need to know the near end rotary stiffness in order to determine the stiffness factor of a member with one internal hinge that is acting passively and attached to another member such as in figure 1.95. We also need this stiffness in order to

distribute an applied moment at a node that is connected to multiple members when one or more of these members has one internal hinge as in figure 1.96. The near end rotary stiffness factor is given by:

$$\frac{M_{\text{near}}}{\theta_{\text{near}} \, 4EI/L} = \frac{3k \, x_H^2}{(3 + 4k)L^2 - 6(L + 2kL)x_H + 3(1 + 4k)x_H^2} \tag{1.9}$$

For any location of the internal hinge, this stiffness factor is always between 0 and $(3 + 4k)/(4 + 4k) \leq 1$. The minimum near end stiffness factor of zero is obtained when the internal hinge is infinitesimally close to the near end while the maximum stiffness factor is obtained when the internal hinge is at the inflection point of a beam with no internal hinges but with the same spring at the far end. When the internal hinge is at the far end then the near end stiffness factor is always 0.75 because the beam becomes effectively freely hinged at the far end. Also, when $x_H > (3+4k)/(3+8k)$, then the near end stiffness factor is always greater or equal to 0.75. In practice, we can use this as follows. When the stiffness factor 'k' is greater or equal to 0.75 then as long as the internal hinge is within $L/3$ (ie. one third the length) away from the spring end then we can take the near end stiffness factor to be approximately 1 instead of some value between 0.75 and 1 which, as was seen in previous examples, leads to good approximate results.

The formula for the near end stiffness factor 1.9 is relatively complex and so we will present it graphically. Figure 1.94 shows a contour plot of the normalized near end stiffness factor. This figure shows contours of the near end stiffness factor given by formula 1.9 divided by the near end stiffness factor of an equivalent beam but with no internal hinge. We note that this normalized stiffness factor must be 1 when the internal hinge is located at the coresponding location of the inflection point in a beam with no internal hinge. The stiffness factor decreases as the internal hinge approaches the near end and increases as the stiffness factor of the far end (ie. 'k') increases.

Having discussed the near end stiffness factor, we note that as the internal hinge gets closer to the near end, the near end stiffness factor tends to zero while the carry-over factor for the moment at the far end tends to infinity. If we have a structure as shown in figure 1.95, then the moment at B depends on the near end stiffness factor of member BC while the moment at C is the product of the moment at B multiplied by the carry-over factor for moments of member BC. It is then natural to ask which has the stronger effect, the stiffness factor at the near end or the carry-over factor for moments? If we multiply the near end stiffness factor given in formula 1.9 by the carry-over factor given in formula 1.8 and we consider the limit as the internal hinge approaches the near end then we find that
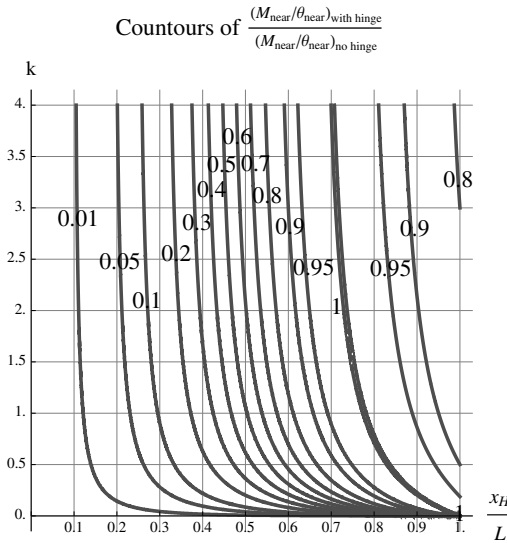
Countours of $\dfrac{(M_{near}/\theta_{near})_{\text{with hinge}}}{(M_{near}/\theta_{near})_{\text{no hinge}}}$

Figure 1.94. Contours of the normalized near end stiffness factor for the beam shown in figure 1.93.

the limit is zero. In other words, in figure 1.95, the moment at B and at C will both tend to zero as the internal hinge approaches node B.

Now we again consider the continuous beam shown in figure 1.95 and consider what can be the worst effect of having an internal hinge on the moment at C. Our concern is of course with the possibly large carry-over factor for moments in member BC due to the presence of the internal hinge. Therefore, we ask where should we locate the internal hinge so that either the moment at B or at C is a maximum. The moment at B is a maximum when the rotary stiffness at B is a maximum and this occurs when the internal hinge is placed at the inflection
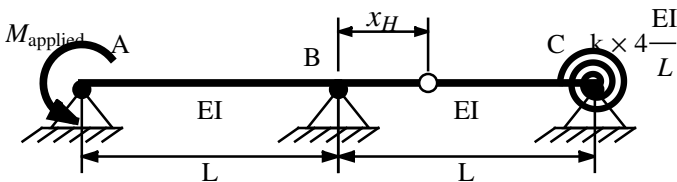
Figure 1.95. Example of a beam with one internal hinge acting as a passive structure in a continuous beam.

point of member BC if that member had no internal hinges. The moment at C is a maximum when the location of the internal hinge is at $x_H \approx (3 + 5k)L/(3 + 9k)$ (maximum error $< 1.6\%$) and the maximum value is equal to $(3 + 4k + \sqrt{9 + 36k + 32k^2})/(6+10k)$ times larger than for a similar beam but with no internal hinge. This last magnification factor is always less than about 1.066. Therefore, we conclude that no matter where we place the internal hinge in member BC, the moment at C cannot be larger than about 6.6% what it would be if member BC had no internal hinge. If the length of AB is allowed to vary from 0 to 10 times the length of member BC then the maximum increase in the moment at C cannot be larger than about 32.5% and occurs when the length of member AB is 10 times that of BC. From this we deduce that when a member with one internal hinge is acting as a passive member and is attached to other passive members on the left and right then the transmitted moment across the member will, in general, not be much higher but may be much less than if that member had no internal hinge.

If a member with an internal hinge is acting passively but has an active member attached at one end then the situation is different then when both sides have passive members. As an example, we consider the structure shown in figure 1.96 where a uniform load is applied on member DB which is then equivalent to having an applied moment M_{applied} on the passive structure ABC. What is then the largest bending moment in member BC at node B and and at node C? The bending moment at node B on member BC is obtained by distributing the applied moment on the two members AB and BC according to their relative stiffness or stiffness factor at B. Specifically, if we call the stiffness factor of member BC at B to be k_{BC} (given by formula 1.9) and the ratio $\beta = (EI_C L)/(EIL_C)$ then the bending moment at node B in member BC equals $M_{\mathrm{applied}} k_{\mathrm{BC}}/(k_{\mathrm{BC}} + \beta)$.
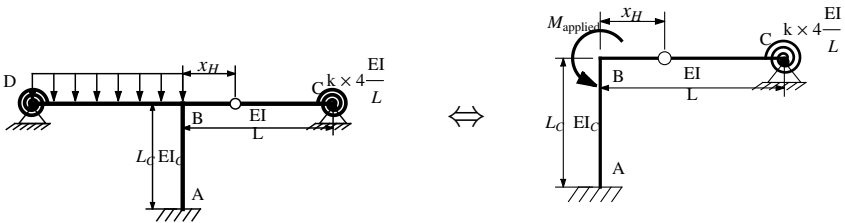
Figure 1.96. Example of a beam with one internal hinge attached to another member with an external moment applied at the common node.

Therefore, the largest bending moment at B in member BC is obtained when k_{BC} is maximum and this occurs when the internal hinge is placed at the inflection point of member BC if that member had no internal hinges. By multiplying the bending moment at B in member BC by the carry-over factor for moments given in formula 1.8, we get the bending moment at node C which is then given by $M_{applied} \, k_{BC} / (k_{BC} + \beta)$ $(L - x_H) / x_H$. The largest bending moment at C in member BC can then be obtained by maximizing this last expression and will next be discussed.

The results of optimizing the location of the internal hinge in member BC of figure 1.96 in order to obtain the maximum moment at C are shown in figure 1.97. In figure 1.97a, we show a contour plot of the maximum bending moment at C at the optimized location of the internal hinge divided by the bending moment at C that would have been obtained if there was no internal hinge in member BC. This magnification factor is generally large and increases indefinitely as the rotary stiffness of the column at node B decreases (ie. as β decreases). For example, when the column length, Young's modulus and moment of inertia of the column is the same as that of the beam (ie. $\beta = 1$) and the stiffness factor $k = 1$, then the magnification factor is about 2.25 and the corresponding location of the internal hinge is at about $0.5L$ from B but when $\beta = 0.1$ (much lower column rotational stiffness at B) then the magnification
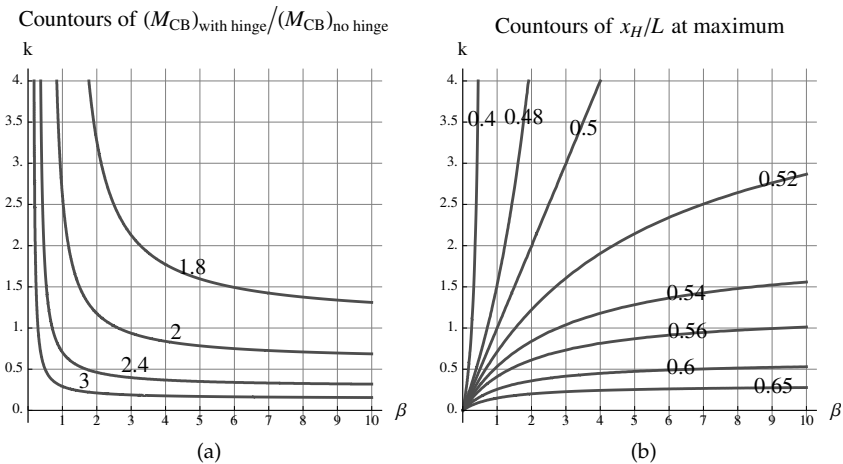
Figure 1.97. Results of optimizing the location of the internal hinge in figure 1.96 to obtain the largest bending moment at C.

factor is about 4.36 and the internal hinge is at about $0.688L$ from B. The location of the internal hinge that gives the worst case moment at C is shown in a contour plot in figure 1.97b. These locations are always closer to the node B than the location of the inflection point if the beam had no internal hinge.

For sketching purposes, we give some examples of the deformed shape of figure 1.93 for various specific locations of the internal hinge and various values of the stiffness factor 'k.' We note that when the internal hinge is closer to the spring than the location of an inflection point that would be present in a similar beam but with no internal hinge then there is a kink (*ie.* sudden change in angle) at the internal hinge forming a convex angle relative to the side containing the chord line (*ie.* the straight line joining the end points) as seen in figure 1.98a, d, e and f. Otherwise, the kink forms a reflex angle as seen in figure 1.98c. When the internal hinge is exactly at the location of the infection point of the similar beam but with no internal hinge then the deformation is continuous at the location of the internal hinge as seen in figure 1.98b.

The bending moment diagrams corresponding to the cases shown in figure 1.98 are shown in figure 1.99. These are all simple straight lines passing through the internal hinge and whose values at the near end equals the applied (counterclockwise) moment. Note that the spring stiffness factor at the right end has no effect on the bending moment diagram as seen by comparing figures 1.99a, b and c or by comparing figures 1.99d and e. Finally, figure 1.99 illustrates a carry-over factor for the moment that is greater than one and must always occur when the internal hinge is closer to the end where the moment is applied.
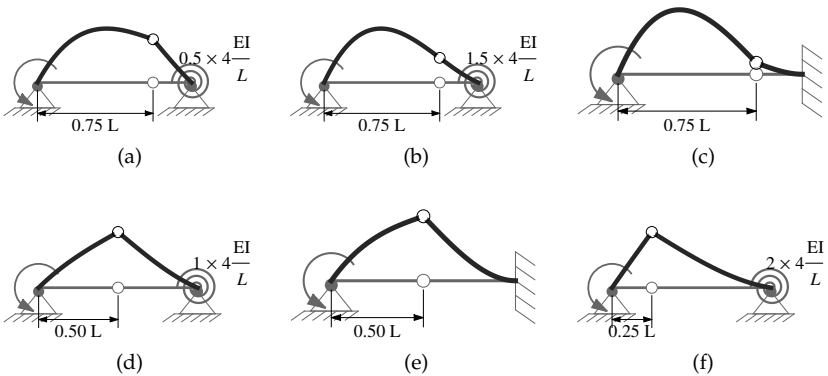
Figure 1.98. Example of deformed shapes for the beam shown in figure 1.93.
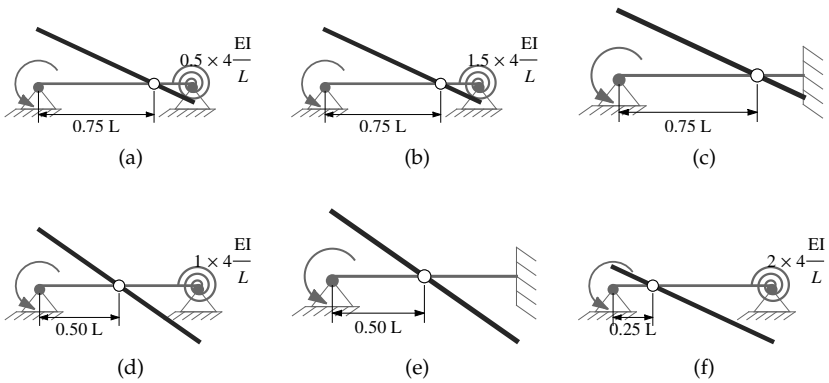
Figure 1.99. Moment diagrams corresponding to the beams shown in figure 1.98.

1.13 Beam with One Internal Hinge and a Uniform Load

We now consider the case when a member with one internal hinge is attached on both ends to passive structures while being loaded over its span. In order for the member to be statically stable, at least one of the stiffness factors at the ends must be non-zero. When this condition applies, then in general, such a loaded member has one inflection point. When we identify this inflection point then we can use statics in a manner similar to that shown in figure 1.30 or in figure 1.58 with one internal hinge replacing the role of the second inflection point. In addition, formulas 1.5 or formula 1.7 may then be used to determine the maximum positive moment and the end moments for a uniform load and a point force load respectively with the location of the internal hinge replacing the location of the second inflection point. We will start by discussing the case of a uniform load.

For a uniform load on a beam with one internal hinge whose coordinate is 'x_H,' beam length 'L' and left and right stiffness factors 'k_L' and 'k_R' respectively, there is one inflection point located at 'x_I' that is given by:

$$x_I = \frac{k_L\left(3\left(L - x_H\right)^2 + k_R\left(3L^2 - 8Lx_H + 6x_H^2\right)\right)}{3k_R\,x_H^2 + k_L\left(3\left(L - x_H\right)^2 + 4k_R\left(L^2 + 3x_H\left(-L + x_H\right)\right)\right)}L \quad (1.10)$$

This formula is somewhat complex and involves three non-trivial independent parameters all of which have non-negligible influence. We note that when other factors are fixed, the inflection point gets closer to

an end whenever the stiffness factor of that end decreases and gets far-
ther from an end as the internal hinge gets closer to that end. We can
also provide a guide in some particular but common cases. If the inter-
nal hinge is within $0.25L$ from one end and the stiffness factor at that
end is greater than 0.75, then formula 1.4 provides a good approxima-
tion for the location of the inflection point near the other end. Using that
formula, the maximum error in locating the inflection point is less than
about $0.083L$ and generally significantly better.

Concerning the bending moments in a beam with one internal hinge,
the maximum possible positive moment is $9(1 + k)^2 qL^2 / \left(8(3 + 4k)^2\right)$
where 'q' is the magnitude of the uniform load, 'k' is the stiffness factor
at the end farthest from the internal hinge and 'L' is the length of the
beam. This maximum occurs when the internal hinge is at one end of
the beam. When the stiffness factor at the end farthest from the internal
hinge is zero then we get a simply supported beam and a maximum
positive moment of $qL^2 / 8$.

The maximum possible negative moment is $qL^2 / 2$ which is 4 times
what is possible without the internal hinge. This maximum negative
bending moment occurs when one end has zero stiffness factor and the
internal hinge is infinitesimally close to that end. This effectively makes
the rest of the beam into a cantilever but with flexible support. This result
is similar to what was discussed for the beam with two internal hinges. If
neither end has zero stiffness factor then the location of the internal hinge
which gives the largest negative end moment is given by a complex ex-
pression. The results for the maximum end moment at the left end and
the corresponding location of the internal hinge are shown in figure 1.100
and examples of configurations that give the maximum moment at the
left end for some choices of the stiffness factors are shown in figure 1.101.

For the purposes of sketching, we now present examples of the de-
formed shape of a uniformly loaded beam with one internal hinge and
passive structures attached at either end. These examples are shown in
figure 1.102. We note that when the location of the internal hinge does
not correspond to a location of an inflection point when the beam has
no internal hinges then there will be a kink (*ie.* sudden change in angle)
in the deformed shape as seen if figures 1.102b, c, d, e and f. The kink
forms a convex angle relative to the side containing the chord line (*ie.* the
straight line joining the end points) whenever the internal hinge is closer
to its nearest end than the inflection point that would have been present
without the internal hinge as seen in figures 1.102b, c and f. Otherwise,
the kink forms a reflex angle as seen in figures 1.102d and e. When the
internal hinge is exactly at the location of the infection point of a similar
beam but with no internal hinge then the deformation is continuous at
the location of the internal hinge as seen in figure 1.102a.

Contours of maximum end moment / $(qL^2/8)$

Contours of x_H/L for maximum moment at left end
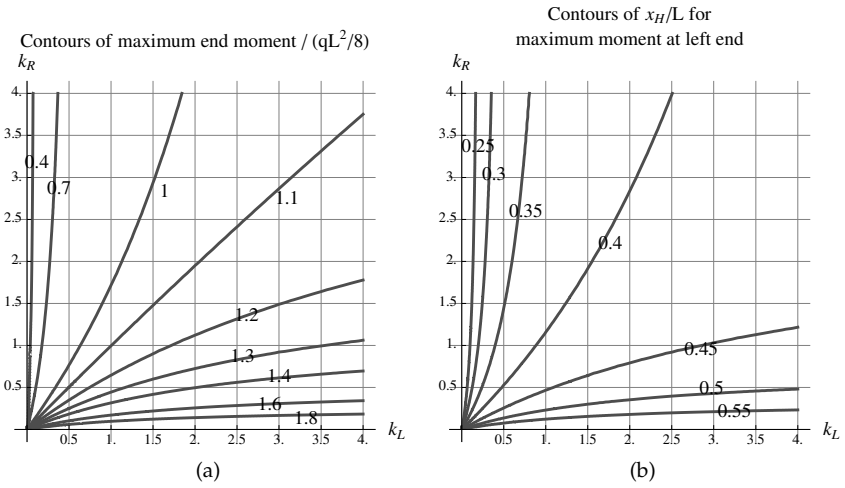
Figure 1.100. Maximum moment at the left end and corresponding locations of the internal hinge for a uniformly loaded beam as a function of the end stiffness factors.
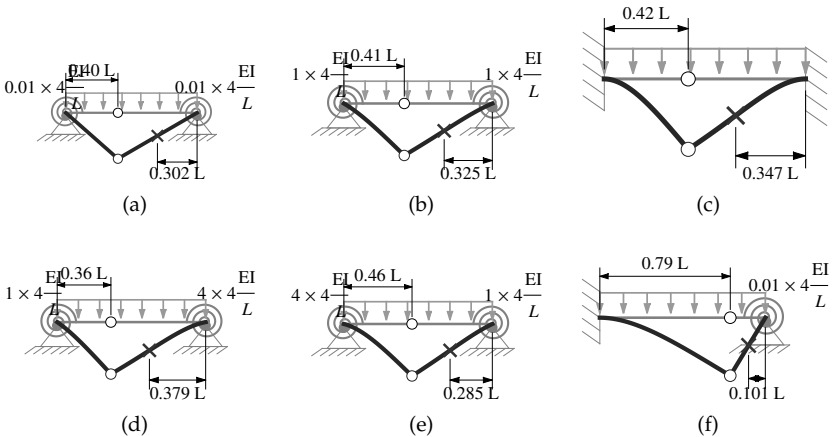
Figure 1.101. Locations of the internal hinge that give the maximum end moment at the left end for specific choices of the end stiffness factors when the beam is loaded by a uniform load.
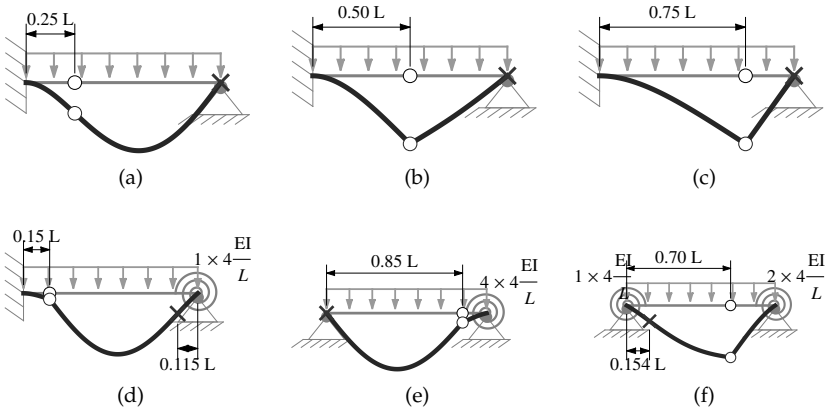
Figure 1.102. Examples of deformed shapes for a uniformly loaded beam with one internal hinge and passive structures attached at either end.

The bending moment diagrams corresponding to the cases shown in figure 1.102 are shown in figure 1.103. These are all parabolas passing through zero at the internal hinge and the inflection point. The location of the maximum positive bending moment always occurs midway between the internal hinge and the inflection point. The values of the moments at either end and at the maximum positive bending moment may all be calculated by statics using formulas 1.5 with the location of the internal hinge calculated using formula 1.10 (or otherwise estimated) replacing the location of the second inflection point in that formula.
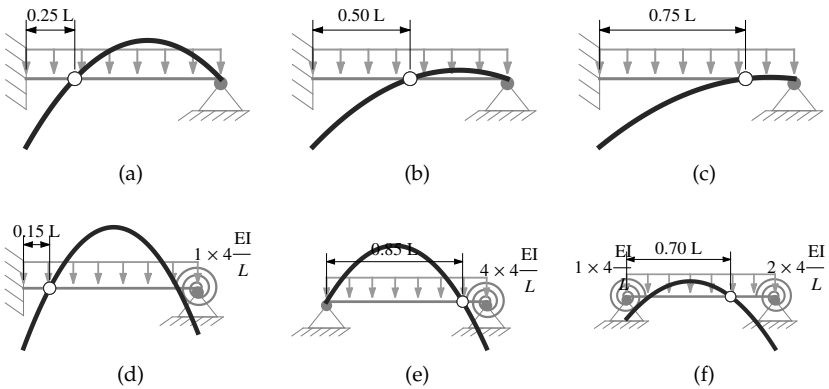
Figure 1.103. Moment diagrams corresponding to the beams shown in figure 1.102.

1.14   Beam with One Internal Hinge and a Point Force

For a point force load on a beam at location 'x_F' with one internal hinge whose coordinate is 'x_H,' beam length 'L' and left and right stiffness factors 'k_L' and 'k_R' respectively, there is one inflection point located at 'x_I' that is given by:

$$x_I = \begin{cases} k_L\, x_F \\ \quad \times \left(\dfrac{\left(L^3(3+4k_R)+2k_R x_F(x_F-3x_H)x_H\right.}{z_1} \right. \\ \qquad \left. + \dfrac{3L(1+4k_R)x_H^2-6L^2(x_H+2k_R x_H))}{z_1} \right) & x_F \le x_H \\[4pt] \dfrac{3L\,k_R\,x_F\,x_H^2 + k_L\left(L^3(3+4k_R)(x_F-x_H)\right)}{z_2} \\ \quad - \dfrac{k_L\left(2k_R x_F^2(x_F-3x_H)x_H\right)}{z_2} \\ \quad - \dfrac{k_L\left(3L^2(1+2k_R)(x_F-x_H)x_H\right)}{z_2} & x_F > x_H \end{cases} \tag{1.11}$$

where

$$z_1 = 3L\,k_R\,x_H\,(-x_F + x_H)$$
$$\quad + k_L\left(L^3\,(3+4k_R) + 2k_R x_F^2\,(x_F - 3x_H)\right.$$
$$\qquad \left. + 3L\,(1+4k_R)\,x_H^2 - 6L^2\,(x_H + 2k_R x_H)\right)$$

$$z_2 = 3L\,k_R\,x_H^2$$
$$\quad + k_L\left(-2k_R x_F^2\,(x_F - 3x_H) + 3L^2\,(1+2k_R)\,(x_F - x_H)\right.$$
$$\qquad \left. - 3L\,(1+4k_R)\,(x_F - x_H)\,x_H\right)$$

This formula is somewhat complex and involves four non-trivial independent parameters all of which have non-negligible influence. We note that when other factors are fixed, the inflection point gets closer to an end whenever the stiffness factor of that end decreases and gets farther from an end as the internal hinge gets closer to that end. We can also provide a guide in some particular but common cases. If the internal hinge is within $0.25L$ from one end whose stiffness factor is greater than 0.75 and the point force is within $0.6L$ from the other end, then formula 1.6 provides a good approximation for the location of the inflection point near the other end. Using that formula, the maximum error in locating the inflection point is less than about $0.1L$ and generally significantly better.

Concerning the bending moments in a beam with one internal hinge, the maximum positive moment is always at the location of the point force. The maximum possible positive moment for any location of the internal hinge and any values of the spring stiffness factors is $PL/4$ where 'P' is the magnitude of the point force load and 'L' is the length of the beam. This maximum occurs when the internal hinge is at one end of the beam and the stiffness factor at the end farthest from the internal hinge is zero. When both spring stiffness factors are non-zero, then the maximum positive moment is well approximated by $PL(1+k)/(4+6k)$ where 'k' is the stiffness factor of the end opposite to the internal hinge and the distance of the point force from the internal hinge at which this maximum positive moment occurs is well approximated by $(1+k)/(2+2.7k)$.

The maximum possible negative moment is PL which is 4 times what is possible without the internal hinge. This maximum negative bending moment occurs when one end has zero stiffness factor and the internal hinge is infinitesimally close to that end. This effectively makes the rest of the beam into a cantilever but with flexible support. This result is similar to what was discussed for the beam with two internal hinges. If neither end has zero stiffness factor then the location of the internal hinge which gives the largest negative end moment occurs when the internal hinge is infinitesimally or very close to the end with the smaller stiffness factor and the point force is at approximately $0.423L$ distance from the other end. The location at which the point force gives the maximum negative moment is independent of the stiffness factors. However, the magnitude of the maximum negative moment depends on the larger of the stiffness factors at the two ends. Specifically, this maximum negative moment is approximately given by $PL\,4k/\left(\sqrt{3}(9+12k)\right)$ where 'P' is the magnitude of the point force, 'L' is the length of the beam and 'k' is the maximum of the left and right stiffness factors.

For the purposes of sketching, we now present examples of the deformed shape of a point force loaded beam with one internal hinge and passive structures attached at either end. These examples are shown in figure 1.104 and 1.106. We first consider the case when the point force is in the middle. We note that when the location of the internal hinge does not correspond to a location of an inflection point when the beam has no internal hinges then there will be a kink (*ie.* sudden change in angle) in the deformed shape as seen if figures 1.104b, c, d, e and f. The kink forms a convex angle relative to the side containing the chord line (*ie.* the straight line joining the end points) whenever the internal hinge is closer to its nearest end than the inflection point that would have been present without the internal hinge as seen in figures 1.104b, c, e and f. Otherwise, the kink forms a reflex angle as seen in figures 1.104d. When the internal hinge is exactly at the location of the infection point of a similar beam but
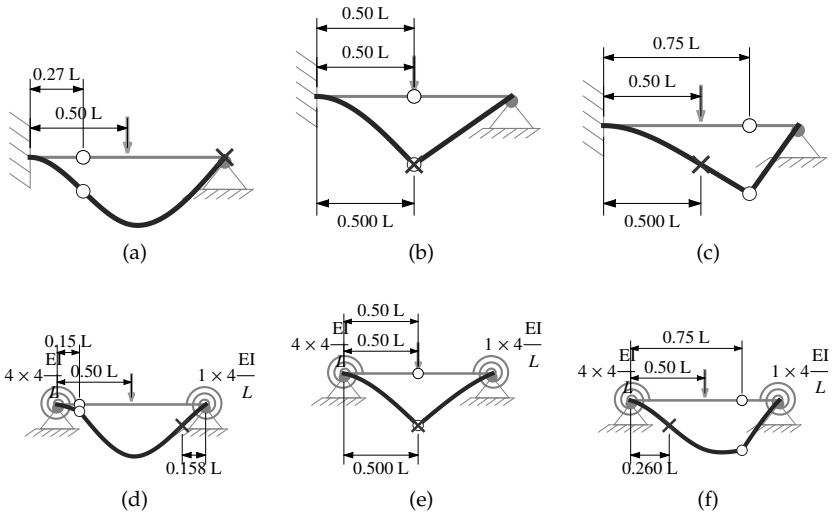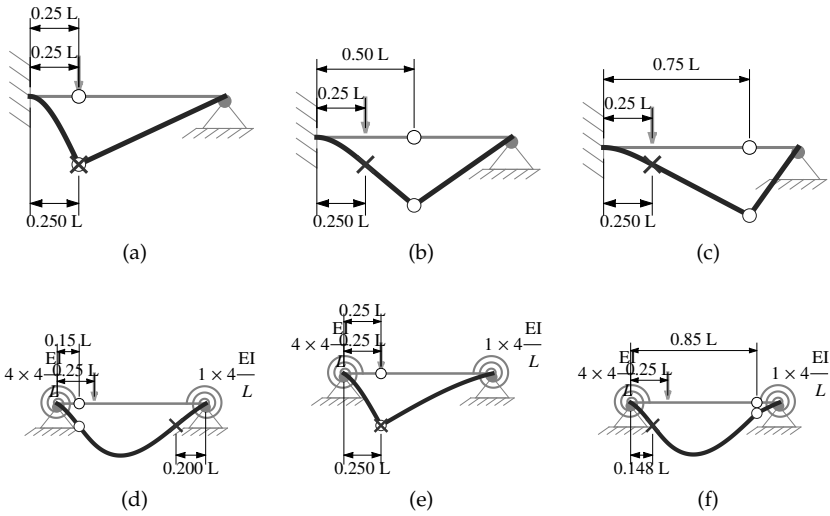
Figure 1.104. Examples of deformed shapes for a point force loaded beam with one internal hinge and passive structures attached at either end.

with no internal hinge then the deformation is continuous at the location of the internal hinge as seen in figure 1.104a. An additional observation is that the internal hinge divides the beam into two pieces. The piece that is free of the point force behaves like a cantilever with flexible support unless the stiffness factor on its side is zero (*ie.* regular hinge) and then it simply rotates rigidly as seen in figure 1.104b and c. The piece that has the point force will, in general, have both positive and negative curvatures but a maximum displacement occurs in that hinge only if that piece is signficantly longer than the other as seen in figures 1.104a and d. This is due to the much higher flexibility of a cantilever relative to a beam with some type of support at each end.

The bending moment diagrams corresponding to the cases shown in figure 1.104 are shown in figure 1.105. These are all piecewise straigh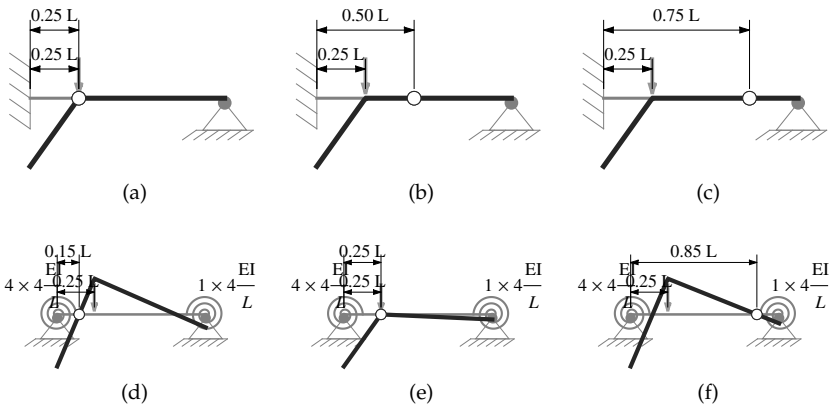t lines passing through zero at the internal hinge and, when it exists, the inflection point. The location of the maximum positive bending moment, if present, always occurs at the location of the point force as in figures 1.105a, d and f. In some cases, there is no maximum positive moment because all the bending moments are negative or zero as seen in figure 1.105b, c and e. This occurs when the piece that is free of the point force has a zero stiffness factor at its end or when the point force is applied exactly at the internal hinge. When the last case occurs then both sides behave like cantilevers with flexible support and the shape always looks similar to figure 1.105e except that the relative magnitudes at the
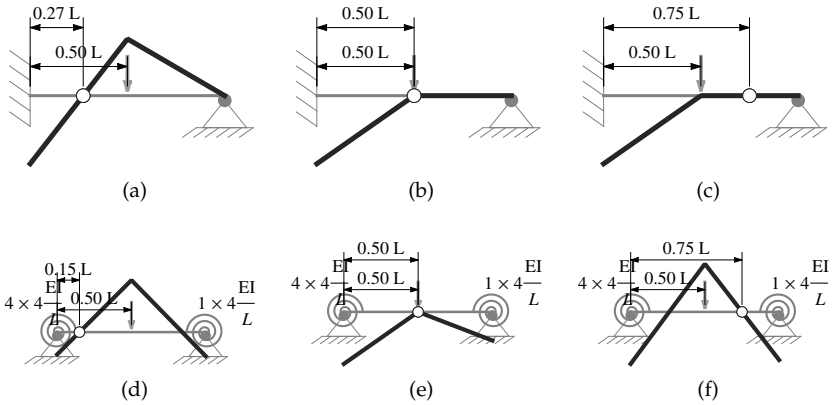
Figure 1.105. Moment diagrams corresponding to the beams shown in figure 1.104.

ends may differ. The values of the moments at either end and at the maximum positive bending moment may all be calculated by statics using formulas 1.7 with the location of the internal hinge calculated using formula 1.11 (or otherwise estimated) replacing the location of the second inflection point in that formula.

The case when the point force is nearer to one end is similar to the case when the point force is at the middle. Again, we note that when the location of the internal hinge does not correspond to a location of an inflection point when the beam has no internal hinges then there will be a kink (*ie.* sudden change in angle) in the deformed shape as seen if figures 1.106a, b, c, e and f. The kink forms a convex angle relative to the side containing the chord line (*ie.* the straight line joining the end points) whenever the internal hinge is closer to its nearest end than the inflection point that would have been present without the internal hinge as seen in figures 1.106a, b, c and e. Otherwise, the kink forms a reflex angle as seen in figure 1.106f. When the internal hinge is exactly at the location of the infection point of a similar beam but with no internal hinge then the deformation is continuous at the location of the internal hinge as seen in figure 1.106d. Again as in the case when the point force is in the middle, the piece of the beam from the internal hinge to a support that is free of the point force behaves like a cantilever with flexible support unless the stiffness factor on its side is zero (*ie.* regular hinge) and then it simply rotates rigidly as seen in figure 1.106a, b and c. The piece that has the point force will, in general, have both positive and negative curvatures but a maximum displacement occurs in that hinge only if that piece is

Figure 1.106. Examples of deformed shapes for a point force loaded beam with one internal hinge and passive structures attached at either end.

signficantly longer than the other as in figures 1.106d and f. This is due to the much higher flexibility of a cantilever relative to a beam with some type of support at each end.

Finally, the bending moment diagrams corresponding to the cases shown in figure 1.106 are shown in figure 1.107. These are all piecewise

Figure 1.107. Moment diagrams corresponding to the beams shown in figure 1.106.

straight lines passing through zero at the internal hinge and, when it exists, the inflection point. The location of the maximum positive bending moment, if present, always occurs at the location of the point force as in figures 1.105d, e and f. In some cases, there is no maximum positive moment because all the bending moments are negative or zero as seen in figure 1.105a, b and c. This occurs when the piece that is free of the point force has a zero stiffness factor at its end or when the point force is applied exactly at the internal hinge. When the last case occurs then both sides behave like cantilevers with flexible support and the shape always looks similar to figure 1.107e except that the relative magnitudes at the ends may differ. The values of the moments at either end and at the maximum positive bending moment may all be calculated by statics using formulas 1.7 with the location of the internal hinge calculated using formula 1.11 (or otherwise estimated) replacing the location of the second inflection point in that formula.

Chapter 2

Approximate Analysis of Frames with Sidesway

2.1 The Cantilever and the Single Floor Portal Frame

In previous chapters, we have analyzed structures where the chord (*ie.* the line joining end points or nodes) of every member remains either at the same or at a parallel location relative to its original position. We say that such structures have no sidesway. When a structure has sidesway, we will consider the effect of applying transverse point forces at only the nodes of members (*ie.* ends of members) with the effect of other loads added later through superposition. By using superposition it is possible to include the effect of other loads that may be present.

The approximate analysis of structures with sidesway depends on a careful study of the stiffness of individual members relative to transverse motion or sidesway. We will call this stiffness the shear stiffness in contrast to the rotary stiffness that we considered previously. There are several ways that shear stiffness may be defined. For members that are free of transverse loads on their span, we define the shear stiffness as the shear force in the member divided by the difference in transverse motion between the ends of the member. This definition is consistent because the shear force is uniform in such a member. We adopt this definition because it is especially useful in analyzing buildings subject to sidesway. The reason is that the shear forces in columns of the same floor are then proportional to their respective shear stiffnesses. This means that by determining or estimating the shear stiffness of columns, we can then determine the shear force in them. By estimating the shear force in columns, we can proceed to calculate or estimate end moments of all the members in a structure subject to sidesway. Therefore, we will next study what

affects the shear stiffness of members and then proceed to develop an
overall method of analyzing structures subject to sidesway.

We begin our study of shear stiffness by considering a cantiliver
attached to some passive structure and subject to a concentrated force
and moment at its end. An example of such a case is the one shown in
figure 2.1a. For such a cantiliver, the effect of the rest of the structure is
a rotary spring at the connection as shown in figure 2.1b. In the limit
when the connected passive structure is relatively very stiff, its effect
may be modeled as a fixed end as shown in figure 2.1c. A cantilever with
rotary spring supports is the most transversely flexible of any member
connected to a passive structure (assuming no transverse flexibility at the
connections) and can thus often be used in estimating the lower bound
on the shear stiffness of a member. The deflection 'δ' at the tip of such a
cantiliver is given by:

$$\delta = \left(\frac{1}{2} + \frac{1}{4k}\right)\frac{L^2}{EI}M_{\text{app}} + \left(\frac{1}{3} + \frac{1}{4k}\right)\frac{L^2}{EI}PL \tag{2.1}$$

where 'L' is the length of the cantilever, 'E' is Young's modulus, 'I' is
the moment of inertia and 'k' is the stiffness factor of the rotary spring
(see figure 2.1b). Note that this is the sum of the deflection of a cantilever
with a fixed end and the deflection of a rigid bar attached to a rotary
spring with stiffness $k \times 4EI/L$. From this deflection, we can infer the
shear stiffness to be:

$$k_{\text{sh}} = \frac{k}{\left((6k+3)\frac{M_{\text{app}}}{PL} + (4k+3)\right)}\frac{12\,EI}{L^3} \tag{2.2}$$

The above shear stiffness is an apparent stiffness which depends on the
ratio of applied moment to applied transverse force times the member's
length. This is important in later discussions but to highlight the role of

(a)   (b)   (c)
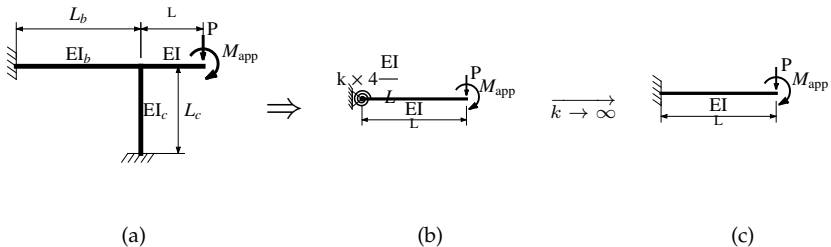
Figure 2.1. Cantiliver attached to a rotationally flexible structure and the limit of
a fixed end.

the passive structure on the shear stiffness we set the applied moment 'M_{app}' to zero. The resulting shear stiffness is given by:

$$k_{\text{sh},P\,\text{only}} = \frac{k}{(4k+3)}\frac{12\,EI}{L^3} \tag{2.3}$$

This shear stiffness is sensitive to the rotary stiffness, especially at stiffness factors between 0 and 3 which is expected to occur in practice for cantilevers. At a stiffness factor of 1, 2 and 3, the tip deflection is about 75%, 37% and 25% more than for a fixed end. Therefore, a careful consideration of the role of the connected members is important in approximately estimating the deflection of cantilevers.

As noted above, the shear stiffness given by formula 2.2 depends on the applied moment. This means that our definition of shear stiffness requires that we know the applied moment or at least that we estimate its value or influence. In particular, we can have an apparent shear stiffness that is either smaller or larger than when the applied force is acting alone. Specifically the shear stiffness is smaller when the applied moment is acting with the applied force and larger otherwise. It is even possible to get infinite shear stiffness as well as negative shear stiffness. The infinite and negative stiffnesses occur when the applied moment, if acting alone, causes an opposing tip displacement that is either equal to or greater than, respectively, the one produced by the applied force acting alone. While infinite and negative stiffness seems to be an undesirable implication of our definition of shear stiffness, this definition along with the role of the applied moment is crucial in understanding and in approximately analyzing portals and multistory buildings as will be discussed next.

Consider the column shown in figure 2.2. Aside from the shear in the beam 'V_{beam},' the column is similar to the cantilever shown in figure 2.1c; to see this rotate the page 90° after you isolate the forces on the column.
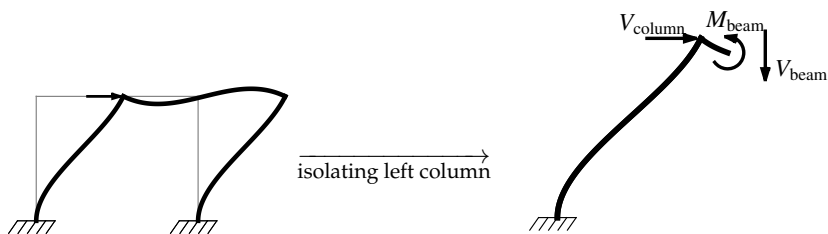
Figure 2.2. Portal frame and the role of the beam's resisting moment.

When the deformations are small, the shear in the beam only causes an axial force in the column. Also, the axial force in the beam has already been included in the shear in the column 'V_{column}.' Therefore, the apparent shear stiffness of the column is given by formula 2.2 with 'k' $\to \infty$, 'P' equal to the shear in the column 'V_{column}' and the applied moment 'M_{app}' equal to the moment from the beam at the connection 'M_{beam}.' This moment 'M_{beam}' acts to give a deformation in the opposite direction as the shear in the column 'V_{column}.' Therefore, the shear stiffness of the column will be larger with the beam than without it. Using equation 2.2 with $k \to \infty$, the column shear stiffness is given by:

$$k_{\text{sh,col}} = \frac{1}{\left(6\frac{M_{\text{beam}}}{V_{\text{column}} \times L_{\text{column}}} + 4\right)} \frac{12\,EI_{\text{column}}}{L_{\text{column}}^3} \qquad (2.4)$$

When the beam is extremely flexible, the moment in the beam is zero (*ie.* $M_{\text{beam}} = 0$) and we find from formula 2.4 that the column shear stiffness is that of a cantilever which equals '$3EI_{\text{column}}/L_{\text{column}}^3$.' By contrast, when the beam is infinitely stiff it prevents all rotation at the connection with the columns. In that case, both ends of the column cannot rotate and must, by symmetry, have the same bending moment. Since by statics, the sum of the bending moments at the ends of a member with no loads on its span must equal the shear times the length of the member, we determine that the bending moment at the ends of each column will be $M_{\text{column}} = (1/2)\,(V_{\text{column}} \times L_{\text{column}})$. By moment equilibrium (*ie.* statics) at the connection between the column and the beam, we deduce that $M_{\text{beam}} = -M_{\text{column}} = -(1/2)\,(V_{\text{column}} \times L_{\text{column}})$. With this value of moment in the beam, we use formula 2.4 to determine that the column shear stiffness equals '$12\,EI_{\text{column}}/L_{\text{column}}^3$.' This stiffness is four times the stiffness when the beam is extremely flexible. This shows that most of the shear stiffness of a portal is developed due to existence of the beams. For the passive portal frame shown in figure 2.2, the resisting moment developed by the beam is between $-1/2$ and 0 so that the shear stiffness of each column is between one and four times the shear stiffness of a cantilever. Although this provides valuable insight into the role of beams in developing transverse stiffness in framed structures, we will prefer to consider beams as providing rotary stiffness to the columns rather than resisting moments in order to arrive at an effective approximate analysis. The reason is that it is easier to estimate a rotary stiffness (as described previously) rather than to estimate a resisting moment and we need to estimate some parameters or variables in order to do an approximate analysis.
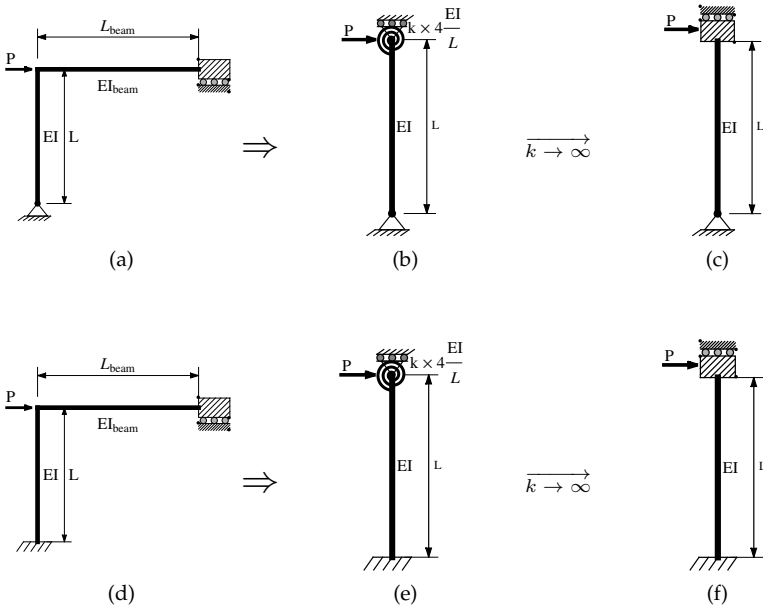
Figure 2.3. Effect of a beam attached to a column is modeled as a rotary stiffness.

We now study the stiffness of a column that is hinged or fixed at the lower end and attached to a beam at the top as shown in figure 2.3. Of course, the rotary stiffness of a beam or beams develop a resisting moment which, for a fixed lower support, we can use formula 2.4 to determine the column's shear stiffness. However, we will develop a formula for the shear stiffness of a column in terms of the rotary stiffness factor of one or more attached beams. This rotary stiffness comes about when we remove an attached beam and replace it by its rotary stiffness as shown in figures 2.3b and e for the hinge and fixed supported columns respectively. In the limit of a very stiff beam, the rotary spring becomes equivalent to a sliding but non-rotating fixed end as shown in figures 2.3c and f. Here the rotary stiffness factor 'k' is calculated in the same way as in the framed structures with no sidesway. In the example of figure 2.3, the rotatry stiffness factor 'k' has the exact value of $((EI_{\text{beam}}/L_{\text{beam}})/(EI/L))$. The shear stiffnesses for the column in figure 2.3b and e are given by:

$$k_{\text{sh}} = \begin{cases} \dfrac{4k}{(3+4k)}\dfrac{3EI}{L^3} & \text{hinge support} \quad \text{(a)} \\[2mm] \dfrac{(1+4k)}{(4+4k)}\dfrac{12\,EI}{L^3} & \text{fixed support} \quad \text{(b)} \\[2mm] 0 & \text{roller support} \quad \text{(c)} \end{cases} \qquad (2.5)$$

The above shear stiffnesses are seen to be sensitive to the stiffness of the attached beam which increase with the stiffness of the attached beam. In particular, the column with the hinged end of figure 2.3a or equivalently 2.3b has zero stiffness if the beam has zero stiffness and hence depends on the beam's stiffness to provide any shear resistance. For the column with the fixed end of figure 2.3b, formula 2.5 indicates that the shear stiffness varies by a factor of 4 from $3EI/L^3$ to $12\,EI/L^3$ as the stiffness of the attached beam varies from 0 to infinity. Note that if more than one beam is attached to the column then this result still applies with the stiffness factor being the sum of the stiffness factors of the attached beams. Sample values for the shear stiffness for these two cases are given in table 2.1. As will be discussed later, the shear stiffnesses of formulas 2.5 are sufficient to approximately analyze any multi-span, single floor portal subject to sidesway. However, to get good accuracy we must do a good estimate of the stiffness factors due to the beams.

Table 2.1. Shear Stiffness of a Column that is Hinged or Fixed on One End and with Rotary Spring with Stiffness Factor 'k' on Other End.

k	$k_{\text{shear}}/\left(EI/L^3\right)$ (hinged end)	$k_{\text{shear}}/\left(EI/L^3\right)$ (fixed end)
0.00	0.00	3.00
0.50	1.20	6.00
0.75	1.50	6.86
1.00	1.71	7.50
1.50	2.00	8.40
2.00	2.18	9.00
3.00	2.40	9.75
4.00	2.53	10.20
5.00	2.61	10.50
6.00	2.67	10.71
∞	3.00	12.00

In addition to the shear stiffness we will also need to calculate the end moments in the columns of figures 2.3a and d. We can express these end moments in terms of the stiffness factors and the shear force in the column. In addition, if needed, we can determine the location of the inflection point either in terms of the end moments using a simple free-body-diagram or directly in terms of the stiffness factor of the

beam or beams. The end moments and location of the inflection point are given by:

$$\begin{pmatrix} M_{\text{inner top}} \\ M_{\text{inner bottom}} \end{pmatrix} = \begin{pmatrix} \frac{2k}{1+4k} \\ -\frac{(1+2k)}{(1+4k)} \end{pmatrix} PL \qquad \text{(fixed end)} \qquad \text{(2.6a)}$$

and

$$\begin{pmatrix} M_{\text{inner top}} \\ M_{\text{inner bottom}} \end{pmatrix} = \begin{pmatrix} 1 \\ 0 \end{pmatrix} PL \qquad \text{(hinged end)} \qquad \text{(2.6b)}$$

$$x_I = \frac{(1+2k)}{(1+4k)} L \qquad \text{(fixed end)} \qquad \text{(2.6c)}$$

and

$$x_I = 0 \quad \text{(or none)} \qquad \text{(hinged end)} \qquad \text{(2.6d)}$$

where:

x_I is the location of the inflection point measured from the bottom and 'L' is the length of the column.

$M_{\text{inner top}}$ and $M_{\text{inner bottom}}$ are the inner moments at the ends of the column at the top and bottom respectively.

We consider $M_{\text{inner top}}$ and $M_{\text{inner bottom}}$ to be positive when counterclockwise and clockwise respectively in conformance with standard conventions of bending moment diagrams.
Note that the difference between the bottom and top moment is always equal to the shear in the column multiplied by the length (*ie. PL*). For a hinged support, there is no inflection point while for a fixed support, the inflection point occurs between '$0.5L$' and '$0.6L$' when the stiffness factor is between 1 and ∞. Finally, for a roller support, the shear force is zero and the bending moment is uniformly zero across the column. A roller support in a column is equivalent to having no column at all in terms of shear stiffness.
While the structures shown in figure 2.3a and d are adequate for representing the columns of single floor portals, the behavior of beams in a portal are generally not passive. For example, in figure 2.4a, the existence of a second column on the right exerts a clockwise moment on the right end of the beam and this violates the assumption that the beam is acting with passive resistance. However, because of symmetry, there is an inflection point at the middle of the beam and this point remains at the same level as the top of the columns. This means that the column on the
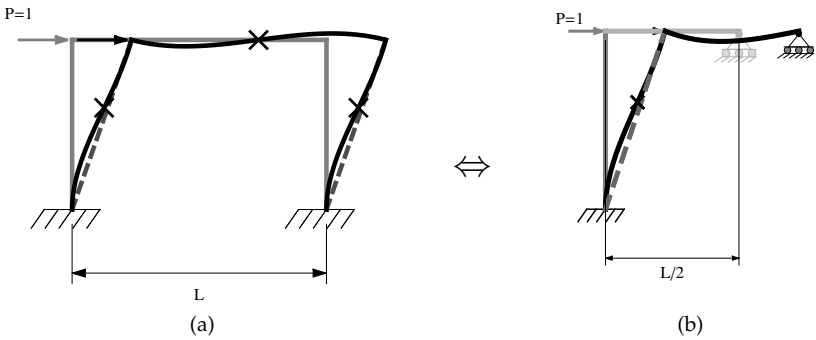
Figure 2.4. Simple portal frame and effective equivalent length of an attached passive beam.

left effectively sees a beam on a roller with half the length of the original beam as indicated in figure 2.4b. By considering both the reduced effective length and the roller support, we conclude that the stiffness factor of the attached beam is 1.5 times the stiffness factor of a passive member that has the conditions of the ones shown in figures 2.3a and d. For this reason, in the approximate method to be described in a later section, we will magnify the stiffness factors of some of the beams connected to columns by this 1.5 factor.

If we want to study the effective stiffness factors of attached beams more carefully, we need to explicitly consider the effect of an active moment applied on the far end of an attached beam. Consider a simple portal but with columns that may differ in their cross-sectional properties as shown in figure 2.5a. The action of the left column on the beam may be modeled as shown in figure 2.5b. Our aim is to determine the effective
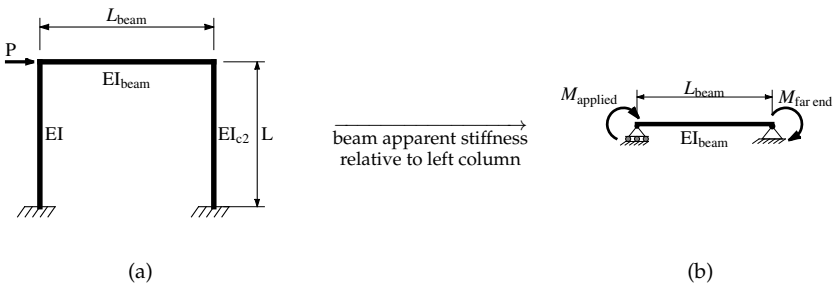
Figure 2.5. Effect of far end resisting moment on the apparent stiffness factors of attached beams.

rotary stiffness factor of such a beam relative to the left column when the far end has a specified resisting moment '$M_{\text{far end}}$.' By solving the beam problem shown in figure 2.5b, we can deduce:

$$k_{\text{apparent}} = \frac{3}{4 - 2\left(M_{\text{far end}}/M_{\text{applied}}\right)} \tag{2.7a}$$

or

$$k_{\text{apparent}} = \frac{3\left(x_I/L_{\text{beam}}\right)}{6\left(x_I/L_{\text{beam}}\right) - 2} \tag{2.7b}$$

where 'x_I' is the distance of the inflection point from the left end.

We note that the apparent stiffness factor is 1 when the resisting or far-end moment is half the applied one and this corresponds to a non-rotating end at the right side as is the case in figures 2.3a and d. Also the apparent stiffness factor is 1.5 when the ratio of far-end to applied moment is 1 which corresponds to the symmetry case considered in figure 2.4a. Therefore, formula 2.7a allows us to model both passive and non-passive resisting beams using a rotary spring as shown in figure 2.3e. However, for the purposes of doing an approximate analysis, we note that at the beginning of an analysis the far-end to near-end applied moments in a beam are unknown and may be difficult to estimate. By contrast, the geometry and approximate ratios of sectional properties are either known or may be estimated and this allows us to estimate rotary stiffness factors under the assumption of passive resisting beams. For that reason, formula 2.7a is not very useful for approximate analysis except if we intend to use an iterative approach. In an iterative approach, we start by assuming that the resisting beams are passive and obtain initial estimates for the end moments in all beams using the approach outlined in the next section. With these estimated end moments, we can use formula 2.7a to obtain updated estimates of the stiffness factors for the beams and then proceed to do an updated approximate analysis. This reanalysis may be done as many times as desired. However, this approach is not recommended because the added complexity and effort of the iterative approach is generally not worth the improvement in accuracy and the convergence properties of such an iterative approach has not been fully studied. Instead of an iterative approach, we recommend use of 2.7a as a guide to make better initial estimates of the stiffness factor of attached beams. For that purpose, its is instructive to plot formulas 2.7a and 2.7b and these are shown in figures 2.6a and 2.7b.

The results shown in figure 2.6a and b indicate several interesting features. First, the effective rotary stiffness factor may be infinite
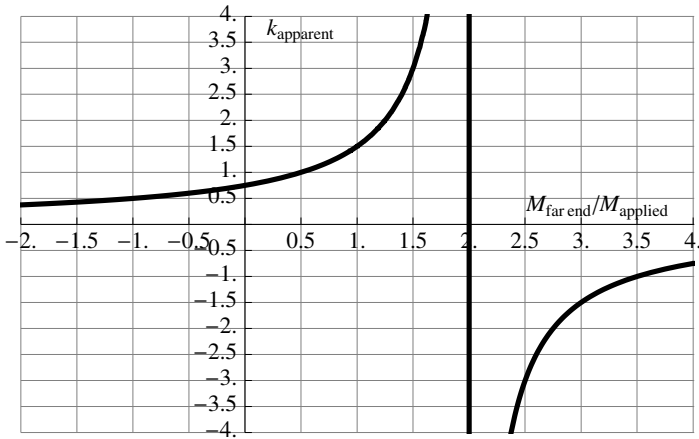
(a)
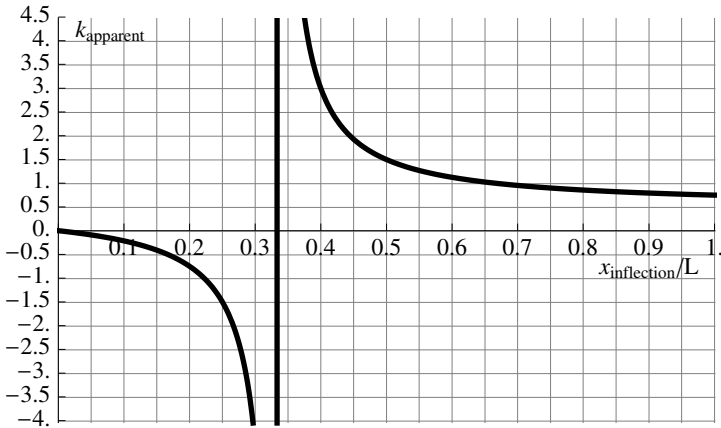
(b)

Figure 2.6. Apparent stiffness factor for a member shown in figure 2.4b.

corresponding to a non-rotating end. This occurs when the far-end mo-
ment is twice the applied one or, equivalently, when the inflection point
is 1/3 times the length from the near end. Second, the effective rotary
stiffness factor may be negative when the far-end moment goes beyond
twice the near end one which causes the near-end to rotate in a sense that
is opposite to the applied moment. Both these effects may occur when the
ratio of shear stiffness between two adjacent columns is very large.
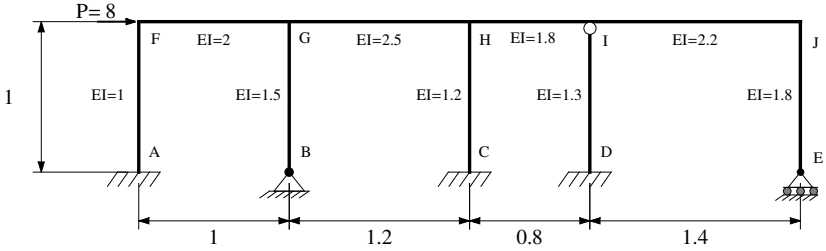
Figure 2.7. Single story sidesway example used to illustrate ideas.

In the next section, we will use the above study of the cantilever and portal and especially formula 2.5 to develop an effective approximate method to analyze any single story multi-span building subject to a side force. In subsequent sections, we will further study the response of a column subject to sidesway in order to develop an effective approximate method for multi-story, multi-span buildings subject to side forces applied at the nodes.

2.2   Approximate Analysis of Single Floor Frames Subject to a Horizontal Load

In the previous section, we have identified that formula 2.5 gives us the shear stiffness of a column with either a fixed or a hinged lower support and beams attached at the top that are characterized by an effective rotary stiffness factor. We will use that formula to develop a method for solving any single story multi-span building subject to a side force. The outline of the method is as follows:

1. Start by estimating the effective rotary stiffness factors at the top of each column.

2. Using the rotary stiffness factors, calculate the shear stiffness of each column using formula 2.5 reproduced below:

$$
k_{\text{sh}} = \begin{cases} \frac{4k}{(3+4k)} \frac{3EI}{L^3} & \text{hinge support} \\ \frac{(1+4k)}{(4+4k)} \frac{12\,EI}{L^3} & \text{fixed support} \\ 0 & \text{roller support} \end{cases}
$$

Using the shear stiffness of each column, calculate the shear force in each column by dividing the net applied side force at that level over

the columns in proportion to their shear stiffness. The net applied side force at a level is the total of all side forces that occur anywhere above the middle of the columns being considered.

3. Using formula 2.6, calculate the end moments and, optionally, the inflection point in each column.

4. Knowing the moment at the top end of each column, apply those moments as point moments on the nodes of the attached beams. Analyze the resulting problem as a continuous beam with point moments on the nodes but with no sidesway using the methods described previously.

In the rest of this section, we will discuss each of the steps of the outline specified above using figure 2.7 as a specific example.

Estimating rotary stiffness factors of beams

We start by discussing how to estimate the rotary stiffness factors at the top of each column. These factors are the sum of the stiffness factors of the beams attached to the top of the columns. The difficulty in accurately estimating these stiffness factors is due to the active nature of the beams. By active we mean that both ends of the beam are acted upon by the attached columns so that neither end behaves like a purely passive rotary spring. In the estimation process, we will discuss a simple approach that gives generally good results ($< 15\%$ error in shear forces) but the errors in some cases may be more. A more careful estimation of the effective stiffness factor of the beams can give much more accurate results ($< 10\%$) but with more effort. Ideas on how to do a more careful estimation will be discussed. However, we note that when the actual stiffness factor is greater than 1 and 2 respectively then the maximum error in estimating the shear stiffness is about 42.9% and 27.3% respectively. Errors in the shear stiffnesses in turn lead to less error in estimating the shear forces in the columns due to the distribution process with all factors being less than one. Therefore, relatively large errors can only occur when the stiffness factor at the top of a column is less than 1 which rarely occurs in practical portals frames. In such cases, the large relative errors are limited to the columns with low shear stiffness and these generally have much lower shear forces and end moments than the other columns and hence are less critical.

In the discussions, we will refer to the column under consideration as the self-column and the beams and columns to the left and right of the self column, if any, as the left beam, right beam, left column and right column respectively as shown in figure 2.8.
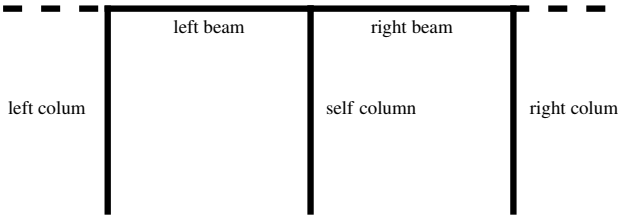
Figure 2.8. Naming convention for a column where we require the stiffness factor of the connected beams.

The stiffness factors may be estimated as follows:

stiffness factor $k \approx$

$$\frac{\sum_{\text{rigidly connected beams}} \left(f_{\text{beam}} \times EI_{\text{beam at top}} / L_{\text{beam at top}} \right)}{EI_{\text{self column}} / L_{\text{self column}}} \quad (2.8)$$

where: $f_{\text{beam}} = 1.5$.

In the above, the sum is taken over all beams that are rigidly connected to the self column. A rigidly connected beam is a beam that does not have an internal hinge at its connection with the self-column. In particular, if the self column has an internal hinge at its top then the stiffness factor is zero for all the connected beams. The factor f_{beam} is taken to be 1.5 because the inflection point in the beams is often near their middle and in the previous section we saw that this gives an equivalent rotational stiffness factor of 1.5 times the regular value.

In general, we get good results for the calculated shear forces in the columns if we use formula 2.8 to estimate the stiffnes factors. However, we can get a better approximation of the shear forces if we improve our estimate of the stiffness factors. Some suggestions on getting better estimates of stiffness factors include:

- If a beam is rigidly connected to the self column but has an internal hinge at the other end then use $f_{\text{beam}} = 0.75$ for that beam.

- If a beam is rigidly connected to the self column and rigidly connected to the neighboring column and the lower support of the self column is a hinge but the neighboring column has a fixed support then use $f_{\text{beam}} = \infty$. This means that assume that the top of the self column has a sliding support but allows no rotation (the stiffness factor $\to \infty$).

- If a beam is rigidly connected to the self column and to the neighboring column and the lower support of the self column is fixed but the neighboring column has a hinge or roller support then use $f_{beam} = 1$.

Using the simple formula 2.8, we can generate the stiffness factors at the top of each column for the structure shown in figure 2.7. The result is shown in table 2.2.

Table 2.2. Stiffness Factors at the Top of the Columns Shown in Figure 2.7.

Approximate analysis of a side loaded building					
Preliminary calculations					
Floor $= 1$					
column	1	2	3	4	5
stiffness factor at top	3.000	4.083	5.417	0	0
stiffness factor at bottom	∞	0	∞	∞	0

Note that the stiffness factor of a column with a roller support at the bottom is always 0.

Calculating shear stiffness and shear force

Once the stiffness factors of all the columns have been estimated, we can directly calculate the shear stiffness of each column using formula 2.5. This is organized and presented in the row titled "shear stiffness" in table 2.3 with the total of the shear stiffness of all the columns shown in the last column. Knowing the shear stiffness in the columns we can express the shear force in each column as the shear stiffness times the sidesway in that column. However, we note the following:

i) The difference between the sidesway of a column and its next neighbor is the axial deformation of the beam between them.

ii) Axial deformations in beams are much smaller than the sidesway bending deformations in columns. Therefore, we neglect the axial deformations in beams.

These first two points imply that the sidesway of adjacent columns are approximately the same.

iii) Since all columns in a portal are joined by beams and the sidesway of adjacent columns are approximately the same then the sidesway of all the columns in a portal are approximately the same.

From the above, we conclude that the shear force in each column is the shear stiffness of that column times a sidesway which is the same for all the columns.

Next, we take a cut across all the columns at the bottom of the columns to get the free body diagram shown in figure 2.9. From this free body diagram and taking the sum of forces in the horizontal direction, we deduce that the sum of the shear forces in all the columns equals the total side forces applied above the cut; in the example of figure 2.7 and 2.9, the total is 8. Therefore, the total side forces equal the sum of the shear stiffnesses multiplied by the sidesway.
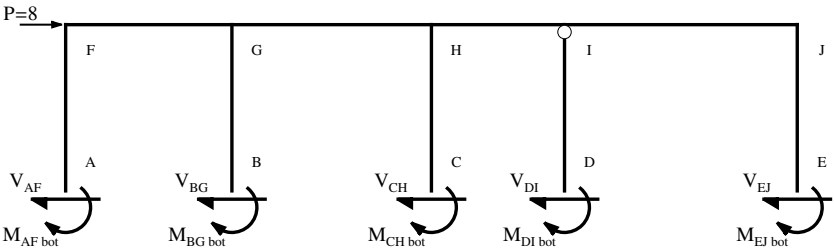
Figure 2.9. Free body diagram (excluding vertical axial forces) of figure 2.7 by taking cut just above the supports.

Symbolically, if we call the sidesway Δ, then we can express the argument described above symbolically as follows:

The total side forces equals the sum of the shear forces in the column:

$$\sum(\text{side forces above cut}) = \sum_{\text{columns in floor}} (\text{shear force in column})$$

The sum of the shear forces is the sum of the shear stiffnesses multiplied by the common sidesway:

$$\sum_{\text{columns in floor}}(\text{shear force in column}) = \sum_{\text{all columns}} (k_{\text{sh column}}\,\Delta)$$

$$= \left(\sum_{\text{all columns}} k_{\text{sh column}}\right)\Delta$$

Therefore, the total side forces above the cut equals the sum of shear stiffnesses multiplied by the common sidesway:

$$\sum(\text{side forces above cut}) = \left(\sum_{\text{all columns}} k_{\text{sh column}}\right)\Delta$$

We now solve the above equation to get the sidesway as follows:

$$\Delta = \frac{\sum(\text{side forces above cut})}{\sum_{\text{columns in floor}} k_{\text{shcolumn}}} \tag{2.9}$$

Once we have the sidesway in terms of the forces and the sum of shear stiffnesses of the columns, we can calculate the shear force in each column in terms of that sidesway as follows:

$$\text{shear force in a column} = k_{\text{sh column}}\Delta$$

$$= k_{\text{sh column}} \frac{\sum(\text{side forces above cut})}{\sum_{\text{columns in floor}} k_{\text{sh column}}}$$

We rearrange the above, putting the shear stiffness terms together to get:

$$\text{shear force in a column} = \frac{k_{\text{sh column}}}{\sum_{\text{columns in floor}} k_{\text{shcolumn}}}$$
$$\times \sum(\text{side forces above cut}) \tag{2.10}$$

Using formula 2.10, we can calculate the shear force in each column. The process of calculating the shear force using formula 2.10 is organized and presented in the rows labeled "relative shear stiffness" and "shear" in table 2.3. For example, the shear force in column AF is given by $P \times k_{\text{sh column AF}}/\sum_{\text{columns in floor}} k_{\text{sh column}} = 8 \times 9.750/30.169 \approx 8 \times 0.323 \approx 2.585$.

Table 2.3. Calculation of Shear Stiffness, Shear Force and End Moments in the Columns Shown in Figure 2.7.

Single floor results						
Floor $= 1$						
column number	1	2	3	4	5	
shear stiffness	9.750	3.802	12.717	3.900	0	30.169
relative shear stiffness	0.323	0.126	0.422	0.129	0	1
shear	2.585	1.008	3.372	1.034	0	8
Internal moment at top	1.193	1.008	1.612	0	0	
Internal moment at bottom	−1.392	0	−1.760	−1.034	0	

Calculating end moments in columns

Once the shear force in each column has been calculated, the end moments in the columns can be obtained using formula 2.6. In those equations, 'P' is the shear force in the particular column. For example, in

column AF, the lower support is fixed and so the top end moment is given by $M_{\text{top}} = (2k/(1 + 4k))PL$ where 'P' is interpreted as the shear force in column AF. Substituting values for k, P and L we get: $M_{\text{top}} = (2 \times 3/(1 + 4 \times 3)) \times 2.585 \times 1 \approx 1.193$. The end moment for all the columns have also been calculated and arranged in the last two rows of table 2.3.

The result of calculating the exact and approximate shear force and end moments in each column for the frame shown in figure 2.7 is shown in figure 2.10. In that figure, the approximate results are shown in paranthesis. We note that the maximum error in the shear force occurs in column BG and is about 13.3%.

Figure 2.10. Shear forces and end moments in the columns of the structure shown in figure 2.7. Note that the approximate results are shown in parentheses under the exact results.

Calculating end moments in beams

Once the moments at the top of the columns are known, these moments are placed as applied moments on the beams that are resting on top of them. We note that those beams may be modeled as being supported on rollers or hinges. This approach is schematically illustrated in figure 2.11. The reason that we can assume that the beams are equivalently resting on rollers or hinges is as follows: i) We can neglect the axial deformations in the columns which implies that the beams at a given floor must remain at the same height. ii) The sideway movement of the columns cause an essentially rigid translation of all the beams together in the same direction. This is so because, as discussed before, the sidesway of all the columns are approximately the same. Therefore, since all the beams remain at the same height and are only subject to a rigid translation sideways which cause no bending deformations, the effect is equivalent to placing the beams on rollers or hinges and applying point moments that are transmitted from the tops of the columns.

Now we need to obtain the moments in a continuous beam resting on rollers and hinges subject to point moments at the nodes. Such a
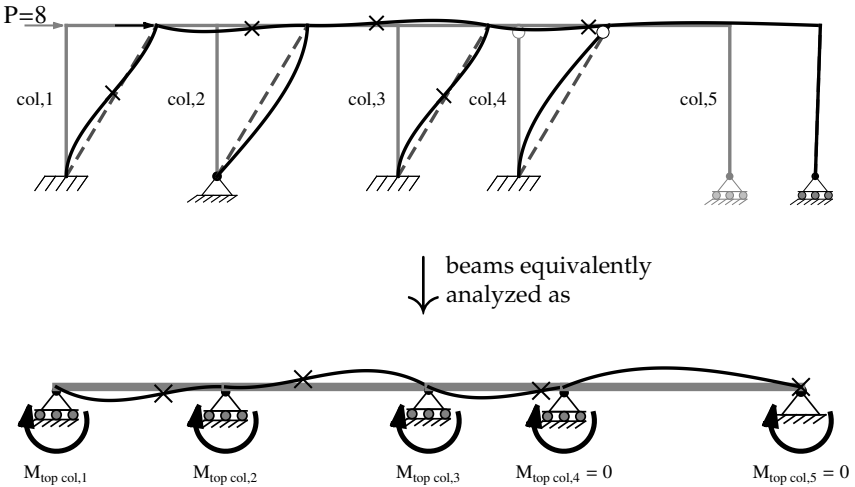
Figure 2.11. Analyzing beams in portals as a continuous beam with no sidesway.

continuous beam has no sidesway and hence may be analyzed by the methods described in the previous chapter. However, due to the way the applied moments are generated and because all the applied moments are usually in the same sense, there's a quick but less accurate way to estimate the end moments in the beams. This is simply to distribute the applied moments at each node to the attached beams in proportion to their relative nominal rotary bending stiffness. This approach usually works because: i) for the extreme left and right ends of the continous beam, the moments in the beams must match the applied moments and ii) for internal nodes of the continuous beam, the influence of the applied moments on the left and right neighboring nodes have an opposing effect to each other and therefore approximately cancel each other out. Of course, this cancellation doesn't always apply such as when the applied moments vary greatly from node to node. In that case, one must revert to the methods of the previous chapter.

Second example of portal frame

As a second example of the method presented, we consider the portal frame shown in figure 2.12. In this problem, we have an internal hinge in beam HI near node H as well as column JE that has zero shear stiffness due to having both a hinge support and an internal hinge.

As in the previous example, we first prepare a table of the stiffness factors at the top of the columns as shown in table 2.4. Note that in this table the stiffness factor of column EJ is zero because of the internal hinge
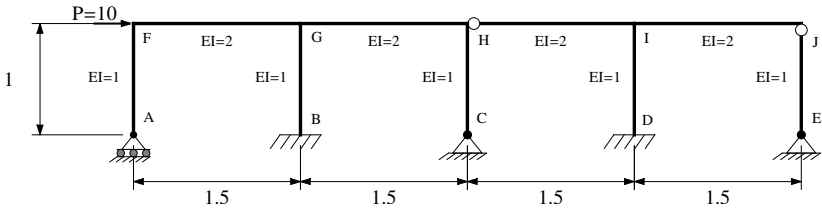
Figure 2.12. Single story sidesway example.

Table 2.4. Stiffness Factors at the Top of the Columns Shown in Figure 2.12.

Approximate analysis of a side loaded building					
Preliminary calculations					
Floor = 1					
column	1	2	3	4	5
stiffness factor at top	0	4.000	2.000	4.000	0
stiffness factor at bottom	0	∞	0	∞	0

near joint J. Also, the contribution of beam HI to column CH is zero because of the internal hinge at H but this beam (beam HI) does give a contribution to column DI. Note that we have used $f_{beam} = 1.5$ throughout although more accurate results can be obtained following previous discussed guidelines.

Once the stiffness factors at the top of the columns are obtained, we calculate the relative shear stiffness (*ie.* shear stiffness over total shear stiffness of all columns) and multiply those by the total side force of 10 to get the shear in each column. Finally, with the shear force and formula 2.6, we obtain the end moments in all columns. The results are shown in table 2.5 and illustrated in figure 2.13 with the approximate

Table 2.5. Calculation of Shear Stiffness, Shear Force and End Moments in the Columns Shown in Figure 2.12.

Single floor results						
Floor = 1						
column number	1	2	3	4	5	
shear stiffness	0	10.200	2.182	10.200	0	22.582
relative shear stiffness	0	0.452	0.097	0.452	0	1
shear	0	4.517	0.966	4.517	0	10
Internal moment at top	0	2.126	0.966	2.126	0	
Internal moment at bottom	0	−2.391	0	−2.391	0	

Figure 2.13. Shear forces and end moments in the columns of the structure shown in figure 2.12. Note that the approximate results are shown in parentheses under the exact results.

results shown in parenthesis below the exact results. The moments in the beams have not been shown because these may be obtained using the methods discussed in the previous chapter.

2.3   Sketching Single Floor Portal Frames

Now that we've discussed how to calculate the shear and bending moments in the columns and beams of a structure subject to sidesway, we turn to the matter of sketching the deformed shape of such structures. In this regards, our objective is to identify the deformation patterns that clarify how the overall structure distibutes the load and that illustrates the relative stiffness of the members. We start with the column that has a fixed lower support and that is subject to a side force which, by equilibrium, must equal the internal shear force. As discussed before, the contribution of beams may be modeled as a rotary spring with stiffness factor 'k' whose values range from zero to infinity. We will next discuss the deformations of columns at some representative values of the stiffness factor of the beams and these are illustrated in figures 2.14a to f.

The case when the stiffness factor is zero corresponds to having an internal hinge at the top of the column as for example is seen in column DI in figure 2.7. In that case, the bending moment is zero at the top and has a value of 'PL' at the bottom where 'P' is the applied force and 'L' is the length of the column. If we rotate the page so that the chord of the column shown as a dashed line in figure 2.14a becomes horizontal then we notice that this column becomes similar to a beam that is hinged at both ends and has an applied moment of 'PL' at one end. We've studied this case before (see figure 1.14a) and we note that this member has no inflection points. We also note that the rotation at the end where the load is applied is twice that at the other end but in the opposite sense relative to the horizontal. If we apply these observations to the column of figure 2.14a, we deduce that the angle that the column makes relative
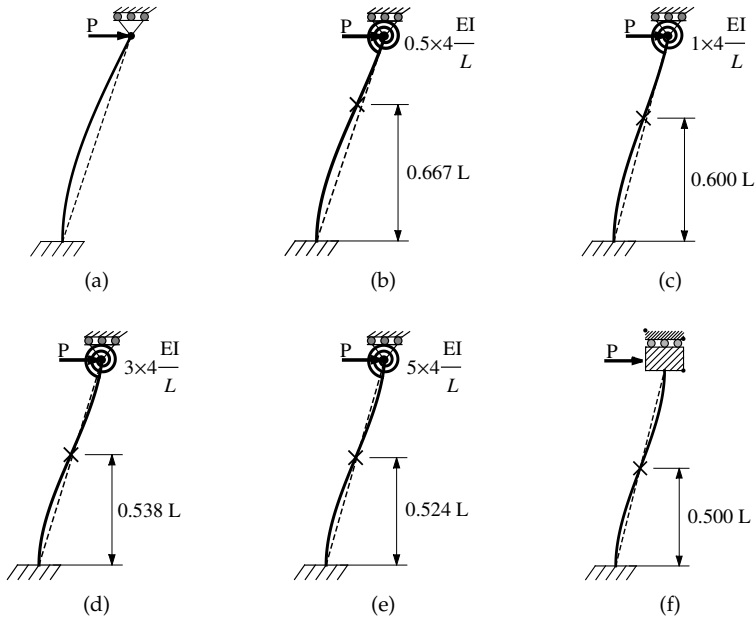
Figure 2.14. Deformation of single floor columns with lower fixed support.

to the chord at the lower end must be twice the angle that it makes with the chord at the top end. In addition, both ends of the column are at the same side of the chord.

As the stiffness factor increases, and by analogy with the hinged beams in figures 1.14, the slope of the column at the top gets closer to the slope of the chord. These two slopes become equal when the stiffness factor equals 0.5 as shown in figure 2.14b. In that case, if we view the column relative to the chord, the top end of the column is similar to a fixed end relative to the equivalent beam problem in figure 1.14f. From this we deduce that the inflection point must be one-third from the top or two-thirds from the bottom as shown in figure 2.14b. We note that although the case when the stiffness factor is 0.5 is interesting, this value rarely occurs in practice because the bending stiffness of beams are usually comparable or higher than those of the connected columns and hence the corresponding stiffness factors are expected to be larger than one.

Cases where the stiffness factor of the beams is larger than one are shown in figure 2.14c to f. All these cases have two common features. First, the top and bottom ends of the column start extending at opposite sides of the chord so that the deformed shape of the column will intersect the chord at some point between the top and bottom but closer to the top.

Therefore, for all these cases, the slope of the column at the top is always between the vertical and the chord. Typical values of stiffness factor usually imply a slope closer to the vertical than that of the column's chord. Second, the inflection point when the stiffness factor is greater than one is always between $0.5L$ and $0.6L$ from the bottom where 'L' is the length of the beam. However, we note that the inflection point is, in general, different from the point of interesction of the column with the chord. In fact, the inflection point usually occurs at the left side of the chord and below the point of intersection of the column with the chord. The point of intersection of the column with the chord equals the location of the inflection point only when the stiffness factor is infinite which implies highly rigid beams relative to the column as shown in figure 2.14f.

We now consider columns that have a hinged lower support and that is subject to a side force which, by equilibrium, must again equal the internal shear force. Again, the contribution of beams may be modeled as a rotary spring with stiffness factor ' k' whose values range from zero to infinity. We will next discuss the deformations of columns at some representative values of the stiffness factor of the beams and these are illustrated in figures 2.15a to d.
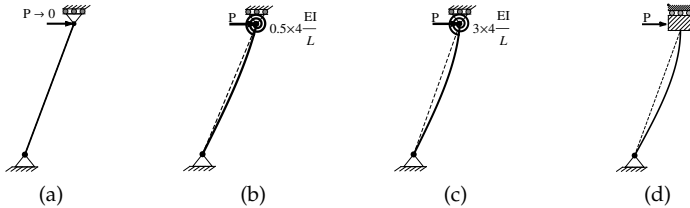
Figure 2.15. Deformation of single floor columns with lower hinged support.

The case when the stiffness factor is zero corresponds to having an internal hinge at the top of the column as for example in column EJ of figure 2.12. In that case, the bending moment is zero throughout the column which simply undergoes a rigid rotation and provides zero shear resistance. As the stiffness factor increases from zero, the rotary spring provides an increasing resistance to deformation and therefore a bending moment at the top while the hinge maintains a zero bending moment at the bottom. If we again rotate the page so that the chord of the column shown as a dashed line in any of the figures 2.15b to d becomes horizontal then we notice that these columns are again similar to a beam that is hinged at both ends and has an applied moment of 'PL' at one end. However, by contrast with the previous case of the fixed lower support, the applied moment is at the right side after rotating the page or at the

top of the column before rotating the page. Again, this case is similar to figure 1.14a which we've studied before but with the left and right ends switched. If we apply the same observations as before to the columns of figure 2.15, we deduce the following: For columns with hinged lower support, the following is true: i) Both ends of the column always extend from the same side of the chord which is to the right of the chord if the column is sheared to the right and vice versa. ii) The rotation of the lower end relative to the chord is half the rotation of the top end relative to the chord and iii) as the applied moment increases, the rotation at the top relative to the chord increases monotonically until in the limit of infinite stiffness factor, the slope at the top of the column becomes vertical as seen in figure 2.15d.

Based on the above discussion, we now discuss how to sketch the deformation of portals. As a specific example, we again consider the portal frame considered in figure 2.7. The steps in sketching the deformed shape of a portal frame are illustrated in figure 2.16 and are as follows:

i) Draw the column and beam chords. In this step, we choose a value of sidesway (ie. sideway movement) and move all the chords of the beams by that amount of sidesway. The chords of these beams are shown as FG, GH, HI and IJ in figure 2.16a. Note that the axial deformation of the beams is neglected because it will be very small compared to the magnitude of the sidesway. Also sketch the chords of all the columns with supports that are either hinged or fixed as shown for columns AF, BG, CH and DI in figure 2.16a. Note that because the axial deformations are neglected, the chords of these columns are all parallel. Also note that the chord of column EJ is not shown because its support is a roller.

ii) Draw the directions or tangents to most columns and beams at the nodes or connections. At fixed supports like nodes A, C and D of figure 2.16b, the tangent must be vertical because the fixed supports restrain rotations. At the top of the columns, we have rotations that must be consistent with the previous discussions. For example, columns AF and CH will have tangents that lie between the vertical and the chord in a manner consistent with figures 2.14c to d because we expect the stiffness factors at the top to be close to the range corresponding to those cases. By contrast, column DI must have a tangent at the top that is similar to figure 2.14a because of the internal hinge at the top.

In contrast to the columns with the fixed lower supports, the column with the hinged lower support which is column BG, must have tangents at the top and bottom that are similar to the figures 2.15b to d. We also
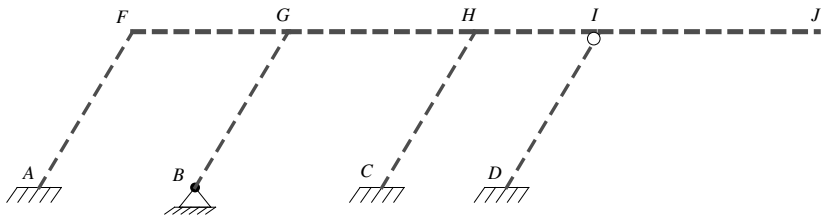
(a) Sketch the chords (dashed lines)
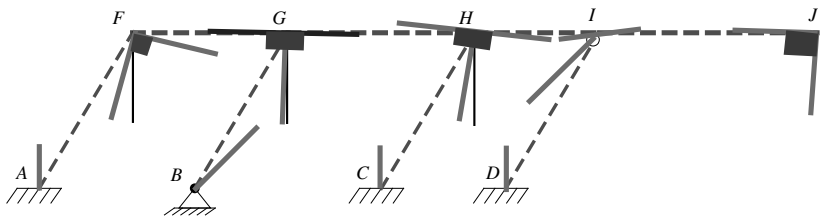
(b) Sketch directions at nodes wherever possible
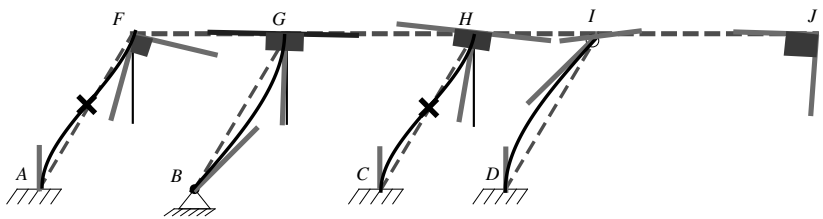
(c) Sketch the columns

Figure 2.16. Steps in sketching the deformed shape of problem 2.7.

note that column BG is attached to beams that are in turn attached to columns on either side that are relatively much more rigid column BG. This causes the inflection point in beams FG and GH to be closer to G which gives an apparently high stiffness factors at the top of column BG. The result is that the tangent at the top of column BG will be close to the vertical and thus close to figure 2.15 which has no rotation at the top.

In order to draw the tangents to the beams, we first note that at rigid connections, such as nodes F, G and H in figure 2.16b, the angles between columns and beams must be maintained after the deformation. Since those connections were orthogonal (*ie.* 90°) before the deformation then the beams must remain orthogonal to the columns after the deformation and we correspondingly draw the tangent to the beams at those
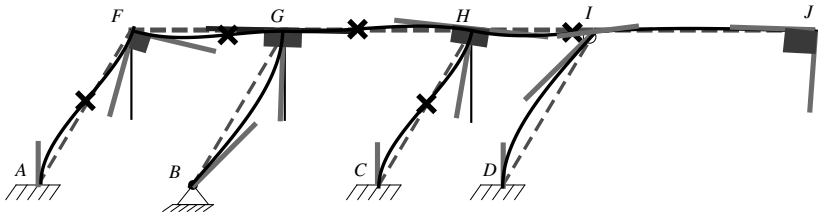
(d) Sketch the beams
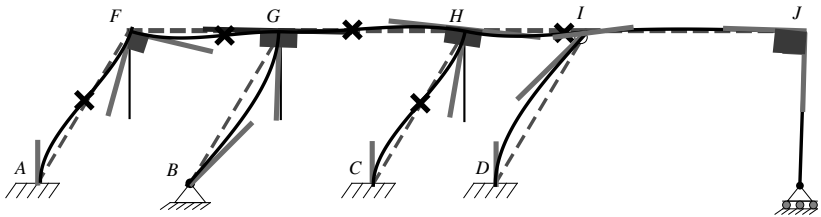
(e) Add column with rollers (rigid rotation)
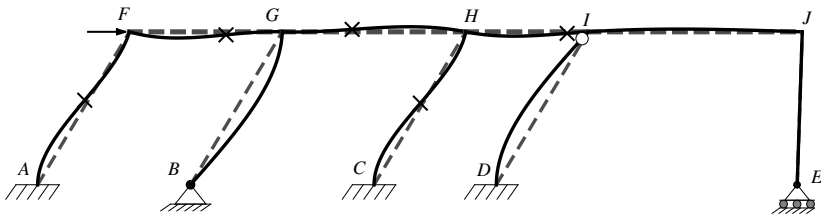
(f) Remove extraneous lines (keep chord lines)

Figure 2.16. *(continued):* Steps in sketching the deformed shape of problem 2.7.

nodes as shown at nodes F, G and H of figure 2.16b. Second, the nodes that are not rigidly connected to columns must deform in a manner consistent with the other beams and in view of the model of figure 2.11. For example, node I is not subjected to a moment transmitted from the top of the column and therefore will act passively in resisting the moment transmitted from node H. This means that the rotation of the beams at node I will be consistent with figure 1.11 with the moment at H viewed as the applied moment and with node I providing a passive rotary stiffness. Consequently, the beams at node I must have a rotation opposite to the rotation of node H and with magnitude less than half the rotation at node H. Finally, we have zero moment at node J because column EJ has zero shear stiffness and thus member IJ is similar to figure 1.14a. This

means the rotation at node J is exactly half the rotation at node I but in the opposite sense than at node J. These are also sketched in figure 2.16b along with the tangent at J to column EJ being orthogonal to the tangent at J to beam IJ because the connection at J is rigid and beams IJ and column EJ were orthogonal before the deformation.

iii) Draw the columns by using the tangents at the nodes and figures 2.14 and 2.15 as a guide. The result of sketching these columns are shown in figure 2.16c. We also add an 'x' marker at the approximate location of the inflection points. Note that columns with fixed lower supports have inflection points whenever the top of the column does not have an internal hinge while columns with a hinged support have no inflection points in all cases.

iv) Draw the beams by using the tangents at the nodes as a guide. The result of sketching these columns are shown in figure 2.16c. We also add an 'x' marker at the approximate location of the inflection points. Note that inflection points are placed closer to the columns with lower shear stiffness.

v) Draw the column or columns with rollers using the tangents as a guide and knowing that those columns must be subject to a rigid rotation. The result of sketching the column is shown in figure 2.16e.

vi) Remove extraneous lines that were used in constructing the sketch in order to get a better looking drawing of the deformed shape. In this step, we recommend that the chords be kept because they help to clarify the deformations of the columns and beams.

As a further example of sketching the deformation of portals subject to sidesway we consider the problem shown in figure 2.12. The deformed shape is shown in figure 2.17. Note that the steps in sketching the deformed shape is similar to the previous case. We start by sketching
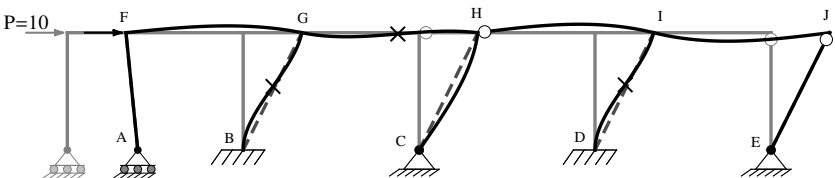
Figure 2.17. Sketch deformed shape of problem 2.12.

the chords, followed by tangents at nodes and so on. Some of the new features are as follows:

- Column EJ has a lower hing support and an internal hinge at the top. Its deformation follows figure 2.15a so that the column rotates as a rigid beam.

- The internal hinge in beam HI at H implies that the tangent at H to beam HI will not be orthogonal to the tangent a H to column CH after deformation. Node H of beam HI will have a rotation that is half the rotation at node I because it behaves in a way similar to the beam in figure 1.14a which we've studied before but with the left and right ends switched.

- The internal hinge in the last column EJ implies that the moment in the beam IJ at node J is also zero. This again implies that beam IJ will behave like the beam in figure 1.14a with the rotation at node J being have the rotation at node I.

Other features such as the deformation of the columns BG, CH, DI and AF in figure 2.17 are similar to corresponding features in the previous problem shown in figure 2.16.

Finally, having described how to sketch the deformation of portals, we note that this requires considerable knowledge of the deformation of various columns and beams as well as an estimation of the relative stiffness of different members. Consequently, as we sketch the deformation of portals, we gain a better understanding of their overall behavior. Conversely, as we have more experience with portals, we can sketch their deformations with more precise features. Therefore, sketching the deformation of portals or of structures with sidesway is an excellent educational tool because we gain a better understanding of the behavior of portals and can demonstrate our increased understanding in ever more precise details that further enhances our understanding. Furthermore, we can quickly answer explorative design questions such as what happens if a support is changed from being fixed to hinged or the effect of adding an internal hinge at any given location.

2.4   The Column with Rotary Springs and Moments at Both Ends

Now that we have a method to approximately analyze a single story portal frame, we will extend it to analyze multi-story frames subject to sidesway. At first, we might think that nothing more is needed and that

we can analyze multi-story frames in the same way that we have analyzed single story portals but on a floor-by-floor basis. The first problem we encounter in trying to do this appears when we try to analyze the second floor of a multi-story frame and notice that the lower supports of the second floor columns are neither fixed nor hinged. In fact, the support for the second floor are the beams and columns of the first floor. In addition, we notice that columns on the second floor and higher are not only connected to beams but also to columns and that all columns on floors other than the top also have their top columns connected to columns as well as beams.

The problem of having the bottom of a column being connected to beams instead of a hinge or fixed support may be handled by having a lower hinge support with a rotary spring in a way similar to how we handled the top of the column being connected to beams with the single story portal frames. In particular, when the lower rotary stiffness factor is zero or tends to infinity then we get the hinge and fixed supports respectively. The rotary stiffness of the supports on the second floor and up comes mainly from the beams and we can neglect the role of columns. The reason is that the columns are subject to sidesway and the rotary stiffness of a member subject to sidesway may generally be neglected as will be discussed next.

Consider a column that is subject to sidesway with an applied moment at one end and a support that provides some rotary resistance as shown in figures 2.18. In figure 2.18a and b, the rotary resistance is infinite while in figures 2.18c and d we have a specified rotary stiffness factor 'k_c.' For each of these figures, we then calculate the rotation at the node where the moment is applied and divide the applied moment by that calculated rotation to get the rotary stiffness of the column. That rotary stiffness is then given by:

$$\text{rotary spring stiffness} = \begin{cases} \left(\frac{EI}{L}\right)_c & \text{for fixed far-end (a)} \\ 4\frac{k_c}{1+4k_c}\left(\frac{EI}{L}\right)_c & \text{for flexible far-end (b)} \end{cases}$$

$$\Rightarrow \frac{\substack{\text{rotary stiffness factor} \\ \text{with sidesway}}}{\substack{\text{rotary stiffness factor} \\ \text{without sidesway}}} = \begin{cases} \frac{1}{4} & \text{for fixed far-end (c)} \\ \frac{4k_c(1+k_c)}{(1+4k_c)(3+4k_c)} \leq \frac{1}{4} & \text{for flexible far-end (d)} \end{cases} \qquad (2.11)$$

The above result indicates that the rotary stiffness factor of a column (or any member) that is subject to sidesway is less or equal to a quarter what it would be if there were no sidesay. In other words, allowing a member to have sidesway reduces its resistance to rotation by at least a factor of four. Therefore, since the stiffness factors of beams are comparable to those of columns and because we are approximating stiffness
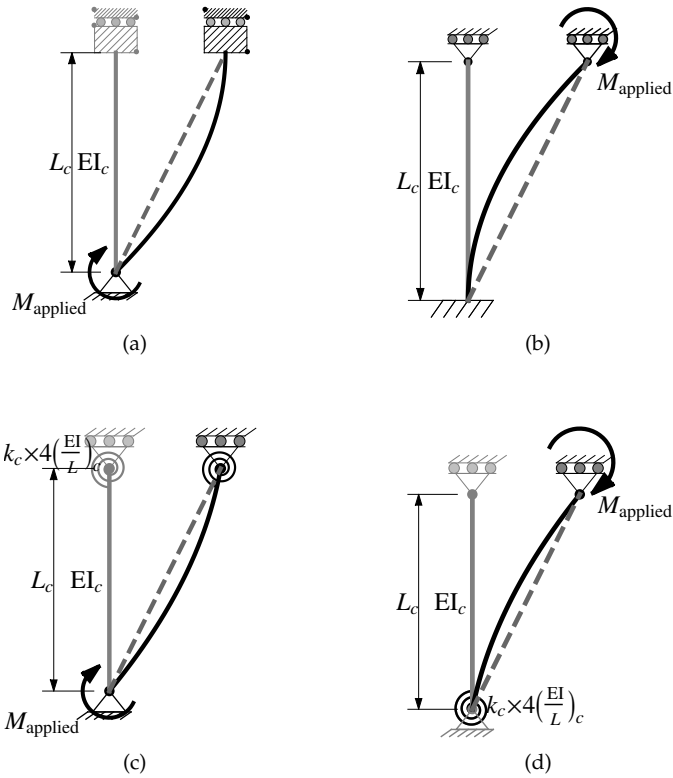
Figure 2.18. Columns used to determine the rotary stiffness of members subject to sidesway.

factors where a difference of a quarter rarely matters, we can neglect the rotary resistance of columns that are undergoing sidesway. Exceptions to this rule includes the case when there are beams and a column attached to another column but the beams that are attached have an internal hinge at that connection. This implies that all the resistance to rotation is provided by the attached column which although small can no longer be neglected.

From the above discussion, we find that we can generally neglect the rotary resistance of attached columns when we approximately analyze frames with sidesway. Although the rotary resistance of attached columns may be neglected, such columns can have a more significant effect on the (apparent) shear stiffness of a column which we will now explore. Consider a multi-story frame subject to sidesway such as the 3-story frame shown in figure 2.19a. Assume we are interested in obtaining
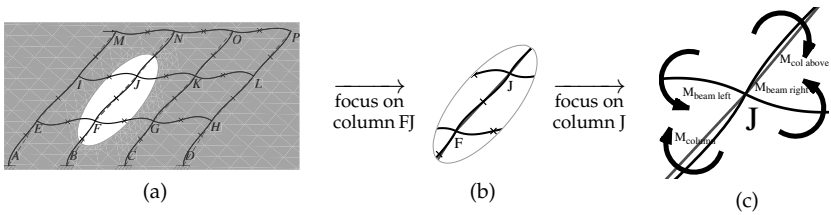
Figure 2.19. Effect of columns on their mutual shear stiffnesses.

the shear stiffness of column FJ in that figure. To that end, we isolate that column as shown in figure 2.19b. In that figure, we note the curvature of the beams and of the columns and beams attached to the top and bottom nodes of column FJ. These curvatures indicate that the bending moments in the beams are resisting the deformation while the bending moments in the columns are increasing the deformation. We can see this better if we isolate either node F or node J as shown in figure 2.19c and then refer to the results associated with the cantilever of figure 2.1b. Physically, the reason that attached columns increase the deformation is because they are also subject to shearing and are not simply passively resisting rotations.

So far, we have determined that beams that are attached at the top or at the bottom of columns help to resist deformations while similarly attached columns help to increase the deformations. In order to translate these observations into results we could use in an approximate analysis, we consider the column shown in figure 2.20. In that figure, the effect of attached beams are modeled as rotary springs both at the top and at the bottom. The effective stiffness factor of these springs at either the top or bottom are determined in the same way that we determined the stiffness factor at the top of the single floor portal. The special case when the lower stiffness factor is zero or tends to infinity corresponds to the column at the ground floor with either a hinge or a fixed support respectively. By contrast with the beams, the effect of an attached column either at the top or at the bottom is modeled as an applied moment corresponding to the bending moment at the connected end of the attached column. We note that these moments are applied on both the column and the rotary springs which can be understood by considering the moments on the nodes in figure 2.19c. For the special case when there is no attached column at a connection such as when we consider the bottom of a ground floor column or the top of a top floor column, then the corresponding applied moment must be zero. This means that with reference to figure 2.20, $M_t = 0$ at a top floor column and $M_b = 0$ at a ground floor
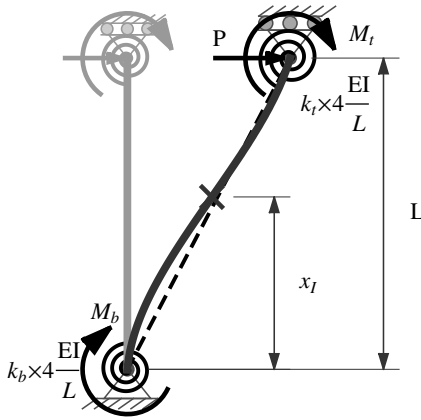
Figure 2.20. Column subject to sidesway with the effect of attached beams and columns at both the top and bottom modeled as rotary springs and applied moments respectively.

column. Finally, we consider the special case where there is an internal node at either end of the column. In that case and at any end where there is an internal hinge in the column, the rotary stiffness of attached beams provides no resistance and attached columns can apply no moment at that end. This means that if we have an internal hinge at the top of a column then we have to set $k_t = 0$ and $M_t = 0$ irrespective of the characteristics of any beams or columns attached at the top. Similiarly, if we have an internal hinge at the bottom of a column then we have to set $k_b = 0$ and $M_b = 0$.

With the model considered in figure 2.20, we now quantitatively explore the effect of attached columns. There are two effects that are of interest in doing an approximate analysis. These are the shear stiffness of the column and the end moments in the column. The shear stiffness 'k_{sh}' of column 2.20 is given by:

$$k_{\text{sh}} = \frac{(k_b+k_t+4k_b\,k_t)}{(3+4k_b+4k_t+4k_b\,k_t)+(3+6k_b)\frac{M_t}{PL}+(3+6k_t)\frac{M_b}{PL}} \times 12\frac{EI}{L^3} \qquad (2.12)$$

where:

'E' is Young's modulus of the column

'I' is the moment of inertia of the column

'L' is the length of the column

'k_b' and 'k_t' are the stiffness factors at the top and bottom respectively

'P' is the shear in the column with P positive according to the convention of figure 2.20

'M_b' and 'M_t' are the moments applied at the top and bottom respectivley with clockwise moments being positive.

We note that, as required, formula 2.12 reduces to formula 2.5a when $k_t = k$, $k_b = 0$, $M_b = M_t = 0$ and to formula 2.5b when $k_t = k$, $k_b \to \infty$, $M_b = M_t = 0$. Also, we note that clockwise applied moments at either the top or the bottom will increase the denominator in formula 2.12 which will therefore decrease the (apparent) shear stiffness of the column. Such clockwise moments are in the same sense as the moments that attached columns would apply on the top and on the bottom connections. Therefore, we generally expect our estimates of shear stiffness to decrease when we include the effect of attached columns versus when we neglect them. We will explore this matter quantitatively for ground floor, middle floor and top floor columns separately.

Ground floor columns in a multistory frame have columns attached only at their tops. We expect that these attached columns will have end moments that are comparable to the ground floor ones and hence we expect that $M_t / PL \lesssim 0.5$. The lower support of ground columns are either fixed or hinged but in either case the moment at the bottom is zero (*ie.* $M_b = 0$). We then plot in figures 2.21a and b the percentage decrease in stiffness for the fixed and hinge support respectively as a function of M_t / PL and for various values of the effective stiffness factor of the top beams. Figures 2.21 indicate that when $M_t / PL \leq 0.5$ then the decrease in stiffness is less than about 40% in all cases. While this maximum is considerable, we note that all the columns in the ground floor
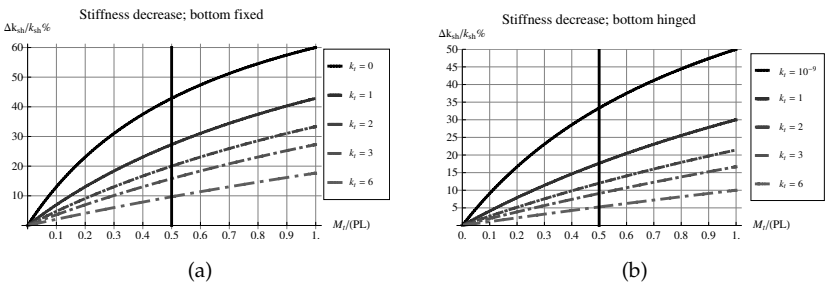
Figure 2.21. Stiffness decrease in ground floor columns due to attached columns at their top.

will generally have a comparable decrease and we need to accurately estimate the relative shear stiffness rather than the absolute shear stiffness. This means that the maximum error in estimating the shear stiffness will translate into a much lower error in estimating the shear forces as will be observed in the examples in the next section. In any case, the estimates of the shear force will improve in a second iteration when we use estimates of M_t/PL obtained from the results of the first iteration.

Top floor columns in a multistory frame have columns attached only at their bottom ends. We expect that these attached columns will have end moments that are comparable to the top floor ones, hence $M_b/PL \lesssim 0.5$. The top of top columns are, by definition, not attached to columns and hence the applied moment at the top is zero (*ie.* $M_t = 0$). We then plot the percentage decrease in stiffness as a function of M_b/PL and for various values of the effective stiffness factor of the bottom beams for two typical values of the stiffness factor of the beams at the top, specifically with $k_t = 1$ and 3 for figures 2.22a and b respectively. Figures 2.22 indicate that when $M_t/PL \leq 0.5$ then the decrease in stiffness is less than about 40% in all cases. While this maximum is considerable, we note that all the columns in the top floor will generally have a comparable decrease and we need to accurately estimate the relative shear stiffness rather than the absolute shear stiffness. This means that the maximum error in estimating the shear stiffness will translate into a much lower error in estimating the shear forces as will be observed in the examples in the next section. In any case, the estimates of the shear force will improve in a second iteration when we use estimates of M_b/PL obtained from the results of the first iteration.

Middle floor columns in a multistory frame have columns attached at both their top and bottom ends. We expect that these attached columns will have end moments that are comparable to their own moments at their ends and hence $M_t/PL \approx M_b/PL \lesssim 0.5$. We then plot the percentage decrease in stiffness as a function of $M_t/PL \approx M_b/PL$ and for various values of the effective stiffness factor at the bottom and top beams which we have taken to be approximately the same in figure 2.23a. That figure indicates that when $M_t/PL \approx M_b/PL \leq 0.5$ then the decrease in stiffness is less than about 50% in all cases. While this maximum is considerable, we note that all the columns in the middle floor will generally have a comparable decrease and we need to accurately estimate the relative shear stiffness rather than the absolute shear stiffness. This means that the maximum error in estimating the shear stiffness will translate into a much lower error in estimating the shear forces as will be observed in the examples in the next section. In any case, the estimates of the shear force will improve in a second iteration when we use estimates of end moments obtained from the results of the first iteration. We have
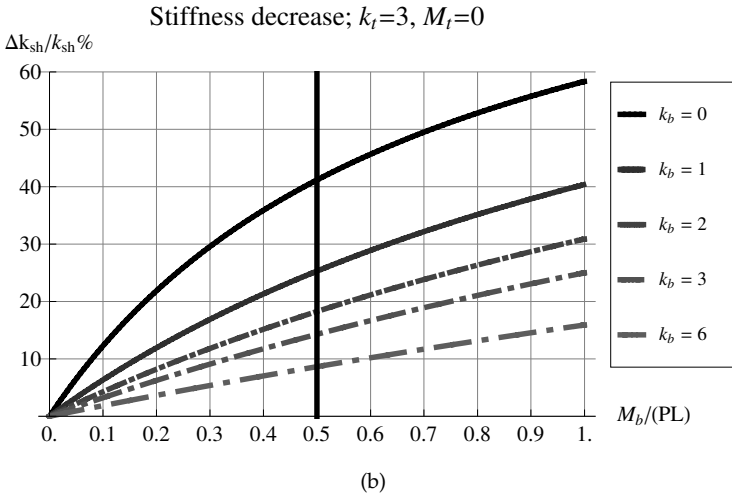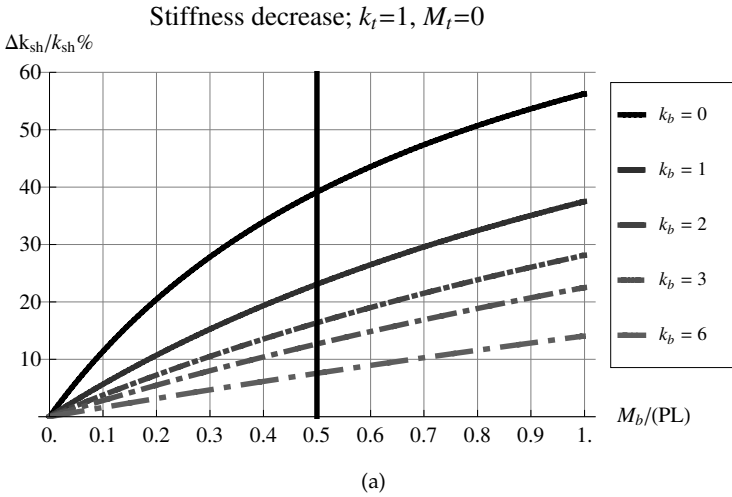
Figure 2.22. Stiffness decrease in top floor columns due to attached columns at their bottom.

also plotted in figure 2.23b the decrease in shear stiffness as a function of the stiffness factor of the connected beams which are assumed to be the approximately the same at the top and bottom of middle columns. These plots indicate that the shear stiffness becomes less sensitive to the action by the attached columns as the relative stiffness of the attached beams
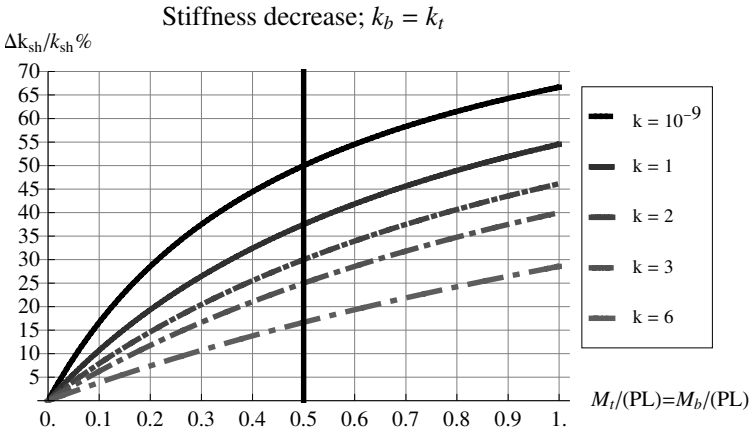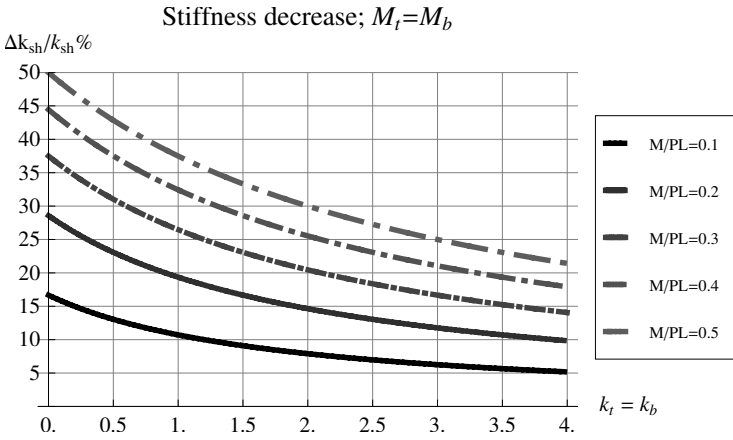
Figure 2.23. Stiffness decrease in top floor columns due to attached columns at their bottom.

increases. The reason is that these attached beams will absorb more of the moment applied by the attached columns and will therefore have a reduced effect on the shear stiffness of the column.

The second effect that is of interest in doing an approximate analysis is an expression for the end moments of column 2.20. These end

moments are given by:

$$
\begin{pmatrix} M_{\text{inner top}} \\ M_{\text{inner bottom}} \end{pmatrix} = \begin{pmatrix} +\frac{k_t+2k_bk_t}{k_b+k_t+4k_bk_t} \\ -\frac{k_b+2k_bk_t}{k_b+k_t+4k_bk_t} \end{pmatrix} PL + \begin{pmatrix} +\frac{k_t}{k_b+k_t+4k_bk_t} \\ +\frac{k_t}{k_b+k_t+4k_bk_t} \end{pmatrix} M_b
$$

$$
+ \begin{pmatrix} -\frac{k_b}{k_b+k_t+4k_bk_t} \\ -\frac{k_b}{k_b+k_t+4k_bk_t} \end{pmatrix} M_t
$$

(2.13)

Note that in the above formulas, the applied moments M_t and M_b are considered positive when clockwise and the applied load P is considered positive when acting to the right. By contrast, the inner bending moments $M_{\text{inner top}}$ and $M_{\text{inner bottom}}$ are considered to be positive when counterclockwise and clockwise respectively in conformance with standard conventions of bending moment diagrams.

By inspective formula 2.13 we find that it reduces to formula 2.6a when $k_t = k$, $k_b \to \infty$, $M_b = M_t = 0$ and to formula 2.6b when $k_t = k$, $k_b = 0$, $M_b = M_t = 0$. Formula 2.13 gives the end moments as the linear superposition of the effect of each of the transverse force P, the applied moment at the top M_t and the applied moment at the bottom M_b. If we only apply a moment at one of the ends (*ie.* only M_b or only M_t), the shear force in the member must be zero and therefore the column must be in a state of pure bending. This means that the bending moment in the column is the same throughout the column. By considering moment equilibrium at the node where the moment is applied, we note that the uniform bending moment plus the moment in the spring must equal the applied moment. This means that the applied moment must be distributed according to the relative stiffness of the rotary spring versus the rotary resistance of the column. The rotary resistance of a column subject to sidesway is given by formula 2.11b. For example, for the moment applied at the bottom, the moment in the column and spring must be in proportion to $k_t/(1+4k_t)$ versus k_b. The bending moment in the column is then given by $(k_t/(1+4k_t))/((k_t/(1+4k_t))+k_b) = k_t/(k_b+k_t+4k_bk_t)$ as indicated by the second terms of formula 2.13. The effect of the applied moment at the top may be similarly verified.

The way that the applied moments affect the column indicates that these will have a relatively small contribution. That will generally be true because the rotary stiffness of a column subject to sidesway will have a relatively low stiffness (as discussed in the context of formula 2.11) relative to the attached beams. For an approximate analysis, this means that most of the error in estimating the bending moments at the ends of a column will be due to errors in estimating the shear force in the column and therefore indirectly due to estimating the shear stiffness of the column.

Related to the end moments is the location of the inflection point because we can deduce that location from the end moments. The location of the inflection point measured from the bottom is given by:

$$x_I = \frac{(k_b+2k_bk_t)-k_t(M_b/(PL))+k_b(M_t/(PL))}{(k_b+k_t+4k_bk_t)} L \qquad \text{(on condition } 0 \leq x_I \leq L\text{)}$$
(2.14)

We note that, as required, formula 2.13 reduces to formula 2.6c when $k_b \to \infty$. Also, when k_b and k_t are both greater than one, which is the usual case, the inflection point is always between $0.4L$ and $0.6L$ when $M_b = M_t = 0$. The effect of M_b and M_t act against each other so that M_b causes the inflection point to shift down while M_t causes the inflection point to shift up. However, in any case, the effect of M_b and M_t on the inflection point location is small for the same reason that their effect on the end moments are small (see previous discussion). However, it is possible for unusually large values of M_b or M_t to cause the column to have no inflection point at all. Although the conditions for this are unusual, these can sometimes occur in a large number of floors multistory building at either the top floor where M_b is acting alone and may be relatively large or the ground floor where M_t is acting alone and may be relatively large.

2.5   Approximate Analysis of Multiple Floor Frames Subject to Horizontal Loads

In the previous section, we have identified that formula 2.12 gives us the shear stiffness of any column in a multi-story building with the attached beams at the top and bottom modeled by effective rotary stiffness factors and the attached columns modeled by applied moments. In addition, we have formula 2.13 which gives us the end moments in each column when given the same kind of information. We will use these two formulas to develop a method for solving any multi-story building subject to a side force. The outline of the method is as follows:

1. Start by estimating the effective rotary stiffness factors at the top and bottom of each column at every floor. Note that the ground floor is special so that the lower spring factor is taken to be infinite for a fixed support or zero for a hinge support. Equivalently, we can use formula 2.5 for the ground floor columns.

2. In a first iteration, assume that columns do not apply moments on each other (*ie.* $M_b = M_t = 0$ in formulas 2.12 and 2.13) and then use the rotary stiffness factors from step 1 to calculate the shear stiffness of each column using formula 2.12.

Using the shear stiffness of each column and with each floor considered separately, calculate the shear force in each column of a specific floor by dividing the net applied side force above that floor over the columns in that floor in proportion to their shear stiffness. The net applied side force at a floor is the total of all side forces that occur anywhere above the middle of the columns of the floor being considered.

3. Using formula 2.13, calculate the end moments and, optionally, using formula 2.14 calculate the inflection point in each column.

4. At this point, we have estimated the moments at the top and bottom of each column. If we now isolate a node or connection joining one or more beams with one or more columns, the moments applied by the columns at a node are known. Because these column moments are known, we can apply their algebraic sum as a point moment applied on the beams at the nodes. To get the beam end moments at a given floor, we then analyze all the beams at that floor as a continuous beam with no sidesway and with known point moments on the nodes applied by the columns. This problem may be approximately analyzed using the methods described in the previous chapter.

5. In a second optional iteration, use the end moments in the columns obtained from step 3 as an estimate of what moment to apply on the columns attached to them (*ie.* estimates of M_b and M_t). Again use formula 2.12 to calculate an updated shear stiffness for each column.

   Using the updated shear stiffness of each column and on each floor considered separately, calculate the shear force in the same manner as in step 2.

6. Repeat step 3 but with the updated shear force and applied moments.

7. Repeat step 4 but with updated estimates of column moments.

In the rest of this section, we will illustrate most of the steps of the outline specified above using figure 2.24 as a specific example.

The first step is to estimate the effective rotary stiffness of the beams on the ends of each column. This is done in the same way we did the single floor portal with two new considerations. First, columns have other columns attached to them as well as beams. In each case and based on previous discussions, we simply neglect the rotary stiffness provided by the columns. For example, at the top of column AD, the rotary stiffness factor is $1.5 \times (EI_{DE}/L_{DE}) / (EI_{AD}/L_{AD}) = 1.5 \times (2/5)/(2/4) = 1.2$. We note that we neglect the stiffness of column DG when obtaining this stiffness factor and the multiplier 1.5 is the same multiplier used
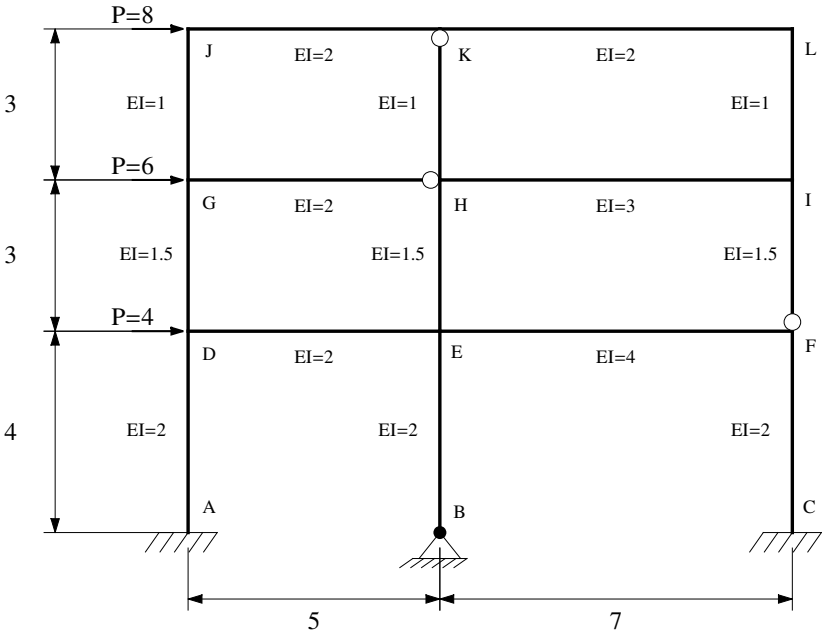
Figure 2.24. Multi-story sidesway example used to illustrate ideas.

in obtaining stiffness factors in single floor portals. The second consideration is that for all columns above the ground floor, we have to estimate the stiffness factor at the bottom as well as at the top of the column. For example, at the bottom of column HE, the rotary stiffness factor is $1.5 \times ((EI_{DE}/L_{DE}) + (EI_{EF}/L_{EF}))/(EI_{AD}/L_{AD}) = 1.5 \times ((2/5) + (4/7))/(1.5/3) \approx 2.914$. We note again that we neglect the stiffness of the attached column which is column EB in this case. The result of calculating the top and bottom stiffness factors for all the columns of all the floors is conveniently organized in table 2.6. As in the single floor portal frame, we note that we can obtain better estimates of the stiffness factors using the same guidelines that were described in the section on single floor portals.

Once we have estimated the rotary stiffness factors at the ends of all columns, we proceed to calculate the shear stiffness for each column. These shear stiffnesses are arranged by floor so that the relative shear stiffness may be calculated on a floor by floor basis. Once the relative shear stiffness is obtained, we determine the total force that must be resisted by the sum of the shear forces in all the columns of the given floor.

Table 2.6. Stiffness Factors at the Top of the Columns Shown in Figure 2.24.

Approximate analysis of a side loaded building		
Preliminary calculations		
Floor = 1		
column	1	2	3
stiffness factor at top	1.200	2.914	1.714
stiffness factor at bottom	∞	0	∞
Floor = 2		
column	1	2	3
stiffness factor at top	1.200	1.286	1.286
stiffness factor at bottom	1.200	2.914	0
Floor = 3		
column	1	2	3
stiffness factor at top	1.800	0	1.286
stiffness factor at bottom	1.800	1.929	1.929

For example, for the second floor of figure 2.24, we consider the free body diagram, with axial forces omitted for aesthetics, shown in figure 2.25. From figure 2.25, we determine that the total force to be resisted by the shear forces in the second floor columns is $8 + 6 = 14$. This total force is then multipied by the relative shear stiffness to obtain the shear force in each column in that second floor. This process is done for each floor and the calculations and results are conveniently organized in table 2.7. In that table, in addition to the shear force in each column of each floor, we
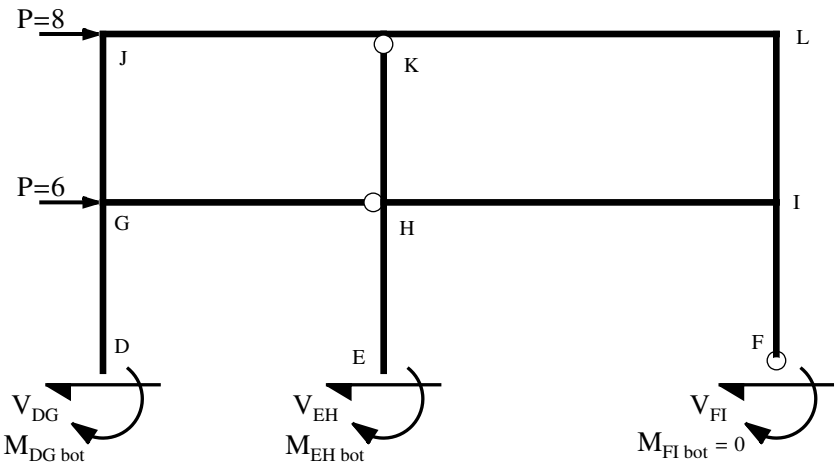
Figure 2.25. Free body diagram (excluding vertical axial forces) of figure 2.24 by taking a cut just above the first floor beams.

Table 2.7. First Iteration Calculations of Shear Stiffness, Shear Force and End Moments in the Columns Shown in Figure 2.24.

	Iteration number $= 1$			
Floor $= 1$				
column number	1	2	3	
shear stiffness	0.247	0.075	0.271	0.593
relative shear stiffness	0.417	0.126	0.458	1
shear	7.501	2.263	8.236	18
Internal moment at top	12.415	9.051	14.376	
Internal moment at bottom	-17.589	0	-18.569	
Floor $= 2$				
column number	1	2	3	
shear stiffness	0.296	0.368	0.105	0.769
relative shear stiffness	0.385	0.478	0.137	1
shear	5.392	6.692	1.916	14
Internal moment at top	8.088	9.186	5.747	
Internal moment at bottom	-8.088	-10.890	0	
Floor $= 3$				
column number	1	2	3	
shear stiffness	0.242	0.080	0.226	0.549
relative shear stiffness	0.442	0.146	0.413	1
shear	3.533	1.166	3.301	8
Internal moment at top	5.300	0	4.708	
Internal moment at bottom	-5.300	-3.498	-5.193	

also calculate the bending moment at the top and bottom of each column of each floor using 2.13 with $M_b = M_t = 0$.

Once we are done with the first iteration, we may do a second iteration. To decide whether a second iteration is needed we note the following:

- In general, the first iteration will give an adequate approximation for a preliminary analysis. If we evaluate the error in the shear force of the columns with the largest such values in each floor then the relative errors in the first iteration will be about 10% to 30%.

- The relative error in all columns decreases as the stiffness contrast between columns in the same floor decreases.

- A second iteration generally improves the results by a relative error of about 10% to 15%.

- Relatively low errors of less than about 5% to 10% in all columns can be achieved only if we carefully estimate and update the rotary stiffness

contribution of the beams on the columns. We must improve such esti-
mates for all the columns simultaneously because if we only improve
such an estimate for only one column then we may actually increase
the errors in the shear stiffness contrast between columns. We note that
it is the shear stiffness contrast between columns that determines how
the total horizontal forces are distributed over the columns.

If we decide to do a second iteration then the process of doing this
is similar to the first iteration but with updated values of M_b and M_t in
formulas 2.12 and 2.13. We start by calculating the shear stiffness of each
column. To that end, for a given column, we use the top bending moment
in the column below it for M_b or zero if it is the ground floor. Also, we use
negative the bottom bending moment of the column above it for M_t or
zero if it is the top floor. The reason we use positive the bending moment
from the column below but negative the bending moment from the col-
umn above in formulas 2.12 and 2.13 is because of conflicting sign con-
ventions. Formulas 2.12 and 2.13 consider clockwise applied moments to
be positive for both the top and bottom applied moments while the con-
vention used for bending moments at the ends of columns imply posi-
tive values for counterclockwise moments transmitted from above and
clockwise from below. Finally, we note that 'P' in formulas 2.12 and 2.13
correspond to the shear force in the colums and this is estimated from
the shear force in the column obtained from the first iteration.

For example, for column DG, $P = 5.392$, $M_b = 12.415$ and $M_t = -(-5.300) = 5.300$. Using formula 2.12 and the rotary stiffness factors
for column DG (*ie.* 1st column of 2nd floor in table 2.6), we get a shear
stiffness of $((1.2 + 1.2 + 4 \times 1.2 \times 1.2)/(3 + 4 \times 1.2 + 4 \times 1.2 + 4 \times 1.2 \times 1.2 + (3 + 6 \times 1.2) \times (5.300/(5.392 \times 3)) + (3 + 6 \times 1.2)(12.415/(5.392 \times 3)))) (12 \times 1.5 /3^3) \approx 0.1842$. This value along with all the other shear
stiffnesses is organized and presented in table 2.8 which has the same
form as the table for the first iteration.

For comparison, figure 2.26 shows the exact and approximate (with
2 iterations) column shears and end moments for the problem of
figure 2.24. We note that most of the shear forces and end moments are
well approximated with errors that are less than about 10% to 20% with
the exception of column DG. In that column, the shear force and the end
moments are significantly overestimated. If we do a third iteration in a
similar way to the second iteration, we find that the errors remain about
the same with less than about 5% change in values. To understand the
source of error in column DG, we must look elsewhere.

To understand the source of error in column DG, we compare
the exact and approximate (with 2 iterations) shear stiffnesses of the
columns and these are shown in table 2.9. We note that most of the shear

Table 2.8. Second Iteration Calculations of Shear Stiffness, Shear Force and End Moments in the Columns Shown in Figure 2.24.

	Iteration number = 1			
Floor = 1				
column number	1	2	3	
shear stiffness	0.209	0.060	0.271	0.540
relative shear stiffness	0.387	0.111	0.503	1
shear	6.960	1.994	9.046	18
Internal moment at top	10.125	7.977	15.790	
Internal moment at bottom	−17.713	0	−20.395	
Floor = 2				
column number	1	2	3	
shear stiffness	0.184	0.296	0.079	0.559
relative shear stiffness	0.329	0.529	0.141	1
shear	4.611	7.413	1.976	14
Internal moment at top	7.962	10.251	5.929	
Internal moment at bottom	−5.869	−11.988	0	
Floor = 3				
column number	1	2	3	
shear stiffness	0.180	0.046	0.182	0.409
relative shear stiffness	0.441	0.113	0.447	1
shear	3.525	0.903	3.572	8
Internal moment at top	6.166	0	5.659	
Internal moment at bottom	−4.408	−2.708	−5.058	

Table 2.9. Comparison Between the Exact and Approximate (2 Iteration) Shear Stiffness of the Columns Shown in Figure 2.24.

shear stiffness	column 1 exact (approx)	column 2 exact (approx)	column 3 exact (approx)
floor 1	0.207 (0.209)	0.062 (0.060)	0.261 (0.271)
floor 2	0.111 (0.184)	0.333 (0.296)	0.081 (0.079)
floor 3	0.126 (0.180)	0.032 (0.046)	0.160 (0.182)

stiffnesses are very well estimated with the biggest exception being column DG (*ie.* column 1 and floor 2). If then consider figure 2.26 and the way in which we have estimated the rotary stiffness of the beams, we can then account for most of this discrepancy. In particular, we have considered beam GH as providing 1.5 times its rotary stiffness to column DG but since it has an internal hinge at end H, it can only provide 0.75 times its rotary stiffness. Therefore, the shear stiffness should be much lower than the standard but simple to apply estimate that we have used in these calculations.
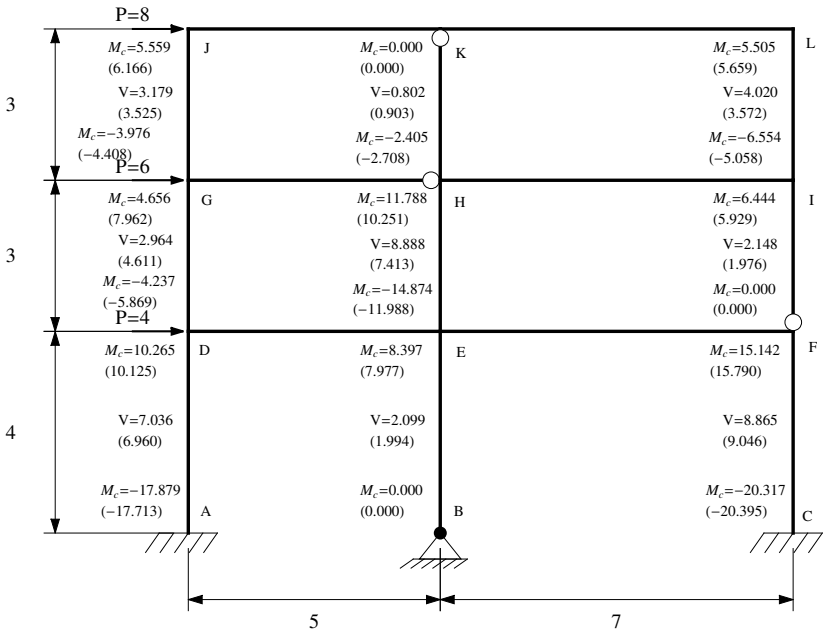
Figure 2.26. Shear forces and end moments in the columns of the structure shown in figure 2.24. Note that the approximate results are shown in parentheses under the exact results.

In addition to column DG, table 2.9 reveals another large discrepancy in the estimate of the shear stiffness. Specifically, column EB (*ie.* column 2 and floor 1) has a stiffness that is again overestimated. However, this overestimate did not lead to the same relatively large errors as in column DG. The reason is that all the columns of the first floor, for different reasons, have been overestimated and what is important in obtaining the shear force and consequently the end moments is the relative shear stiffness. If we apply the previously discussed recommendations on getting improved estimates of the rotary stiffness of the resisting beams then we would get much better overall shear stiffness, shear and end moment estimates for column DG, EB as well as for all the other columns.

As a second example, we analyze the problem shown in figure 2.27. The analysis steps are the same as in the previous example. First, we obtain the effective rotary stiffness factors at the top and bottom of each column at every floor and this is summarized in table 2.10. Next, we calculate the shear stiffness using formula 2.12 from which we then obtain the relative shear stiffness and the shear force in each column. With the
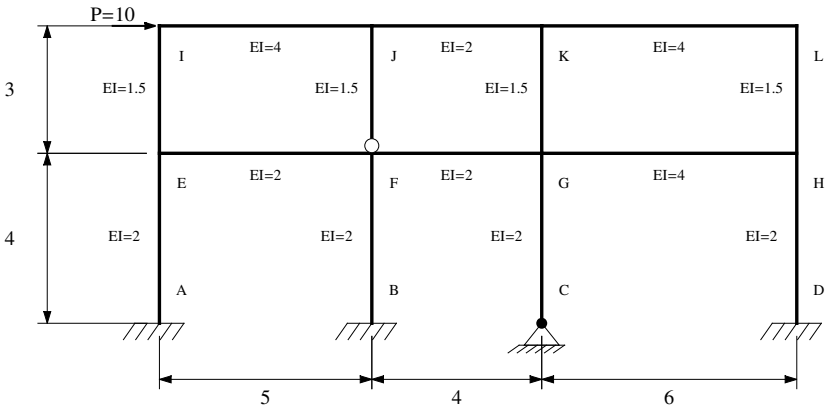
Figure 2.27. Multi-story sidesway example used to illustrate ideas.

Table 2.10. Stiffness Factors at the Top of the Columns Shown in Figure 2.27.

Approximate analysis of a side loaded building			
Preliminary calculations			
Floor $= 1$			
column	1	2	3	4
stiffness factor at top	1.200	2.700	3.500	2.000
stiffness factor at bottom	∞	∞	0	∞
Floor $= 2$			
column	1	2	3	4
stiffness factor at top	2.400	3.900	3.500	2.000
stiffness factor at bottom	1.200	0	3.500	2.000

shear force in each column known, we may then calculate the end mo-
ments using formula 2.13 with 'P' in that formula being the shear force
in each respective column. At the beginning, the values of 'M_b' and 'M_t'
in formulas 2.12 and 2.13 are taken to be zero for every column and the
results obtained using that assumption are identified as a first iteration
result and are shown in table 2.11.

At this point, the first iteration results may be considered as a rough
approximation that is suitable for preliminary analysis. In the problem
of figure 2.27, the maximum relative error in the shear forces in all the
columns is about 29% while the mean of the absolute value of the rela-
tive errors is about 16%. If we decide to do a second iteration analysis,
we will have to use updated values of 'M_b' and 'M_t' that we obtain from
the end moments in the columns of the first iteration. The result of doing

Table 2.11. First Iteration Calculations of Shear Stiffness, Shear Force and End Moments in the Columns Shown in Figure 2.27.

	Iteration number = 1				
Floor = 1					
column number	1	2	3	4	
shear stiffness	0.247	0.299	0.077	0.281	0.905
relative shear stiffness	0.273	0.331	0.085	0.311	1
shear	2.732	3.305	0.853	3.109	10
Internal moment at top	4.522	6.050	3.414	5.527	
Internal moment at bottom	−6.407	−7.171	0	−6.909	
Floor = 2					
column number	1	2	3	4	
shear stiffness	0.349	0.140	0.467	0.381	1.336
relative shear stiffness	0.261	0.105	0.349	0.285	1
shear	2.609	1.046	3.493	2.852	10
Internal moment at top	4.224	3.139	5.240	4.277	
Internal moment at bottom	−3.603	0	−5.240	−4.277	

Table 2.12. Second Iteration Calculations of Shear Stiffness, Shear Force and End Moments in the Columns Shown in Figure 2.27.

	Iteration number = 2				
Floor = 1					
column number	1	2	3	4	
shear stiffness	0.202	0.299	0.061	0.240	0.802
relative shear stiffness	0.252	0.373	0.076	0.299	1
shear	2.518	3.730	0.758	2.994	10
Internal moment at top	3.546	6.828	3.032	4.848	
Internal moment at bottom	−6.525	−8.093	0	−7.129	
Floor = 2					
column number	1	2	3	4	
shear stiffness	0.259	0.140	0.425	0.298	1.122
relative shear stiffness	0.231	0.125	0.379	0.266	1
shear	2.305	1.246	3.789	2.659	10
Internal moment at top	4.450	3.738	5.897	4.542	
Internal moment at bottom	−2.466	0	−5.471	−3.436	

a second calculation is shown in table 2.12 and are compared with the exact results in figure 2.28. By doing this second iteration, we find that the maximum relative error in the shear force in all the columns is about 14% (*ie.* a 15% improvement in the column shears) and the mean of the absolute value of the relative errors is about 6% (*ie.* about 10% improvement from the first iteration).
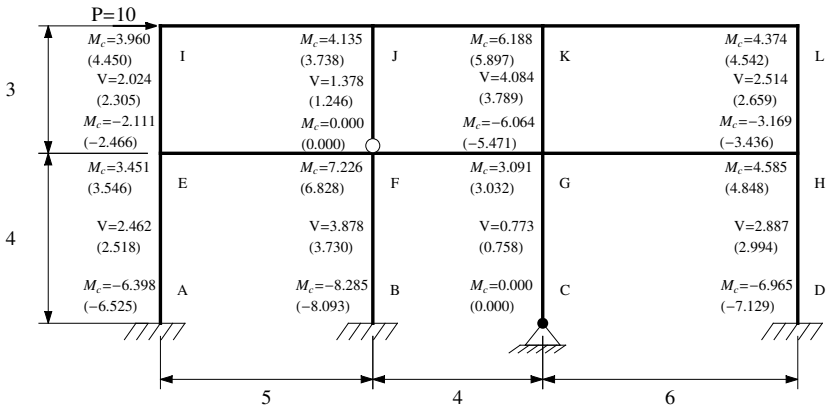
Figure 2.28. Shear forces and end moments in the columns of the structure shown in figure 2.27. Note that the approximate results are shown in parentheses under the exact results.

Table 2.13. Comparison Between the Exact and Approximate (2 Iteration) Shear Stiffness of the Columns Shown in Figure 2.27.

shear stiffness	column 1	column 2	column 3	column 4
	exact (approx)	exact (approx)	exact (approx)	exact (approx)
floor 1	0.198 (0.202)	0.311 (0.299)	0.062 (0.061)	0.232 (0.240)
floor 2	0.222 (0.259)	0.151 (0.140)	0.449 (0.425)	0276 (0.298)

In order to identify the main source of the error in the problem of figure 2.27, we again compare the exact versus (second iteration) approximate shear stiffness of the columns. This comparison is shown in table 2.13. The results indicate that the maximum error in the shear force and in the shear stiffness correspond to the same column. In order to improve the results obtained, we will find that a third iteration will not be effective. If we do a third iteration for the problem of figure 2.27, we will get a maximum relative error in the shear forces in all the columns of about 15% (a slight improvement of 1% over the second iteration) and a mean of the absolute value of the relative errors of about 8% (a 2% worsening over the second iteration). In fact, these iterations appear to converge but not to the exact results unless we input better estimates of the effective rotary stiffness provided by the beams to the columns. We note that if we use the recommendations identified previously, the biggest change in the effective rotary stiffness would be precisely in the columns with the largest errors. By improving our estimates of the rotary stiffness

factors, the shear stiffness estimates improve and consequetly the shear force and all the other results improve as well.

2.6   A Note on the Lumped Mass Model for Buildings

Before we consider how to sketch the deformed shape of frames subject to sidesway, we will discuss a particular model of a building subject to side forces which will be useful in identifying the general deformation pattern of a frame subject to sidesway. That model is often used in structural dynamics analysis and is called the lumped-mass model. The lumped mass model simplifies a building so that each floor is modeled as one mass and so that consecutive floors are attached to each other by linear springs in series. For example, the frame in figure 2.29 would be modeled as four masses attached to springs in series as shown in figure 2.30a. In addition to the springs, dashpot units may also be attached between consecutive floors in a way similar to that of the springs. In this section, we will use the concepts developed in previous sections to discuss those aspects of the lumped-mass model associated with calculating the shear stiffness in columns.
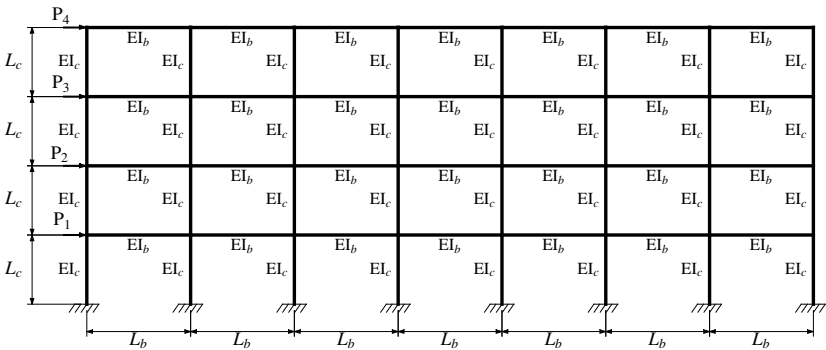
Figure 2.29. Frame building type analyzed to compare lumped mass shear stiffness with exact shear stiffness.

The basic assumption of the lumped-mass model is that the beams attached to the columns are so stiff that the rotations at the ends of columns are negligible. If we use formula 2.12, we find that this implies that the shear stiffness of a column is $12\,EI_c/L_c^3$ (see symbol definitions below formula 2.12). To assess this assumption, we compare this stiffness with the apparent shear stiffness of buildings like the one shown in
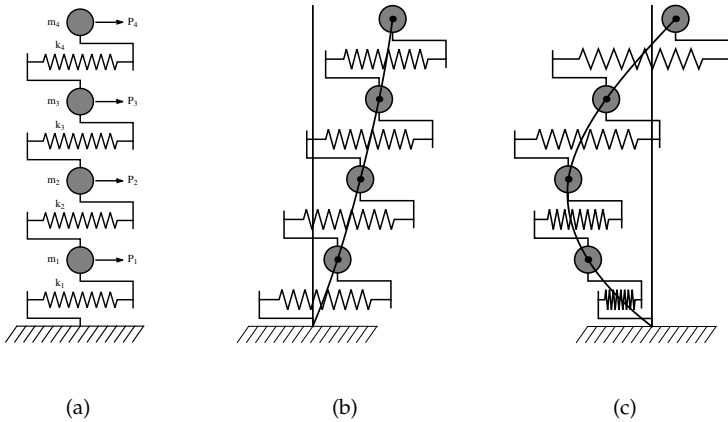
Figure 2.30. Lumped-mass system for a framed building with the first two modes of deformation assuming all columns have the same stiffness.

figure 2.29 having all its beams similar to each other and all its column similar to each other and with exactly seven beam spans but with a variable number of floors and with a variable ratio of the beam to column rotary stiffness (*ie.* $(EI_c/L_c)/(EI_b/L_b)$).

When we do an exact analysis, we find that, unlike the mass model, the shear stiffness of the columns depend on the pattern of applied side forces 'P_i.' The reason is that the shear stiffness of a column also depends on the moments transmitted from the columns above and below it (see figure 2.19 and 2.20) which in turn depends on the pattern of applied side forces. In order to decide on what pattern of side forces is most relevant for analysis, we need to consider how we typically use the lumped-mass model in structural dynamics. In structural dynamics, after we obtain the parameters of the lumped-mass model, we usually do a modal analysis. This modal analysis gives the natural frequencies of the building and for each natural frequency we obtain a pattern of deformation called an eigenmode. If we rank the frequencies and their eigenmodes in order of increasing frequency, the one with the lowest frequency is called the first mode, the second the second mode and so on. For example, the first and second modes of the lumped-mass model shown in figure 2.30a are shown in figures 2.30b and c for some typical configurational parameters.

In many buildings, it is often considered sufficiently accurate to consider relatively few eigenmodes when doing a structural dynamics study. Therefore, to test the assumptions of the lumped-mass model, we

will consider an applied load pattern that roughly corresponds to the
the first two modes of deformation. An example of such loads and the
response of the frame shown in figure 2.29 is shown in figure 2.31 for the
first mode and in figure 2.34 for the second mode. We will next discuss
how the shear stiffness of each of those modes compare with those of the
lumped-mass model.
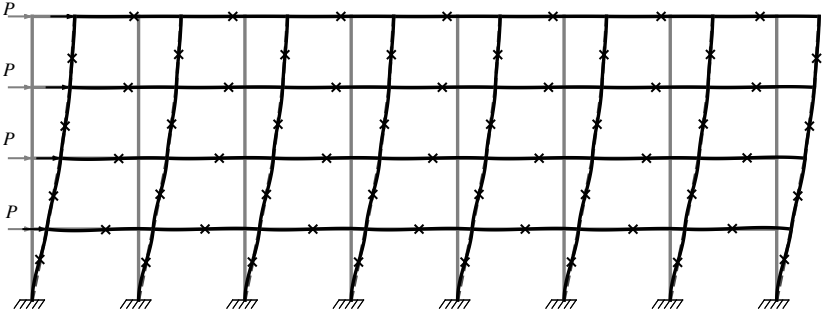
Figure 2.31. Frame building type analyzed to compare lumped mass shear
stiffness with exact shear stiffness for an approximate first mode pattern of
deformation.

First we consider the first mode and to that purpose we consider
the loading shown in figure 2.31. By analyzing that frame, we find that
the shear stiffness of columns within one floor varies from column to
column. However, since the lumped-mass model uses a single spring
to represent a whole floor, we will compare the mean shear stiffness of
columns in a floor with the uniform value identified by the lumped-mass
model. The normalized mean shear stiffness (*ie.* shear stiffness divided
by EI_c/L_c^3) when the relative rotary stiffness of a beam to a column is 1
and 3 are shown in tables 2.14 and 2.15 respectively. In addition to the
normalized mean shear stiffness, the tables also show the ratio of the
maximum shear stiffness to the minimum shear stiffness in the columns
of each floor and these are shown in parenthesis. Those tables indicate
the following:

i) The shear stiffness factor is significantly less than 12 and we note that
the values of rotary stiffness considered are within the typical range
for buildings.

ii) The columns at the ground floor have higher stiffnesses than those at
the rest of the floors because of their fixed supports.

iii) The columns at floors above the ground floor have approximately the same mean shear stiffness (*eg.* about 4.5 and 7.5 when the relative rotary stiffness of beams to columns is 1 and 3).

iv) The mean shear stiffness of columns at floors above the ground floor are relatively insensitive to the number of floors.

Table 2.14. Mean and Maximum Over Minimum Ratios of the Normalized Shear Stiffness of Columns by Floor for the Building Type Shown in Figure 2.29 for Various Number of Floors with $P_i = P$ (Same) at all Floors and $(EI/L)_{beam}/(EI/L)_{column} = 1$ for All Beams and Columns.

Normalized shear stiffness at floor (mean and max/min)

number of floors →	1	2	3	4	5	6	7
floor = 7							4.14 (2.02)
floor = 6						4.14 (2.02)	4.33 (1.74)
floor = 5					4.14 (2.02)	4.33 (1.74)	4.34 (1.76)
floor = 4				4.15 (2.02)	4.34 (1.74)	4.34 (1.76)	4.35 (1.76)
floor = 3			4.21 (1.96)	4.38 (1.71)	4.38 (1.73)	4.37 (1.73)	4.37 (1.74)
floor = 2		4.58 (2.01)	4.65 (1.75)	4.62 (1.77)	4.59 (1.77)	4.58 (1.76)	4.57 (1.76)
floor = 1	8.60 (1.30)	7.77 (1.22)	7.40 (1.26)	7.22 (1.27)	7.12 (1.28)	7.05 (1.28)	7.00 (1.29)

Table 2.15. Mean and Maximum Over Minimum Ratios of the Normalized Shear Stiffness of Columns by Floor for the Building Type Shown in Figure 2.29 for Various Number of Floors with $P_i = P$ (Same) at All Floors and $(EI/L)_{beam}/(EI/L)_{column} = 3$ for All Beams and Columns.

Normalized shear stiffness at floor (mean and max/min)

number of floors →	1	2	3	4	5	6	7
floor = 7							7.38 (1.57)
floor = 6						7.38 (1.57)	7.46 (1.51)
floor = 5					7.38 (1.57)	7.46 (1.51)	7.46 (1.51)
floor = 4				7.38 (1.57)	7.46 (1.51)	7.46 (1.51)	7.46 (1.51)
floor = 3			7.39 (1.56)	7.47 (1.50)	7.47 (1.51)	7.47 (1.51)	7.47 (1.51)
floor = 2		7.53 (1.63)	7.56 (1.55)	7.55 (1.55)	7.54 (1.54)	7.54 (1.54)	7.54 (1.54)
floor = 1	10.43 (1.18)	9.89 (1.18)	9.68 (1.20)	9.58 (1.21)	9.52 (1.22)	9.48 (1.22)	9.45 (1.22)

Further parametric studies also indicate that the mean shear stiffness of columns at floors above the ground floor are relatively insensitive to the number of spans above 2 spans and relatively insensitive to the distribution of side-forces as long as they are all in the same direction and the top floor is loaded. Therefore, the lumped-mass model generally overes-

timates the stiffness of a frame and the the error may not be fixed by simply multiplying the stiffness of all columns by some factor because the ground floor columns have a different stiffness from those at the other floors. However, if the building has many stories, the pattern of deformation should match the exact one except for a possible discrepancy at the first floor.

To get an indication of how the shear stiffness varies with the relative rotary stiffness of beams to columns, we plot in figure 2.32 the normalized mean shear stiffness of the columns at the fifth floor in a ten story building as a function of the relative beam to column stiffness. As expected, this normalized stiffness tends to 12 as the beams become infinitely stiff. However, the rate at which this happens is rather slow with typical values of beam to column rotary stiffness having normalized shear stiffness values that are significantly lower than the limit of 12. We note that when the relative rotary stiffness of beams to columns approaches zero, the normalized mean shear stiffness of columns approaches a small but non-zero value which, in the case of figure 2.32 is about 0.04. A rational expression curve fitted to the data of figure 2.32
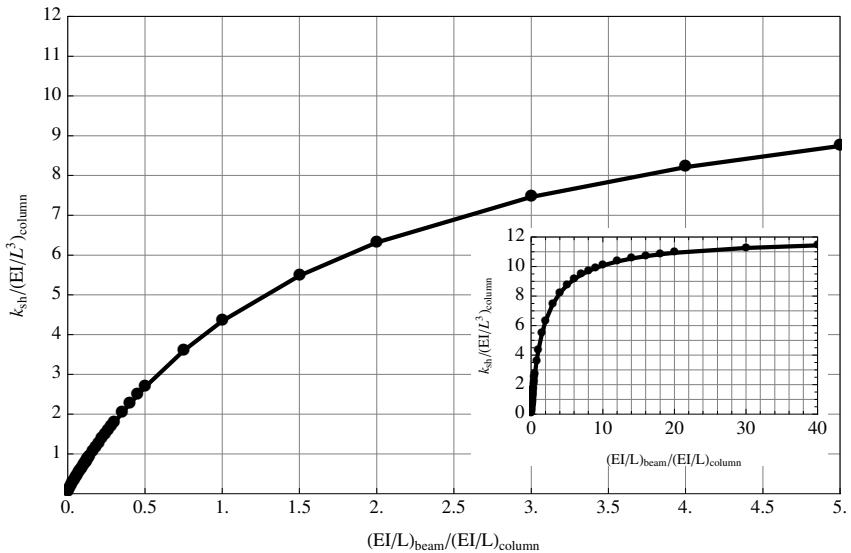
Figure 2.32. Mean normalized shear stiffness of 5th floor columns in a 10 floor framed building as a function of the relative rotary stiffness of a beam versus a column. Building system configuration assumes that $P_i = P$ (same), all beams have same sectional properties and all columns have same sectional properties.

and to comparable data for the ground floor gives the following result for the mean shear stiffness:

$$
k_{\text{sh mean}} =
\begin{cases}
\left(\dfrac{1+72k}{11+6k}\right) \times \dfrac{EI_c}{L_c} & \text{mid floor} \\[2ex]
\left(\dfrac{1+132k}{9+11k}\right) \times \dfrac{EI_c}{L_c} & \text{ground floor}
\end{cases}
\tag{2.15}
$$

where: $k = (EI_b/L_b)/(EI_c/L_c)$ and is the relative rotary stiffness of a beam to a column.

The above formula 2.15 is qualitatively applicable and often approximately accurate to spans above 3 and number of floors above 3 and to a wide variety of side-force loading patterns.

In addition to the mean normalized shear stiffness, tables 2.14 and 2.15 also present the ratio of maximum to minimum shear stiffness in the floors of a column. This ratio is relevant to another approximate method used for portal frames and called the portal method. The portal method assumes that all inner columns take twice the shear of the two outer columns which is equivalent to assuming that the inner columns have twice the stiffness of the outer columns. Based on the plot shown in figure 2.33, this assumption has significant errors even for a highly patterned building of the type shown in figure 2.29. Figure 2.33 indicates that typical values of the ratio of inner to outer column shears is somewhere between 1.4 and 1.7 but may reach a maximum of 1.92 at the atypical rotary stiffness ratio of about 0.174. Of course, geometrical and configurational variation of columns and beams cannot be addressed by the portal method but can be simply analyzed using the methods previously discussed.

Next we consider the second mode and to that purpose we consider the loading shown in figure 2.34. By analyzing that frame, we find that the shear stiffness of columns within one floor varies from column to column. However, since the lumped-mass model uses a single spring to represent a whole floor, we will compare the mean shear stiffness of columns in a floor with the uniform value identified by the lumped-mass model. The normalized mean shear stiffness (*ie.* shear stiffness divided by EI_c/L_c^3) when the relative rotary stiffness of a beam to a column is 1 and 3 are shown in tables 2.16 and 2.17 respectively. In addition to the normalized mean shear stiffness, the tables also show the ratio of the maximum shear stiffness to the minimum shear stiffness in the columns of each floor and these are shown in parenthesis. Those tables indicate the following:

i) The shear stiffness factor is significantly less than 12 and we note that the values of rotary stiffness considered are within the typical range for buildings.
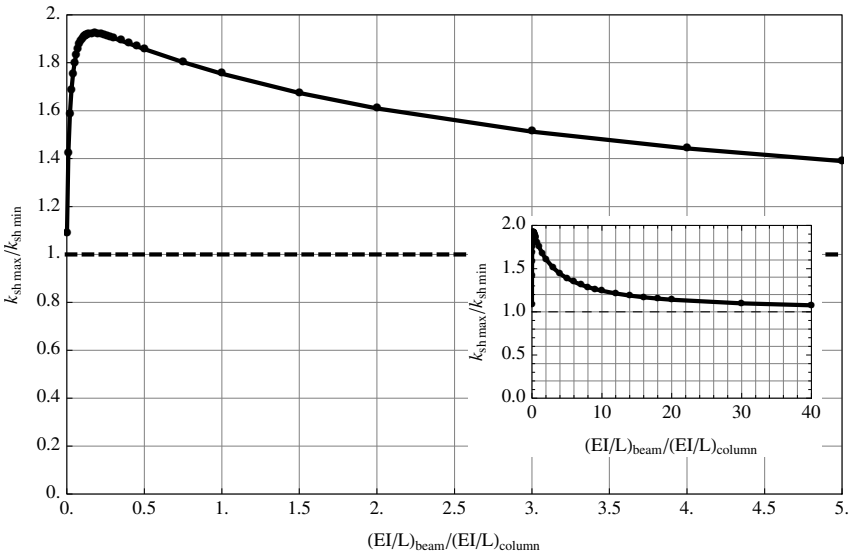
Figure 2.33. Maximum over minimum ratios of the shear stiffness of 5th floor columns in a 10 floor framed building as a function of the relative rotary stiffness of a beam versus a column. Building system configuration assumes that $P_i = P$ (same), all beams have same sectional properties and all columns have same sectional properties.
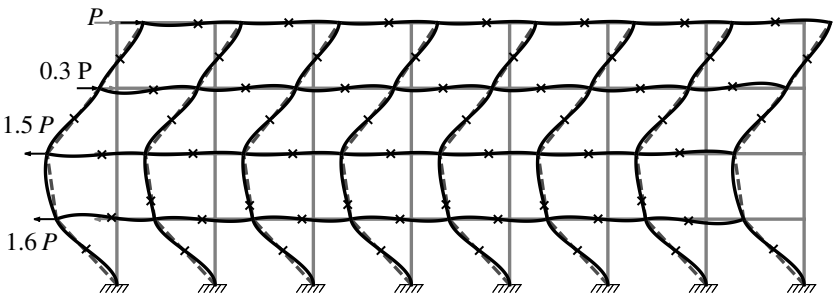
Figure 2.34. Frame building type analyzed to compare lumped mass shear stiffness with exact shear stiffness for second mode.

ii) The columns at the ground floor have higher stiffness than those at the rest of the floors because of their fixed supports. In one case, when we have only two floors, the normalized mean shear stiffness of the columns at the ground floor exceeds 12 and will be explained below.

Table 2.16. Mean and Maximum over Minimum Ratios of the Normalized Shear Stiffness of Columns by Floor for the Building Type Shown in Figure 2.29 for Various Number of Floors with $P_{top} = P$, $P_{mid} = -1.6\,P$ and $P_{other} = 0$ at All Floors and $(EI/L)_{beam}/(EI/L)_{column} = 1$ for All Beams and Columns.

Normalized shear stiffness at floor (mean and max/min)

number of floors →	2	4	6	8	10
floor = 10					5.13 (1.70)
floor = 9					4.42 (1.72)
floor = 8				5.13 (1.70)	4.37 (1.75)
floor = 7				4.44 (1.71)	4.49 (1.76)
floor = 6			5.15 (1.69)	4.49 (1.76)	6.06 (1.39)
floor = 5			4.57 (1.73)	6.06 (1.39)	8.24 (1.20)
floor = 4		5.33 (1.70)	6.08 (1.39)	8.25 (1.20)	4.59 (1.77)
floor = 3		6.19 (1.37)	8.31 (1.20)	4.61 (1.75)	4.39 (1.72)
floor = 2	7.49 (1.34)	8.84 (1.20)	4.79 (1.77)	4.55 (1.74)	4.52 (1.76)
floor = 1	17.22 (1.04)	7.25 (1.33)	6.79 (1.30)	6.73 (1.31)	6.73 (1.31)

Table 2.17. Mean and Maximum over Minimum Ratios of the Normalized Shear Stiffness of Columns by Floor for the Building Type Shown in Figure 2.29 for Various Number of Floors with $P_{top} = P$, $P_{mid} = -1.6\,P$ and $P_{other} = 0$ at All Floors and $(EI/L)_{beam}/(EI/L)_{column} = 3$ for All Beams and Columns.

Normalized shear stiffness at floor (mean and max/min)

number of floors →	2	4	6	8	10
floor = 10					8.22 (1.43)
floor = 9					7.49 (1.52)
floor = 8				8.22 (1.43)	7.46 (1.51)
floor = 7				7.49 (1.51)	7.51 (1.53)
floor = 6			8.22 (1.42)	7.51 (1.53)	8.85 (1.29)
floor = 5			7.54 (1.53)	8.85 (1.29)	10.11 (1.16)
floor = 4		8.27 (1.44)	8.86 (1.29)	10.11 (1.16)	7.54 (1.54)
floor = 3		8.89 (1.29)	10.12 (1.16)	7.54 (1.54)	7.47 (1.50)
floor = 2	9.88 (1.21)	10.22 (1.18)	7.60 (1.57)	7.52 (1.53)	7.52 (1.54)
floor = 1	13.37 (1.05)	9.40 (1.27)	9.29 (1.23)	9.29 (1.24)	9.29 (1.24)

iii) The columns at floors above the ground floor have approximately the same mean shear stiffness (*eg.* about 4.5 and 7.5 when the relative rotary stiffness of beams to columns is 1 and 3) except near the floor where the reversal in deflection starts.

iv) The mean shear stiffness of columns at floors above the ground floor are relatively insensitive to the number of floors except near the floor where the reversal in deflection starts.

Further parametric studies also indicate that the mean shear stiffness of columns at floors above the ground floor are relatively insensitive to the number of spans above 2 spans and relatively insensitive to the distribution of side-forces as long as there is one reversal in displacement occuring at the same level in the building. Therefore, the lumped-mass model generally overestimates the stiffness of a frame and the error may not be fixed by simply multiplying the stiffness of all columns by some factor because the ground floor columns have a different stiffness from those at the other floors. Furthermore, even when the building has many stories, the exact pattern of deformation may significantly differ from that of the lumped-mass model and these two patterns may not be reconciled by a simple scaling factor. The additional difficulty in this second mode of deformation is that we do not know a-priori where the displacement reversal will occur because this depends on the pattern of shear stiffness between adjacent floors which the lumped-mass model assumes up front. In that regards, we note that figure 2.19 and 2.20 and the associated formula 2.12 can be used to understand why the relative shear stiffness increases in the columns of the floors where the displacement starts to reverse. Specifically, when the displacement reverses, the moment at the top of the column is acting to restrict and thus to stiffen the connected column while such moments for the other columns enhance and thus reduce the stiffness of connected columns. In particular, when there is only one story, the effect of restricting moment is more pronounced and leads to column stiffnesses at the ground floor that may exceed a normalized mean shear stiffness of 12.

In summary, the lumped-mass model overestimates the shear stiffness of columns but may give acceptable patterns of deformation for the first mode of deformation. Furthermore, by using some scaling factor, it may be also possible to get a good approximation between this first mode's natural frequency and the exact one. Unfortunately, for modes higher than one, this simple fix may not be reliably possible. However, most of the deformation of a tall building (usually above 80%) may be accounted for by the first mode of deformation so that the lumped-mass model remains a useful model to study.

2.7 Sketching Multiple Floor Frames Subject to Horizontal Loads

Now that we've discussed how to calculate the shear and bending moments in the columns and beams of a multi-story frame subject to sidesway and we've discussed the relatively simpler lumped-mass model and its deformation patterns, we turn to the matter of sketching the deformed

shape of frames subject to sidesway. In this regards, we will extend the procedure developed for sketching single floor portal frames. The steps remain the same and these are repeated concisely below:

   i) Draw the column and beam chords.

  ii) Draw the directions or tangents to most columns and beams at the nodes or connections.

 iii) Draw the columns by using the tangents at the nodes and figures 2.14 and 2.15 as a guide for the ground floor and figure 2.20 for the other floors.

  iv) Draw the beams by using the tangents at the nodes as a guide.

   v) Draw the column or columns with rollers (if any) using the tangents as a guide and knowing that those columns must be subject to a rigid rotation.

  vi) Remove extraneous lines that were used in constructing the sketch in order to get a better looking drawing of the deformed shape. In this step, we recommend that the chords be kept because they help to clarify the deformations of the columns and beams.

   In the above steps, we will give additional suggestions on how to sketch the chords of columns and the deformed columns themselves. This is additional information related to steps (i) and (iii) above. The rest of the steps are similar to sketching the previously discussed single floor portal.

   We start by discussing how to sketch the column chords. In a single floor portal, we simply choose a convenient slope for the chord of any column and all the other chords of the columns must be parallel to that one. This observation still applies on a floor by floor basis in a multi-story frame. Once we choose the sidesway or slope of one of the chords of the columns in a given floor then all the other chords of the columns on the same floor must be parallel to that one. What remains to be discussed is the relative slopes of the chords at different floors. In that regards, we will find it useful to define a frame's chord-line to be the line joining a representative chord of a column from each floor connected to other representative columns in successive floors all the way from the ground to the top floor.

   The shape of a frame's chord-line depends on how the total shear stiffness of all columns in a floor vary from floor to floor and on the pattern of side loading. To estimate this shape, we can use the lumped-mass model with the shear stiffness of the columns adjusted according to the

methods of previous sections. We start by considering the deformation pattern when we apply a side force at only the top floor of a regular frame as shown in figures 2.35. In that case, the total shear force in the columns of any given floor is the same for all floors. This total shear force divided by the total shear stiffnesses of the columns in a given floor gives the sidesway for that floor. When there is some regularity in the frame, the total shear stiffness of the floors are all about the same with relatively large deviation only at the ground floor. Therefore, the sidesway of the floors will all be about the same and this leads to the frame chord-line being approximately linear. This trend is apparent in all of figures 2.35 that have more than one floor with small deviations at the ground floor due to the relatively large deviation in that floor's shear stiffness.
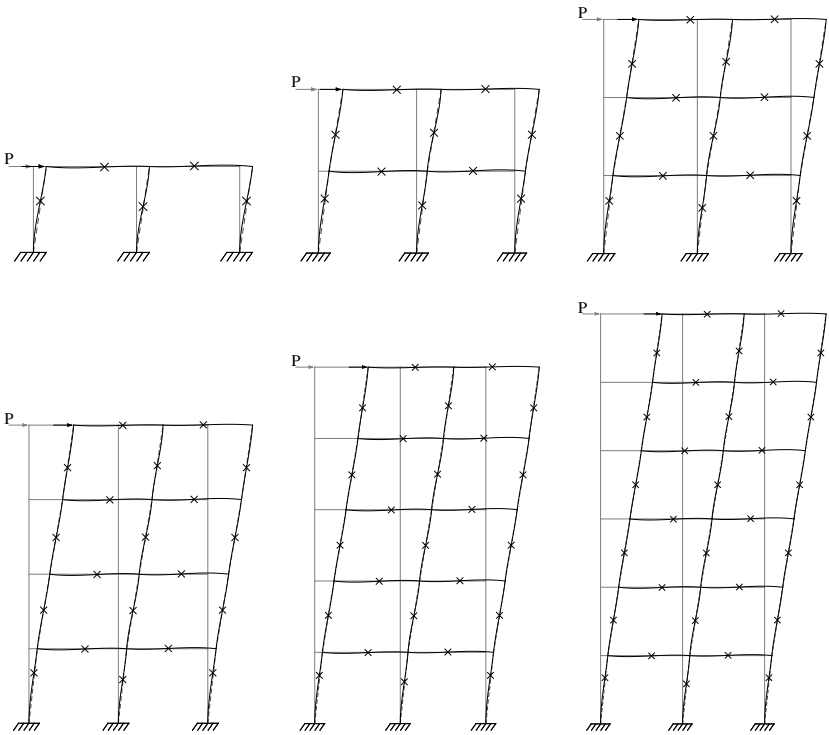
Figure 2.35. Deformation pattern for side-loaded frames with only the top floor loaded.

Next we consider the deformation pattern when we apply the same side force at each floor of a regular frame as shown in figures 2.36. In that case, the total shear force in the columns of any given floor decreases
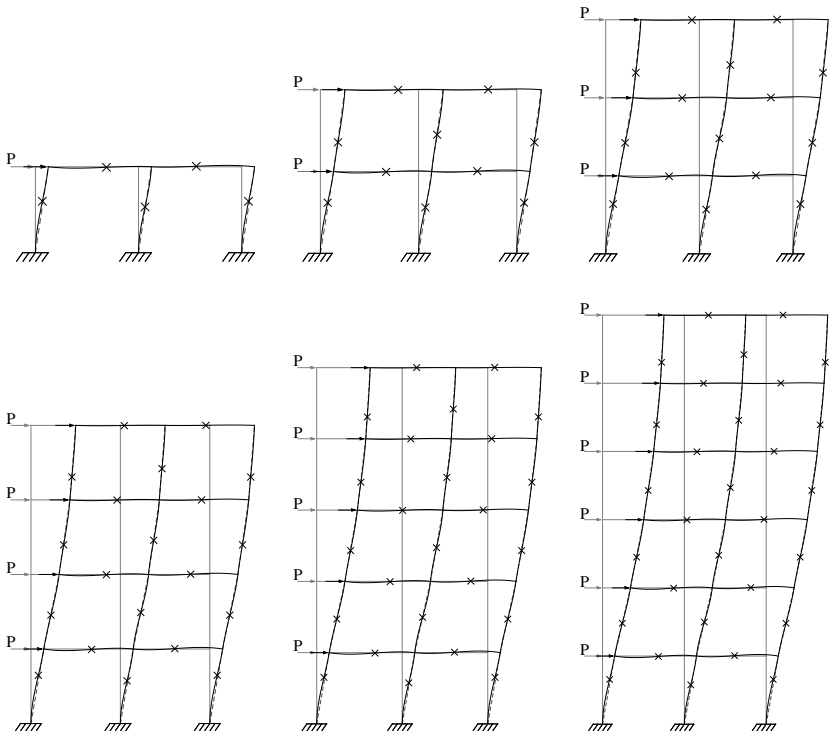
Figure 2.36. Deformation pattern for side-loaded frames with a uniform distribution of loads per floor.

linearly from the ground floor where this total shear force equals the total of all side forces on the ground floor until the top floor where this total shear force equals only the side force applied at the top floor. As before, when there is some regularity in the frame, the total shear stiffness of the floors are all about the same with relatively large deviation only at the ground floor. Therefore, the sidesway of the floors will vary in an approximately linear manner and this leads to the frame chord-line being approximately parabolic. This trend is apparent in all of figures 2.36 that have more than two floors with small deviations at the ground floor due to the relatively large deviation in that floor's shear stiffness.

Next we consider the deformation pattern when we only apply a side force at the top floor but there is a discontinuity in shear stiffness in one of the floors as shown in figures 2.37 and 2.38. The discontinuity in figure 2.37 is due to placing internal hinges at the top of all the columns of one of the floors which significantly reduces the shear stiffness of that
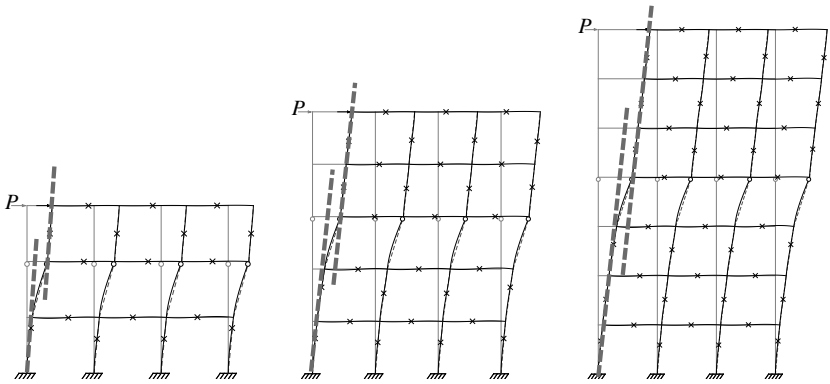
Figure 2.37. Deformation pattern for side-loaded frames with only the top floor loaded and all the columns of the middle floor have internal hinges at their tops.
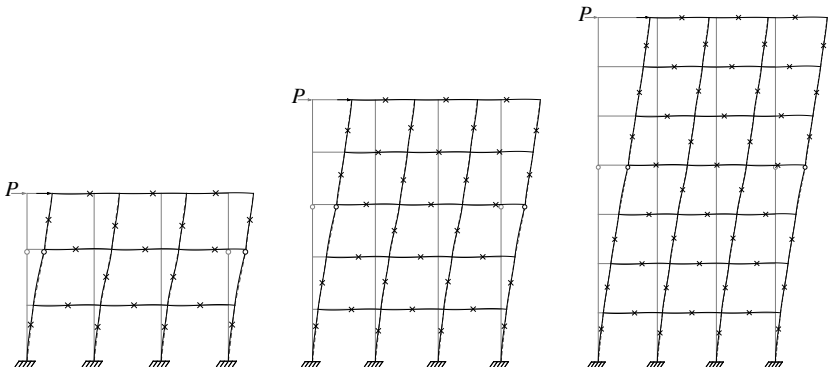
Figure 2.38. Deformation pattern for side-loaded frames with only the top floor loaded and only outer columns of middle floor have internal hinges at their tops.

floor. In that case, we find that the slope before and after the more flexible floor are the same as those of the frame without the internal hinges. In comparison with that uniform frame, the main deviation is localized at only the floor with the internal hinges as seen in figure 2.37. By contrast to the frames of figure 2.37, the discontinuity in the frames of figure 2.38 is due to placing internal hinges at the top of only the outer columns of one of the floors. This again causes a signficant reduction of shear stiff-ness in that floor but about half of that than in the frames of figure 2.37. The result in deformations of the frames of figure 2.38 are similar to those of the frames of figure 2.37 but the localized deviation in slope is much less than for the case of the frames of figure 2.37.

The next aspect that we will discuss concerns a detail in sketching the individual columns of the floors after the column chords have been sketched. In particular, we found that when the rotary stiffness factor at the top of a column is larger than 0.5, which is almost always the case, then the slope of the column at the top must be between the chord of the column and the vertical. Do the slopes of the column tops and bottoms also usually lie between the chord and the vertical when there is more than one floor? When there is more than one floor, there are 4 possible cases to consider (see figure 2.39) as follows:
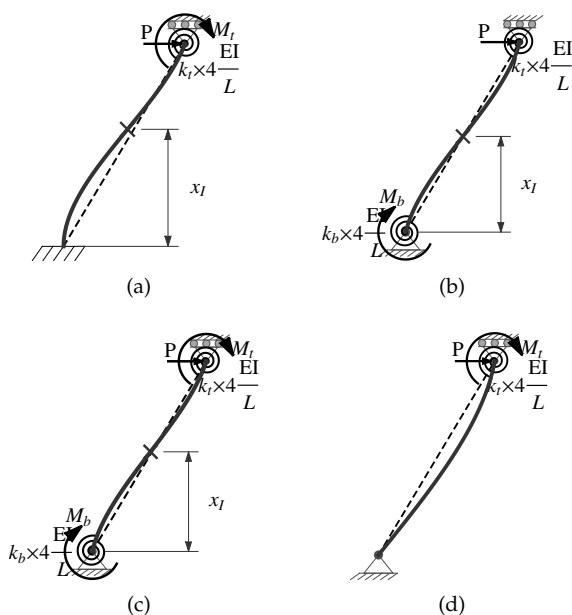
Figure 2.39. Column cases considered in regards to sketching their deformations.

- The ground floor column with a fixed lower end as shown in figure 2.39a: In this case, in order for the top of the column to be along the column chord, the value of the top rotary stiffness factor k_t must be related to the applied top moment M_t that is transmitted from the column above it by the relation given in formula 2.16a and plotted in figure 2.40a. Since the normalized applied top moment is usually below 0.5, the top of the column will be between the chord and the vertical whenever the rotary stiffness factor at the top k_t is larger than 1.25 which is usually the case.

Combinations where top slope tangent to chord

Case: $M_b=0$, $k_b \to \infty$

M_t/PL

(a)

Combinations where lower slope tangent to chord

Case: $M_t=0$

M_b/PL

(b)
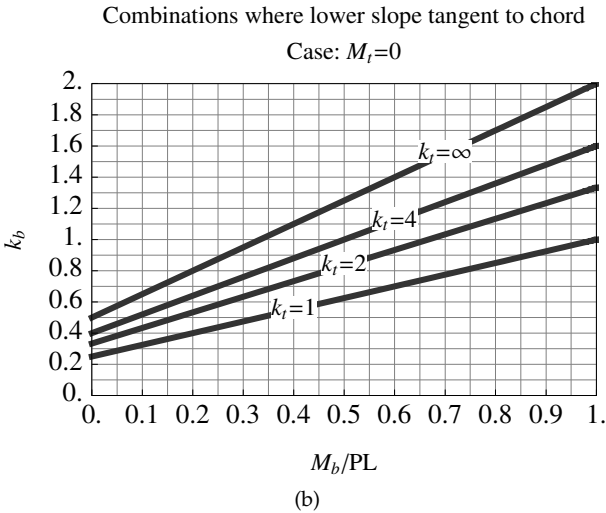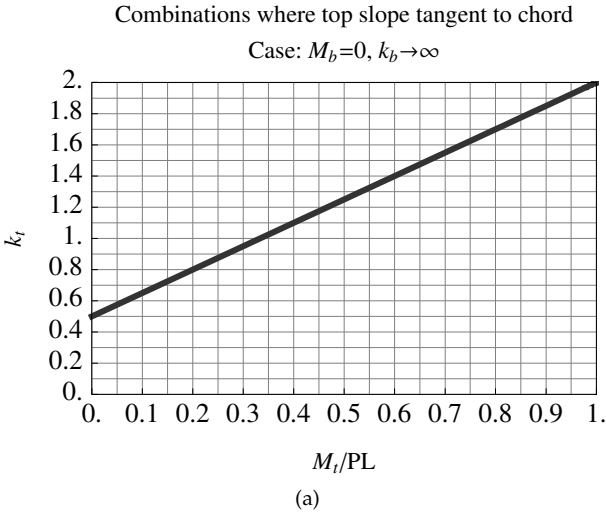
Figure 2.40. Conditions where a column's slope is tangent to the chord for the cases of figure 2.39a, b and c. Figure 2.39d never has the column line tangent to its chord. For figure 2.39c only the special case when $M_b = M_t$ is shown. *(Continued below.)*

Combinations where upper slope tangent to chord

Case: $M_t=M_b=M$

(c)
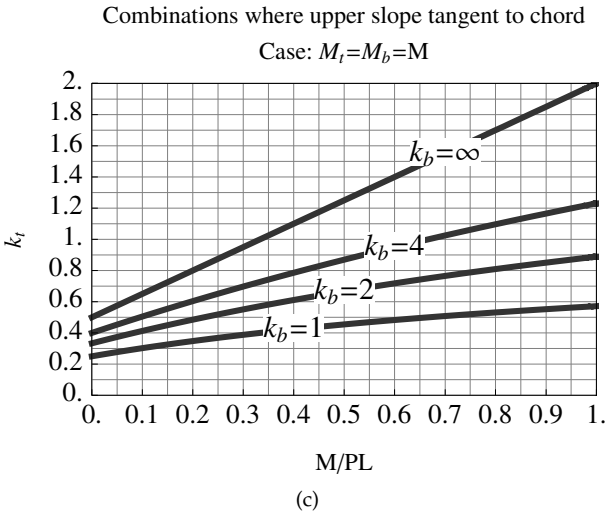
Figure 2.40. *(Continued from above.)* Conditions where a column's slope is tangent to the chord for the cases of figure 2.39a, b and c. Figure 2.39d never has the column line tangent to its chord. For figure 2.39c only the special case when $M_b = M_t$ is shown.

- The top floor column with only an applied moment M_b at the bottom as shown in figure 2.39b: In this case, in order for the bottom of the column to be along the column chord, the relation between the rotary stiffness factor at the top k_t, at the bottom k_b and the bottom applied moment M_b that is transmitted from the column below it must be related by formula 2.16b and this is plotted for some parameters in figure 2.40b. Since the normalized applied bottom moment is usually below 1, the top of the column will be between the chord and the vertical whenever the rotary stiffness factor at the bottom k_b is larger than 2 which is often the case.

- The mid-floor column with an applied moment at the bottom M_b and the top M_t as shown in figure 2.39c: In this case, in order for the bottom and top of the column to be along the column chord, the relation between the rotary stiffness factor at the top k_t, at the bottom k_b and the applied moment at the top M_t and bottom M_b must be related by formula 2.16c and this is plotted for some parameters and for the special but important case when $M_b = M_t$ in figure 2.40c. Since the moments at the top and bottom are usually close to each other and both below a normalized value of 0.5, the top and bottom of the column will be be-

tween the chord and the vertical whenever the rotary stiffness factors at the bottom k_b and top k_t are both larger than 1.25 which is usually the case.

• The ground floor column with a hinged lower end as shown in figure 2.39b: In this case the slope at the top will always be between the vertical and the chord and the slope at the bottom will always be between the chord and the horizontal.

To summarize, excluding the slope at a hinge support or at an internal hinge, the slopes of all columns at both the top and bottom will usually be between the vertical and the chord of the column and should usually be sketched in that manner. Conditions where the slope of a column is along the chord are given in formulas 2.16 below:

$$k_t = \frac{(1 + 3M_t)}{2} \qquad \text{(tangent at top)} \qquad (2.16a)$$

$$k_b = \frac{k_t + 3k_t\, M_b}{2\,(1 + k_t)} \qquad \text{(tangent at bottom)} \qquad (2.16b)$$

$$\begin{cases} k_t = \frac{k_b + 3k_b\, M_t}{2 + 2k_b + 3M_b} & \text{(tangent at top)} \\ k_b = \frac{k_t + 3k_t\, M_b}{2 + 2k_t + 3M_t} & \text{(tangent at bottom)} \end{cases} \qquad (2.16c)$$

Having described the guidelines needed to sketch the deformed shape of a frame subject to sidesway, we now consider specific examples. For that purpose, we will again consider the frames shown in figure 2.24 and 2.27.

The steps in sketching the deformed shape of the frame of figure 2.24 are illustrated in figure 2.41. First we sketch the chords of the columns and beams. For the given pattern of side forces, the frame's chord-line will be between a linear and parabolic shape. Since we only have three floors, the disctinction will be minor and we will simply draw a linear chord-line as shown in figure 2.41a. Next we sketch the column and beam slopes using short stubs at either end of each member as shown in figure 2.41b. In this regards and for all columns, we follow the recommendation related to column slopes at all ends where there is neither an internal hinge or a hinge support. Namely that the column slope at an end must be between the vertical and the column chord. At an internal hinge or at a hinge support, the slope of the member (beam or column) at the hinge relative to the chord of the member is half the slope at the other end. Using these guidelines we may sketch all the column slopes or stubs. Next we discuss how to draw the stubs for the beams.

Whenever there is a rigid connection, the rotation of all the connected stubs must be the same. This imposes a constraint on the column slopes when they are attached to the same node and allows us to draw
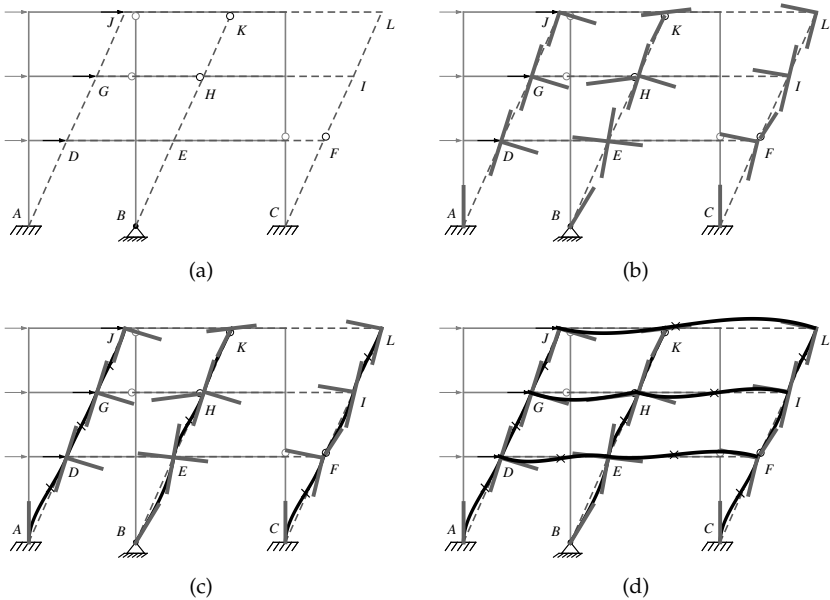
Figure 2.41. Steps in sketching the deformed shape of problem 2.24.

stubs at the ends of all beams where there is a rigid connection. At beam ends that are connected to a node where all the attached columns have an internal hinge at that connection (for example node K in figure 2.41), the rotation of the beams at the connection is dictated by the beam rotations at the other ends of those beams. In this regards, we need to use the methods related to sketching the deformation of beams with no sidesway because the beams of each floor behave as shown in figure 2.11.

Once the stubs at all beam and column endings have been sketched, we then sketch the column lines. These follow the same guidelines as those for the single floor portal and is shown in figure 2.41c. Finally, the deformed shape of all beams are sketched using the methods of beams with no sidesway and this is shown in figure 2.41d. By removing extraneous lines including the stubs constructed in figure 2.41b, we get a cleaner looking sketch of the deformed frame and this is shown in figure 2.42.

The steps in sketching the deformed shape of the frame of figure 2.27 are illustrated in figure 2.43. These are similar to the previous case. First we sketch the column chords as shown in figure 2.43a. Second, we sketch stubs indicating the slopes at the ends of all columns and beams. Unlike the previous example, in this case the rotation of all beams are dictated by the rotation of the columns and the result is shown in figure 2.43b.
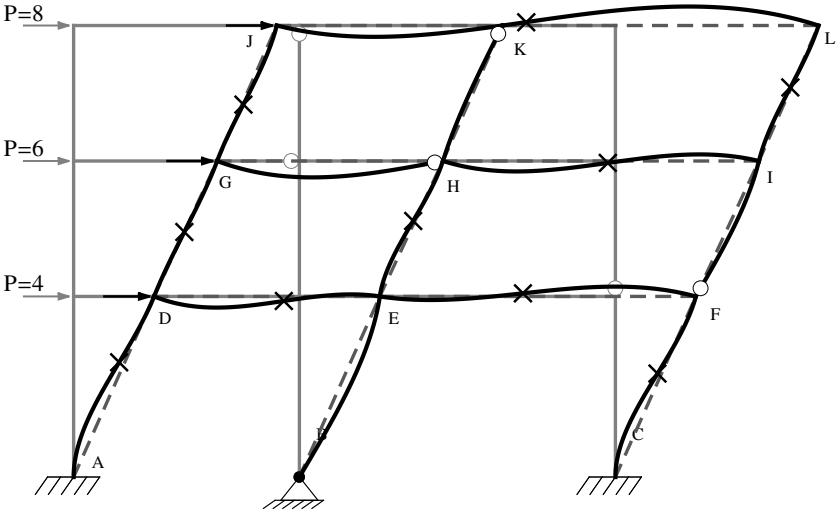
Figure 2.42. Sketch of deformed shape of problem 2.24.

(a)

(b)

(c)

(d)
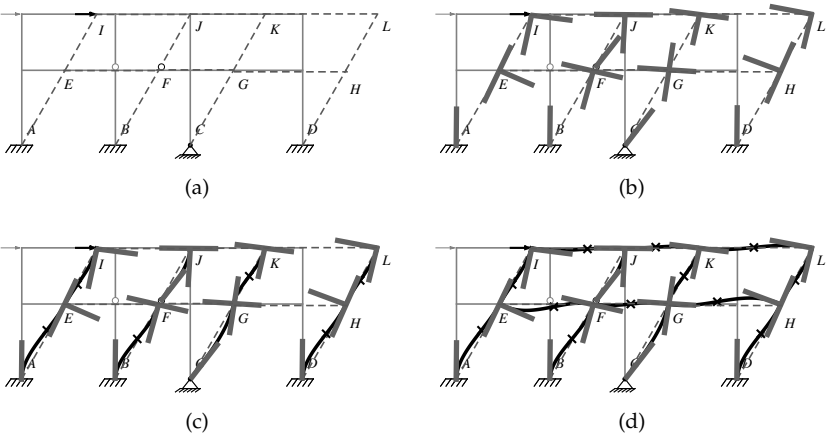
Figure 2.43. Steps in sketching the deformed shape of problem 2.27.

Having sketched the stubs, it becomes simple to sketch first the column lines as shown in figure 2.43c and the beam lines as shown in figure 2.43d. Finally, by removing extraneous lines, we get a cleaner looking sketch of the deformed frame and this is shown in figure 2.44.
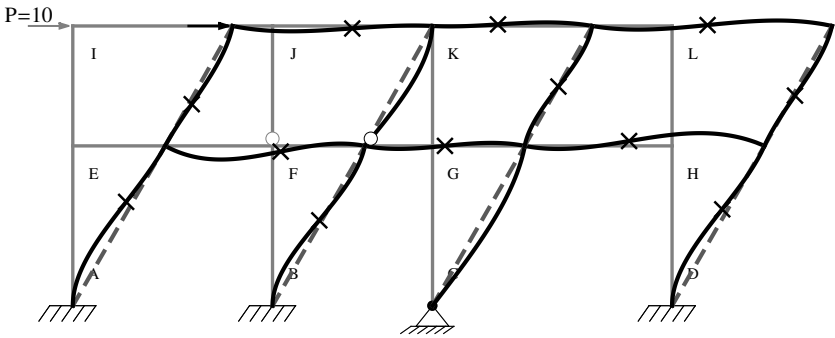
Figure 2.44. Sketch deformed shape of problem 2.27.

2.8   Notes on Sidesway Due to Vertical Loads or Applied Couples

Having discussed sidesway due to side forces, we will now consider some aspects of sidesway due to vertical loads and applied couples. Specifically, we will consider the following three questions:

- When there is sidesway due to vertical loads or applied couples, how do we approximately analyze the problem?

- When there is sidesway due to vertical loads or applied couples, what is the direction of the sidesway? By knowing the direction of sidesway, we may identify whether the bending moment in each member of such frames will have a higher or lower value when sidesway is either considered or neglected.

- Under what conditions may we neglect the effect of sidesway due to vertical loads or applied nodal moments even when sidesway is possible? We will consider an answer to this question for a limited class of frames but the results will be suggestive to other frames.

We start by describing how to approximately analyze a frame with either vertical loads or with applied couples at nodes but the frame has
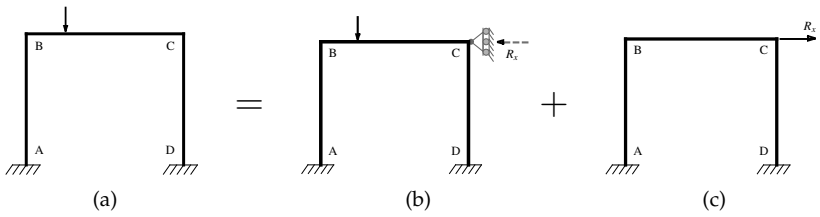
Figure 2.45. Superposition to analyze a frame subject to a vertical load and that may have sidesway.

no constraints on having sidesway such as in figure 2.45a. We analyze such a problem using superposition by first applying a restraint against the sidesway as shown in figure 2.45b and then we apply an equal and opposite force to the reaction at the restraint as shown in figure 2.45c. For a general frame, restraints must be applied at each floor in order to inhibit the sidesway at each floor. The frame without sidesway may be approximately analyzed using the techniques of the first chapter while the frame with transverse point forces at only the nodes of the floors may be analyzed using the methods of the current chapter. The only new aspect is in how to determine the reaction forces at the restraints used to inhibit sidesway and this will be discussed next.

Consider a frame with vertical forces that has an horizontal restraint in order to inhibit sidesway such as the one shown in figure 2.46a. First, we draw the free body diagram of the whole frame (*eg.* figure 2.46b) from which we deduce that the restraining horizontal force (*ie.* R_x in figure 2.46b) equals negative the total shear forces in the columns. Note that if we have more than one floor then we have to add the shear forces in
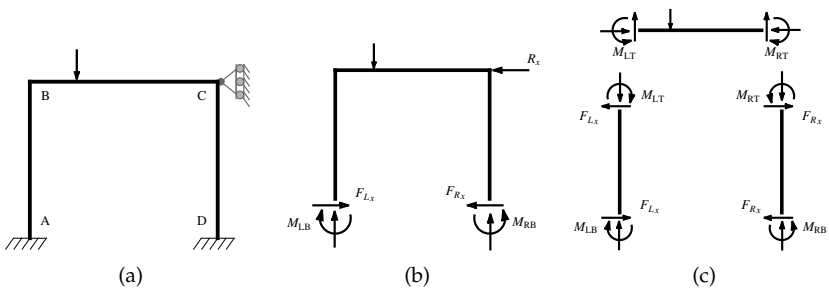
Figure 2.46. Figures showing free body diagrams that are useful to identify which side the frame moves if the horizontal roller at C is removed.

all the columns above and below the floor under consideration. Finally, to determine the shear forces in the columns, we use free body diagrams such as the ones shown in figure 2.46c to deduce that the shear force in a column is the sum of the end moments in that column divided by the column length. The reaction force in the horizontal direction at a constraint is then given by:

$$
R_x = \begin{cases} \displaystyle\sum_{\text{all columns}} \dfrac{\left(M_{\text{end points top}} + M_{\text{end point bottom}}\right)}{L_{\text{column}}} & \text{single floor} \\[2em] \displaystyle\sum_{\substack{\text{all columns} \\ \text{above and below}}} \dfrac{\left(M_{\text{end points top}} + M_{\text{end point bottom}}\right)}{L_{\text{column}}} & \text{multiple floors} \end{cases}
\tag{2.17}
$$

where the reaction force is positive in the x-direction and the moment at an endpoint is positive if it is counter-clockwise and negative if clockwise.

Having discussed how to approximately analyze frames with vertical loads or applied moments, the question of determining the direction of sidesway becomes straightforward. Consider the illustration of superposition shown in figure 2.45. This superposition applies to internal forces and moments as well as to displacements. In particular, the deformation of the frame in figure 2.45c may include a sidesway but not those of the frame of figure 2.45b. This implies that the direction of the sidesway is opposite to the direction of the reaction force. Since the reaction force is the sum of all the counter-clockwise end moments of all the columns then the direction of sidesway of a floor is to the right if the sum of the end moments of all the columns above and below the floor in question when sidesway is inhibited is clockwise.

To clarify how the direction of sidesway may be determined, we will consider a simple frame with three kinds of loading as shown in figures 2.47. In those frames, the sectional properties of all three members
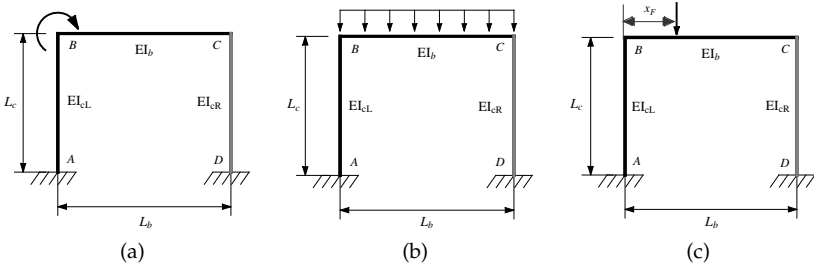
Figure 2.47. Cases considered in clarifying conditions that determine whether the sidesway is to the left or to the right.

may be different and the length of the columns and the beam may be independently chosen. In addition, for figure 2.47c, the location of the point force may vary across the beam. As a reference, we give the exact result for the sidesway in those frames which is as follows:

$$\Delta = \begin{cases} \frac{(k_L - k_R)}{16z} \frac{L_c L_b^3}{EI_b} q & \text{uniform load} \\ \frac{(2k_L - k_R + 2k_L k_R)}{4z} \frac{L_c L_b}{EI_b} M_{\text{app}} & \text{applied moment} \\ (1 - \hat{x}_F)\, \hat{x}_F & \\ \quad \times \left(\frac{(2k_L - k_R + 2k_L k_R)}{4z} \right. & \text{point force} \\ \quad \left. - \frac{(k_L + k_R + 4k_L k_R)\hat{x}_F}{4z} \right) \frac{L_c L_b^2}{EI_b} P & \end{cases} \qquad (2.18)$$

where:

$$z = 3k_L + k_L^2 + 3k_R + 11k_L k_R + k_L^2 k_R + k_R^2 + k_L k_R^2$$

$$k_L = (EI_{cL}/L_c)\,/\,(EI_b/L_b)$$

$$k_R = (EI_{cR}/L_c)\,/\,(EI_b/L_b)$$

'q' is the magnitude of the uniform load

'M_{app}' is the magnitude of the applied moment

'P' is the magnitude of the point force

$\hat{x} = x_F/L_b$ where x_F is the distance of the point force from the left end

In all the cases considered in figure 2.47, we note the following:

- In all cases, the top end moments of the left column are clockwise and those of the top right column are counter-clocwise.

- In all cases, the bottom end moments of a column are half the top ones and are of the same sign.

Therefore, in all cases, if the top end moment on the left column is higher than the corresponding one on the right column then the sidesway will be to the right and it will be to the left otherwise. We next consider each of the three cases separately.

First we consider the frame in figure 2.47a with a clockwise applied moment. For the three cases considered in figure 2.48, we note the following:

- The applied moment is distributed on the beam and on the left column in proportion to their rotary stiffness which is approximately proportional to the sectional property 'EI' where 'E' is Young's modulus and 'I' is the moment of inertia.
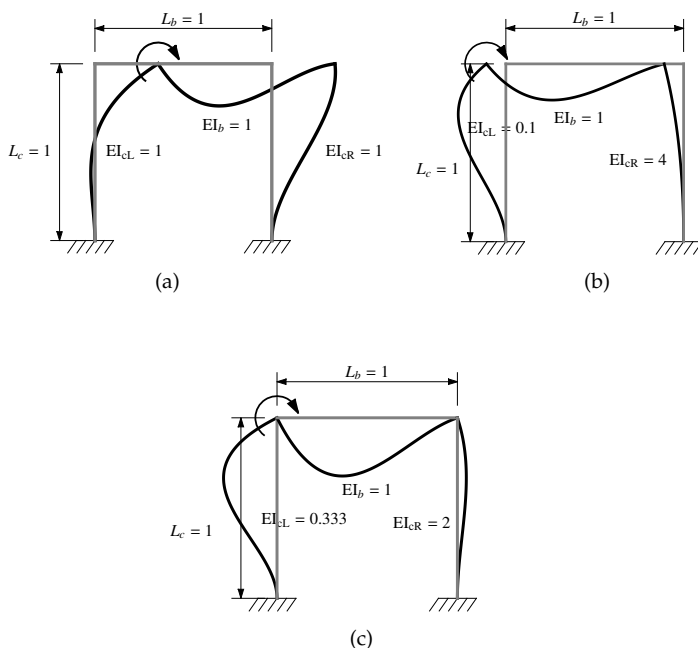
Figure 2.48. Cases considered in clarifying conditions that determine whether the sidesway is to the left or to the right.

- The moment on the right column is equal to the moment on the right end of the beam which is equal to the moment on the left end of the beam times a carry-over factor. This carry-over factor depends on the relative stiffness of the sectional property 'EI' of the column divided by that of the beam. This carry-over factor increases with 'EI_{cR}' and reaches a maximum of a half.

   With the above observation, we now consider each of the cases in figure 2.48:

- When the sectional properties of the columns are the same (as in figure 2.48a), the moment distributed to the left column will be about half the applied moment while that on the right column it will be less than half (*ie.* carry-over factor) of half the applied moment (*ie.* applied moment distributed to the beam). Therefore, the end moments on the left column are higher and the frame will move to the right.

- When the sectional properties of the column on the left is one-tenth that of the beam (figure 2.48b), the moment distributed to the left column will be less than one-tenth the applied moment while that on the

right column will be close to half of nine-tenth the applied moment. Therefore, the end moments on the right column are higher and the frame will move to the left.

• When the sectional properties of the column are as is shown in figure 2.48c, an approximate analysis of the frame with sidesway inhibited gives end moments in the columns that are about the same. Therefore, sidesway will be zero or negligible.

Next we consider the frame in figure 2.47b. For the three cases considered in figure 2.49, we note the following:

• The moments at the ends of the beam equal the moments at the top of the columns.

• The moments at the ends of the beam are related to the rotary stiffness factors at the ends. In particular, the end with the higher rotary stiffness factor will have a higher end moment. This means that the end with a higher value of 'EI' will have a higher end moment because the length of the columns are identical.

With the above observation, we now consider each of the cases in figure 2.49:

(a)

(b)

(c)
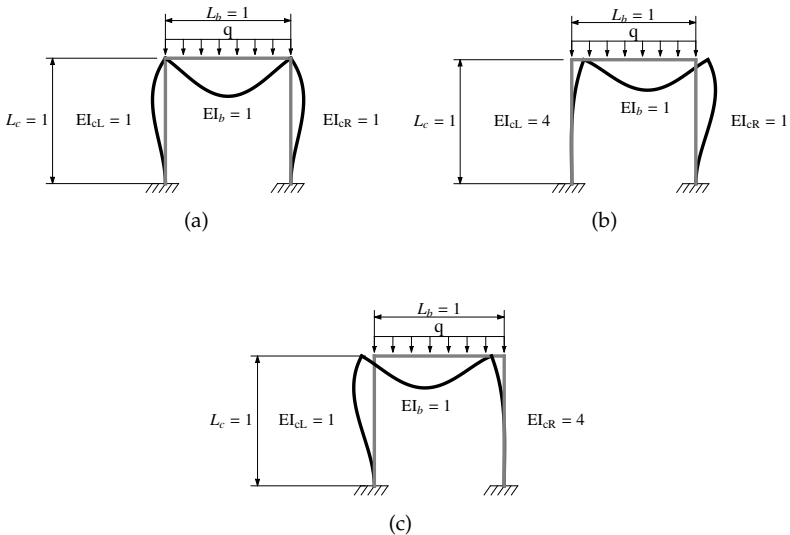
Figure 2.49. Cases considered in clarifying conditions that determine whether the sidesway is to the left or to the right.

- When the sectional properties of the columns are the same as in figure 2.49a then the end moments on the columns are the same and there is no sidesway. Note that, in this case, we could also have deduced this fact based on the simultaneous symmetry of the geometry, material and loading.

- When the rotary stiffness of the left column is higher as in figure 2.49b then the sidesway is to the right and when this is lower as in figure 2.49c then the sidesway is to the left.

Next we consider the frame in figure 2.47c with an applied point force. For the six cases considered in figure 2.50, we note the following:

- The moments at the ends of the beam equal the moments at the top of the columns.

- The moments at the ends of the beam are related to the rotary stiffness factors at the ends. In particular, the end moment at an end increases with the rotary stiffness factor at that end.

- The moments at the ends of the beam are also related to the location of the point force. In particular, for the same material properties, as the point force approaches an end, the moment at that end will tend to increase relative to the other end.

- The above observations taken together imply that there are two competing effects, the location of the point force and the relative rotary stiffness factors of the columns.

With the above observation, we now consider each of the cases in figure 2.50:

- When the sectional properties of the columns are the same and the point force is at the middle of the beam as in figure 2.50a then the end moments on the columns are the same and there is no sidesway. Note that, in this case, we could also have deduced this based on the simultaneous symmetry of the geometry, material and loading.

- When the sectional properties of the columns are the same and the point force is closer to the left end of the beam as in figure 2.50b then the end moments on the left columns are higher and sidesway is to the right. This is because the rotary stiffness factor does not favor any side in terms of higher internal moments but the point force favors the left side column.
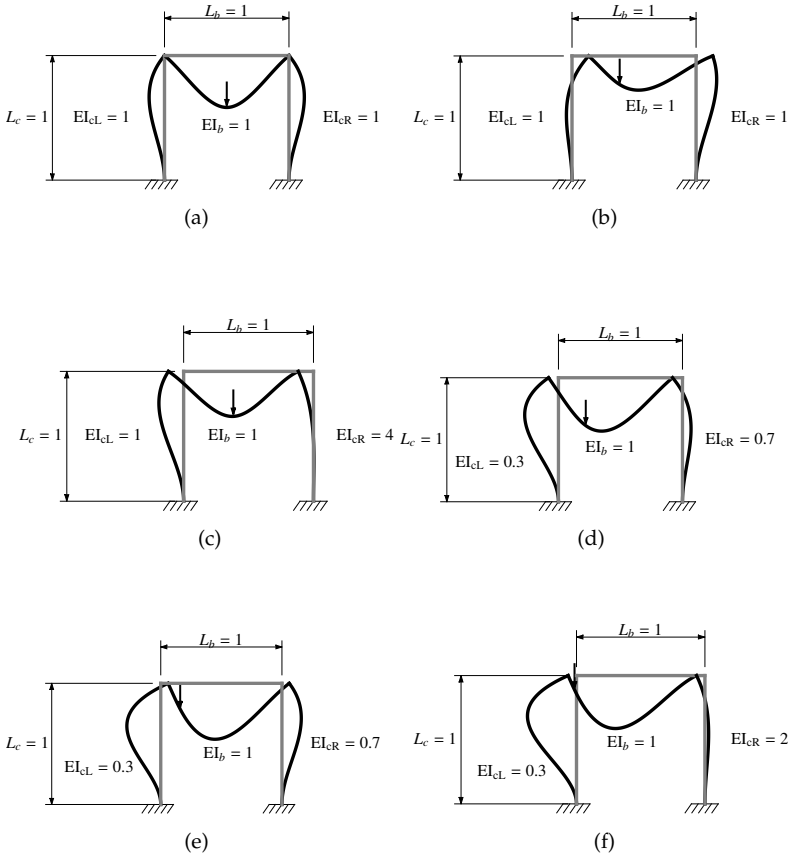
Figure 2.50. Cases considered in clarifying conditions that determine whether the sidesway is to the left or to the right.

- When the sectional properties of the columns are such that the rotary stiffness factor on the right are higher than at the left and the point force is at the middle of the beam as in figure 2.50b then the end moments on the right columns are higher and sidesway is to the left. This is because the rotary stiffness factor favor the right hand column in terms of higher internal moments but the point force does not favor any side.

- The cases shown in figures 2.50d, e and f all have a competition between the effect of the location of the point force and the contrast in rotary stiffness factors. For a moderate contrast between the rotary

stiffness factors of the columns, the sidesway is to the left when the point force is not sufficiently close to the left end as in figure 2.50d and it is to the right when it gets sufficiently close to the left end as in figure 2.50e. However, when the stiffness contrast between the rotary stiffness factors of the columns is above a threshold as in figure 2.50f then the effect of the location of the point force will always be weaker than the effect of rotary stiffness contrast and the frame will always have a sidesway to the left.

Finally, we consider the question of whether we can neglect the effect of sidesway due to vertical loads or applied nodal moments even when sidesway is possible. In order to study this question, we consider a single floor but multi-bay portal frame subject to either an applied moment at the leftmost end as in figures 2.51, or to an applied uniform load on the leftmost beam as in figure 2.52, or to an applied point force on the leftmost beam as in figure 2.54. In each case, we consider the internal moment at the left end of the leftmost beam when the sidesway is inhibited as in figures 2.51a, 2.52a and 2.54a and when sidesway is allowed as in figures 2.51b, b and b. The reason we consider the internal moment at the left end of the leftmost beam is that this is usually the largest (or close to the largest) internal moment in the frame.

(a) variable number of bays or spans   (b) variable number of bays or spans
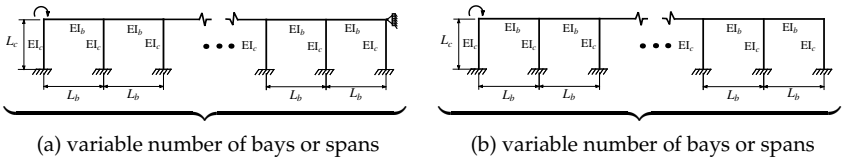
Figure 2.51. A single floor regular portal frame with variable number of bays subject to a point moment at only the leftmost node.

(a) variable number of bays or spans   (b) variable number of bays or spans
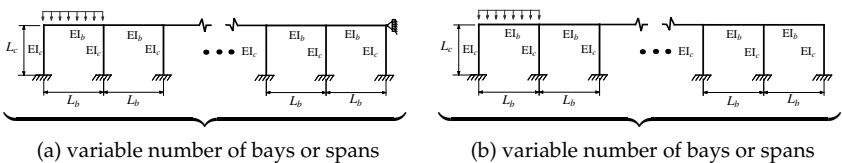
Figure 2.52. A single floor regular portal frame with variable number of bays subject to a uniform load on only the leftmost span.
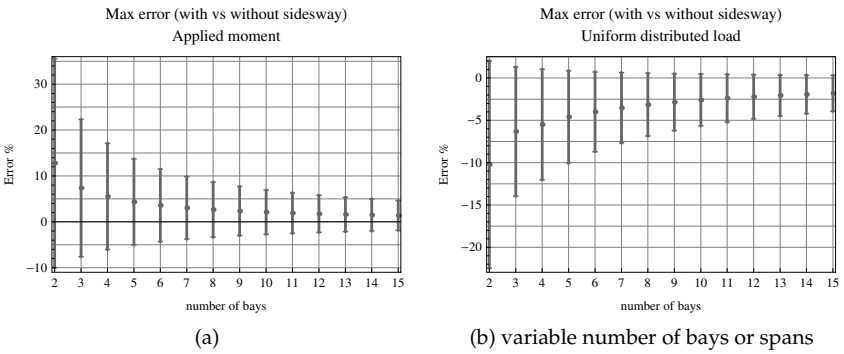
Figure 2.53. Percent error between the leftmost moments of the leftmost beams when the sidesway is neglected or when it is included versus the number of bays or spans. Figure 2.53a is for an applied moment at the leftmost node and figure 2.53b is for an applied uniform load on the leftmost span. In both figures, $0.5 \leq (EI_c/L_c) / (EI_b/L_b) \leq 2$ and $0.8 \leq L_b/L_c \leq 2$.

First, we consider the cases of an applied moment (figures 2.51) and of an applied uniform load (figures 2.52). In those cases, there are effectively two parameters that affect the relative error between the above specified internal moment when there is and when there is no sidesway. These parameters are the relative length of a column to a beam (*ie.* L_b/L_c) and the relative rotary stiffness factor of a column to a beam (*ie.* $(EI_c/L_c) / (EI_b/L_b)$). For each configuration, we consider the largest positive and negative errors for any value of these parameters within a range typical for those parameters (see related figure captions) and plot the error range as a function of the number of bays as shown in figure 2.53a and b for the applied moment and for the uniform load cases respectively. The results shown in the plots indicate that the error decreases as the number of bays increases so that if we allow a maximum
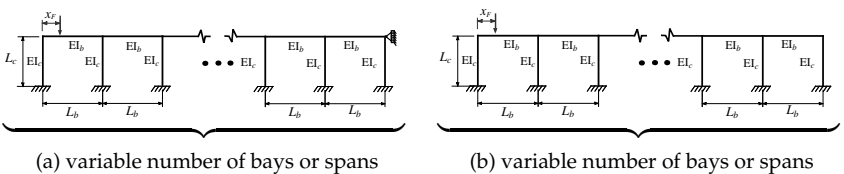
Figure 2.54. A single floor regular portal frame with variable number of bays subject to a point force on only the leftmost span.

Max error (with vs without sidesway)
Point force: $x_F/L = 1/2$

(a)

Max error (with vs without sidesway)
Point force: $1/3 \leq x_F/L \leq 2/3$

(b)
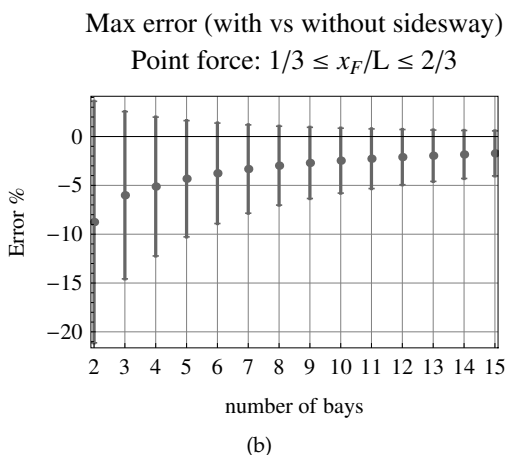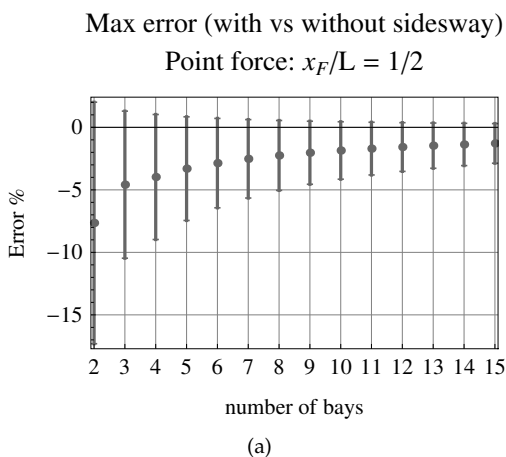
Figure 2.55. *(Continued below.)*

error of about 15% then we may neglect sidesway when the number of bays is larger than four. The trend for these results may be understood by noting the following:

i) The internal moments when sidesway is inhibited is largest in the the first two leftmost columns (*ie.* nearest to the load) and decreases rapidly relative to those values as we consider columns farther away from those columns.
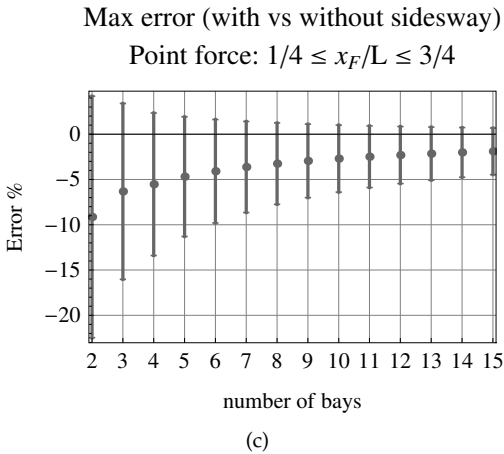
Figure 2.55. *(Continued from above.)* Percent error between the leftmost mo-
ments of the leftmost beams when the sidesway is neglected or when it is in-
cluded versus the number of bays or spans. The figures are for an applied point
force on the leftmost beam with the location of the point force restricted to the
center for figure 2.55a, the middle third of the span for figure 2.55b and the middle
half of the span for figure 2.55c. In both figures, $0.5 \leq (EI_c/L_c) / (EI_b/L_b) \leq 2$
and $0.8 \leq L_b/L_c \leq 2$.

ii) Negative the restraining force inhibiting sidesway will be distributed
   over all the columns when we superpose back the effect of the restrain-
   ing force in order to get the unrestrained case (*eg.* see figure 2.45 and
   related explanations).

   The above two observations implies that the restraining force when
sidesway is inhibited changes relatively little as the number of bays in-
creases but negative this restraining force gets distributed over a larger
number of columns producing progressively less end moments in those
columns to be superposed back in order to get the unrestrained case.
Hence, the error between the cases when sidesway is inhibited and when
it is not inhibited will decrease with the number of bays.

   For the case when a point force is applied on the leftmost beam as
in figures 2.54, we have an additional parameter which is the location of
the point force on the beam. For each configuration specified by (L_b/L_c),
$(EI_c/L_c) / (EI_b/L_b)$ and (x_F/L_b), we again consider the largest positive
and negative errors for any value of these parameters within a range
typical for those parameters (see related figure captions) and plot those
as a function of the number of bays as shown in figure 2.55a, b and c. The
cases differ in the range that is allowed for the location of the point force.

The results shown in the plots indicate that the error again decreases as the number of bays increases so that if we allow a maximum error of about 15% then we may neglect sidesway when the number of bays is about three for all three ranges of the location of the point force. The trend for these results may be understood in the same way as those for the applied moment or applied uniform load.

This page intentionally left blank

Chapter 3

Estimating Displacements in Beams and Frames

3.1 Maximum Vertical Displacements in Beams

In this chapter, we will discuss deflections and rotations in beams and frames. Some of the material will overlap with previous discussions related to the sketching of beams and frames but the emphasis here is on calculating or estimating the maximum deflection or rotation. In this section, we will graphically present deflection results in terms of stiffness factors. To estimate the maximum deflection in any beam that is attached to a passive structure, we first estimate the stiffness factors at the ends and then use the appropriate plot or formula to obtain the maximum displacement. For convenience, simpler approximate formulas are presented in this section with exact formulas being relegated to the appendices.

We start our presentation with the case of an applied moment at an end and a passive resistance at the other as shown in figure 3.1a. In this case, the maximum deflection always occurs nearer to the end where the moment is applied at a distance between about 0.333 and 0.423 times the length of the member and occur when the stiffness factor is 0 and ∞ respectively. The value of the maximum deflection is between about 0.0370 and 0.0642 times $M_{app}L^2/EI$ where 'M_{app}' is the magnitude of the applied moment, 'L' is the length of the beam and 'EI' is the moment of inertia of the beam. We note that the largest maximum deflection is $\sqrt{3}$ (≈ 1.732) times the smallest maximum deflection. The results of both the location and value of the maximum deflection are shown in
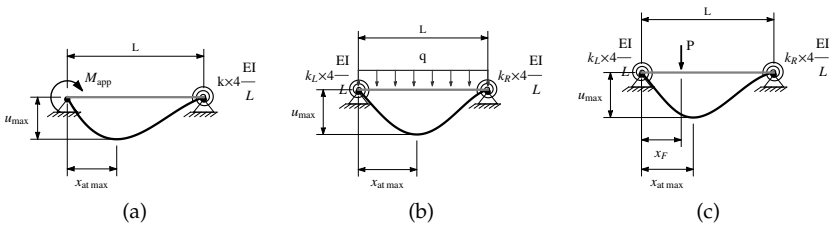
Figure 3.1. Cases considered in calculating maximum deflections.
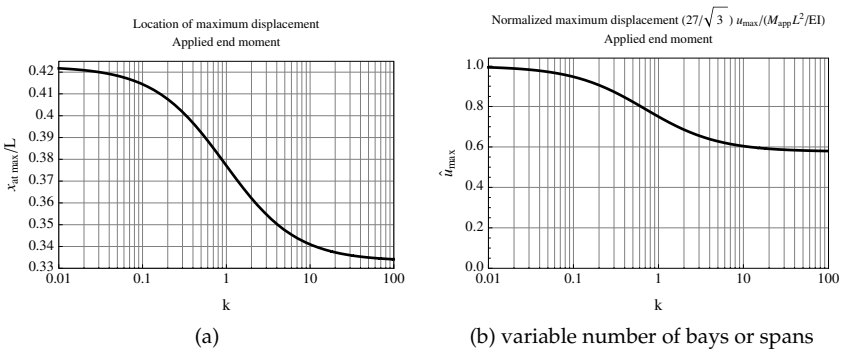
Figure 3.2. Location and value of the maximum deflection for the case shown in figure 3.1a.

figures 3.2. Finally, an aproximate formula for the maximum deflection is given by:

$$u_{\max \text{Mapp}} \approx \frac{(1 + 0.8k)}{(16 + 22k)} \frac{M_{\text{app}} L^2}{EI} \qquad (3.1)$$

We note that the above approximate formula always underestimates the deflection and has a maximum error that is always less than 1.82% which occurs when $k = 0$.

The next case we consider is that of a uniform load with passive supports on each side as shown in figure 3.1b. In this case the maximum deflection always occurs closer to the more flexible side (*ie.* the side whose stiffness factor is lower) and always lies between about 0.422 and 0.578 times the length of the beam. In other words, the location of the maximum is within about 7.84% of the length of the beam from the
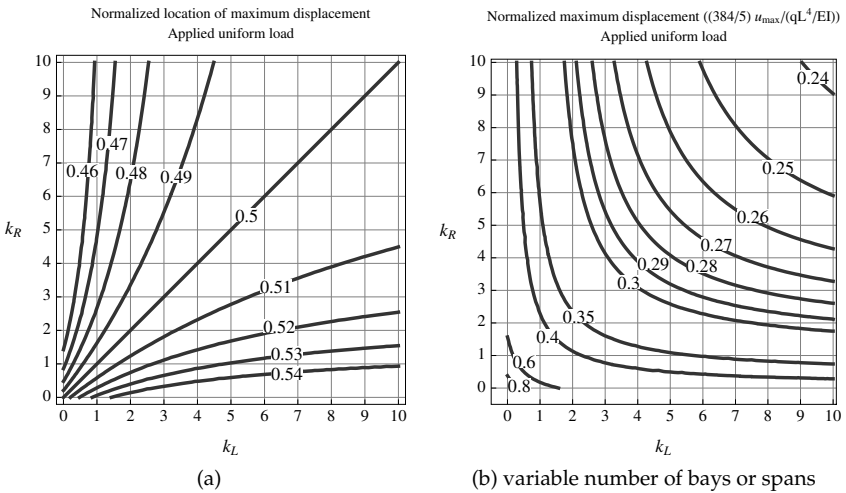
Figure 3.3. Location and value of the maximum deflection for the case shown in figure 3.1b.

center. The value of the maximum deflection is between 1 and 5 times $q\,L^4/(384EI)$ where 'q' is the magnitude of the uniform load, 'L' is the length of the beam and 'EI' is the moment of inertia of the beam. We note that the largest maximum deflection which occurs when the beam is simply supported is 5 times the smallest maximum deflection which occurs when both ends are fixed. The results of both the location and value of the maximum deflection are shown in figures 3.3. Finally, an aproximate formula for the maximum deflection is given by:

$$u_{\max\,UL} \approx \frac{(1 + 0.57k_L + 0.57k_R + 0.29k_L\,k_R)}{(77 + 106k_L + 106k_R + 112k_Lk_R)}\frac{qL^4}{EI} \qquad (3.2)$$

We note that the above approximate formula has a maximum error of 0.72% and occurs when one end is hinged and the other fixed.

The final case we consider is that of a point load with passive supports on each side as shown in figure 3.1c. In this case, the influence of the location of the point force has the largest effect on the location of the maximum deflection. However, the location of the maximum deflection always lies in the middle third of the beam for any location of the point force on the beam and for any passive supports at the ends. The maximum deflection occurs at one third of the beam's length when the point force is almost at one end of the beam, that end is hinged and the other

end is a fixed end. When the point force is within the middle third of the beam, the location of maximum deflection is at most a distance of one sixth the length from that of the point force for any passive supports. The value of the maximum deflection when the point force is at the middle of the beam is between 2 and 8 times $PL^3/(384EI)$ (*ie.* between $PL^3/(192EI)$ and $PL^3/(48EI)$) where 'P' is the magnitude of the uniform load, 'L' is the length of the beam and 'EI' is the moment of inertia of the beam. These two limits occur for the simply supported beam and the beam that is fixed at both ends. When the point force is not at the middle of the beam, the expression of the maximum deflection is more complex but generally decreases as the point force moves away from the center with the maximum possible deflection being for the simply supported beam and central loading (*ie.* $8PL^3/(384EI)$). The value of the maximum deflection remains about the same if the point force remains close to the center. In other words, the variation of the maximum deflection is insensitive to the location of the point force when the point force is near the center. For example, when the point force is within the middle 10% and 20% of the beam then the maximum deflection is always within about 8.1% and 21.3% respectively of the maximum deflection when the point force is at the middle. The results of the location of the maximum deflection are shown in figures 3.4 and those of the value of the maximum deflection are shown in figures 3.5 for selected values of the location of the point force. Finally, an approximate formula for the maximum deflection is given by:

$$u_{\max PF} \approx \left(\frac{2.5k_L\left(3 - 2\hat{x}_F\right)\hat{x}_F + 6k_L\,k_R\left(1 - \hat{x}_F\right)\hat{x}_F}{z} \right.$$
$$\left. + \frac{\left(3 - 2\hat{x}_F\right)\left(1 + 2\hat{x}_F\right) + 2.5k_R\left(1 - \hat{x}_F\right)\left(1 + 2\hat{x}_F\right)}{z} \right)$$
$$\times \left(1 - \hat{x}_F\right)\hat{x}_F \times \tfrac{PL^3}{EI} \tag{3.3}$$

where $z = 48 + 66k_L + 66k_R + 72k_L\,k_R$

We note that the above approximate formula has a maximum error of 8.77% when the max deflection is less than $0.2PL^3/(48EI)$.
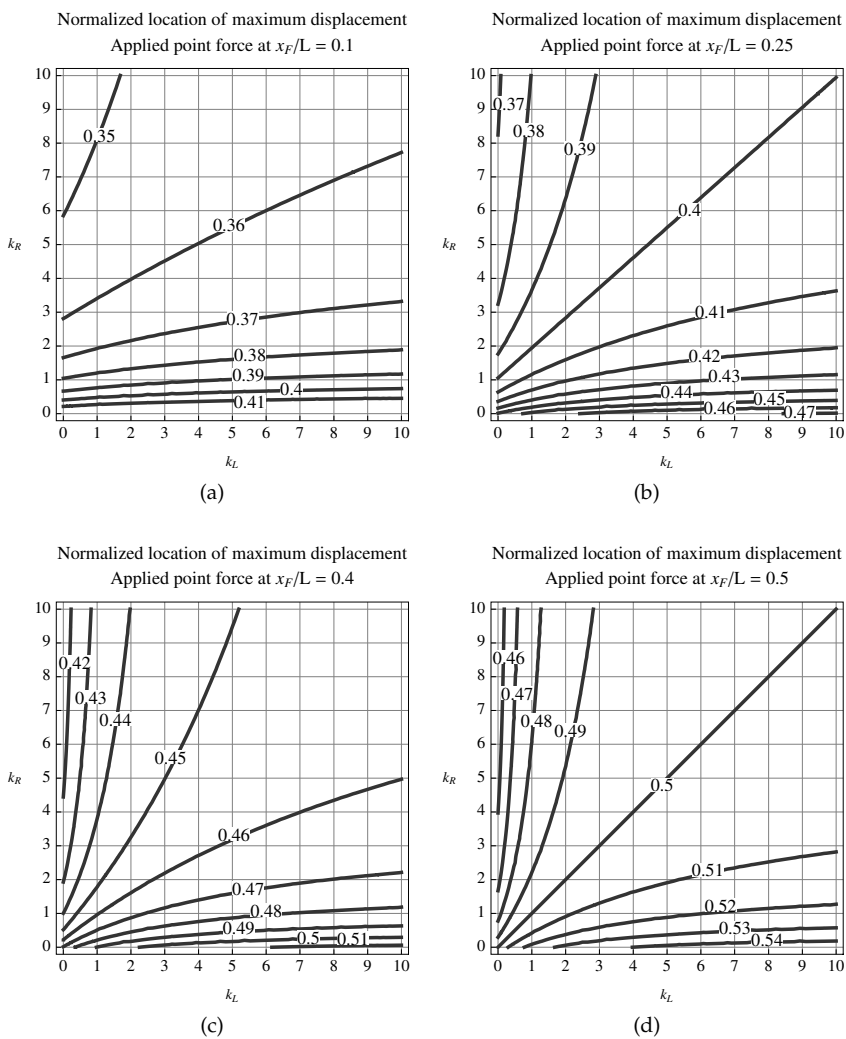
Figure 3.4. Location of the maximum deflection for the case shown in figure 3.1c.

Normalized max displacement (48 u_{max}/(PL^3/EI))
Applied point force at x_F/L = 0.1

(a)

Normalized max displacement (48 u_{max}/(PL^3/EI))
Applied point force at x_F/L = 0.25

(b)

Normalized max displacement (48 u_{max}/(PL^3/EI))
Applied point force at x_F/L = 0.4

(c)

Normalized max displacement (48 u_{max}/(PL^3/EI))
Applied point force at x_F/L = 0.5

(d)
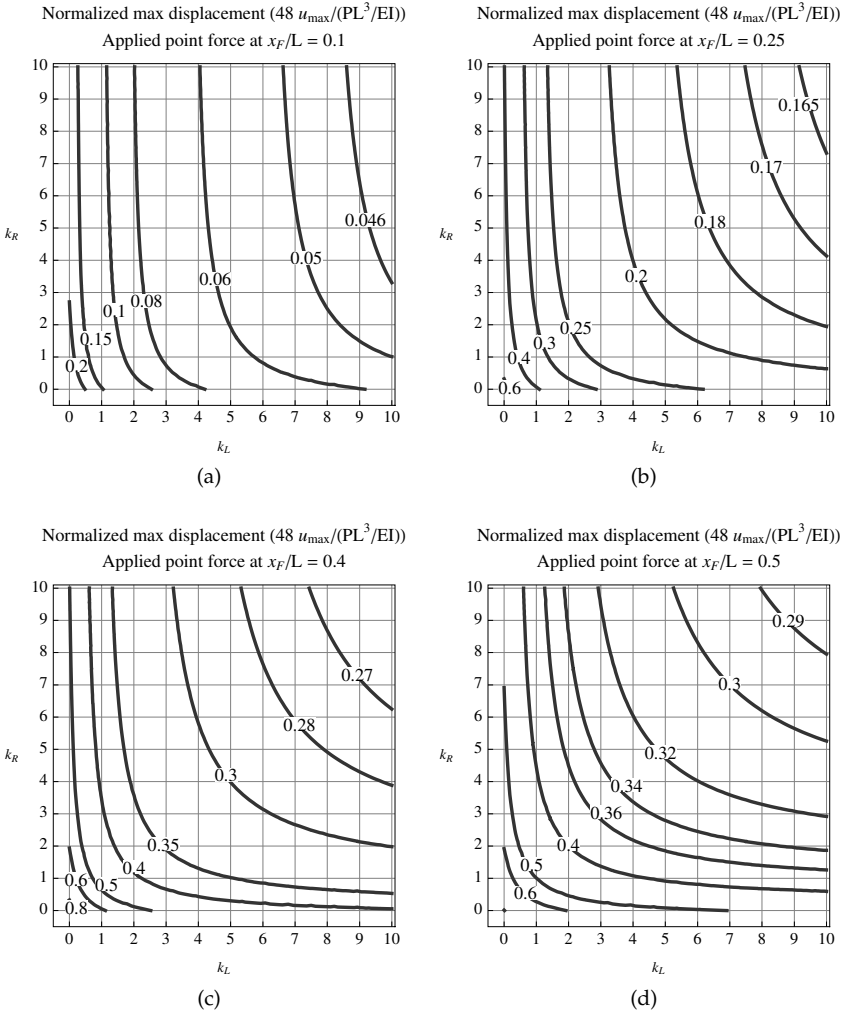
Figure 3.5. Value of the maximum deflection for the case shown in figure 3.1c.

3.2   Estimating Moment of Inertia

For an actual beam, we can, with practice or experience, make a good estimate of its dimensions simply by looking at it. Also, by being familiar with the concept of area and with some practice or experience, we can also estimate areas of cross-sections by a visual inspection and some minor calculations. For example, one approach to estimate areas is to mentally rearrange the cross-section, without stretching or leaving gaps, into an equivalent rectangle whose area we then calculate based on our estimates of dimensions. By contrast, rules to estimate the moment of inertia are not obvious but such a skill would be useful for a structural engineer because formulas for deflections and bending stresses prominently involve the moment of inertia. This is especially important in optimization where we seek the relative advantage of different shapes both in regards to constructability and in regards to providing the largest moment of inertia for a given weight. In this section, we will develop some guidance in estimating moments of inertia for arbitrary sections, in quickly sorting various sectional shapes in terms of their moments of inertia and in identifying what features in the shape most affect the moments of inertia.

We will consider shape transformations that either do not change the moment of inertia or change it in a simple and easy to calculate manner. In this discussion, we will focus on the moment of inertia relative to an horizontal axis. A similar discussion may be done for the moment of inertia relative to a vertical axis which can be easily deduced after rotating the page by 90°. The first transformation we consider leaves the moment of inertia relative to an horizontal axis invariant. That transformation consists of any shape change that maintains unchanged the net width at every horizontal cut. Note that this transformation also leaves the area invariant. For example, consider the shapes shown in figure 3.6. By sliding the middle portions of the box section (figure 3.6a) from both left and right towards the center, we get the I-beam (figure 3.6b) with the net width at each height remaining the same. Furthermore, by sliding the middle portion of the I-beam to the far right, we get the C-channel (figure 3.6c). Therefore, we deduce that all three sections shown in figures 3.6 have the same moment of inertia relative to an horizontal axis.

A special case of the transformation discussed above is that of a linear sideways shearing. A uniform sideways shear leaves the net width at each horizontal cut unchanged and therefore will also leave the moment of inertia unchanged. As an example, figures 3.7 shows an isosceles triangle (figure 3.7a) that is uniformly sheared into a right triangle (figure 3.7b) and then into an obtuse triangle (figure 3.7c). Therefore, the three triangles in figures 3.7 all have the same moment of inertia
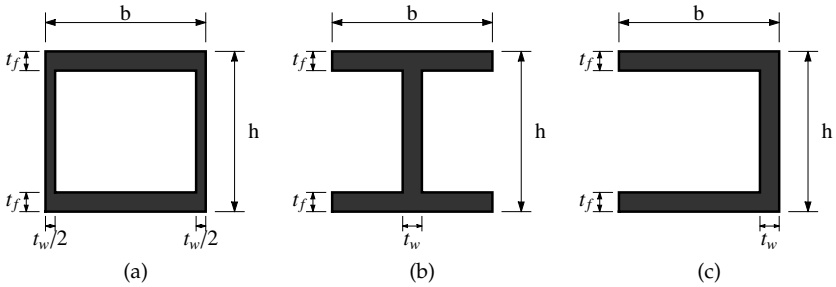
Figure 3.6. Shapes 3.6a, b and c above all have the same area, moment of inertia about any horizontal axis and radius of gyration about any horizontal axis. These sectional properties remain the same when the net width at every horizontal cut remains the same.
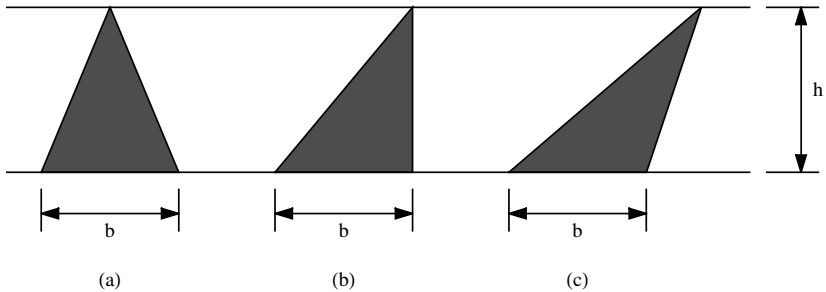
Figure 3.7. Shapes 3.7a, b and c above all have the same area, moment of inertia about any horizontal axis and radius of gyration about any horizontal axis. These sectional properties remain the same when there is uniform shearing in the horizontal direction because such shearing leaves the net width at every horizontal cut invariant.

relative to an horizontal axis. Note that the characteristic of a linear sideways shearing transformation is that straight lines are transformed into straight lines of the same height. For example, transforming a rectangle into a parallelogram of the same height and base also leaves the moment of inertia invariant.

The third transformation we will consider changes the value of the moment of inertia but in a simple manner. If we uniformly stretch or contract (*ie.* scale) a cross-section horizontally so that the width at every horizontal cut is multiplied or divided by the same factor then both the area and the moment of inertia will be multiplied or divided by the
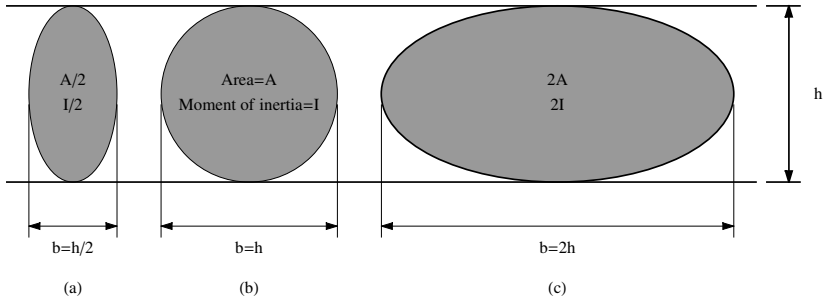
Figure 3.8. Shapes 3.8a, b and c above have area, moment of inertia about any horizontal axis and radius of gyration about any horizontal axis that scale with the width. These sectional properties increase proportionately to the amount of scaling in the horizontal direction.

same factor. As an example, we consider a disk that is either contracted or stretched by a factor of 2 as shown in figures 3.8. In that case, the thin ellipse in figure 3.8a will have half the area and half the moment of inertia relative to an horizontal axis as that of the disk in figure 3.8b. Similarly, the wide ellipse in figure 3.8c will have twice those same quantities as the disk. We note that because this transformation scales both the moment of inertia and the area by the same factor, then the radius of gyration which is the square root of their ratio is invariant under this transformation. In addition, since the height remains the same, the ratio of the moment of inertia divided by the maximum moment of inertia also remains invariant under this transformation. As will be discussed below, since this ratio may be used as a measure of the efficiency of a given shape, therefore an horizontal scaling does not change the efficiency of a cross-sectional shape.

The next transformation we will consider relates the moment of inertia of a symmetric section with that of an unsymmetric one. We start with a cross-section that is symmetric relative to an horizontal axis but is otherwise unconstrained as for example the cross-section shown in figure 3.9a. If we now remove an arbitrary piece of this cross-section, reflect it relative to the horizontal axis of symmetry and add it to the reflected side, we then get an unsymmetric cross-section. For example, we have used this process to transform the cross-section of figure 3.9a into that of figure 3.9b, however, we have additionally horizontally slid the reflected piece in order to enhance clarity. Such a further horizontal sliding does not affect the moment of inertia relative to an horizontal axis because it

(a)   (b)
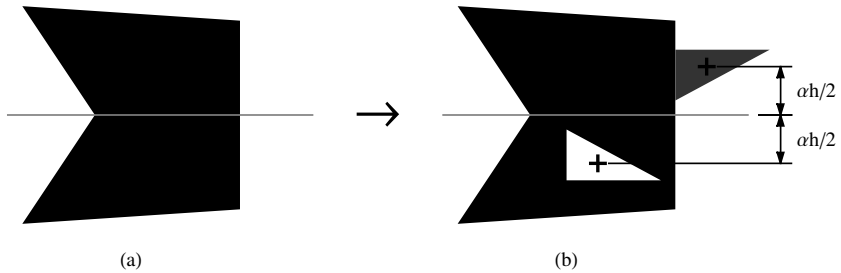
Figure 3.9. Transformation of a symmetric section into an unsymmetric section by reflecting an arbitrary part from one side of the line symmetry to the other side. For clarity, the part that is reflected is further slid horizontally to the edge of the cross-section. Such an horizontal sliding does not change the moment of inertia relative to a horizontal axis.

does not change the net width at any horizontal cut. The result of this transformation leaves the area the same but changes both the center of gravity and the moment of inertia. The moment of inertia of the unsymmetric section '$I_{\text{unsymmetric}}$' can be related to the symmetric one '$I_{\text{symmetric}}$' as follows:

$$\left(I_{\text{unsymmetric}}/I_{\text{max}}\right) = \left(I_{\text{symmetric}}/I_{\text{max}}\right) - 4(\Delta A/A)^2\alpha^2 \qquad (3.4)$$

where:

A is the area of the cross-section

ΔA is the area of the piece that is reflected

h is the height of the cross-section

$\alpha h/2$ is the the distance from the midline of the symmetric section to the center of gravity of the reflected piece

$I_{\text{max}} = Ah^2/4$ which is the maximum possible moment of inertia for the specified area and height

As an example of using the above formula, consider a rectangular section of height 'b' and width 'h.' The value of the ratio $I_{\text{symmetric}}/I_{\text{max}}$ is $(bh^3/12)/(bh\,h^2/4) = 1/3$. If we reflect all of the lower area which equals half the area and reflect it to the top, we get a new rectangle with width '$2b$' and height '$h/2$.' This new cross section has $I/I_{\text{max}} = (2b(h/2)^3/12)/(bh\,h^2/4) = 1/12$. The formula 3.4 gives $I_{\text{unsymmetric}}/I_{\text{max}} = 1/3 - 4(1/2)^2(1/2)^2 = 1/12$. Note that I_{max} is always

relative to the original height even if all the area on one side is being reflected.

There are several things that are interesting in formula 3.4 which include:

- The formula applies for both ΔA positive (removal then reflection of area) as well as negative (adding then reflecting negative area).

- $I_{\text{unsymmetric}}$ is always less than $I_{\text{symmetric}}$ because the difference is always negative. Note that this does not mean that all unsymmetric sections have lower moments of inertia than symmetric ones. However, it does mean that if an unsymmetric section can be related to a symmetric one through such a transformation then the symmetric section will have a higher moment of inertia. It also means that the above described transformation always lowers the moment of inertia of a symmetric section. Furthermore, the result can be used to prove that for a fixed area and height, the maximum moment of inertia is that of the ideal I-beam with all the areas being symmetrically placed at the farthest allowable locations.

- If we remove and reflect a piece from only one side then $(\Delta A/A) \leq 1/2$ and $\alpha \leq 1$. This implies that the difference between $I_{\text{unsymmetric}}/I_{\text{max}}$ and $I_{\text{symmetric}}/I_{\text{max}}$ is always less or equal to one.

- The decrease in the moment of inertia is quadratic with '$\Delta A/A$' and with 'α.' Since these are both less than one if we are removing and reflecting area from only one side then the change in moment of inertia between a symmetric section and its associated unsymmetric section will generally be a relatively small change. For example, if we remove and reflect at most 20% of the area from one side (*ie.* 10% of the total area) then the change in moment of inertia will be less than 24% for all shapes that are at least as efficient as a diamond shape (see table 3.2 and related discussions).

To clarify the effect of this last transformation, we study two cross-sectional shapes, namely the I-beam with a negligible web width but finite flange thickness and the rectangular cross-section. For the I-beam, we use formula 3.4 to plot the ratio of moment of inertia of the unsymmetric to the symmetric one versus the ratio of top to bottom flange width. As expected, the maximum occurs for the symmetric section and the variation is parabolic near that maximum and this is shown in figure 3.10a for $(b/h)_{\text{symmetric}} = 1$ and in figure 3.10b for $(b/h)_{\text{symmetric}} = 2$. Note that even when the non-symmetric I-beam has a side whose width is twice (or half) the other side, its moment of inertia is about 92.7% and
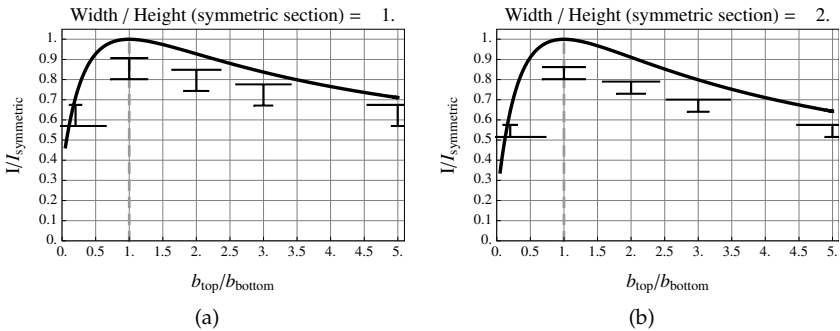
Figure 3.10. Relation between the moment of inertia relative to an horizontal axis and the deviation from symmetry of an ideal I-beam at fixed area and height.

91.1% that of the symmetric one for figures 3.10a and b respectively. This shows that even with rather large deviations from symmetry we get relatively small changes in the moment of inertia.

For the rectangular cross-section, we take a rectangular piece from the top half and add it to the lower part and then shift areas horizontally to obtain a symmetric section. Note that horizontally shifting areas does not change the moment of inertia relative to a horizontal axis. The net transformation gives an inverted T-beam. In this case, we again use formula 3.4 to obtain a relation between the ratio of moment of inertia of the unsymmetric to the symmetric one versus the ratio of the top width of the unsymmetric sections over the width of the symmetric one. Simplifying the expression for this case in terms of the parameters chosen leads to the following formula which is surprisingly independent of the aspect ratio of the associated symmetric rectangular section:

$$I_{\text{unsymm}}/I_{\text{symm}} = (1/4)\left(1 + 6\left(b_{\text{top}}/b_{\text{top sym}}\right) - 3\left(b_{\text{top}}/b_{\text{top sym}}\right)^2\right) \tag{3.5}$$

$$\text{(for rectangular section)}$$

The above formula 3.5 is plotted in figure 3.11 which again shows that the maximum occurs for the symmetric section and that the variation is parabolic near that maximum. Note that also in this case, large deviations from symmetry cause a relatively small change in the moment of inertia. For example, if we start with a rectangular section and reflect half the area of the top to get the T-beams shown in figure 3.11 at $b_{\text{top}}/b_{\text{top symm}} = 0.5$ we get that the change in moment of inertia is only 18.75%.

In the final transformation, we consider the effect of adding a rectangular area 'ΔA' with height 'Δh' centered around the center of gravity of the cross-section as for example shown in figure 3.12. The resulting

$I/I_{\text{symmetric}}$ versus $b_{\text{top}}/b_{\text{top symmetric}}$
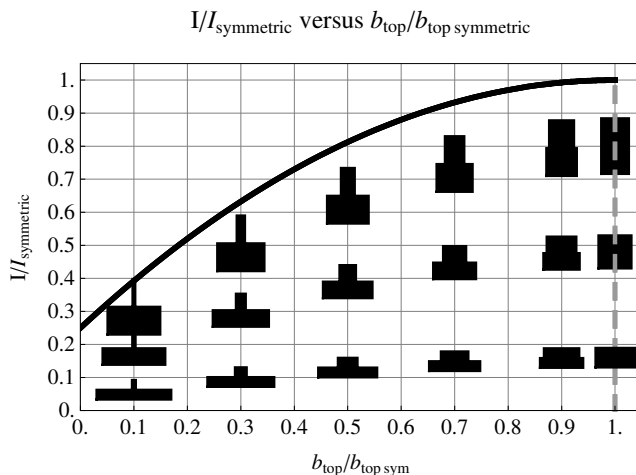
Figure 3.11. Relation between the moment of inertia relative to an horizontal axis of an inverted T-beam as it gets closer in shape to that of a rectangular section of the same area and height.
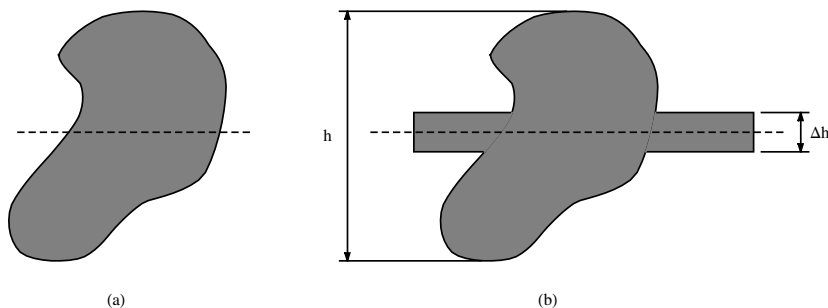
Figure 3.12. The middle augmentation transform consists of adding a rectangular area centrally located around the center of gravity.

moment of inertia is given by:

$$I_{\text{new}}/I_{\text{max}} = I_{\text{old}}/I_{\text{max}} + (1/3)(\Delta A/A)(\Delta h/h)^2 \qquad (3.6)$$

This transformation is interesting because the increase in the moment of inertia is usually negligible for the purposes of a rough estimate. For example, if $\Delta A \leq 1$ (*ie.* up to doubling the area) and the height of the material added is such that $\Delta h \leq 0.2h$ (*ie.* less than 20% the overall height)

then the change in moment of inertia will always be less than 10% for all the shapes shown in table 3.2. For the same maximum change in area, if the height of the material added is such that $\Delta h \leq h/3$ (*ie.* less than one third the overall height) then the change in moment of inertia will always be less than 26% for those same shapes. Therefore, this transformation can have quite substantial changes in the shape and area but will produce relatively little change in the moment of inertia.
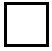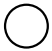
A summary of the above transformations, as well as one addition (horizontal slide) is presented in table 3.1. All these transformations are important because we can use them to estimate the moment of inertia of a new shape by transforming that shape to some other known or close to a known shape whose moment of inertia is known exactly or approximately. Of course, this assumes that we have familiarity with a family of basic shapes with which to do the comparison. Therefore, we will next consider such family of shapes and sort them according to their moments of inertia.

Table 3.1. Shape Transformations and their Effect on the Moment of Inertia Relative to an Horizontal Axis.

Transformation name	Description	Effect on moment of inertia
width invariant transformation	Any shape change that maintains unchanged the net width at every horizontal cut	no change
horizontal slide	Any horizontal slice may be rigidly shifted horizontally by any amount	no change
linear sideways shearing	A uniform horizontal shearing such that straight lines are transformed into straight lines of the same height	no change
horizontal scaling	Uniformly stretch or contract (*ie.* scale) a cross-section horizontally so that the width at every horizontal cut is multiplied or divided by the same factor	Multiplied by same factor multiplying width
reflection from symmetry	Remove an arbitrary piece of the cross-section, reflect it relative to the horizontal axis of symmetry and add it to the reflected side	reduced by $(\Delta A/A)^2 \alpha^2 A h^2$ (see figure 3.9)
middle augmentation	Add a rectangular area centered around the center of gravity (see figure 3.12)	increases by $(1/12)(\Delta A/A)(\Delta h/h)^2 A h^2$ (see figure 3.12)

Table 3.2. Relation Between Shape, Radius of Gyration and Height of Cross-Sections for Symmetric Sections. The Cross-Sectional Shapes are Rankedin (Usually) Decreasing Order of $I/I_{\max}$ where 'I' is the Moment of Inertia of the Cross-Section Relative to an Horizontal Axis and $I_{\max} = Ah^2/4$ is the Maximum Possible Moment of Inertia Relative to an Horizontal Axis for a Fixed Area 'A' and Height 'h.'

Note: In the table below, 'A' is the area, 'b' is the width, 'h' is the height, 'ρ' is the radius of gyration around an horizontal axis through the center of gravity, 'I' is the moment of inertia around an horizontal axis through the center of gravity, '$I_{\max}$' is the maximum possible moment of inertia, 'r' is the radius of a circle (if present) and 't' is a thickness (if present).

Name	Shape	Area (A)	ρ/h	$I/I_{\max}$
ideal I-beam		$2bt$	$\frac{1}{2} = 0.5$	1
I-beam $(A_{\text{web}} \ll A_{\text{flange}})$		$A_{\text{flange}} + A_{\text{web}}$	$\approx \frac{1}{2}\left(1 - \frac{1}{2}\frac{A_{\text{web}}}{A_{\text{flange}}}\right)$	$\approx \left(1 - \frac{A_{\text{web}}}{A_{\text{flange}}}\right)$
hollow square		$\approx 4ht$	$\approx \frac{1}{2\sqrt{1.5}}\left(1 - \frac{t}{h}\right)$	$\approx \left(1 - 2\frac{t}{h}\right)$
sharp-edged parabolic hourglass		$\frac{1}{3}bh$	$\approx \frac{1}{2\sqrt{1.842}} = 0.368$	≈ 0.543
sharp-edged linear hourglass		$\frac{1}{2}bh$	$\frac{1}{2\sqrt{2}} \approx 0.354$	$\frac{1}{2}$
hollow circular disk		$\approx \pi rt$	$\approx \frac{1}{2\sqrt{2}}\left(1 - \frac{t}{4r}\right)$	$\approx \frac{1}{2}\left(1 - \frac{t}{2r}\right)$
rectangle		bh	$\frac{1}{2\sqrt{3}} \approx 0.289$	$\frac{1}{3}$
elliptic disk (includes circular)		$\frac{\pi}{4}bh$	$\frac{1}{2\times\sqrt{4}} = 0.250$	$\frac{1}{4}$
facing parabolas		$\frac{2}{3}bh$	$\frac{1}{2\sqrt{4.375}} \approx 0.239$	$\frac{1}{4.375}$
diamond		$\frac{1}{2}bh$	$\frac{1}{2\sqrt{6}} \approx 0.204$	$\frac{1}{6}$
parabolas-sided diamond		$\frac{1}{3}bh$	$\frac{1}{2\sqrt{7}} \approx 0.189$	$\frac{1}{7}$

In order to compare and sort the moments of inertia we normalize the moment of inertia relative to an horizontal axis by the maximum possible moment of inertia which is $I_{\max} = Ah^2/4$. This gives a ratio which is always between zero and one. Also, since the displacement is inversely proportional to the moment of inertia, this ratio gives the rel-

ative rigidity of a given cross-section for a fixed area and height. The higher the ratio, the higher the rigidity of the cross-section with a ratio of one corresponding to the shapes with the highest possible rigidity for a given area and height. In addition, for symmetric cross-sections, the maximum stress is also inversely proportional to the moment of inertia for a fixed area, height and maximum bending moment. Therefore, the ratio $I/I_{\max}$ also gives the relative strength of a symmetric cross-section for a fixed area and height. For example, a diamond shape and a rectangular shape (see table 3.2) have $I/I_{\max}$ equal to $1/6$ and $1/3$ respectively. Therefore, a beam with a rectangular cross-section is $(1/3)/(1/6) = 2$ times as strong and as rigid as a diamond shaped cross-section for the same area and height.

We start by discussing a set of cross-sectional shapes that are symmetric relative to a horizontal axis and these are shown in table 3.2 (second column). From the definition of the moment of inertia, we expect the moment of inertia for a given area to increase as more of the area is placed as far as possible from the center of gravity. In the limit, we get the 'ideal I-beam' which has the area placed symmetrically at half the height away from the center of gravity. This configuration gives the highest possible moment of inertia so that $I/I_{\max} = 1$. The next configuration allows for a web or some material to be placed to connect the two areas placed at the farthest point. This gives an I-beam that can actually be constructed and has a relatively lower moment of inertia than the ideal I-beam. A shape that may be equivalent to a real I-beam in terms of moment of inertia is the hollow square (see figure 3.6) and is shown as the third entry in table 3.2. The next two shapes considered allow for the width to taper as we get closer to the center of gravity. They are both hour-glass shaped but one has parabolic borders and the one after that has straight line borders. Both these hour-glass shaped cross-section would need some small amount of material to be placed at and near the center of gravity in order to have a well-connected section but these do not much affect the moment of inertia. In any case, the parabolic and linear hour-glass $I/I_{\max}$ equal about 0.543 and 0.5 respectively. The next shape is that of the hollow circular disk which, depending on its thickness 't,' may or may not be more efficient than the rectangular section which has $I/I_{\max} = 1/3$. The rectangular cross-section is a delimiting case between the shapes that taper out as we get farther from the center of gravity and those that taper in. Of course, shapes that taper out will have relatively higher moment of inertia for the same area and height. Among the rest of the shapes, we note the elliptic cross-sections which include the disk and all of these sections have $I/I_{\max} = 1/4$. We also note the diamond shape with straight edges which has $I/I_{\max} = 1/6$.

Note that, with all the cross sections, if we have a specified height and area, then this determines the width 'b' or thickness 't' for a chosen shape. In particular, for the elliptic cross-sections, if we specify the height and area, the width is then determined and this will generally not correspond to a disk or circular border. In any case, the formula for the area is also given in order to obtain cross-sections that are comparable in terms of the moment of inertia when we specify both the area and the height. Finally, the radius of gyration relative to an horizontal axis is also given since this could be useful in some applications.

Table 3.3. Relation Between Shape, Radius of Gyration and Height of Cross-Sections for Non-Symmetric Sections with Monotonically Varying Width. The Cross-Sectional Shapes are Ranked in (Mostly) Decreasing Order of $I/I_{\max}$ where 'I' is the Moment of Inertia of the Cross-Section and $I_{\max} = Ah^2/4$ is the Maximum Possible Moment of Inertia for the Same Area 'A' and Height 'h' of the Cross Section. The Result for a Rectangle is also Given as a Limiting Case of the Trapezoid.

Note: In the table below, 'A' is the area, 'b' is the width, 'h' is the height, 'ρ' is the radius of gyration around an horizontal axis through the center of gravity, 'I' is the moment of inertia around an horizontal axis through the center of gravity, '$I_{\max}$' is the maximum possible moment of inertia, 'r' is the radius of a circle (if present) and 't' is a thickness (if present).

Name	Shape	Area (A)	ρ/h	$I/I_{\max}$
rectangle		bh	$\sqrt{\frac{1}{12}}$	$\frac{1}{3}$
Trapezoid		$\frac{(b_b+b_t)}{2}h$	$\frac{\sqrt{b_b^2+4b_bb_t+b_t^2}}{\sqrt{9/8(b_b+b_t)}}$	$\frac{2}{9}\frac{(b_b^2+4b_bb_t+b_t^2)}{(b_b+b_t)^2}$
semi-elliptic		$\frac{\pi}{4}bh$	$\frac{\sqrt{9\pi^2-64}}{6\pi}\approx$ $\sqrt{\frac{1}{14.31}}$	$1-\frac{64}{9\pi^2}\approx\frac{1}{3.58}$
outer-parabola		$\frac{2}{3}bh$	$\sqrt{\frac{1}{14.59}}$	$\frac{1}{3.65}$
triangle		$\frac{1}{2}bh$	$\sqrt{\frac{1}{18}}$	$\frac{1}{4.5}$
inner-parabola		$\frac{1}{3}bh$	$\approx\sqrt{\frac{1}{18.92}}$	$\approx\frac{1}{4.73}$
$\perp-$ beam (flange thickness $<< h$)		A_w+A_f	$\approx\sqrt{\frac{1}{12}}\sqrt{\frac{A_w}{A}}$	$\approx\frac{1}{3}\frac{A_w}{A}$
$\perp-$ beam negligible web		A	≈ 0	≈ 0

Finally, we discuss a set of cross-sectional shapes that are unsymmetric relative to an horizontal axis and these are shown in table 3.3 (second column). These shapes all have the property that the width is monotonically decreasing (or more precisely non-increasing) with the height. Of course, these are a small subset of all possible shapes but the reflection from symmetry and the middle augmentation allows us to estimate a much wider set of non-symmetric shapes. As a delimiting case, we first consider the rectangular cross-section which remains constant through the height direction. This case which has $I/I_{\max} = 1/3$ is an upper bound on all the other shapes in this set. For example, if we maximize the value of $I/I_{\max}$ for the trapezoidal shape over all possible values of b_b (bottom width) and b_t (upper width), we find that the maximum of $1/3$ occurs only when those widths are equal which gives a rectangular cross-section. Some interesting results in table 3.3 include:

- The semi-elliptic cross-section is about 10.55% more efficient than the elliptic cross-section. Note that this does not violate the reflection from symmetry because such a transformation cannot change an elliptic into a semi-elliptic cross-section.

- The triangular cross-section is about 55.6% less efficient than the straight-edged hour-glass but only 33.3% more effficient than the straight-edged diamond both of which can be constructed from triangles.

3.3 Relative Vertical Displacements versus Strain in Beams

The formulas and results presented so far require a knowledge of both the load magnitude and the moment of inertia in order to determine the displacements. In some cases, such as during a visual inspection of a built structure or in preliminary design, it may be sufficient to approximately determine the range of displacements of a member. For such a case, an approach that only uses geometrical variables (*ie.* dimensions and strain) will be desirable and related formulas and discussions for this purpose will be developed in this section.

To illustrate the basic idea, we start with a simply supported beam subject to a uniformly distributed load (figure 3.1b with $k_L = k_R = 0$). The maximum displacement for that case occurs at the middle and is given by:

$$\delta_{\text{applied max}} = \frac{5}{384}\frac{qL^4}{EI} \quad \text{(simply-supported beam)} \qquad (3.7)$$

where:

$\delta_{\textbf{applied}\,\text{max}}$ is the displacement at the middle of the beam which is the maximum for this case

q is the magnitude of the unifrom load

L is the length of the beam

E is Young's modulus

I is the moment of inertia

For that same case, the maximum bending stress also occurs at the middle and has a magnitude given by:

$$\sigma_{\text{applied max}} = \tfrac{1}{8}\frac{qL^2}{I}\frac{h}{2}\beta \qquad \text{(simply-supported beam)} \qquad (3.8a)$$

$$\beta = \frac{d_{\text{CG to farthest edge}}}{h/2} \qquad (3.8b)$$

where:

$\sigma_{\textbf{applied max}}$ is the displacement at the middle of the beam

h is the height of the cross-section of the beam

$d_{\textbf{CG to farthest edge}}$ is the maximum vertical distance between the centroid and the border of the cross-section

We note that $\beta = 1$ for all symmetric sections and is between 1 and 2 for an unsymmetric section. If we now divide the maximum stress by Young's modulue 'E,' we get the maximum applied bending strain $\epsilon_{\text{applied max}}$. We now divide the maximum displacement by the maximum applied strain and simplify to get:

$$\frac{\delta_{\text{applied max}}}{h} = \frac{5}{24}\left(\frac{L}{h}\right)^2 \frac{1}{\beta}\left(\frac{\epsilon_{\text{applied max}}}{\epsilon_{\text{max}}}\right)\epsilon_{\text{max}}$$

$$\text{(simply-supported beam; uniform load)} \quad (3.9)$$

where:

$\epsilon_{\textbf{applied max}}$ is the maximum strain in the beam due to the applied loads

$\epsilon_{\textbf{max}}$ is the maximum strain that may be applied to the material of the beam before yielding or failure

If we now repeat this analysis for a centrally located point force, we get the following result:

$$\frac{\delta_{\text{applied max}}}{h} = \frac{1}{6} \left(\frac{L}{h}\right)^2 \frac{1}{\beta} \left(\frac{\epsilon_{\text{applied max}}}{\epsilon_{\text{max}}}\right) \epsilon_{\text{max}}$$

<div align="center">(simply-supported beam; central point force)   (3.10)</div>

If the point force is not centrally located then we get a displacement correction factor 'γ' as follows:

$$\frac{\delta_{\text{applied max}}}{h} = \gamma\left(x_F\right) \frac{1}{6} \left(\frac{L}{h}\right)^2 \frac{1}{\beta} \left(\frac{\epsilon_{\text{applied max}}}{\epsilon_{\text{max}}}\right) \epsilon_{\text{max}}$$

<div align="center">(simply-supported beam; point force; any location)   (3.11a)</div>

$$\gamma\left(x_F\right) \approx 1 - 0.92 \left(\frac{x_F}{L} - \frac{1}{2}\right)^2$$

<div align="center">(simply-supported beam; point force; any location)   (3.11b)</div>

where: x_F is the location of the point force along the beam measured from the left end (see figure 3.1c).

Note that the exact correction factor 'γ' in formula 3.11a for the simply supported beam with a central point force is such that $0.77 \lesssim \gamma \leq 1$. The above analysis may be generalized for the uniform load to obtain an expression that is applicable for all passive supports (see figure 3.1b) with stiffness factors 'k_L' and 'k_R' as follows:

$$\frac{\delta_{\text{applied max}}}{h} = \gamma\left(k_L, k_R\right) \frac{5}{24} \left(\frac{L}{h}\right)^2 \frac{1}{\beta} \left(\frac{\epsilon_{\text{applied max}}}{\epsilon_{\text{max}}}\right) \epsilon_{\text{max}}$$

<div align="center">(uniform load)   (3.12a)</div>

$$\gamma\left(k_L, k_R\right) \approx \frac{15k_L^2 + 2k_L^3 + 4k_L^2 k_R + 15k_R^2 + 4k_L\, k_R^2 + 2k_R^3}{15k_L^2 + 3k_L^3 + 7k_L^2 k_R + 15k_R^2 + 7k_L\, k_R^2 + 3k_R^3}$$

<div align="center">(uniform load)   (3.12b)</div>

$$\gamma(k, k) = \frac{15 + 6k}{15 + 10k}$$

<div align="center">(uniform load; $k_L = k_R = k$)   (3.12c)</div>

The exact expression for $\gamma\left(k_L, k_R\right)$ for the uniform load case is plotted in figure 3.13. The results show that 'γ' varies slowly (note the logarithmic scale) and, by optimizing the values of 'γ,' we determine that 'γ' is always between 0.6 and 1 for the uniform load case.

$\gamma(k_L, k_R)$ for uniform load
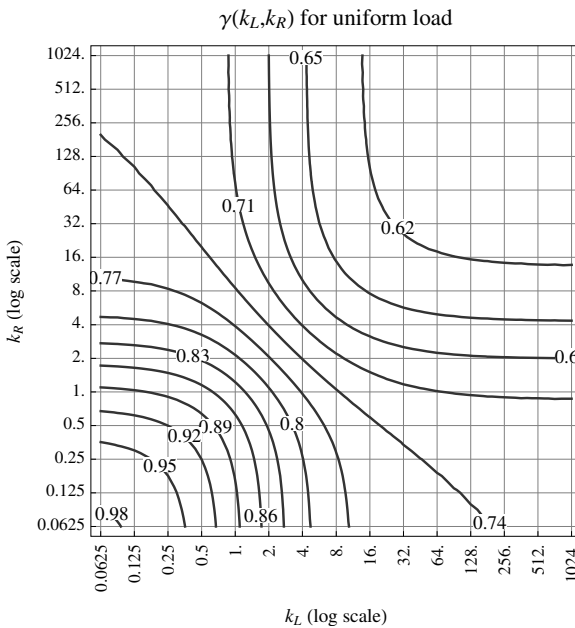
Figure 3.13. Displacement correction factor for the uniform load. Note that the value of γ is always between 0.6 and 1.

The analysis for a point force is somewhat more complicated and simple expressions have not been obtained for the general case. For the case of a centrally located support with symmetric supports (*ie.* $k_L = k_R = k$), we get an exact result:

$$\frac{\delta_{\text{applied max}}}{h} = \gamma\left(k, k, x_F = L/2\right) \frac{1}{6}\left(\frac{L}{h}\right)^2 \frac{1}{\beta}\left(\frac{\epsilon_{\text{applied max}}}{\epsilon_{\text{max}}}\right)\epsilon_{\text{max}}$$

(point force; central load; symmetric supports)
(3.13a)

$$\gamma(k, k, x_F = L/2) = \frac{2+k}{2+2k}$$

(point force; central load; symmetric supports)
(3.13b)

The general case for the point force may be calculated and plotted and the result is shown in figures 3.14 for three different values of 'x_F.' The results show that 'γ' varies slowly (note the logarithmic scale) and by

$\gamma(k_L, k_R, x_F)$ for point force; $x_F/L = 0.1$

(a)

$\gamma(k_L, k_R, x_F)$ for point force; $x_F/L = 0.3$
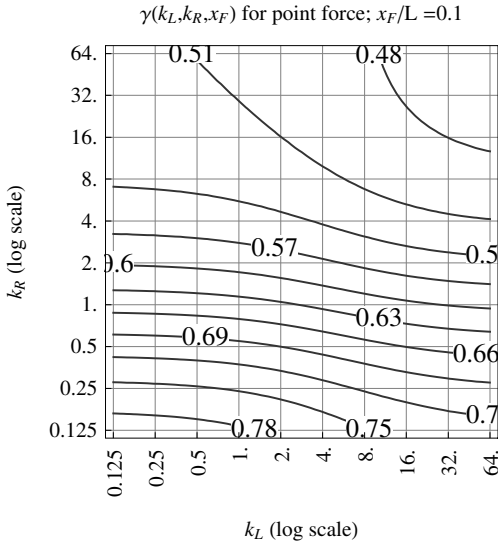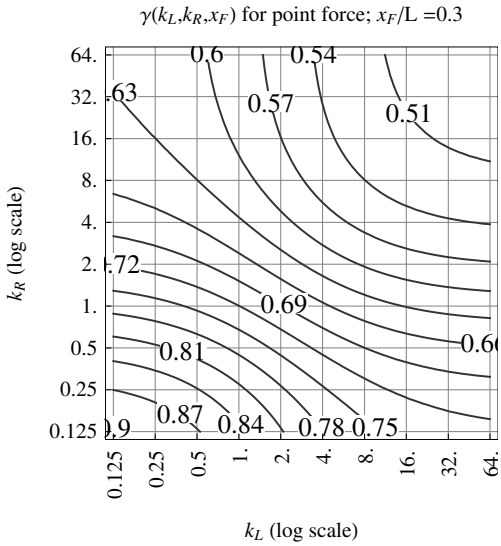
(b)

Figure 3.14. *(Continued below.)*

$\gamma(k_L, k_R, x_F)$ for point force; $x_F/L = 0.5$

k_R (log scale)

k_L (log scale)

(c)
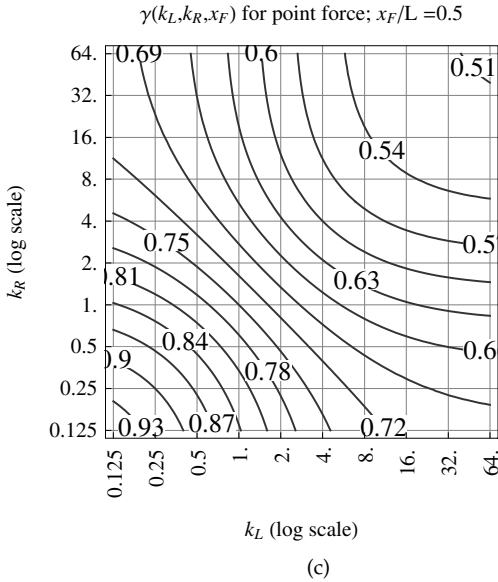
Figure 3.14. *(Continued from above.)* Displacement correction factor for the point load. Note that the value of γ is always between about 0.444 and 1.

optimizing the values of 'γ,' we determine that 'γ' is always between $4/9 \approx 0.444$ and 1 for the general point force location and between 0.5 and 1 for the centrally located point force.

Therefore, for either a uniform load or a point force, we get the following general form and constraints:

$$\frac{\delta_{\text{applied max}}}{h} = c_\delta \left(\frac{L}{h}\right)^2 \frac{1}{\beta} \left(\frac{\epsilon_{\text{applied max}}}{\epsilon_{\text{max}}}\right) \epsilon_{\text{max}}$$

(all cases) $\qquad\qquad$ (3.14a)

$$\frac{\delta_{\text{max}}}{h} = c_\delta \left(\frac{L}{h}\right)^2 \frac{1}{\beta} \epsilon_{\text{max}}$$

(all cases) $\qquad\qquad$ (3.14b)

$$0.037 \left(\frac{L}{h}\right)^2 \epsilon_{\text{max}} \lesssim \frac{\delta_{\text{max}}}{h} \lesssim 0.208 \left(\frac{L}{h}\right)^2 \epsilon_{\text{max}}$$

(all cases) $\qquad\qquad$ (3.14c)

$$\frac{2}{27} \le c_\delta \le \frac{5}{24}$$
$$(ie.\ 0.0741 \lesssim c_\delta \lesssim 0.208) \tag{3.14d}$$

$$\beta = \begin{cases} 1 & \text{symmetric cross section} \\ 1 < \beta < 2 & \text{non-symmetric cross-section} \end{cases} \tag{3.14e}$$

$$\frac{\epsilon_{\text{applied max}}}{\epsilon_{\text{max}}} \le 1 \tag{3.14f}$$

where: δ_{max} is the maximum possible displacement before the maximum allowable strain 'ϵ_{max}' is reached somewhere in the beam.

The formula 3.14a is interesting for several reasons including:

- The maximum displacement (δ_{max}) is independent of Young's modulus, the area of the cross-section, the width of the cross-section and, for a symmetric cross-section, the moment of inertia. In particular, we can avoid calculating the maximum load as an intermediate step in determining the maximum displacement.

- The maximum over minimum value of c_δ is about 2.8 so that all beams with a uniform or a point force load and with any type of passive connections will be within a relatively narrow range when the other variables in formula 3.14a are specified.

- An upper bound on the maximum displacement (δ_{max}) depends only on the ratio of length over height, height and material property 'ϵ_{max}.' This means that if we can estimate the material property 'ϵ_{max}' of the beam and, by a simple visual inspection, estimate the length and height of the beam, then we can estimate an upper bound on the maximum displacement.

Using the relations in 3.14 we can get upper bounds on the maximum displacement for different materials that may be encountered in structural engineering. Typical values of 'ϵ_{max}' for some of those materials are given in table 3.4. The table indicates that most materials have a maximum strain in the range of 0.1% to 1%. This means that the maximum displacement for those materials must have an upper bound between $0.000037(L/h)^2h$ and $0.0021(L/h)^2h$. If the length to height ratio is between 5 to 20 then this means that the maximum possible displacement must have an upper bound between $0.0009h$ and $0.85h$. This is a wide range but it covers a very wide range of materials, loading conditions, length to height ratios and support conditions. For more precise

Table 3.4. Range of Maximum Strain in Common Structural Materials.

Material	Typical range of ϵ_{max}	note
Steel	0.1% to 0.3%	Based on yield strengths of typical structural steels
Aluminum	0.1% to 0.7%	Based on yield strength of wide range of Aluminum types
Concrete	0.3% to 0.5%	Based on ultimate strengths of low to high strength concrete
Wood	0.02% to 0.08%	Based on the compression proportionality limit of soft and hard woods
Thermoplastics	may be several percent	Varies widely, may be several percent

estimates, we may use a more specific formula from the ones presented above.

For example, consider a steel beam with symmetric cross-section with $\epsilon_{max} = 0.001$ subject to a centrally applied point force which is half the maximum possible. In addition, the beam has a span of 5m and height of 0.5m and it is connected to either side by identical beams. In this case, the maximum deflection may be estimated as follows: We start by using formula 3.13a with the stiffness factor $k \approx 1$ and the ratio of applied maximum to maximum possible strain $\left(\epsilon_{\text{applied max}}/\epsilon_{max}\right) = 0.5$. Using formula 3.13b or figure 3.14c, we get that $\gamma = 3/4$ and this then leads to an estimate of the maximum deflection to be $(3/4) \times (1/6) \times (5\text{m}/0.5\text{m}) \times 1 \times (0.5) \times 0.001 \times 0.5\text{m} \approx 0.0003125\text{m} = 0.3125\text{mm}$. Note that this is the maximum displacement due to half the failure load. For the full failure load due to a point force, we get double the previous displacement which is equivalent to $0.00125h$ (*ie.* within the bounds identified previously).

For completion, we also present the formula equivalent to 3.14 for a cantilever that is either uniformly loaded or loaded by a point force at its tip. The results are as follows:

$$\frac{\delta_{max}}{h} = \frac{1}{2}\left(\frac{L}{h}\right)^2 \frac{1}{\beta}\left(\frac{\epsilon_{\text{applied max}}}{\epsilon_{max}}\right)\epsilon_{max}$$

(uniform loaded cantilever)   (3.15a)

$$\frac{\delta_{max}}{h} = \frac{2}{3}\left(\frac{L}{h}\right)^2 \frac{1}{\beta}\left(\frac{\epsilon_{\text{applied max}}}{\epsilon_{max}}\right)\epsilon_{max}$$

(point force at tip of a cantilever)   (3.15b)

Note that the result of the point force may be inferred from the central point force on a simply supported beam by doubling the effective length of the beam. The uniform load case cannot be similarly inferred because doubling the length with symmetry does not give a simply-supported beam with a uniform load. We note that the cantilever has a significantly higher maximum displacement at any given strain level and, in particular, at failure than beams supported at both sides.

3.4   Side Displacements of Frames Subject to Side Loads

In this section, we will describe how to estimate the sidesway in a regular frame that would usually be part of a building. So far in our analysis, we have assumed that axial deformations in the analysis of a frame may be neglected since they are much smaller than the bending deformations. While this will turn out to be true for most practical frames with fewer than about 10 to 20 floors, we will investigate quantitatively the conditions under which if we neglect axial deformations then we still obtain good approximation for the sideway movement of a frame.

To explore the conditions where we can neglect axial deformations, we consider a class of frames where all the beams have the same sectional properties and all the columns have the same sectional properties such as the frame shown in figure 3.15. In addition, all the columns have the same height and all the beams have the same length with a single side force applied at the top floor. We then consider the side deflection at the point where the load is applied and compare that value to the one we would obtain if we neglect the axial deformations or equivalently when $EA_c \to \infty$ in figure 3.15. Based on this, we define the shear deformation fraction as the side deflection at the top floor when we neglect the axial deformations divided by the same deflection when we do not neglect those axial deformations. The shear deformation fraction must always be between zero and one When this fraction is close to one then we may neglect axial deformations and conversely, when this fraction is close to zero then we may neglect shear deformations.

As a first step in our discussion, we derive an approximate expression for both the shear and bending deformations for the class of buildings depicted in figure 3.15. These expressions will be useful in clarifying the mechanisms and non-dimensional parameters that affect the shear deformation fraction and in providing a more convenient expression to do parametric studies.

We start by considering the top floor displacements due to shear deformations. This top floor displacement is the sum of the sidesways
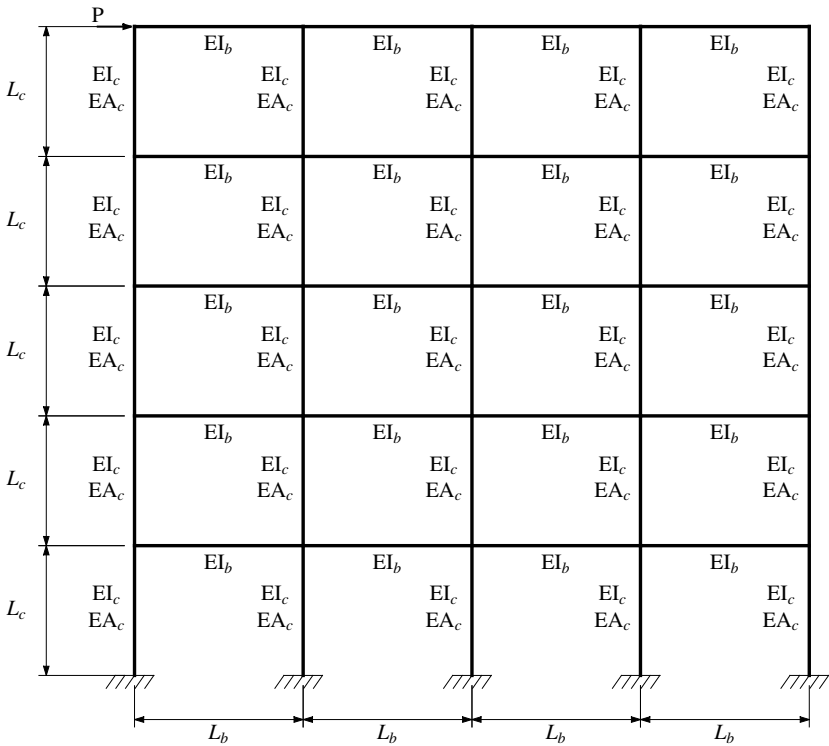
Figure 3.15. Class of building analyzed to identify contribution of bending versus axial deformations due to horizontal loads.

(*ie.* difference in sideway movement of columns) of all the floors. In addition, using free body diagrams at each floor and considering horizontal equilibrium, we find that the total of the shear forces in all the columns in any given floor equals the same force 'P' that is applied at the top floor. Using the previously defined shear stiffness of a column, the sidesway of a given floor is then given by 'P' divided by the total of the column shear stiffnesses in that floor (*eg.* refer to the derivation of formula 2.9). Therefore, the horizontal displacement of one floor is given by:

$$\text{sidesway of one floor} \approx \frac{P}{\text{stiffness of one floor}}$$

$$\approx \frac{1}{5 \text{ to } 12} \frac{P L_c^3}{E I_c} \times \frac{1}{\text{spans} + 1} \approx \left(\frac{11 + 6k}{1 + 72k} \right) \frac{P L_c^3}{E I_c} \times \frac{1}{\text{spans} + 1} \quad (3.16)$$

where:

P is the applied horizontal force at the top floor

L_c is the height of the columns

E is Young's modulus

I_c is a column's moment of inertia (assumed all uniform)

k is the ratio of a beam's rotary stiffness divided by a column's rotary stiffness (ie. $k = (EI_b/L_b) / (EI_c/L_c)$)

spans is the number of spans (or bays) and spans $+1$ equals the number of columns in each floor

Note that to estimate the stiffness of a column in a building, we have used formula 2.15 in spite of its limited applicability. By using formula 3.16 and summing over all floors, we get that the top floor displacement is given by:

$$
\begin{aligned}
\delta_{\text{sheartop}} &\approx \left(\frac{11 + 6k}{1 + 72k} \right) \frac{PL_c^3}{EI_c} \times \frac{\text{floors}}{\text{spans} + 1} \\[2mm]
&= \left(\frac{11 + 6k}{1 + 72k} \right) \frac{PL_c^2 L_b}{EI_c} \times \left(\frac{H}{W} \right) \frac{\text{spans}}{\text{spans} + 1} \qquad (3.17) \\[2mm]
&= \left(\frac{11 + 6k}{1 + 72k} \right) \frac{PL_c^2 L_b}{EI_c} \times \left(\frac{H}{W} \right) \frac{\text{floors}}{\text{floors} + (H/W)(L_b/L_c)}
\end{aligned}
$$

where:

δ_{sheartop} is the side deflection of the top floor due to shear deformations

floors is the number of floors in the frame

H is the total height of the frame or building

W is the total width of the frame or building

Using parametric studies with EA_c being very large, we find that formula 3.17 gives results that have usually less than a few percent error in the range of values that are of interest in subsequent discussions. We note that in all these studies, we assume that the axial elongations of the beams are negligible even when the axial deformations in the columns are taken into account.

Having considered the shear deformations in the class of frames considered, we now focus on estimating the bending deformations in such frames. To that purpose, we start by modelling the frame as an effective cantilever subject to bending deformations only (*ie.* the usual Bernoulli beam or column). The top deflection of such a cantilever is given by:

$$\delta_{\text{bending top}} = \frac{1}{3}\frac{PH^3}{EI_{\text{eff}}}$$

where:

$\delta_{\textbf{bending top}}$ is the side deflection of the top floor due to bending deformations

$\boldsymbol{I_{\textbf{eff}}}$ is the effective moment of inertia of the frame at any given floor

Therefore, we need to determine the effective moment of inertia in order to obtain the required expression. To that purpose, we start (naively) to assume that each column acts like an area at a point with the centroid being at the midpoint of any given floor. By summing up the contribution of each column, we get the following result:

$$I_{\text{eff}} \approx \tfrac{1}{2}A_cW^2\frac{(1+\ \text{spans})(2+\ \text{spans})}{6\ \text{spans}} \tag{3.18}$$

Combining the above two expressions, we get:

$$\delta_{\text{bending top}} \approx \frac{2}{3}\frac{PH}{EA_c}\left(\frac{H}{W}\right)^2\frac{6\ \text{spans}}{(1+\ \text{spans})(2+\ \text{spans})}$$

$$= \frac{2}{3}\frac{PH}{EA_c}\left(\frac{H}{W}\right)^3 \times \tag{3.19}$$

$$\times\ \frac{6\,(L_b/L_c)\,\text{floors}}{\big(\text{floors} + (L_b/L_c)\,(H/W)\big)\big(\text{floors} + 2\,(L_b/L_c)\,(H/W)\big)}$$

Using parametric studies, we find that while the above formula often gives the right trend but it can have relatively large errors in the range of values that are of interest in subsequent discussions. Therefore, we need to do a more careful study in order to obtain a more accurate expression. However, the conceptual development of the above formula is simple and thus provides an overall idea of how we think about bending deformations.

In order to get a more accurate expression for the bending deformations, we will consider a more detailed and discrete view of how bending

Normalized axial forces in ground floor columns

$L_b/L_c = 1.5;$ $(EI_b/L_b)/(EI_c/L_c) = 3$

Floors = 20;   Spans = 8
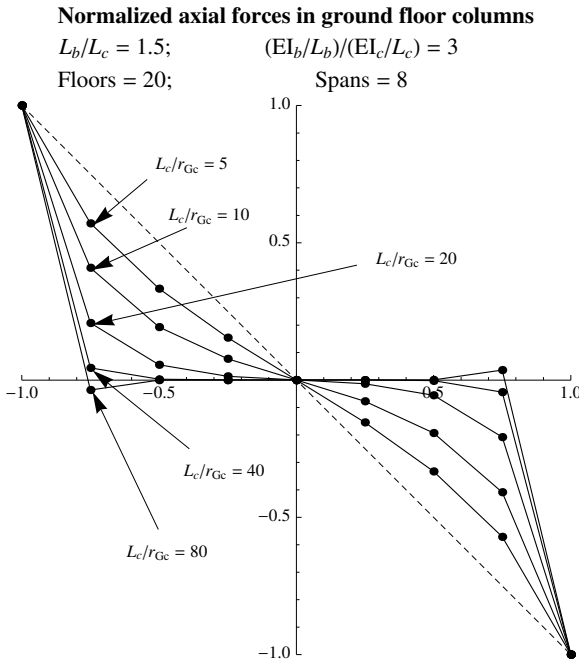
Figure 3.16. Axial force variation as the slenderness ratio varies from a (very) short column to a slender column.

deformations develop in a frame. We start by considering the axial forces in columns when a frame is subject to side forces. To get insight into this problem we plot the normalized axial forces in the columns of the ground floor of a frame with 20 floors and 8 spans and keeping other parameters fixed, we vary the slenderness ratio of the columns as shown in figure 3.16. For realistic values of the slenderness ratio, we find that the distribution of axial deformations is far from linear. If we want to approximate the axial forces, a suitable assumption is to consider that the only non-zero axial forces are in the two outer columns.

The observation that only the outer columns have appreciable axial forces could be understood using the previously developed methods for analyzing frames with sidesway. In particular, we note that for the type of frame considered, and indeed for most frames that do not have internal hinges, the inner columns all carry approximately the same amount of shear and, also, the shear in the outer columns are not much smaller. This leads to end moments in the columns of the same floor being ap-

proximately equal. This in turn leads to end moments in beams of the same floor that are approximately equal. Since the shear force in a beam equals the sum of end moments divided by the length of the beam, we deduce that the shear force in beams at the same floor are all approximately equal. Using free body diagrams of the nodes, we can then determine that the axial force in a column is the difference of shear forces between adjacent beams plus the transmitted axial force from the column above. Since the shear forces between adjacent beams approximately cancel except at the outer columns where there is only one connected beam, we deduce that the axial forces in the columns are approximately zero except at the outer columns.

In order to verify the observation concerning axial forces in columns, we do more extensive parametric studies and these are shown in figure 3.17. These parametric studies show a wide variation in the pattern of axial forces in the columns but do indicate that the assumption that the outer columns have the only non-negligible axial forces is a much better one than that of a linear variation in axial forces.

Based on the assumption that only the outer columns have non-zero axial forces, we can approximately determine those axial forces in each floor using equilibrium. To that end, we consider a free body diagram of the frame with a cut at the middle of a specific floor. We choose the cut to pass through the middle of the floor so that the cut approximately passes through the inflection points of the columns. Hence, at that cut, the bending moment in the columns are approximately zero and the moment developed by the side force at the top floor must approximately equal the moment developed by the axial forces in the outer columns. Therefore, the axial force in an outer column is given by:

$$F_{\text{floor } i} \approx \frac{H - (i - 1/2)L_c}{W} P$$

where:

'i' is the floor number with $i = 1$ being the ground floor and $i =$ floors being the top floor

$F_{\text{floor} i}$ is the axial force in an outer column in floor number *'i'*

The axial forces in the columns cause elongations in those columns and the difference in elongations divided by the width of the frame gives a floor rotation. This floor rotation multiplied by the distance from the floor to the top contributes to a side displacement at the top floor. By adding the effect of rotations at all the floors, we can obtain the top floor

(a)

(b)

Figure 3.17. *(Continued below.)*

Normalized axial forces in ground floor columns

$L_b/L_c = 1.5$; L_c/r_{Gc} (slenderness ratio) = 20

$(EI_b/L_b)/(EI_c/L_c) = 1$;   Max floors = 10;   Max spans = 10

(c)

Normalized axial forces in ground floor columns

$L_b/L_c = 1.$; L_c/r_{Gc} (slenderness ratio) = 40

$(EI_b/L_b)/(EI_c/L_c) = 1$;   Max floors = 10;   Max spans = 10

(d)

Figure 3.17. *(Continued from above and continued below.)*

Normalized axial forces in ground floor columns

$L_b/L_c = 1.$; L_c/r_{Gc} (slenderness ratio) = 40

$(EI_b/L_b)/(EI_c/L_c) = 3$;   Max floors = 10;   Max spans = 10

(e)

Normalized axial forces in ground floor columns

$L_b/L_c = 1.5$; L_c/r_{Gc} (slenderness ratio) = 40

$(EI_b/L_b)/(EI_c/L_c) = 1$;   Max floors = 10;   Max spans = 10

(f)

Figure 3.17. *(Continued from above.)* Distributions of axial forces in the ground floor columns for variable number of floors, spans and other configurational parameters. The parametric studies indicate that most of the resisting moment that is due to the axial forces is developed by the outer columns and that the variation of axial forces is far from linear.

displacement. The rotation $\Delta\theta_{\text{floor}i}$ at the ith floor is given by:

$$\Delta\theta_{\text{floor } i} \approx 2 \frac{F_{\text{floor } i} L_c}{E A_c} \bigg/ W = \frac{H - (i - 1/2)L_c}{E A_c W} 2 L_c P$$

Multiplying this rotation by the distance from the floor to the top and adding the effect of all floors gives the top displacement:

$$\delta_{\text{bending top}} \approx \frac{(1 + \text{floors})(4\,\text{floors} - 1)}{6\,\text{floors}^2} \frac{PH}{E A_c} \left(\frac{H}{W}\right)^2 \tag{3.20}$$

Using parametric studies, we find that formula 3.20 gives results with errors that are usually less than about 15% and generally much lower in the range of values that are of interest in subsequent discussions. Based on formulas 3.17 and 3.20, we obtain the shear deformation fraction as:

$$\text{shear fraction} = \frac{\delta_{\text{shear top}}}{\delta_{\text{total}}} = \frac{\delta_{\text{shear top}}}{\delta_{\text{shear top}} + \delta_{\text{bending top}}}$$

$$\Rightarrow \text{ shear fraction} \approx \frac{1}{1 + \frac{(\text{floors} +1)(4\,\text{floors} -1)(\text{spans} +1)}{6\,\text{floors}^2} \left(\frac{1+72k}{11+6k}\right) \left(\frac{L_c}{r_{Gc}}\right)^2 \left(\frac{H}{W}\right)^2}$$

$$\Rightarrow \text{ shear fraction} = z \tag{3.21}$$

where:

$$z = \frac{1}{1 + \frac{2}{3} \frac{(\text{floors}+1)(\text{floors}-\frac{1}{4})(\text{floors}+(H/W)(L_b/L_c))}{\text{floors}^2} \left(\frac{1+72k}{11+6k}\right) \left(\frac{r_{Gc}}{L_c}\right)^2 \left(\frac{H}{W}\right) \left(\frac{L_c}{L_b}\right)}$$

and:

r_{Gc} is the radius of gyration of the column

(L_c/r_{Gc}) is the slenderness ratio

Parametric studies were done in order to determine the accuracy of formula 3.21 for the class of frames represented by figure 3.15. Specifically, 500 cases were generated using the following rules:

- 'k,' the slenderness ratio and L_b/L_c were chosen randomly based on uniform distributions between 1 and 5, between 10 and 100 and between 1 and 2 respectively.

- The number of floors was randomly chosen from the list (5, 10, 20, 40).
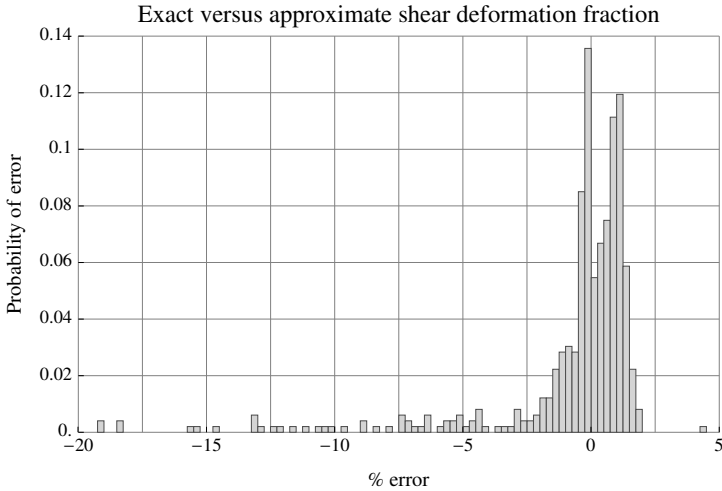
Figure 3.18. Exact versus approximate shear stiffness factor for 500 cases of buildings generated semi-randomly (see text). Note that the sum of probabilities between -5 and $2 \approx 0.9$ (90%). This means that in 90% of the cases, the errors are between -5% and 2%.

- H/W was chosen randomly based on a uniform distribution between 0.5 and 5 with the condition that the number of spans must be an integer between 1 and 10.

The result of the parametric studies are shown as a probability normalized histogram in figure 3.18. The mean error is about -1.03% and the standard deviation is about 4.3%. With these results, we considered the accuracy of formula 3.21 to be sufficient for the following analysis.

Having formula 3.21, we can now quantitatively answer the question of when we can neglect axial deformations. For the class of frames considered in figure 3.15, we will assume that we can approximately neglect axial deformations when at least 80% of the deformation at the top floor may be attributed to shear deformations. This means that we can neglect the axial deformations when formula 3.21 gives a value above 0.8. To explore the conditions under which this occurs, we plot contours of constant value 0.8 for the shear deformation fraction as a function of height over width (H/W) of the frame and of the slenderness ratio. In addition, separate contours are shown when the number of floors is 5, 10, 20, 40 and 80 and different contour plots are given for various combinations of the parameters 'k' and L_b/L_c as shown in figures 3.19.

Shear deformation fraction of total = 80%

$(EI_b/L_b)/(EI_c/L_c)=1;$ $L_b/L_c=1$

height / width of building (fewer spans)

slenderness ratio

(a)

Shear deformation fraction of total = 80%

$(EI_b/L_b)/(EI_c/L_c)=1;$ $L_b/L_c=2$

height / width of building (fewer spans)

slenderness ratio

(b)
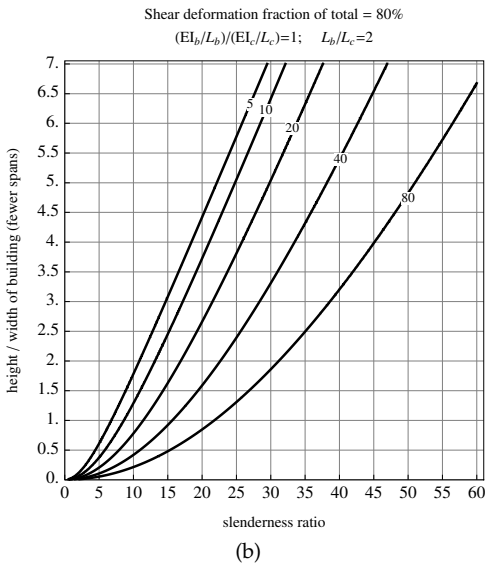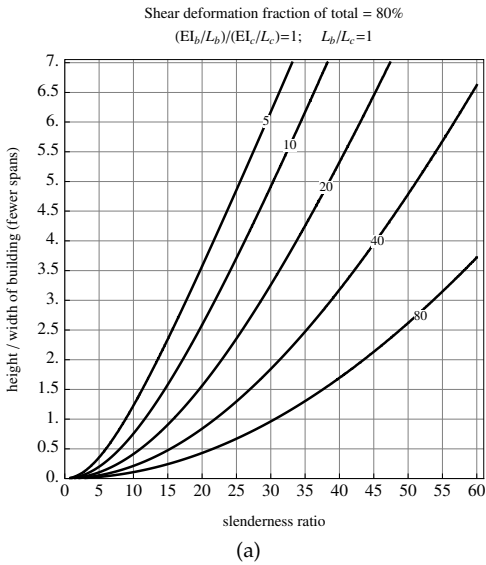
Figure 3.19. *(Continued below.)*
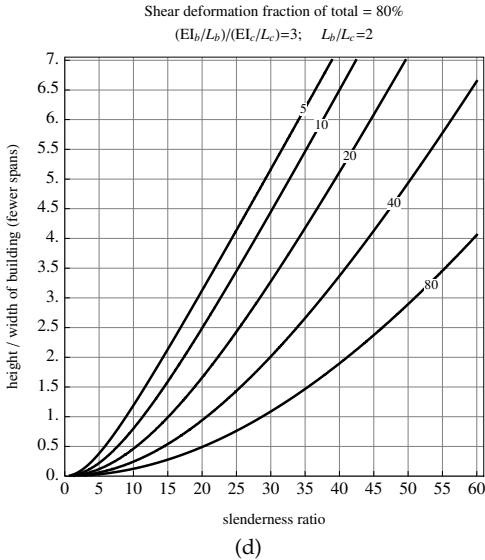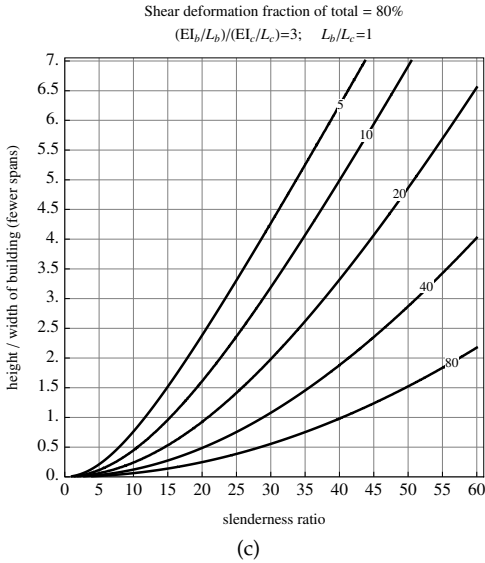
Figure 3.19. *(Continued from above.)* Fraction of top-left displacement attributed to shear in a building where only the top floor is loaded by a side-force. Curves are labelled according to the number of floors (5, 10, 20, 40 and 80 floors) and their pattern indicate the fraction that may be attributed to shear deformation. The contours correspond to a shear deformation fraction of 80% of the total deformation.

To evaluate these results, we note the following:

- In figures 3.19, the points that lie to the right of each shown curve correspond to having shear deformation fractions larger than 80%. Note that each point in the plane of those figures corresponds to a building with a particular combination of values of the column slendernesss ratio and height over width. Therefore buildings associated with points to the left of a specific curve is a building with that curve's number of floors and where that building may be approximately analyzed while neglecting axial deformations. We note that for any number of floors, axial deformations may be neglected if the slenderness ratio of the columns are large enough or if the height over width of the building is small enough. Of course, design constraints of real buildings preclude some combinations of such pairs of values. Therefore as the number of floors in a building increases, the region where axial deformations may be neglected becomes smaller and, if we include design constraints, it becomes gradually unfeasible to neglect axial deformations as the height of a building increases.

- The aspect ratio of a building which correspond to H/W is generally between 0 and 7. Skyscrapers with number of floors usually above 80, generally have an aspect ratio above 4. For example, Dubai tower, Taipei 101, the Empire state building and the Sears tower have aspect ratios of about 9.1, 5, 4.25 and 6.5 respectively and number of floors 162, 101, 102 and 108 respectively. Regular high rise buildings with number of floors between 20 and 60 generally have aspect ratios below 4.5 while buildings with less than 20 floors usually have aspect ratios less than about 3 or 4.

- Concrete and steel columns are considered slender when their slenderness ratio is above about 30 and 50 respectively.

With the above remarks and based on the results of figure 3.19, we note that we may generally neglect axial or bending deformations for frames or buildings with less than about 10 to 20 floors. In general, we may use formula 3.21 to calculate the shear deformation fraction for a proposed frame and based on that value, we can decide whether our analysis may neglect bending deformations.

Finally, we note that the implications of whether bending deformations may be neglected has important consequences on the conceptual design of a building. For example, if bending deformations are important then we have already determined that only the outer columns contribute significantly in resisting such deformations. Hence, one approach in designing tall buildings is the so-called tubular design where a high

percent of the area of all columns are preferentially positioned on the outside of the building. Other approaches that use local or global cross-bracings may also be used either to enhance the contribution of inner columns or to provide an independent second system that is resistant to bending. However, the design of tall buildings is outside the scope of this book. Based on the above study, the methods presented in this book for analyzing frames with sidesway are mostly suitable for buildings with less than about 10 to 20 floors.

3.5   Obtaining Rotary Stiffness Factors from Slope Measurements in Beams

In this book, we have extensively relied on the notion of rotary stiffness factors in order to approximately analyze beams and frames. In this section, we will consider how we can indirectly identify the stiffness factors at the ends of a member in a beam or frame by measuring slopes on that member. A procedure of this kind is important in providing a non-destructive test to determine whether the assumptions used in designing a continuous beam or a frame structure are actually realized in the built structure. This procedure is also important in doing a structural integrity assessment of a structure that may have been damaged due to environmental factors such as earthquakes or due to man-made factors such as accidents.

In designing a process to identify the stiffness factors, we must decide on what to measure, what and how much load to apply and how to process the data to obtain the rotary stiffness factors. We also need to determine the accuracy of our results and especially their sensitivity to measurement errors. We will discuss each of these items next.

First, we consider the choice of what to measure. In general, we need to measure some aspect of deformation such as strain, displacements or rotations. Preparing a member for strain measurements is tedious and time-consuming especially on a built structure. On the other hand, displacement measurements require some reliable fixed datum which may be difficult to achieve. Finally, slope measurements seem to be both economical and relatively fast. Of course, in any such choice, we will be measuring changes in the chosen variable due to an applied load increment. For slope measurements, we place an inclinometer (*ie.* device for measuring slope), make a measurement before we apply a load increment and this will be our datum. As a subsequent step, we load the member and then get a new measurement. The change in slope due to the increment in load that we have applied will be the measurement which we will use to determine the rotary stiffness factors.

Since we are proposing to measure slope, it is useful to first identify the resolution with which the slope may be measured. This resolution will determine whether such an approach is feasible, the magnitude of the incremental load to apply and the limits in accuracy with which we can infer the stiffness factors. For example, if the maximum possible load increment causes failure at slopes below the resolution of the available inclinometers then we cannot use slope measurements, at the current technology, to indirectly measure rotary stiffness factors. As the resolution gets sufficiently fine, we then get a trade-off between applying smaller load increments and having higher accuracy in the inferred stiffness factors. If the load increment is too small then we may again fall below the resolution of our measuring instrument. On the other hand, we must generally stay well below the load at which failure occurs. It would be useful in our analysis to specify a minimum load increment. For this purpose, we choose a minimum load increment which should be both convenient and safe to be around 20% of the maximum possible load. Of course, this value is somewhat arbitrary and for different applications, this minimum load increment may be varied subject to an analysis of the implied errors.

In order to determine whether a particular resolution in the measurement of slope is sufficient, we compare it with the maximum possible slope when subjected to the minimum load increment. For that purpose, we can determine the maximum applied rotation in a beam in terms of the maximum possible strain similar to what we have done in a previous section with the maximum applied displacement. The result is given by:

$$\theta_{\text{applied max}} = c_\theta \left(\frac{L}{h}\right) \frac{1}{\beta} \left(\frac{\epsilon_{\text{applied max}}}{\epsilon_{\text{max}}}\right) \epsilon_{\text{max}} \qquad (3.22a)$$

$$\tfrac{1}{4} \leq c_\theta \leq \tfrac{2}{3} \quad (\textit{ie. } 0.25 \lesssim c_\delta \lesssim 0.667) \qquad (3.22b)$$

In addition, at the time of the writing of this book (late 2009), commercially available and relatively cheap inclinometers have resolutions of less than about 1.74×10^{-5} radians (*ie.* less than 0.001°). Now that we have a formula for the maximum proposed slope that we need to measure and a resolution limit for available measuring devices, we can compare the two to determine whether the proposed method is feasible. For example, if we consider a beam with length over height of 8, with a symmetric section, with a maximum load increment of 20% and a maximum possible strain of 0.001, then the maximum applied slope in the beam must be less than $(1/4) \times (8) \times (1) \times (0.2) \times 0.001 \approx 0.0004$. This value is then $0.0004/0.0000174 \approx 23$ times the resolution limit. Therefore, for this case, we expect slope increments over a considerable part

of the span to be above the measurement resolution limit. However, the resolution limit is about 4.35% of the maximum slope that we propose to measure. Whether this implies an adequately low potential error to allow a determination of the stiffness factors within a sufficiently narrow range is a subject of further study which will be partially addressed in this section.

We now consider the setup and the process for doing the measurements and for inferring the stiffness factors. As before, we consider a beam with passive supports as shown in figure 3.20. We propose to measure the change in slopes at four locations due to a point force applied at the middle of the beam. Specifically, the locations are at either end and and at a quarter the length from each end as indicated in figure 3.20. The procedure consists of the following steps: i) we measure the slopes before any load is applied, ii) we apply a point force at the middle, iii) measure the slopes again and iv) the change in slopes at each of the four locations are the measurements we will use to infer the rotary stiffness factors. Note that it is possible, but much more cumbersome and error prone, to do the procedure with a single tiltmeter. This would require placing the tiltmeter at each of the locations in turn, taking a reference or datum measurement with no load applied anywhere on the beam, placing the point force at the middle of the beam and repeating the measurements at each location with the load kept in place.
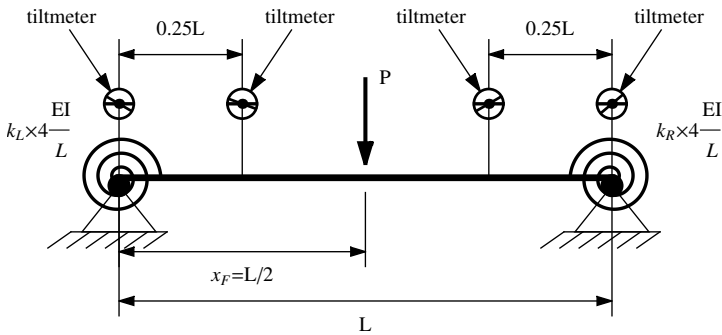
Figure 3.20. Setup for experimentally identifying the stiffness factors k_L and k_R.

The reason for choosing the specific locations shown in figure 3.20 is that, in this case, we can obtain each of the two stiffness factors separately in terms of the measured changes in slope. We start by determining the slopes in terms of the central point force which are given as:

$$\Delta\theta_0 = -\frac{3 + 2k_R}{48 + 64k_L + 64k_R + 64k_L\,k_R}\frac{PL^2}{EI} + e_0 \tag{3.23a}$$

$$\Delta\theta_{1/4} = -\frac{18 + 13k_L + 11k_R + 8k_L\,k_R}{384 + 512k_L + 512k_R + 512k_L\,k_R}\frac{PL^2}{EI} + e_{1/4} \tag{3.23b}$$

$$\Delta\theta_{3/4} = \frac{18 + 11k_L + 13k_R + 8k_L\,k_R}{384 + 512k_L + 512k_R + 512k_L\,k_R}\frac{PL^2}{EI} + e_{3/4} \tag{3.23c}$$

$$\Delta\theta_1 = \frac{3 + 2k_L}{48 + 64k_L + 64k_R + 64k_L\,k_R}\frac{PL^2}{EI} + e_1 \tag{3.23d}$$

where:

$\Delta\theta_0$, $\Delta\theta_{1/4}$, $\Delta\theta_{3/4}$ and $\Delta\theta_1$ are the four changes in slope from left to right in figure 3.20

k_L and k_R are the left and right rotary stiffness factors

P is the magnitude of the point force applied at the middle of the beam

L is the length of the beam

E is Young's modulus

I is the moment of inertia

e_0, $e_{1/4}$, $e_{3/4}$ and e_1 are the errors in measurements

Assuming for now that the errors e_0, $e_{1/4}$, $e_{3/4}$ and e_1 are zero, we now calculate the following combinations of the changes in slopes:

$$m_L = |\Delta\theta_0|\Big/\Big(|\Delta\theta_{1/4}| + |\Delta\theta_{3/4}|\Big) = 2/(3 + 2k_L) \tag{3.24a}$$

$$m_R = |\Delta\theta_1|\Big/\Big(|\Delta\theta_{1/4}| + |\Delta\theta_{3/4}|\Big) = 2/(3 + 2k_R) \tag{3.24b}$$

where: $|\cdot|$ denotes the absolute value of a quantity

Note that since the stiffness factors must be positive, then the combinations m_L and m_R must be between 0 and 2/3. From formulas 3.24a and b, we can solve for the stiffness factors as follows:

$$k_L = \frac{2 - 3m_L}{2m_L} \tag{3.25a}$$

$$k_R = \frac{2 - 3m_R}{2m_R} \tag{3.25b}$$
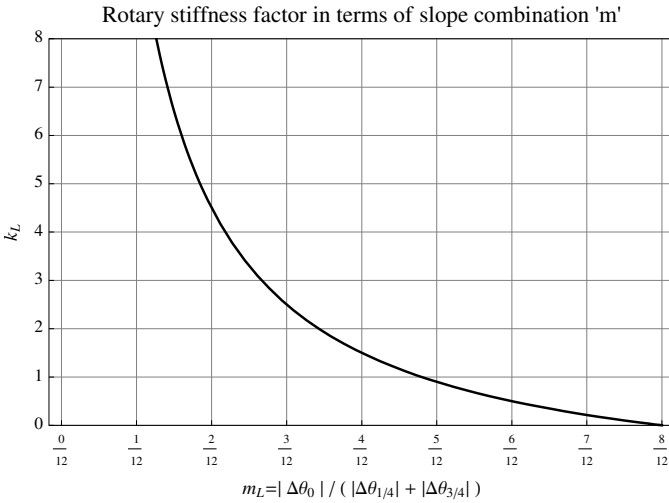
Figure 3.21. Rotary stiffness factor 'k_L' in terms of the slopes combination 'm_L' given in formula 3.25a. The rotary stiffness factor 'k_R' is similarly related to the slopes combination 'm_R' given in formula 3.25b.

The formula 3.25a for 'k_L' is plotted in figure 3.21 while the plot for formula 3.25b would be identical when 'k_L' and 'm_L' are replaced with 'k_R' and 'm_R' respectively. Note that the determination of 'k_L' is highly sensitive to the value of 'm_L' when 'm_L' is small (*eg.* less than about 3/12) and much less sensitive at higher values. This means that small errors in 'm_L' when 'm_L' is relatively small leads to large errors in 'k_L.' Fortunately, we are generally interested in higher accuracy in the determination of the rotary stiffness factors when these are relatively small (*eg.* less than about 3) than when these rotary stiffness factors are large. The reason is that the structural behavior of beams is much more senstive to changes in the rotary stiffness factors at these smaller values.

    Having described the measurements and the process of determining the rotary stiffness factors, we note that due to the choice of where to measure the slopes and how to combine the measurements, we were able to obtain rather simple expressions (*ie.* formulas 3.25) for each of the rotary stiffness factors. In general, choosing a different set of locations for the tiltmeters would require solving nonlinear equations to extract the rotary stiffness factors. This would lead to more complex postprocessing of the measured data but may possibly lead to results that are more robust against errors. For this study, we will use the locations specified in

figure 3.20 and will next consider the role of errors, such as those due to limited resolution in the slope measurements, on the determination of the rotary stiffness factors.

In expressing the measured changes in slopes in formulas 3.23a to d, we have included an error term for each. We note that the maximum possible rotation or slope in a beam due to a centrally applied point force is '$(1/32)PL^2/EI$.' If we now factor out that term from each expression, we get:

$$\Delta\theta_0 = \left(-\frac{6+4k_R}{3+4k_L+4k_R+4k_L\,k_R} + \frac{e_0}{\Delta\theta_{\text{ref max}}}\right)\Delta\theta_{\text{ref max}} \qquad (3.26a)$$

$$\Delta\theta_{1/4} = \left(-\frac{18+13k_L+11k_R+8k_L\,k_R}{12+16k_L+16k_R+16k_L\,k_R} + \frac{e_{1/4}}{\Delta\theta_{\text{ref max}}}\right)\Delta\theta_{\text{ref max}} \qquad (3.26b)$$

$$\Delta\theta_{3/4} = \left(\frac{18+11k_L+13k_R+8k_L\,k_R}{12+16k_L+16k_R+16k_L\,k_R} + \frac{e_{3/4}}{\Delta\theta_{\text{ref max}}}\right)\Delta\theta_{\text{ref max}} \qquad (3.26c)$$

$$\Delta\theta_1 = \left(\frac{6+4k_L}{3+4k_L+4k_R+4k_L\,k_R} + \frac{e_1}{\Delta\theta_{\text{ref max}}}\right)\Delta\theta_{\text{ref max}} \qquad (3.26d)$$

$$\Delta\theta_{\text{ref max}} = \frac{1}{32}\frac{PL^2}{EI} \qquad (3.26e)$$

With the above formulas, we can now calculate 'm_L' and 'm_R' again, but we now include the error terms. We will assume that each of the error terms divided by the reference value $\Delta\theta_{\text{ref max}}$ is bounded by a value 'err_{max}.' This means that:

$$\left|\frac{e_0}{\Delta\theta_{\text{ref max}}}\right|, \left|\frac{e_{1/2}}{\Delta\theta_{\text{ref max}}}\right|, \left|\frac{e_{3/4}}{\Delta\theta_{\text{ref max}}}\right| \text{ and } \left|\frac{e_1}{\Delta\theta_{\text{ref max}}}\right| \le \text{err}_{\text{max}} \qquad (3.27)$$

This then implies that there is a range of values for the observed slope combinations 'm_L' and 'm_R' in terms of 'k_L' and 'k_R' and the normalized error terms 'err_{max}.' If we use this range of values of 'm_L' and 'm_R' in formulas 3.25a and b, we get a range of values of 'k_L' and 'k_R.' From this, we can finally determine the maximum error in either 'k_L' and 'k_R' in terms of 'k_L,' 'k_R' and 'err_{max}.' Some examples of the maximum error in 'k_L' as a function of 'k_L' and 'k_R' are shown in the contour plots of figure 3.22(a), (b), and (c) for a maximum normalized error (ie. $\text{err}_{\text{max}} = e/\Delta\theta_{\text{refmax}}$) of 1%, 2.5% and 5% respectively. The maximum error in 'k_R' (ie. maximum Δk_R) will have identical contour plots when we switch 'k_L' with 'k_R' in the plots of figure 3.22.

Based on the results shown in figure 3.22, we make the following observations:

• The error in determining the rotary stiffness factor Δk_L depends mostly on k_L and weakly on k_R. Conversely, the error in determining

the rotary stiffness factor Δk_R depends mostly on k_R and weakly on k_L.

- The error in determining the rotary stiffness factor Δk_L increases with k_L and this is consistent with the observations made in regards to figure 3.21.

(a)

(b)

(c)
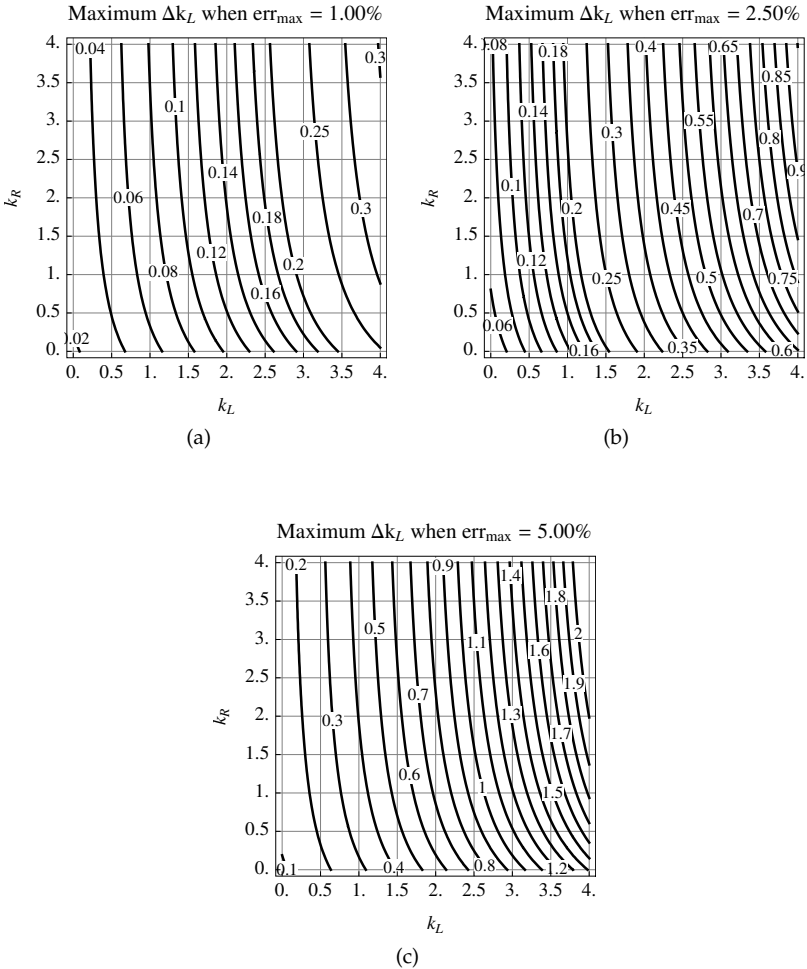
Figure 3.22. *(Continued from above.)* Maximum error in the left rotary stiffness factor as a function of both the left and right rotary stiffness factors at three different values of the upper bound on the maximum error divided by the reference maximum rotation (*ie.* $\Delta\theta_{\text{ref max}}$).

- The values of Δk_L are neither expected errors nor confidence interval width. They are bounds on the error in determining the rotary stiffness factor when the errors have a strict upper bound. Thus, while these results do not have a probabilistic interpretation, they are sufficient for the purposes of giving an indication of the expected accuracy in determining rotary stiffness factors due to a limitation in the resolution of the measuring instruments.

Finally, based on the above study, we conclude that using current technology, it is plausible to indirectly measure rotary stiffness factors using tiltmeters and reasonable loads applied on beams that are part of a larger structure. A process was outlined on how to do the measurements, how to postprocess them and how to estimate errors in the determination of rotary stiffness factors due to possible measurement errors. What is not available at this time is an experimental study that verifies these statements. The usefulness of such a study in the structural integrity assessment of framed structures could be significant.

This page intentionally left blank

Chapter 4

Approximate Influence Lines for Indeterminate Beams

4.1   Introduction to Influence Lines

In structural analysis, we are often interested in the effect of moving loads. For example, to design a bridge against failure, we would need to know how the bending moment at its middle varies as a 'standard' car or truck moves across its span. This requires consideration of the bending moment at a fixed point for every possible location of the car or truck. Using basic structural analysis, we would parametrize the location of the car or truck on the bridge and then plot the bending moment at the center versus this variable location. This plot would then constitute a succinct description of the influence of the car or truck on the bending moment at the middle of the bridge. If, in this process, we replace the car or truck by a unit point force (*ie.* a single point force with magnitude one) then we get the influence line for the bending moment at the middle point of the bridge. Using that influence line, we can then use linear superposition to obtain the previously considered influence of a car or truck.

In general, we consider a frame or continuous beam as shown in figure 4.1 and a unit point force moving across that structure. As that unit point force moves across the continuous beam ABCD, we monitor or calculate a response at any chosen but fixed point E. We call the fixed point E to be the point of influence or the influence point. If we plot the response at point E as a function of the location of the unit point force along the continuous beam then we get the influence line of that response as shown in figure 4.1. In general, the choice of response may be the displacement, the rotation, the shear or the bending moment at the chosen point. In addition, if the response is at a support, then the response may also be chosen as any of the reactions at that support.
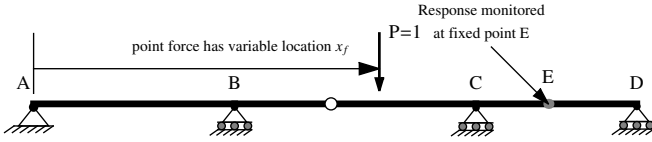
(a) Continuous beam with one internal hinge.
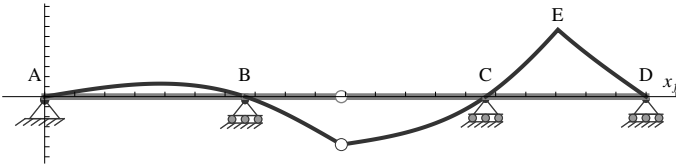
(b) Influence line for the response at point E (in this example the bending moment at E)

Figure 4.1. Figures explaining what is an influence line. In the figures above, as a unit point force traverses the beam ABCD, we monitor the response at a fixed point E. The resulting plot of response versus location of the unit load is called an influence line for that response.

The definition of an influence line suggests a way to directly construct it. We place the unit point force at successive locations from left to right on the beam and for each position, we do a structural analysis and calculate the desired response at the fixed point of interest. We could choose a finite number of locations for the point force across the beam and get a finite number of points to approximately plot the influence line. Alternatively, we could parametrically describe the position of the point force and, using analytic techniques, we then get an analytic expression for the influence line. Although both approaches are feasible they are both better-suited to computer implementations and we will mainly focus on an alternative approach.

The alternative approach is based on the Müller-Breslau principle which is in turn based on the reciprocity or Betti's theorem. The reciprocity theorem relates the external loads and external deformations of two different set of loads applied separately on the same structure. To describe the idea, we will use an example of a continuous beam ABCD that is separately loaded by two point forces as shown in figure 4.2. Each of these loads lead to distinct deformations. The reciprocity theorem then asserts the following:

$$P_E \times u_{E \text{ due to } P_F} = P_F \times u_{F \text{ due to } P_E} \qquad (4.1)$$
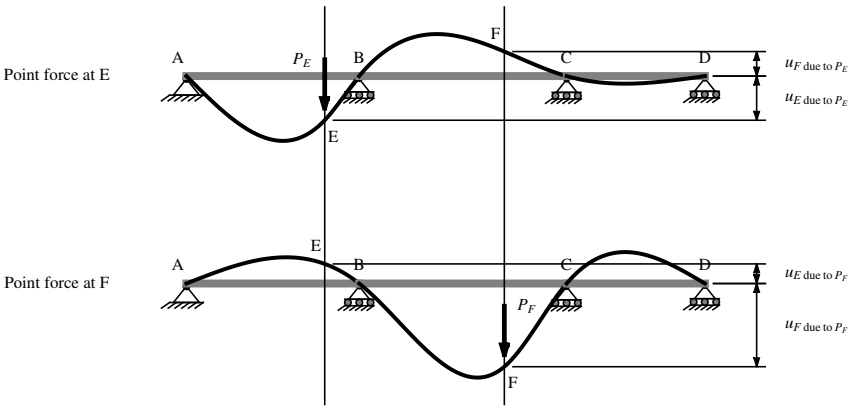
Figure 4.2. The reciprocity theorem considers the same structure but under two different set of loads. In the above, the work done by the point force at E over a displacement at E due to point force F equals the work done by the point force at F over a displacement at F due to point force E.

where the terms above are illustrated in figure 4.2 and are as follows:

P_E is the magnitude of the force at point E

P_F is the magnitude of the force at point F

$u_{E \text{ due to } P_F}$ is the displacement at E due to the point force at F

$u_{F \text{ due to } P_E}$ is the displacement at F due to the point force at E

Note that the displacements and forces are algebraic quantities that may be positive or negative depending on the sense of the chosen coordinate system. Also note that each of the terms in equation 4.1 has the form of a work quantity but with the load and the corresponding deformations being taken from separate load cases applied on the same structure. In general, the reciprocity theorem applies to all types of external loads with their corresponding deformations. Specifically, the reciprocity theorem states that if we are given two independently applied set of loads with their corresponding deformations then the work done from one set of loading on the corresponding deformations of the second set equals work done from the second set of loading on the corresponding deformations of the first. Note that the deformations corresponding to a point force and a point moment are the displacement at the location

of the point force and the rotation at the location of the point moment respectively.

While we will not present a proof of the reciprocity theorem, we will indicate the scope of its applicability. First the reciprocity theorem is based on the principle of virtual work. This principle requires that the external and internal forces be in equilibrium. Furthermore, the principle of virtual work also requires that the internal deformation measures, which are the beam and column curvatures, be compatible with the specified external supports such as rollers, hinges or fixed ends. In addition to these requirements, the reciprocity theorem additionally requires that the material responds in a linear elastic fashion. Fortunately, the specific values of the linear elastic material parameters is immaterial to the theorem. An implication of this restriction is that the reciprocity theorem is inapplicable when there is either material yielding or material cracking or damage. Since the Müller-Breslau principle is based on the reciprocity theorem, we may construct influence lines using this principle only when the material is linear elastic and there is no yielding or damage in the material.

The Müller-Breslau principle states that the influence line of a response monitored at a specific point equals the displacement obtained by applying a unit quantity of the work-associated variable. For example, to construct the influence line for the displacement at point E in the beam shown in figure 4.3a, we must first apply the work-assocatied variable at point E. The work-associated variable to a displacement is a point force at the same location. Therefore, we apply a unit force at point E and calculate the resulting displacement as shown in figure 4.3a. That displacement is numerically equal to the desired influence line at every point on the beam. The reason the Müller-Breslau principle works in this case may be directly inferred from the equation 4.1 by choosing both P_E and P_F equal to one. The result is then:

$$u_{E \text{ due to } P_F} = u_{F \text{ due to } P_E} \qquad (4.2)$$

If we interpret the point F as a variable location for a unit point force, then equation 4.2 is interpreted as follows. The displacement at point E due to a unit moving load at any point F equals the displacement at that point F due to a unit force applied at point E. Therefore, the influence line for the displacement at point E is the displaced beam due to a unit force applied at point E.

In a similar way, we can construct the influence lines for the force reaction at point E (figure 4.3b), the shear force at point E (figure 4.3c) and the bending moment at point (figure 4.3d). In each of those cases, we apply a unit of the work-associated variable at point E and calculate the displacements in the beam. There are some subtleties in applying
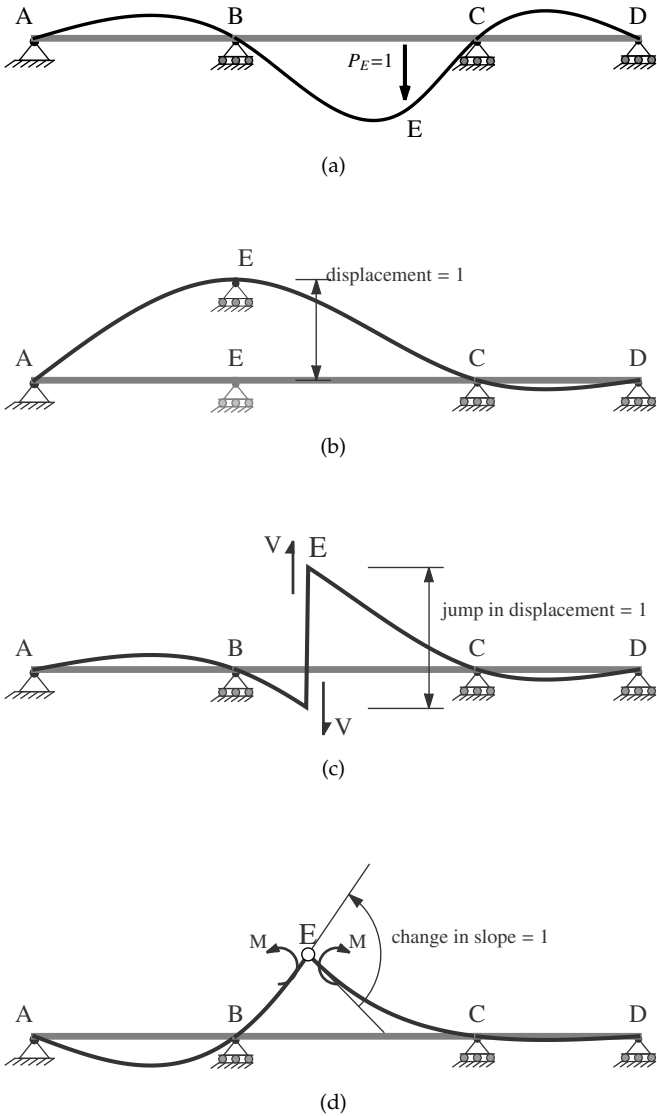
Figure 4.3. Influence lines for the displacement (a), the vertical force reaction (b), the shear force (c) and the bending moment (d) at point E. These influence lines are the equal to the displacements of the beam when subject to the work-associated variable and are illustrated in the figures above.

the unit work-associated variable at point E. Specifically, we note the following:

- For the influence line of the vertical reaction (see figure 4.3b), a unit displacement is applied at the support with an associated unknown reaction force. In particular, we do not apply an external point moment at point E unless it also happens to have a fixed support.

- For the influence line of the shear force (see figure 4.3c), a unit jump in the displacement is applied with an associated unknown equal and opposite forces 'V.' This unit jump causes a discontinuity in the beam, but the slope before and after point E must be the same. In addition, there is an internal bending moment at point E. Also note that the jump in displacement must be up when going from the left to the right of the beam at point E and is implied by the shear force convention used in this book. In addition, the individual displacements before and after point E are unknown (*ie.* only the jump is known) and must be calculated using structural analysis.

- For the influence line of the bending moment (see figure 4.3d), a unit change in the slope is applied with associated unknown equal and opposite moments 'M.' This unit change in slope causes a discontinuity in the slope of the beam but there is no discontinuity in the displacement. In addition, there is an internal shear force at point E. Also note that the change in slope must be clockwise as shown in the figure when going from the left to the right of the beam at point E and is based on the bending moment convention used in this book. In addition, the individual slopes before and after point E are unknown (*ie.* only the change in slope is known) and must be calculated using structural analysis.

In the next sections, we will use the Müller-Breslau principle to construct influence lines for both statically determinate and statically indeterminate structures. The principle applies to both cases, but for statically determinate structures, we can always manually construct the exact influence line. In the case of statically indeterminate structures, we will describe methods to sketch an approximation to the influence lines with approximate values calculated at notable points such as the maximum and minimum values in each span.

Using the Müller-Breslau principle we can identify rules for constructing influence lines for both statically determinate and statically indeterminate structures in the case of force reactions, shear forces and bending moments. Some of these rules are specific for the considered response variable and some are common. The common rules are as follows:

1. The influence line passes through zero at all supports except for one case. That case occurs only at one support on the beam and only when we consider the influence line for the force reaction at that support. In that case, that particular support moves up by one unit (*eg.* figure 4.3b).

2. The influence line is continuous (*ie.* no step jumps) except for one case. That case occurs only at one location on the beam and only when we consider the influence line for the shear force at that location. In that case, the discontinuity is a unit step jump at that location (*eg.* figure 4.3c).

3. The influence line away from internal hinges is smooth (*ie.* continuous slope) except for one case. That case occurs only at one location on the beam and only when we consider the influence line for the bending moment at that location. In that case, there is a sudden change in slope of one unit at that location (*eg.* figure 4.3d). Of course, there may be changes in slopes at internal hinges.

In addition to the above rules, we have a rule that applies to all statically stable beams, specifically:

4. The influence line for statically stable beams is piecwise smooth. The influence line is then a sequence of possibly distinct smooth lines (*ie.* derivative is continuous) with possible step jumps and sudden changes in direction between segments as outlined in the previous rules.

In addition to the above rules, we have one additional rule that is a special case of rule (4) above but only applies to statically determinate beams, specifically:

5. For statically determinate beams, the influence line is piecwise linear. The influence line is then a sequence of possibly distinct straight lines with possible step jumps and sudden changes in direction between segments as outlined in the previous rules.

It is this last rule that allows us to relatively easily construct the exact influence lines for statically determinate beams in the case of force reactions, shear forces and bending moments. Further details and examples for constructing the influence lines of statically determinate beams is considered next.

4.2   Exact Influence Lines for Statically Determinate Beams

4.2.1   Introduction to Sketching the Influence Line for Statically Determinate Beams

For statically determinate beams, it is relatively easy to construct the exact influence lines for reactions, shear forces and bending moments using the few simple rules considered above. However, we must first verify that we are indeed trying to analyze a statically determinate beam before using those rules. The simplest statically determinate beams have either a hinge and a roller support or have one fixed end (*eg.* see beams in figures 4.4). If we add a roller support or a fixed support to a statically determinate beam then we must also add one or two internal hinges respectively or some equivalent internal constraints in order to maintain the statical determinacy. Of course, as we add internal hinges, we must be careful to maintain statical stability.

For our purposes in this section, we only need statical determinacy as related to shear forces and bending moments. This means that, for the cases considered in this section, we must be able to fully determine shear forces and bending moments based on the equations of statics alone. Indeterminacy with respect to axial forces is immaterial to the discussions of this section. Therefore, the rules for constructing influence lines remain the same as those of statically determinate beams if one or more hinge supports are replaced with a horizontal roller as long as there remains at least one reaction in the horizontal direction on the beam to restrict horizontal translations.

In what follows, we will present examples and discuss them in order to clarify how the identified rules may be used to construct influence lines. Note however that the examples considered are extensive but not comprehensive of all possible configurations. The examples progress from having no internal hinges to having one then two internal hinges.

4.2.2   Sketching Influence Lines for Vertical Force Reactions

In the first examples of the influence lines for vertical reaction forces, we consider statically determinate beams with no internal hinges as shown in figure 4.4a and b. In such cases, the influence line for a vertical reaction force is a single straight line. When there is a hinge and roller support, the influence line has a value of one at the support considered and passes through zero at the other support. Using the equation of a straight line or equivalently using similar triangles, we can then determine the value of
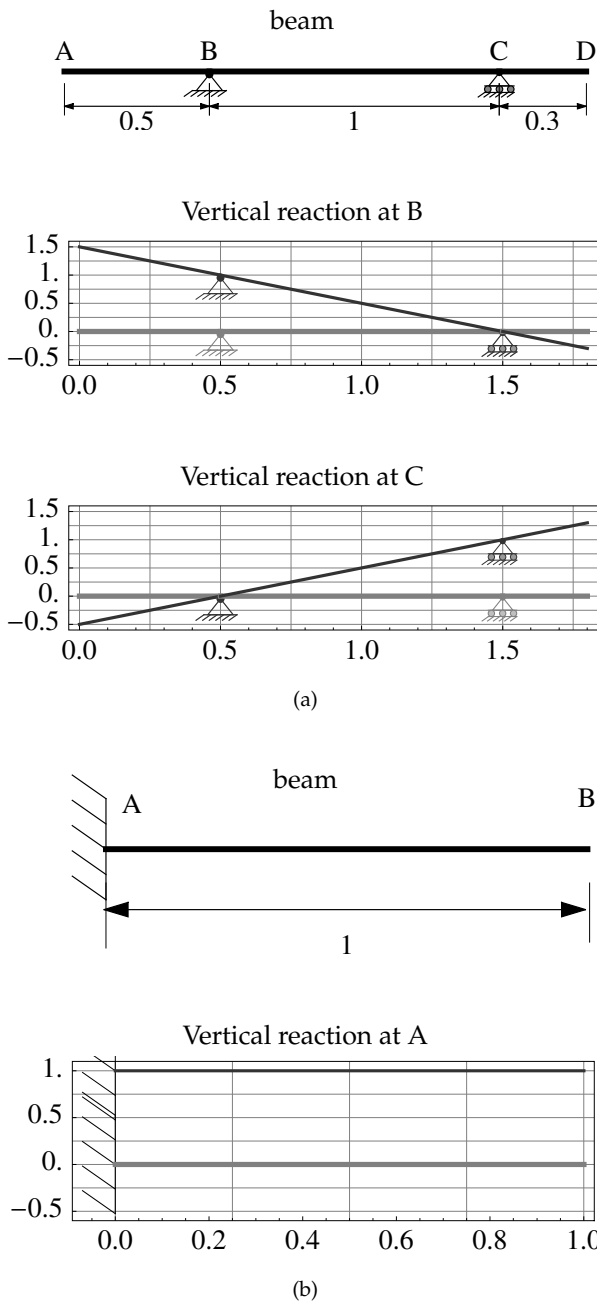
Figure 4.4. Influence lines for the vertical reaction force for statically determinate beams with no internal hinges.

the influence line at any other point. With a fixed end, the influence line is constant and has a uniform value of one. The reason for that uniform value is that when we move the fixed end support up by one unit, we must still keep the moment reaction. Keeping the moment reaction at that fixed end maintains the slope at zero and so we have a uniform value of one.

Next consider statically determinate beams with one internal hinge as shown in figures 4.5a and b. In such cases, the influence line for a vertical reaction force is two connected straight lines with a change in
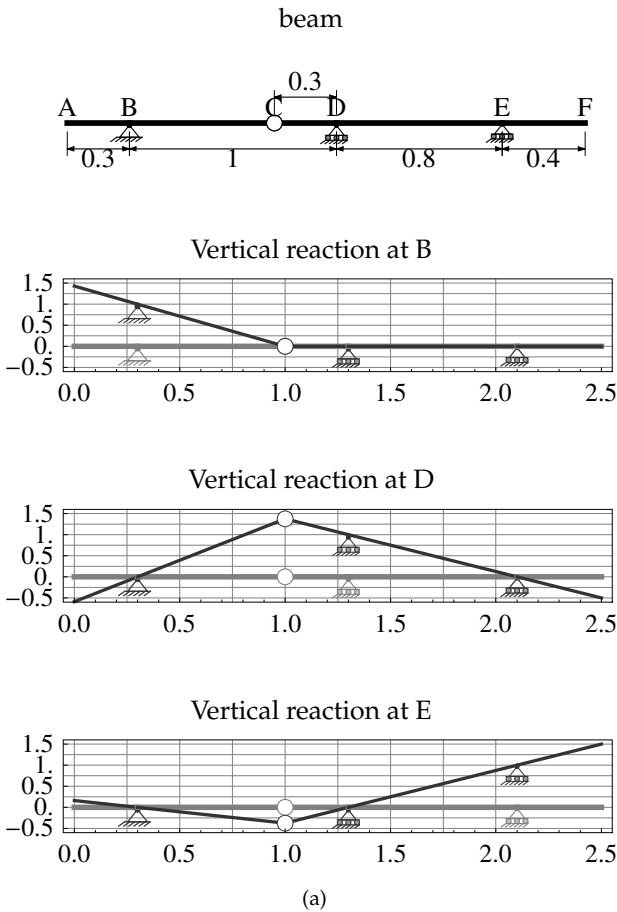
Figure 4.5. Influence lines for the vertical reaction force for statically determinate beams with one internal hinge. *(Continued below.)*
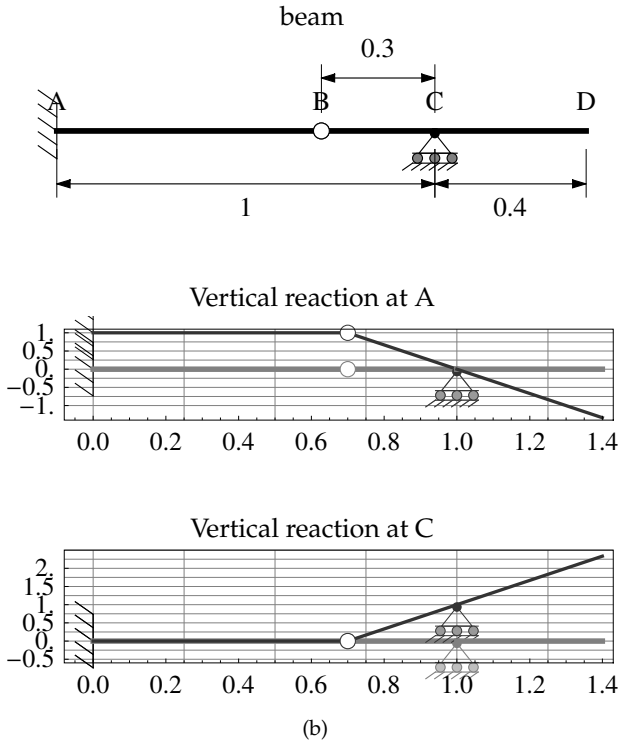
Figure 4.5. *(Continued from above.)* Influence lines for the vertical reaction force for statically determinate beams with one internal hinge.

slope occuring only at the internal hinge. Note that when the influence line must pass through two non-moving consecutive supports with no internal hinge between them, the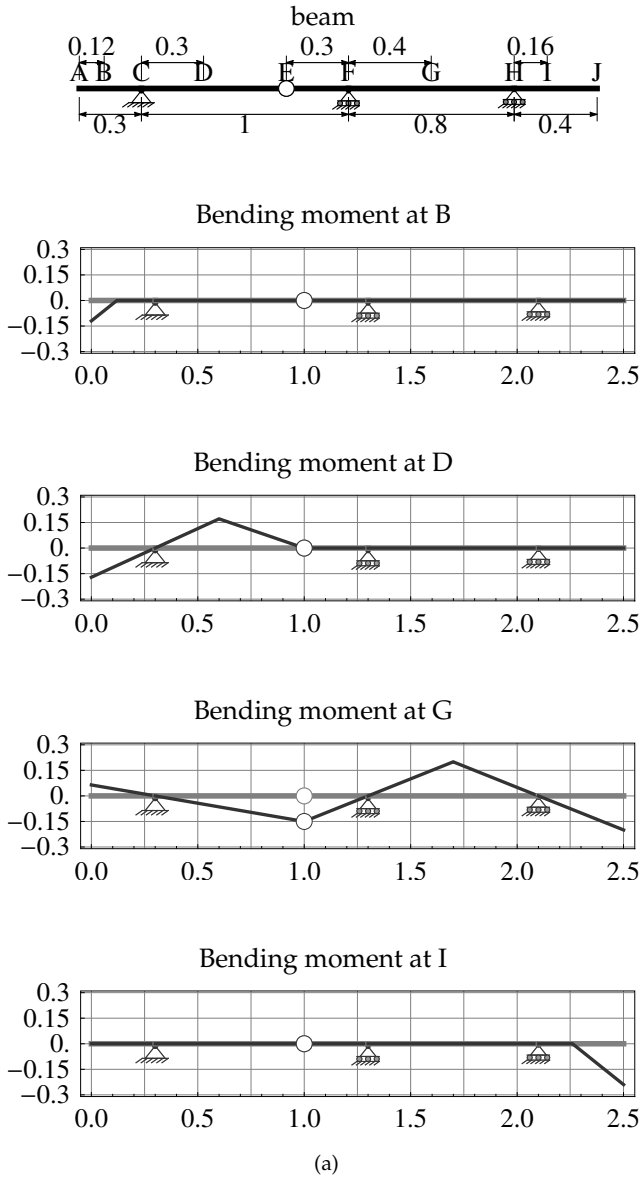n that section of the beam will be zero throughout until either the end of the beam or an internal hinge is met. For example, this occurs in figure 4.5a for the influence line of the reaction at B for the section CDEF with D and E being the non-moving consecutive supports. For the case of one internal hinge with one fixed end, the slope in the segment containing the fixed end must always be zero and a change in slope may only occur at an internal hinge. For example, this occurs in figures 4.5b for the influence lines of the reactions both at A and at C.

In the last examples, we consider statically determinate beams with two internal hinges as shown in figures 4.6a and b and in figure 4.7. In such cases, the influence line for a vertical force reaction is a sequence of up to three connected straight lines with two possible changes in slope
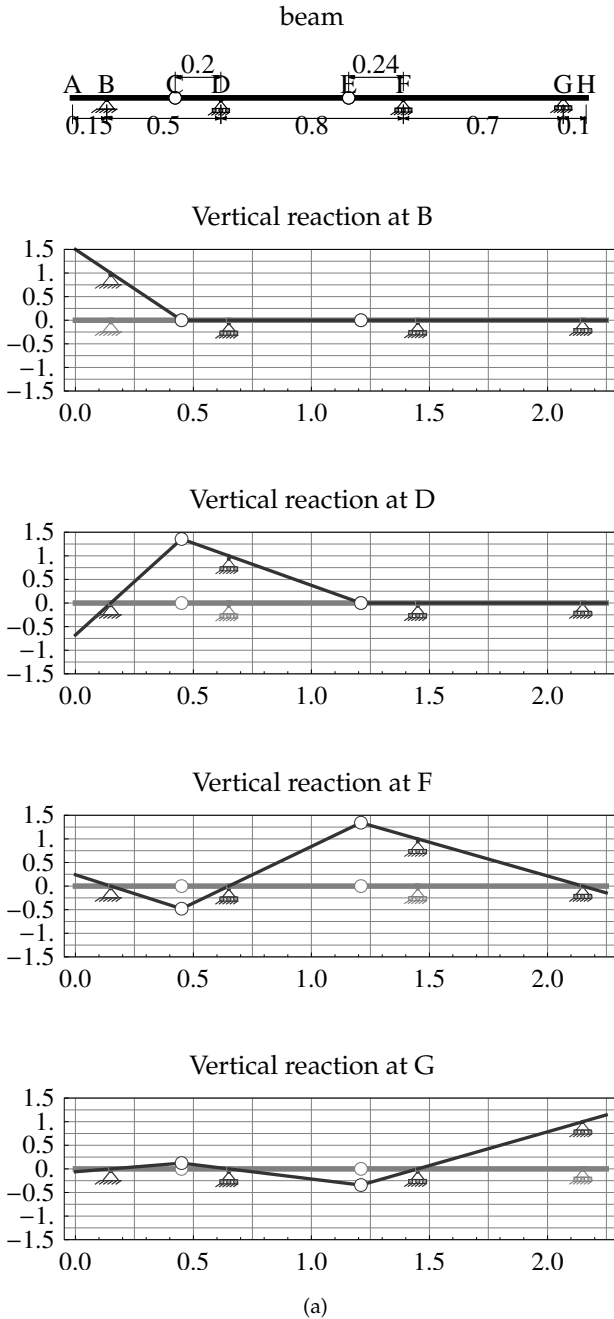
Figure 4.6. Influence lines for the vertical reaction force for statically determinate beams with two internal hinges and no fixed ends. *(Continued below.)*
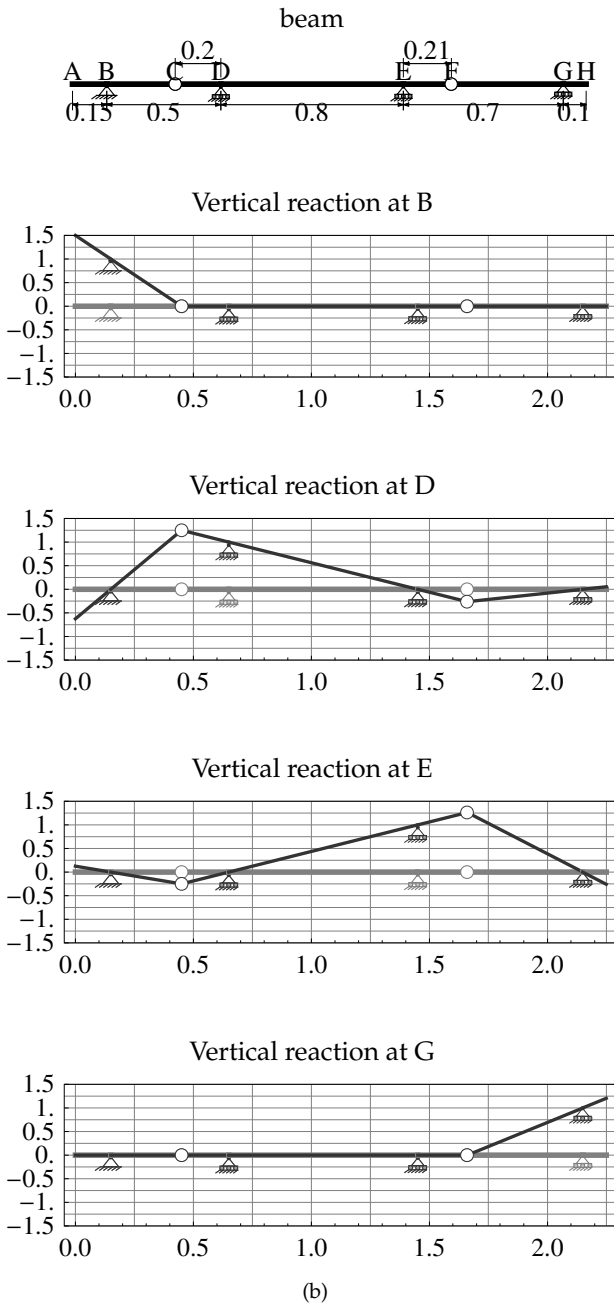
Figure 4.6. *(Continued from above.)* Influence lines for the vertical reaction force for statically determinate beams with two internal hinges and no fixed ends.
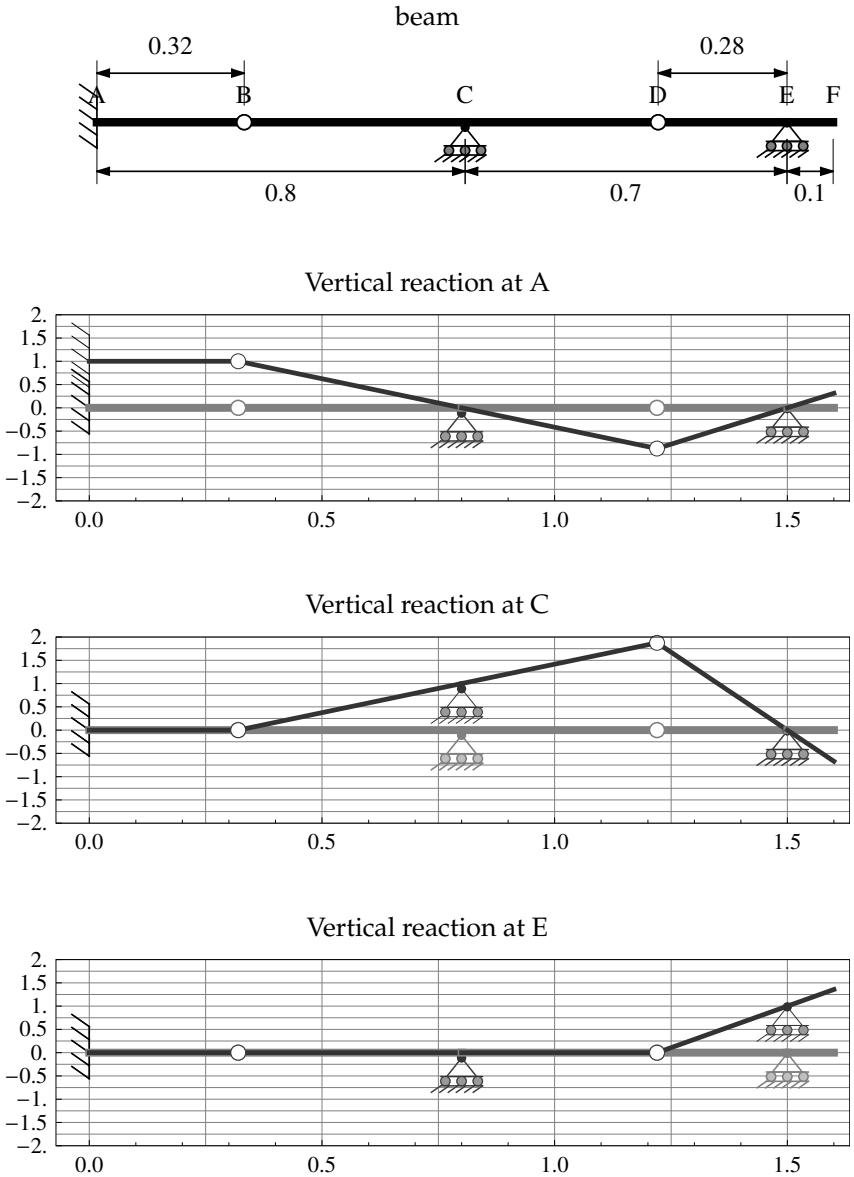
Figure 4.7. Influence lines for the vertical reaction force for statically determinate beams with two internal hinges and one fixed end.

that may only occur at the two internal hinges. Figures 4.6a and b gives two sets of examples of a beam having a hinge and two rol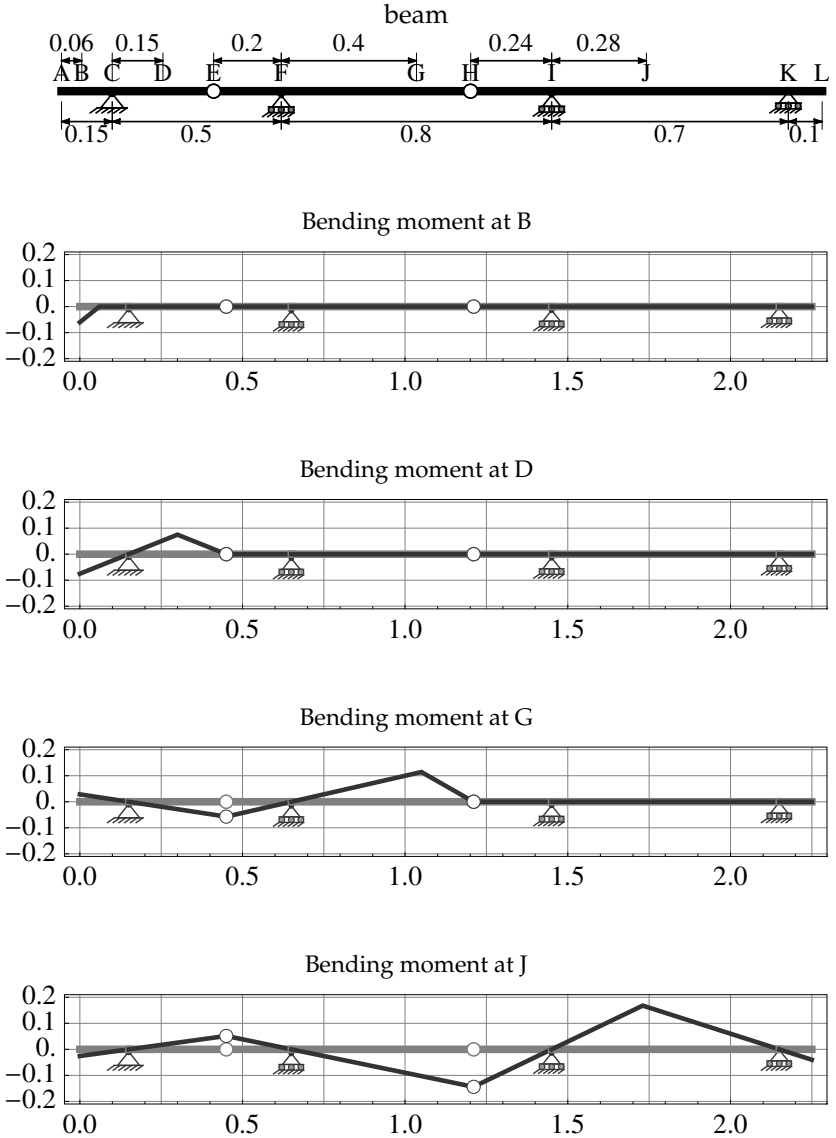lers with two internal hinges while figure 4.7 gives a set of examples of a beam with a fixed end and two rollers with two internal hinges.

In all cases of statically determinate beams without fixed ends, we can first determine the values at all points of the line segment containing the support that is moved up by a unit. In that line segment, we know the coordinates of two points which completely defines the equation of the straight line segment. For example, in figures 4.6a we first determine the line segment ABC, CDE, EFGH and EFGH for the influence line of the reactions at B, D, F and G respectively. The first known coordinate in those segments is the support being moved since its height is one unit and its horizontal position is known. For the second known coordinate, there are two possibilities. If there is a support adjacent to the support being moved and such that there is no internal hinge between the two supports then that adjacent support is the second coordinate with height zero. That adjacent support must be connected by a straight line to the support being moved because slope changes may only occur at internal hinges and it must have a height of zero because it is a support. For example, in figures 4.6a for the influence lines of the reaction at F, the nearest support with no internal hinge in-between is support G and for the reaction at G, the nearest support with no internal hinge in-between is support F. Similarly in figures 4.6b, the influence line for the reaction at D, the moving support D has the nearest support point E with no internal hinge in-between. Also in figure 4.6b, for the influence line for the reaction at E, the moving support E has the nearest support point D with no internal hinge in-between. All those adjacent supports with no internal hinge in-between them and the moving support have zero height and are connected to the moving support by a straight line segment as shown in the corresponding figures.

In the second possiblity, we have either a free end or an internal hinge on either side of the support being moved by one unit. If there is one adjacent free end and one adjacent internal hinge then the internal hinge must have zero height otherwise the beam is statically unstable. For example, in figure 4.6a with the influence line for the reaction at B, one side of the moving support B is free (point A) and the other is an internal hinge (point C). Therefore, the internal hinge (point C) must have zero height. A similar situation occurs in the examples for the influence lines for the vertical reactions at B and at G in figures 4.6b. If the two adjacent ends have internal hinges then one and only one of those internal hinges must have zero height. The one internal hinge with the zero height is determined by considering the kinematics of the rest of the beam. In figure 4.6b with the influence line for the reaction at D,

both sides of the moving support D are internal hinges (points C and E). Due to kinematic constraints on the right side of the beam, the right-side internal hinge (point E) must have zero height. The kinematic constraint on the right consists of two adjacent supports with no internal hinge between them and this necessarily means that the beam remains at zero over that segment until an internal hinge or a free end is met at either end.

In the case when we have a fixed end in a beam with two or more internal hinges, then we consider two cases. First, if the fixed support moves up by one unit then the line segment from that fixed support to the nearest internal hinge must have a uniform value of one. The nearest internal hinge must be nearer to the fixed end than the next support otherwise the beam will not be statically determinate. In the second case, if a roller moves up by one unit then the case is similar to having only hinges and rollers as supports with the added condition that the internal hinge nearest to a fixed end always has a height of zero. The reason for the zero height is that the fixed end must have zero slope and zero height and that the fixed end and nearest internal hinge must be connected by a straight line. Those two condition imply a straight line between them that is uniformly zero.

In all cases, once the first line segment has been constructed, the rest of the line segments are similarly determined by starting at the ends of a known line segment whose coordinates have already been found and determining the equations of the adjacent segments. Those adjacent segments are similarly determined by the coordinates of the known end points and the coordinates of the next adjacent support with no internal hinges in between. If an internal hinge occurs before then next adjacent support then that internal hinge must have zero height otherwise the beam is statically unstable. In all cases, the coordinates of adjacent line segments are determined until the influence line of the whole beam is constructed.

4.2.3   Sketching Influence Lines for Shear Forces

The influence lines for shear forces look similar to those of the vertical force reactions except for the distinctive unit step jump at the monitored location. For example, figure 4.8 shows the influence line for the shear force at point P with the distinctive unit step jump. The jump below and above zero at point P in figure 4.8 may be determined based on the following conditions: i) the total jump has a value of one and ii) the slope just before and just after the jump must be the same. Using these two conditions and the fact that the influence line for a statically determinate
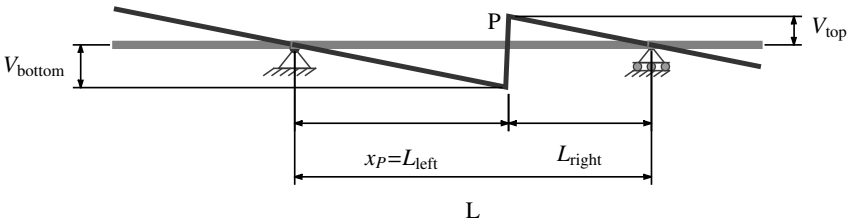
Figure 4.8. Influence line for the shear force at point P shows the distinctive unit step jump at point P. The jump below and above zero (*ie.* V_{bottom} and V_{top}) may be computed using simple equations.

beam is piecewise linear, we get the following equations:

$$V_{\text{bottom}} + V_{\text{top}} = 1 \tag{4.3a}$$

$$V_{\text{bottom}}/L_{\text{left}} = V_{\text{top}}/L_{\text{right}} \tag{4.3b}$$

$$\Rightarrow \quad V_{\text{bottom}} = \frac{L_{\text{left}}}{L} = \frac{x_P}{L} \tag{4.3c}$$

$$V_{\text{top}} = \frac{L_{\text{right}}}{L} = 1 - \frac{x_P}{L} \tag{4.3d}$$

where:

V_{bottom} and V_{top} are the values of the influence line just before and just after point P respectively

L_{left} and L_{right} are the distances between the left support and point P and between point P and the right support respectively

L is the length of the span containing point P

point P is the point at which we are calculating the influence line for shear

x_P is the abscissa (*ie.* x-coordinate) of point P when the origin is taken at the left support of the span containing P

Note that the value of the influence line at just before point P depends on the distance of point P from the left support. This value, denoted by V_{bottom} in figure 4.8, varies linearly with the location of point P (*ie.* with x_P) as that location varies from being at the left support to being at the right. Specifically, V_{bottom} is zero when point P is at the left support and is one when point P is at the right support. The influence line at

just after point P also varies linearly with location but starts at one at the left support and ends at zero at the right support. Once the values of the influence line at just before and at just after point P are determined, we then use the same approach that we used for the influence lines for vertical force reactions to construct the influence line for the shear force. In what follows are examples that further clarify such a construction.

In the first examples of the influence lines for shear forces, we consider statically determinate beams with no internal hinges as shown in figure 4.9a and b. In such cases, the influence line for a shear force consists of two consecutive straight line segments having the same slope and with a unit discontinuity between them. Whenever the point of influence is within an overhang (*ie.* a segment with a free end), the influence line is uniform from the free end up to the point at which influence is calculated and then the rest of the influence line is identically zero. In these cases of the point of influence occuring in an overhang, the uniformity or zero slope of the influence line is required to maintain slope continuity in the beam before and after the point of influence. For example, in figure 4.9a, the influence line for the shear force at B is minus one in segment AB and zero for the rest of the beam. In this case, the shear force must be negative in the left portion AB because the unit step jump condition requires a step up going left to right and the right part of the beam must remain at zero due to having two consecutive supports with no internal hinge between them. By contrast, in figure 4.9a for the influence line for the shear force at F and in figure 4.9b for the influence line for the shear force at B, the left side of the beam before the point of influence is zero and the rest is at positive one. This is again due to constraints imposed by the supports on the left side of the beam and the requirement of stepping up by one unit from left to right at the point of influence. Finally, a case when we need to calculate the influence between a hinge and a roller is shown in figure 4.9a for the influence line for the shear force at D. The value of the influence line just before and just after point D is calculated using formulas 4.3c and d and the rest of the beam is constructed in a manner similar to that described in the section for vertical force reactions.

Next consider statically determinate beams with one internal hinge as shown in figures 4.10a and b. In such cases, the influence line for the shear force is up to three connected straight lines with a change in slope occuring only at the internal hinge. Again when the influence line must pass through two non-moving consecutive supports with no internal hinge between them, then that section of the beam will be zero throughout until either the end of the beam or an internal hinge is met. For example, this occurs in figure 4.10a for the influence line of the shear force at D. As for the case of the influence line for the shear force in an overhang segment, a beam with any number of internal hinges is handled
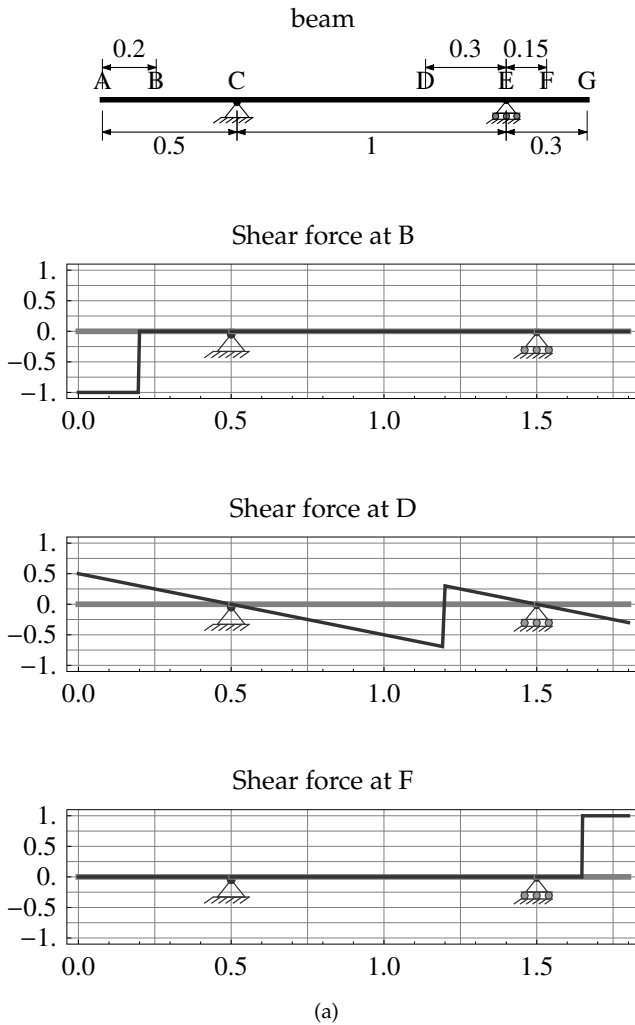
Figure 4.9. Influence lines for the shear force for statically determinate beams with no internal hinges. *(Continued below.)*

exactly as before irrespective of the presence of the internal hinge. Of course, an internal hinge may not occur in an overhang to avoid statical instability.

Next we consider statically determinate beams with two internal hinges as shown in figures 4.11 and in figure 4.12. In such cases, the influence line for a shear force is a sequence of up to four connected straight
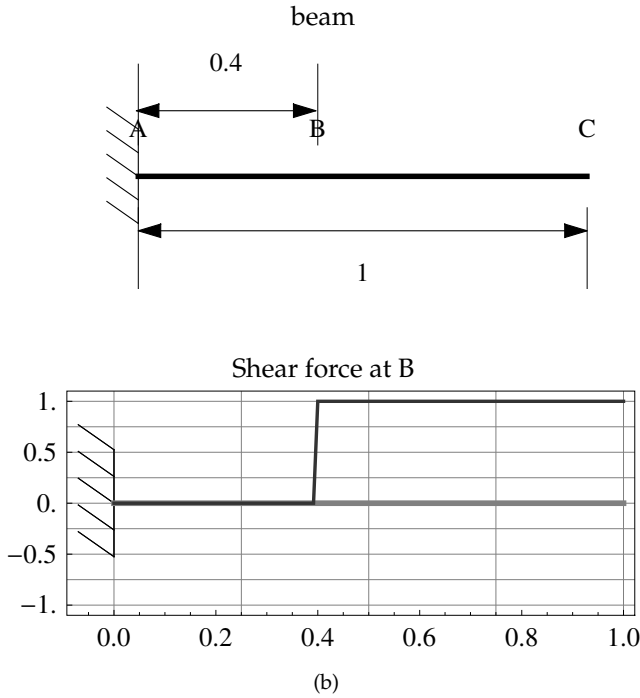
beam

Figure 4.9. *(Continued from above.)* Influence lines for the shear force for statically determinate beams with no internal hinges.

lines with two possible changes in slope that may only occur at the two internal hinges. Figures 4.11 gives two set of examples of a beam having a hinge and two rollers with two internal hinges while figure 4.12 gives a set of examples of a beam with a fixed end and two rollers with two internal hinges.

In one of those examples, specifically figure 4.12 for the shear force at B, we consider the influence line for a point between a left-end fixed support and a roller support when the point monitored occurs to the left of the internal hinge in that span. In that case, the influence line is zero from the support (*ie.* point A) to the point of influence (*ie.* point B) because the slope and value in that segment are constrained by the fixed end. The influence line then jumps up to one at the point of influence (*ie.* point B) and maintains that uniform value of one until we reach the internal hinge (*ie.* point D). This jump is required based on the Müller-Breslau principle for shear forces and the uniform value implies a zero slope which is required to match slopes before and after the jump.

beam

Shear force at B

Shear force at D

Shear force at G

Shear force at I

(a)
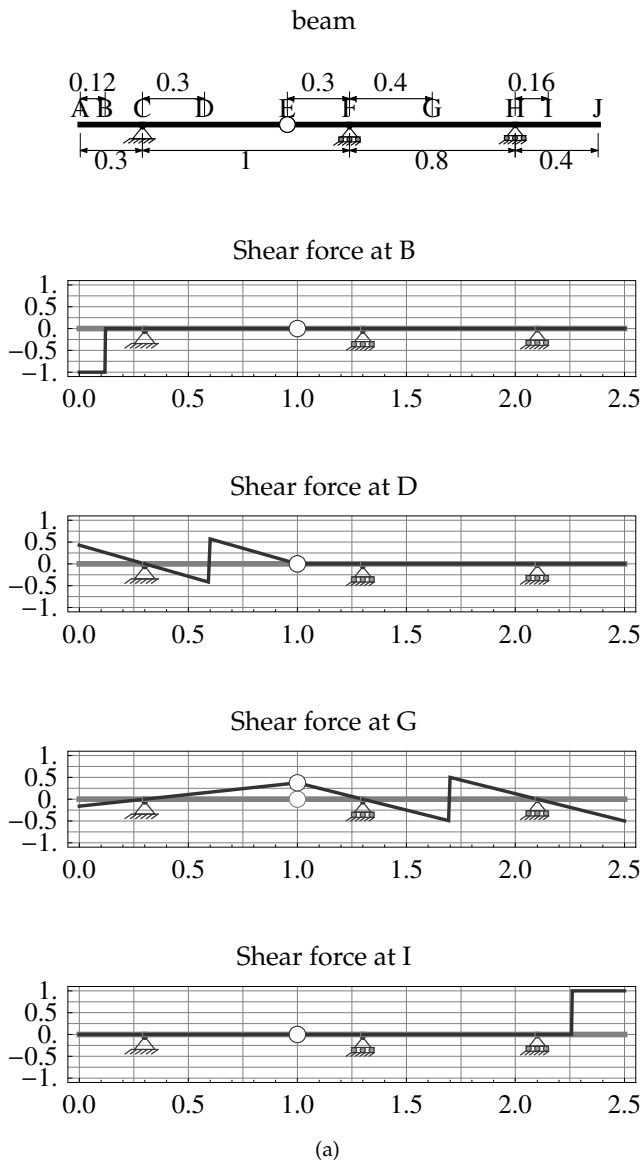
Figure 4.10. Influence lines for the shear force for statically determinate beams with one internal hinge. *(Continued below.)*
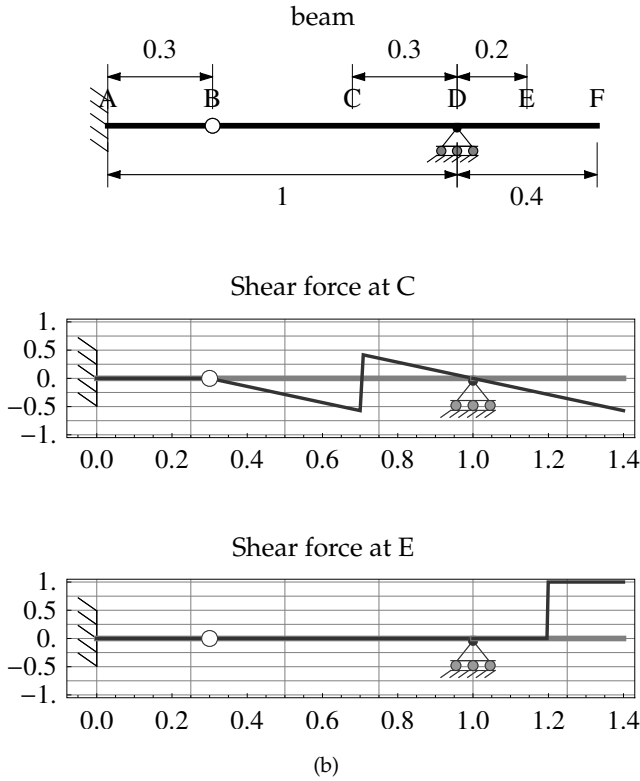
Figure 4.10. *(Continued from above.)* Influence lines for the shear force for statically determinate beams with one internal hinge.

Finally, at the internal hinge (*ie.* point C), the influence line changes direction in order to meet the roller support (*ie.* point D) at zero.

The previous case considered is to be contrasted with the case in a similar span with a left-end fixed support but when the point of influence occurs after the internal hinge such as in figure 4.10b for the shear force at C. In that case, the influence line is zero until the internal hinge which is again due to the fixed end constraints. At the internal hinge, the influence line changes direction downwards until we reach the point of influence (*ie.* point C). At the point of influence (*ie.* point C), the influence line jumps up by one unit as required by the Müller-Breslau principle for shear forces. Finally, the influence line then goes downwards again at the same slope as before the jump in order to meet the roller support at zero. Note that, in this case, a change in direction downwards at the internal
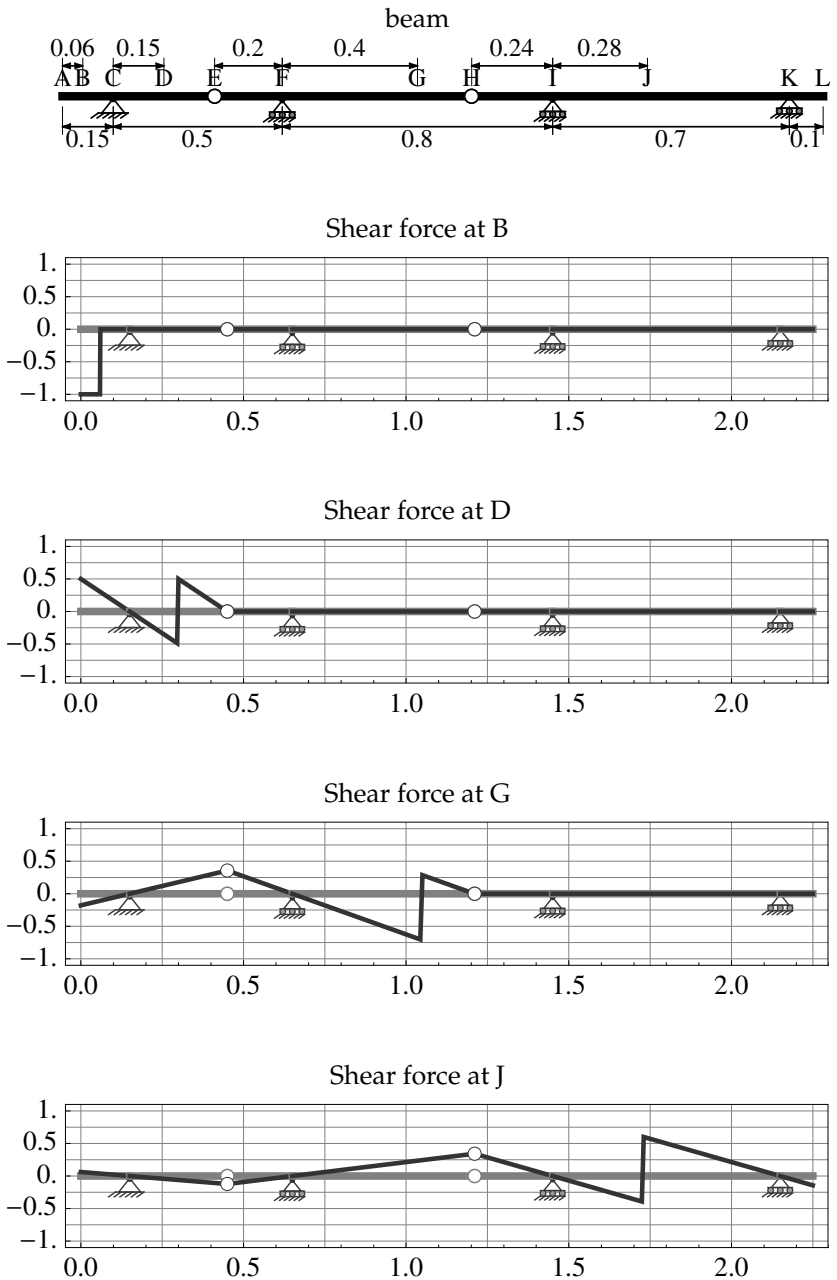
Figure 4.11. Influence lines for the shear force for statically determinate beams with two internal hinges and no fixed ends.
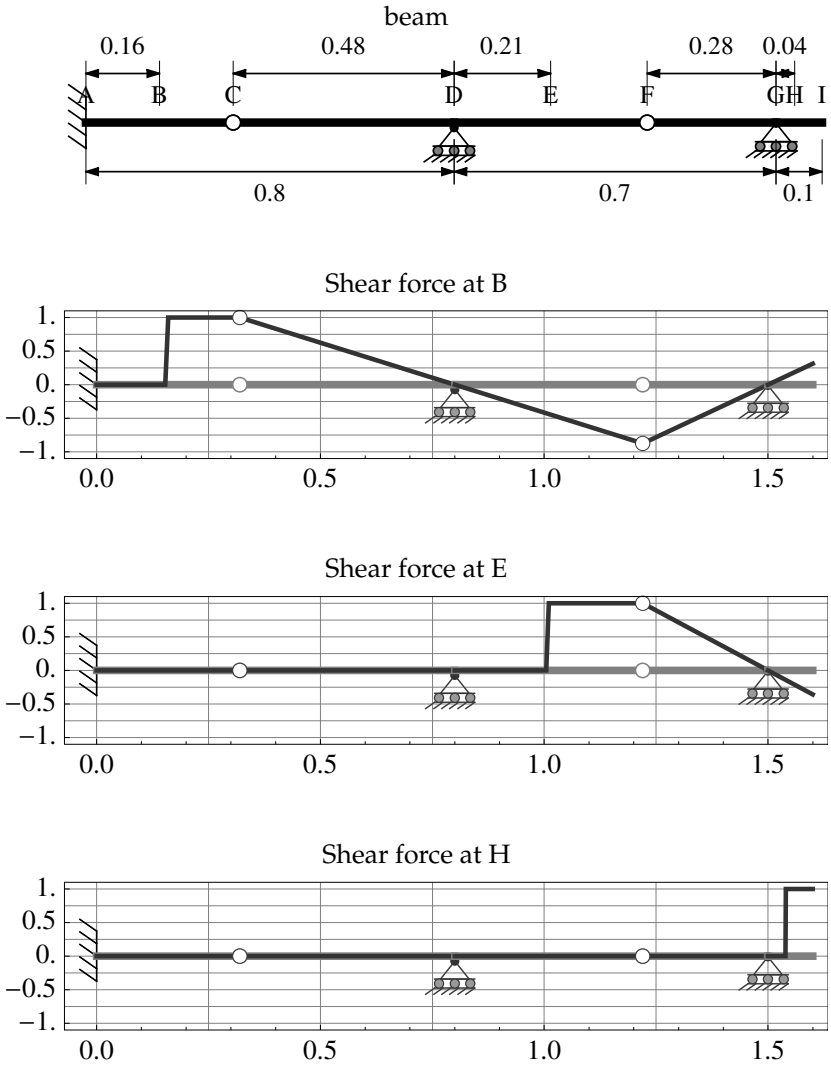
Figure 4.12. Influence lines for the shear force for statically determinate beams with two internal hinges and one fixed end.

hinge (*ie.* point B) is required in order to both have a jump at the point of influence (*ie.* point C) and to maintain the same slope at either end of that point. Also in this case, the values before and after the jump (*ie.* point C) are given by formulas 4.3c and d on condition that we consider the location of the internal hinge (*ie.* point B) to act like a second support. This

means that the effective span 'L' is considered to be the distance between the internal hinge and the roller support (*ie.* distance between B and D). Cases when the fixed support is at the right are similar but with opposite signs as those of fixed supports at the left that were discussed and may be similarly reasoned and constructed.

Finally, we consider the special cases of influence lines for the shear forces at the location of supports, shown in the examples of figures 4.13a and b. In such cases, we must specify whether the point being monitored is slightly to the left or slightly to the right of the support. If the support is slightly to the left, as in figure 4.13a for the shear force at B−, then the value just before the support equals minus one in order to have a jump of one from left to right and to reach zero at the support. By contrast, if the support is slightly to the right, as in figure 4.13a for the shear force at B+, then the value just after the support equals one in order to have a jump of one from the support which must always be at zero. If the support is at the left end of the beam, such as in figure 4.13b for the shear force at A, then we can only consider the shear force slightly to the right of that support. In that case, the influence line for the shear force equals the influence line for the vertical reaction at the support because the reaction at that support equals the shear force slightly to the right of it when the force is at any point to the right of that end point. The case for a support at the right end of the beam is similar except that the influence line for the shear force is negative that of the vertical reaction force at that support. The reason has to do with the convention used to define negative and positive shear forces in beams.

4.2.4 Sketching Influence Lines for Bending Moments

The influence lines for bending moments again look similar to those of the vertical force reactions except for the distinctive change of direction or kink at the monitored location. For example, figure 4.14 shows the influence line for the bending moment at point P with the distinctive kink. The value of the influence line at point P in figure 4.14 may be determined based on the following conditions: i) the total change in angle has a value of one at the kink and ii) the influence line is continuous at P. Using these two conditions and the fact that the influence line for a statically determinate beam is piecewise linear, we get the following equation:

$$\left(M_{\text{at influence}}/L_{\text{left}}\right) + \left(M_{\text{at influence}}/L_{\text{right}}\right) = 1 \qquad (4.4a)$$

$$\Rightarrow \quad M_{\text{at influence}} = \frac{L_{\text{left}} \times L_{\text{right}}}{L} = \frac{x_P}{L}\left(1 - \frac{x_P}{L}\right) L \qquad (4.4b)$$

beam

Shear force at B−

Shear force at B+

(a)

beam

Shear force at A

(b)
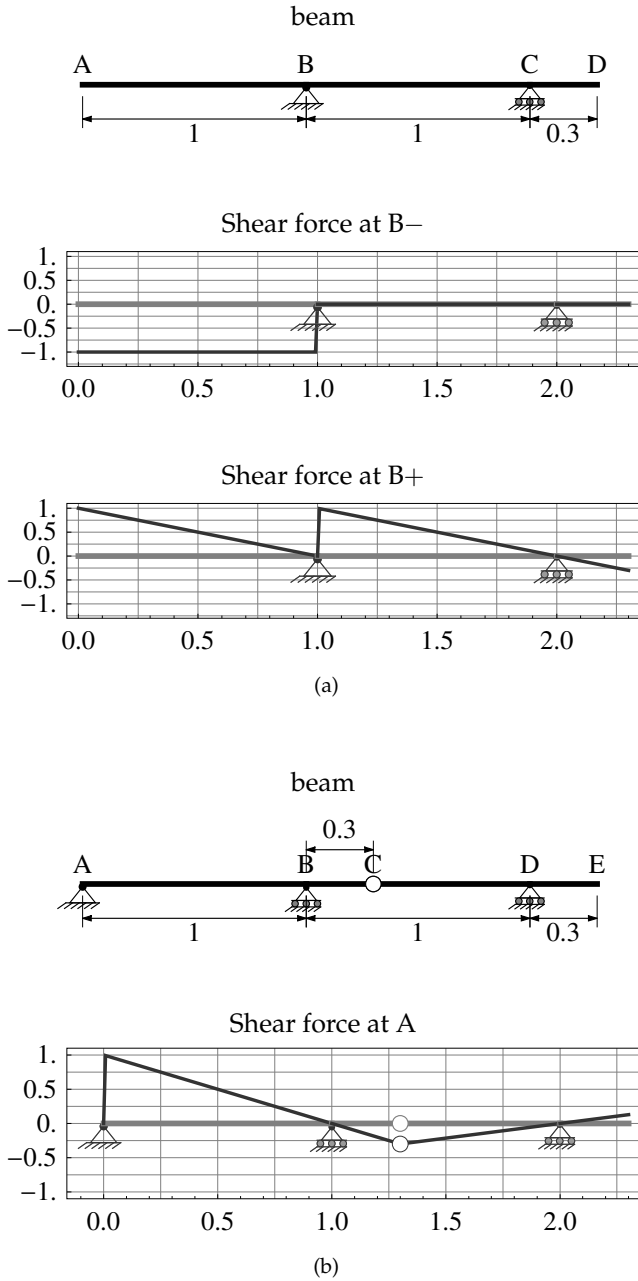
Figure 4.13. Influence lines for the shear force for statically determinate beams near supports.
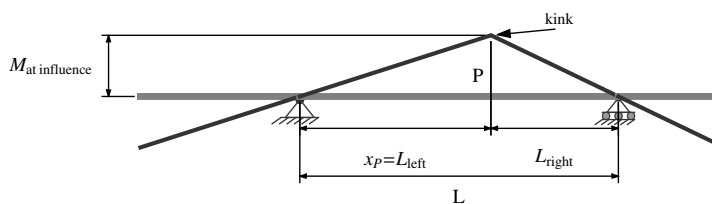
Figure 4.14. Influence line for the bending moment at point P shows the distinctive kink or change in direction at point P. The value of the infuence line at point P (*ie.* $M_{\text{at influence}}$) may be computed using simple equations.

where:

$M_{\text{at influence}}$ is the value of the influence line at point P

L_{left} **and** L_{right} are the distances between the left support and point P and between point P and the right support respectively

L is the length of the span containing point P

point P is the point at which we are calculating the influence line for shear

x_P is the abscissa (*ie.* x-coordinate) of point P when the origin is taken at the left support of the span containing P

Note that the value of the influence line at point P depends on the distance of point P from the left support. This value, which is denoted by $M_{\text{at influence}}$ in figure 4.14, varies parabolically with the location of point P (*ie.* with x_P) as that location varies from being at the left support to being at the right. Specifically, $M_{\text{at influence}}$ is zero when point P is at the left support, reaches a maximum of '$L/4$' when point P is at the midpoint of the span and is again zero when point P is at the right support. Once the values of the influence line at point P is determined, we then use the same approach that we used for the influence lines for vertical force reactions to construct the influence line for the bending moment. In what follows are examples that further clarify such a construction.

In the first examples of the influence lines for bending moments, we consider statically determinate beams with no internal hinges as shown in figure 4.15a and b. In such cases, the influence line for a bending moment consists of two consecutive straight line segments with a change in slope or kink between them. Whenever the point of influence is within an
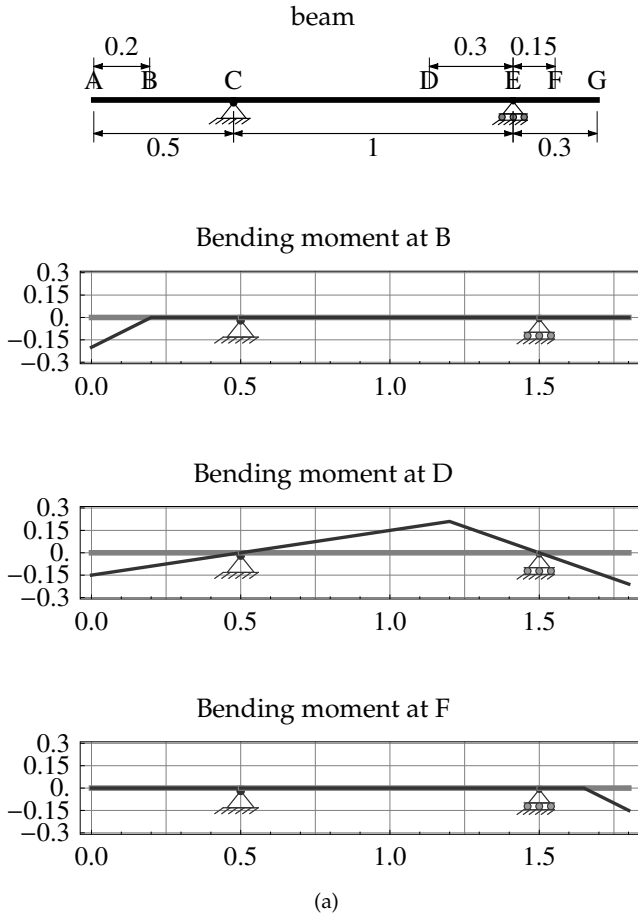
Figure 4.15. Influence lines for the bending moment for statically determinate beams with no internal hinges. *(Continued below.)*

overhang (*ie.* a segment with a free end), the influence line is linear from the end to the point of influence and then the rest of the influence line is identically zero. In these cases of the point of influence occuring in an overhang, the influence line at the point monitored is zero and the slope is either minus or plus one between that point till the end of the beam. For example, in figure 4.15a, the influence line for the bending moment at B starts at A with a value of -0.2 and with a slope of one in order to reach zero at point B which is the point of influence or point being monitored. In that example, the rest of the beam from B to G is identically zero. By contrast, in figure 4.15a for the influence line for the bending
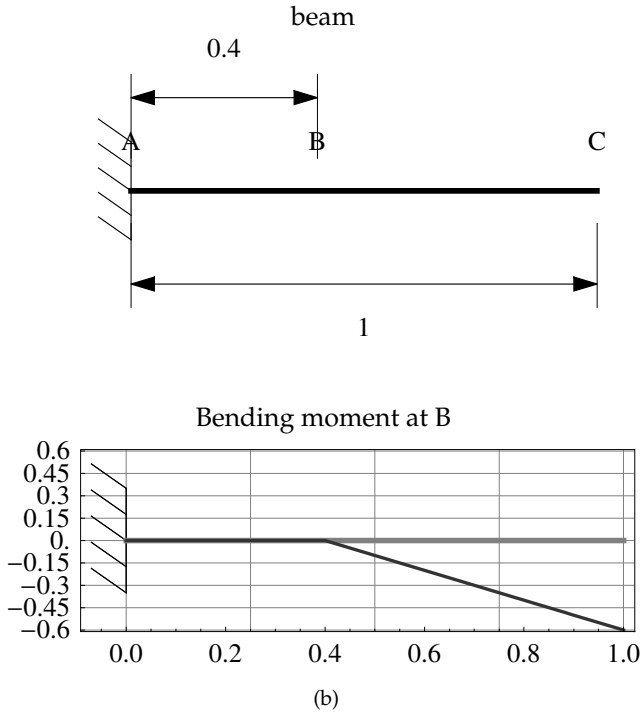
Figure 4.15. *(Continued from above.)* Influence lines for the bending moment for statically determinate beams with no internal hinges.

moment at F and in figure 4.9b for the influence line for the bending moment at B, the left side of the beam before the point of influence is zero and the rest is a straight line with slope minus one and a value of zero at the point of influence. Finally, a case when we need to calculate the influence between a hinge and a roller is show in figure 4.15a for the influence line for the bending moment at D. The value of the influence line at point D is calculated using formula 4.4b and the rest of the beam is constructed in a manner similar to that described in the section for vertical force reactions.

Next consider statically determinate beams with one internal hinge as shown in figures 4.16a and b. In such cases, the influence line for the bending moment is up to three connected straight lines with a change in slope occuring in the internal hinge and a unit change in slope occurring at the point of influence. Again when the influence line must pass through two non-moving consecutive supports with no internal hinge between them, then that section of the beam will be zero throughout

Figure 4.16. Influence lines for the bending moment for statically determinate beams with one internal hinge. *(Continued below.)*
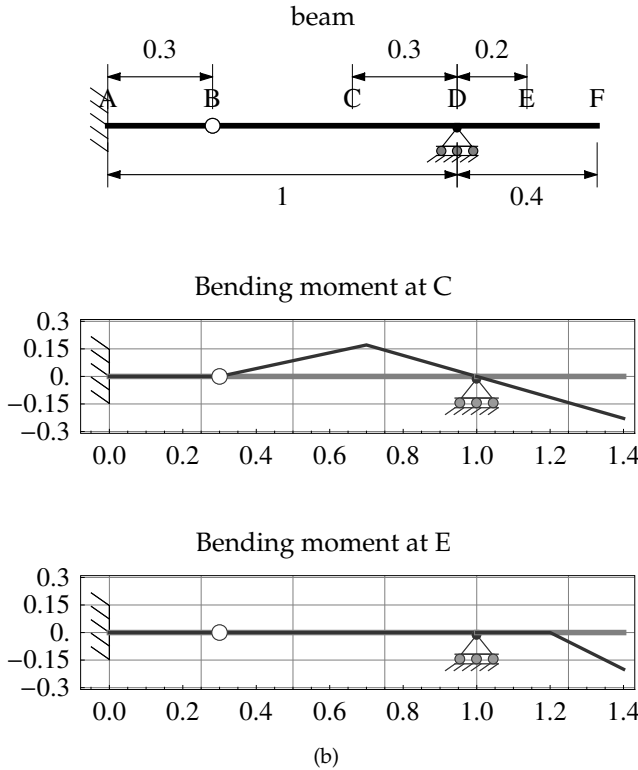
Figure 4.16. *(Continued from above.)* Influence lines for the bending moment for statically determinate beams with one internal hinge.

until either the end of the beam or an internal hinge is met. For example, this occurs in figure 4.16a for the influence line of the bending moment at D. The cases when we consider the influence line for the bending moment in an overhang part of a beam, we handle it the same as for the examples of figure 4.15 irrespective of the number internal hinges in the rest of the beam. Of course, as before, an internal hinge may not occur in an overhang to avoid statical instability.

Next we consider statically determinate beams with two internal hinges as shown in figures 4.18 and in figure 4.19. In such cases, the influence line for a bending moment is a sequence of up to four connected straight lines with two possible changes in slope that may occur at the two internal hinges and one mandatory unit change in slope that must occur at the point of influence. Figures 4.18 gives two set of examples of a beam having a hinge and two rollers with two internal hinges while

Figure 4.17. Influence lines for the bending moment for statically determinate beams with two internal hinges and no fixed ends.
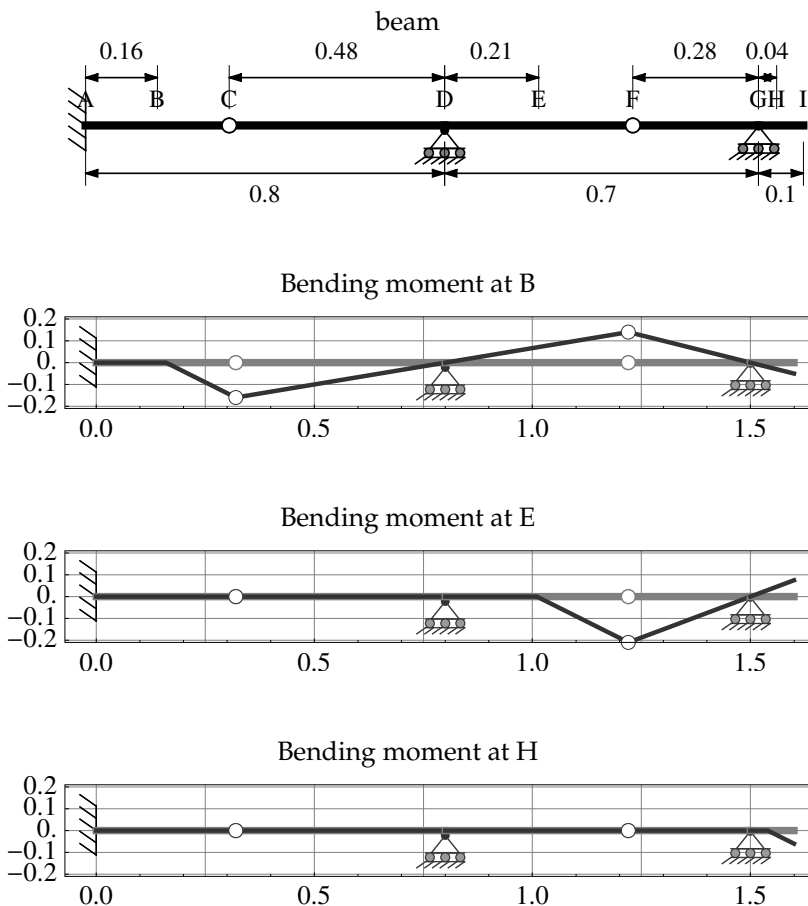
Figure 4.18. Influence lines for the bending moment for statically determinate beams with two internal hinges and one fixed end.

figure 4.19 gives a set of examples of a beam with a fixed end and two rollers with two internal hinges.

In one of those examples, specifically figure 4.18 for the bending moment at B, we consider the influence line for a point between a left-end fixed support and a roller support when the point monitored occurs to the left of the internal hinge in that span. In that case, the influence line is zero from the support (*ie.* point A) to the point of influence (*ie.* point B) because the slope and value in that segment are constrained by the fixed end. The influence line then changes direction to have a slope of minus one just after the point of influence (*ie.* point B) and maintains that slope
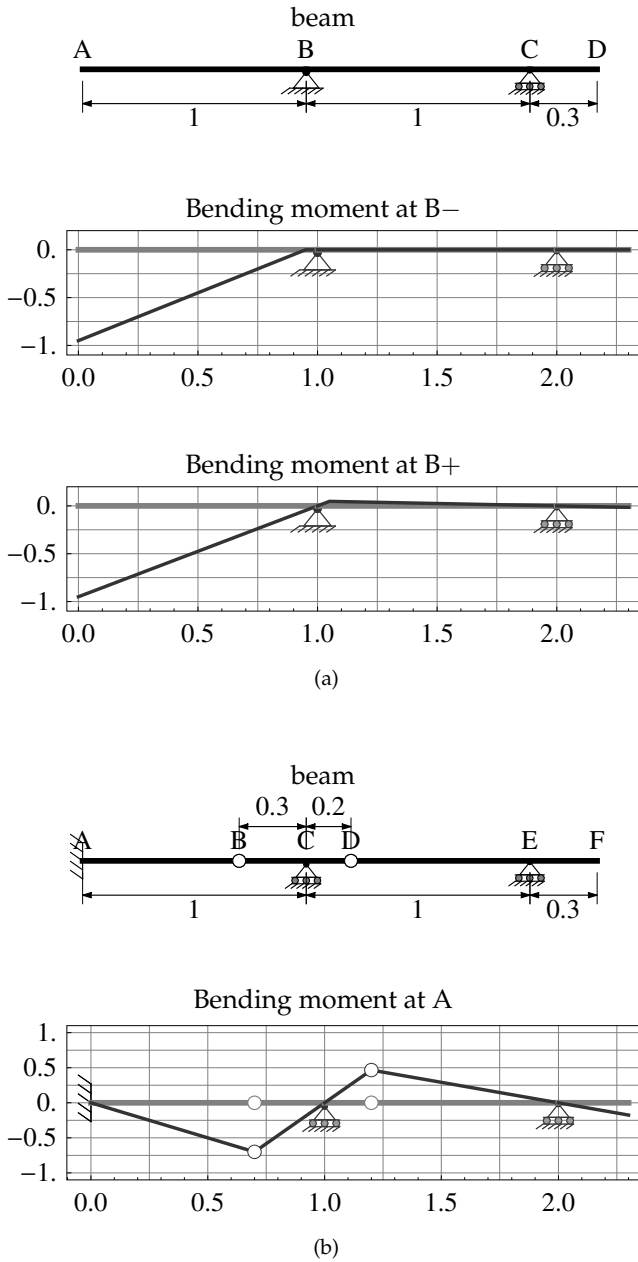
Figure 4.19. Influence lines for the bending moment for statically determinate beams near supports.

until we reach the internal hinge (*ie.* point D). The resulting net change in direction of one at the point of influence (*ie.* point B) is required based on the Müller-Breslau principle for bending moments. Finally, at the internal hinge (*ie.* point C), the influence line changes direction again in order to meet the roller support (*ie.* point D) at zero.

The previous case considered is to be contrasted with the case in a similar span with a left-end fixed support but when the point of influence occurs after the internal hinge such as in figure 4.16b for the bending moment at C. In that case, the influence line is zero until the internal hinge which is again due to the fixed end constraints. At the internal hinge, the influence line changes direction upwards until we reach the point of influence (*ie.* point C). At the point of influence (*ie.* point C), the influence line changes slope by one unit as required by the Müller-Breslau principle for bending moments. Finally, with the change in direction, the influence line then goes downwards to meet the roller support at zero. Note that, in this case, a change in direction upwards at the internal hinge (*ie.* point B) is required in order to both have a unit change in slope at the point of influence (*ie.* point C) and to subsequently meet the next support (*ie.* point D) at zero. Also in this case, the value at the point of influence (*ie.* point C) is given by formula 4.4b on condition that we consider the location of the internal hinge (*ie.* point B) to act like a second support. This means that the effective span 'L' is considered to be the distance between the internal hinge and the roller support (*ie.* distance between B and D). Cases when the fixed support is at the right are similar but with opposite signs as those of fixed supports at the left that were discussed and may be similarly reasoned and constructed.

Finally, we consider the special cases of influence lines for the bending moments at the location of supports as shown in the examples of figures 4.19a and b. In such cases, and unlike the influence line for shear forces, there is no difference whether the point of influence is slightly to the left or slightly to the right of the support. In either case, as in figures 4.19a for the bending moments at B− and at B+, the only novel feature is that the influence line at the point of influence must be zero at the support. If the support is a hinge or roller that is at neither end of the beam, then this will imply, for statically determinate beams, that the slope is zero at one side of the point of influence and the slope is plus or minus one at the other side depending on whether this slope occurs before or after the support respectively.

If we consider the influence line for the bending moment at a support and that support is at either end of a statically determinate beam then we have two cases. If the end support is a hinge or roller, then the influence line for the bending moment is identically zero throughout the whole beam. This may be simply understood by noting that the bending

moment at a free hinge or roller support at either end of a beam must be zero irrespective of any loads applied within the beam. The second case considered is when the end support is a fixed end. In that case, we can better understand the construction of the influence line if we consider the point of influence to be a small distance away from the fixed end. This case is then similar to figure 4.18 for the bending moment at B but with point B being much close to point A. In the limit as the point of influence tends towards the fixed end (*eg.* point B tends to point A in figure 4.18 for the bending moment at B), the horizontal line segment between the fixed support and the point of influence is omitted and we get an immediate change in slope of one at the fixed end as shown in figure 4.19b for the bending moment at A. Incidentally, this influence line for the bending moment at the fixed support must be the same as the influence line for the moment reaction at the fixed support except for sign (*ie.* positive or negative) which depend on the chosen sign convention for bending moments and moment reactions.

4.3   Approximate Influence Lines for Statically Indeterminate Structures

4.3.1   Introduction to Sketching the Influence Line for Statically Indeterminate Beams

In the introduction to influence lines, we detailed rules for constructing the influence lines for statically determinate and indeterminate beams using the Müller-Breslau principle. Based on that principle, sketching an influence line is equivalent to sketching the deformed shape for a specific type of loading. The three types of loading of primary interest are shown in figures 4.3b, c and d which are used to obtain the influence lines for the vertical support reactions, the shear forces and the bending moments respectively. Under these types of loading, the deformations of statically determinate beams are piecewise linear while those for indeterminate ones are, in general, piecewise cubic. In addition, the magnitudes and shapes of the deformed statically indeterminate beams depend on the cross-sectional properties as well as on the length of the spans. Also in these cases, exact calculation of the deformed shape requires exactly solving statically indeterminate beams subject to the associated loadings. Since such solutions are, in general, complex and better suited for computer implementations, we will develop approximate approaches to sketch the deformations due to the special type of loadings identified in figures 4.3b, c and d which then gives approximate influence lines for the statically indeterminate beams.

The approximate approach to sketch the deformation associated with a desired influence line is as follows:

1. Isolate the part in which the special type of loading is present and replace the rest of the passive structure by rotary springs. In the case of influence lines for shear forces and moments, the isolated part is just the member that contains the point of influence. Figure 4.29a, b and c show examples for the influence line for the bending moment while figure 4.26 shows an example for the influence line for the shear force. In the case of influence lines for vertical reaction forces, the isolated part depends on the location of the support. If the support is at either end then the isolated part is the member containing the support as shown, for example, in figures 4.20a and b. If the support is internal to the beam then the isolated part are both members on either side of the support as shown, for example, in figure 4.23.

2. Analyze the deformation of the isolated part to obtain the approximate value and location of the maximum and minimum deformations in that part. Also, obtain the rotations at both ends of that isolated part.

3. Based on known end rotations of the attached members, obtain the approximate value and location of the maximum or minimum deformation as shown in figure 4.32. Also, obtain the rotation at the opposing end of that member. With the new end rotations, this third step is recursively used to obtain the deformations of all the rest of the members.

In what follows, we will do the following:

1. For each of the three types of influence lines identified in figures 4.3b, c and d, we will present an analysis of the isolated part. This includes describing how to sketch the deformed shape of the isolated part and to approximately identify maxima, minima and end rotations.

2. We will present and discuss the results needed to carry out the third step above. This will apply to all types of influence lines for all members outside the isolated part.

3. Finally, for each of the three types of influence lines considered, we will present examples and discuss them in order to clarify how the obtained results may be used to construct influence lines. Note however that the examples considered are extensive but not comprehensive of all possible configurations.

4.3.2   Influence Line for Vertical Reaction Forces in An Isolated Member

The first type of special loading we consider is that of a unit support movement as shown in figures 4.20 and 4.21. As in other parts of this book, the passive response of the rest of the structure is modeled by rotary springs at the ends of the isolated member. This deformation corresponds to the influence line for the vertical reaction force at the displaced support. For this type of loading, we consider two cases, namely, when the support is at an end of a beam as in figures 4.20a and b and when the support is a middle support as in figure 4.21. When the support is at an end of a beam, the maximum displacement and hence influence is right at the support and has a value of one. The interpretation is simply that the largest vertical reaction on an end support due to an applied point force occurs when that point force is right on top of the support. Since we are considering a unit point force, the maximum reaction equals one.
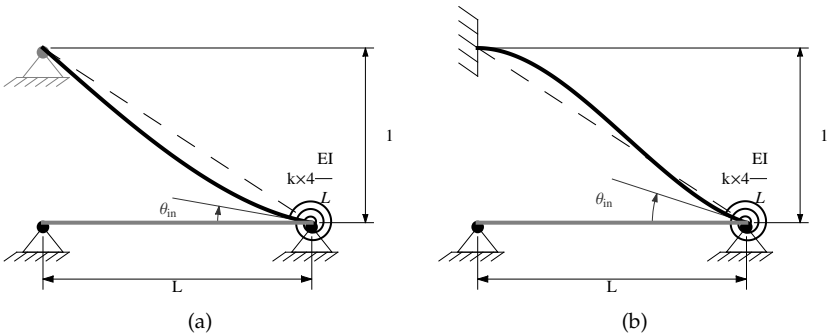
Figure 4.20. Influence lines for the vertical reaction at an end support of a beam with a rotary spring at the other end . The end support may either be a hinge (a) or a fixed support (b).

The shape of the deformation due to a unit movement of an end support differs depending on whether that support is a hinge or is a fixed support. In the case of a hinge end support, the deformed shape always has positive curvature and lies below the chord as shown in figure 4.20a and the slope at the internal support (*ie.* θ_{in} in figure 4.20a is always less or equal to one. Figures 4.21a, b, c and d show the range of behavior obtained as a function of the rotary stiffness factor. When the rotary stiffness factor is zero, we have a statically determinate simply supported beam and the influence line for the vertical reaction force is simply a straight line (see figure 4.21a). As the rotary stiffness factor increases, the
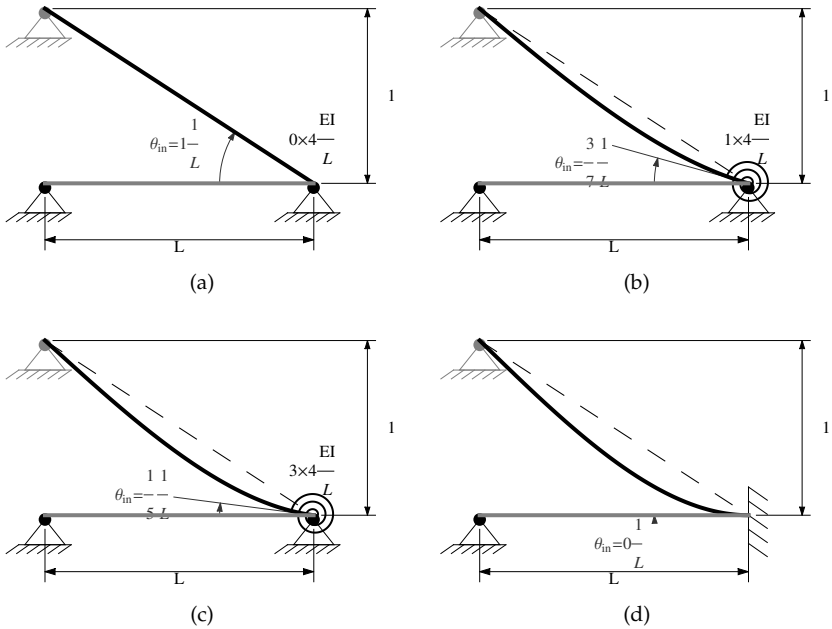
Figure 4.21. Influence lines for the vertical reaction at a hinge end support of a beam as the relative stiffness of the connected beam increases from zero (a) to one (b) to three (c) and to infinity which leads to a fixed end (d).

slope at the connected end decreases from $1/L$ to 0 where 'L' is the length of the span (see figures 4.21b, c and d).

By contrast with the hinge end support, when the end support is fixed then the deformed shape starts with negative curvature at that end and, in general, ends with a positive curvature at the inner support. The exception is when the inner support is itself a hinge or roller, as shown in figure 4.22a where the deformed shape has a negative curvature throughout the beam. With a fixed end, the slope at the inner support (*ie.* θ_{in} in figure 4.20b) is always less than $1.5/L$. The inner slope is exactly $1.5/L$ when the rotary stiffness factor equals zero as shown in figure 4.22a, and is exactly equal to $1/L$ and therefore tangent with the chord, when the rotary stiffness factor equals half as shown in figure 4.22b. When the rotary stiffness factor is greater than half then the inner slope is less than $1/L$ such as shown for a rotary stiffness factor of one in figure 4.21c. In the limit of an infinite rotary stiffness factor and hence a fixed inner support, the slope is zero at the inner support.
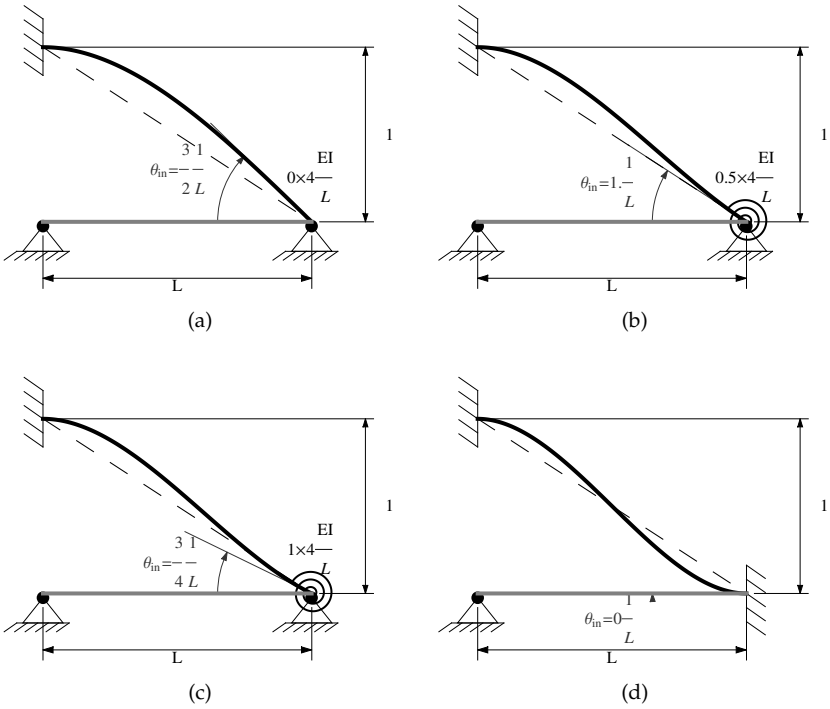
Figure 4.22. Influence lines for the vertical reaction at a fixed end support of a beam as the relative stiffness of the connected beam increases from zero (a) to half (b) to one (c) and to infinity which leads to a fixed end (d). The case of a rotary stiffness factor of half gives a slope at the inner end which is tangent with the chord.

In order to approximately identify the maximum deformation of the inner attached member, we need to quantitatively determine the slope at the inner support. This is given by:

$$\theta_{in} = \begin{cases} \dfrac{3}{3+4k}\dfrac{1}{L} & \text{hinge or roller support at end} \quad (4.5a) \\[3mm] \dfrac{3}{2+2k}\dfrac{1}{L} & \text{fixed support at end} \quad (4.5b) \end{cases}$$

where:

θ_{in} is the slope at the internal support (see figures 4.20)

k is the rotary stiffness factor at the internal support

L is the length of the beam
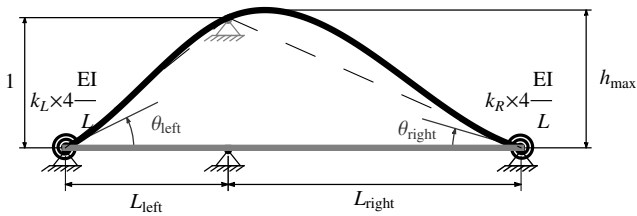
Figure 4.23. Influence lines for the vertical reaction at an internal support of a beam with rotary springs at both ends.

An example of the influence line for the vertical reaction force at an internal support is shown in figure 4.23. The deformed shape, when the sectional properties of the two beams are identical, is simply that of a beam with passive supports at its ends, whose span is the sum of the spans of the two beams and with a point force applied upwards at the location of the middle support. Sketching such deformations was covered extensively in the first chapter. Note that the deformation and hence influence line for a mid-reaction is always positive within the spans adjacent to the support considered. In this case, the maximum displacement is generally greater than one and always occurs within the middle third of the sum of the two spans. For the purposes of approximating the influence line, we need to identify the maximum displacement (*ie.* $h_{\max}$) and we also need to know the end slopes. The end slopes are needed in order to construct the influence lines of the attached members.

The maximum influence (*ie.* $h_{\max}$ in figure 4.23) when the left and right spans on either side of the support have the same sectional properties is approximately given by:

$$h_{\max} \approx 1 + \frac{\left(1 - \left(L_{\text{right}}/L_{\text{left}}\right)\right)^2}{5\left(L_{\text{right}}/L_{\text{left}}\right)} = \frac{L_{\text{right}}}{5L_{\text{left}}} + \frac{L_{\text{left}}}{5L_{\text{right}}} + \frac{3}{5} \qquad (4.6)$$

where:

$h_{\mathbf{max}}$ is the maximum value of the influence line (see figure 4.3)

$L_{\mathbf{left}}$ **and** $L_{\mathbf{right}}$ are the lengths of the left and right spans respectively (see figure 4.23).

Note that formula 4.6 gives a value always greater or equal to one, is symmetric with respect to L_{left} and L_{right} and gives a maximum error of 11% relative to the exact result when the ratio of the spans is between

half and two (*ie.* neither span is longer than twice the other). In that case, the exact value for the maximum possible influence equals about 1.23 and occurs when one span is twice the other with the shorter span being fixed and the longer span being hinged. This also happens to be the case where formula 4.6 has the largest errors relative to the exact results. In general, formula 4.6 is more accurate when the stiffness factors on both sides (*ie.* k_L and k_R in figure 4.23) are both one or larger in which case the maximum error is always less than 5% when the ratio of the spans is between half and two.

The other quantitative result we present for the case of the influence line of the vertical reaction force at an internal support is that of the end slopes. Approximate expressions for those end slopes are given by:

$$\theta_{\text{left}} \approx \frac{3}{4 + 4k_L}\left(\frac{1}{L_{\text{left}}} + \frac{1}{L_{\text{right}}}\right) \tag{4.7a}$$

$$\theta_{\text{right}} \approx \frac{3}{4 + 4k_R}\left(\frac{1}{L_{\text{left}}} + \frac{1}{L_{\text{right}}}\right) \tag{4.7b}$$

where:

θ_{left} **and** θ_{right} are the slopes of the left and right ends respectively (see figure 4.21)

L_{left} **and** L_{right} are the lengths of the left and right spans respectively (see figure 4.21)

k_L **and** k_R are the rotary stiffness factors on the left and right respectively (see figure 4.21). Note that these stiffness factors are relative to the left and right spans respectively which would be different than for those of the two combined spans

Note that formulas 4.7a and b give a maximum possible error of 25% relative to the exact result when the ratio of the spans is between half and two (*ie.* neither span is longer than twice the other). If in addition the rotary stiffness factors on either side are larger than one then the maximum possible error is reduced to 10%.

In order to gain some familiarity with the shape of the influence line in this case, figures 4.24 and 4.25 provide some examples. In figures 4.24, the beams on either side of the inner support are equal. When both sides are hinged, the resulting shape is shown in figure 4.24a. As the stiffness on either side increases, the slope decreases somewhat similar to the cases shown for the fixed end support in figures 4.22. In each case, formula 4.6 may be used to estimate the end slopes and formula 4.7 may be used to estimate the slopes at either end.
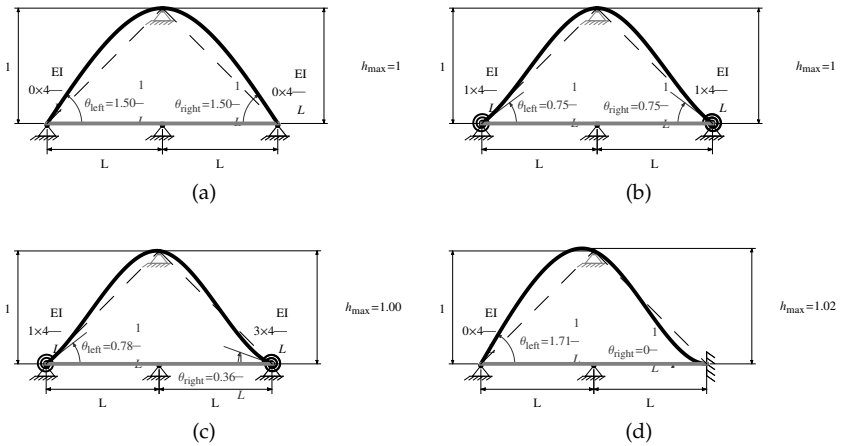
Figure 4.24. Influence lines for the vertical reaction at an internal support of a beam with rotary springs at both ends. In all cases the beams on either side of the inner support are equal with various combinations of the rotary stiffness factors at each end shown. Even when one side is fixed and the other hinged, the maximum displacement barely increases above one as shown in case (d).
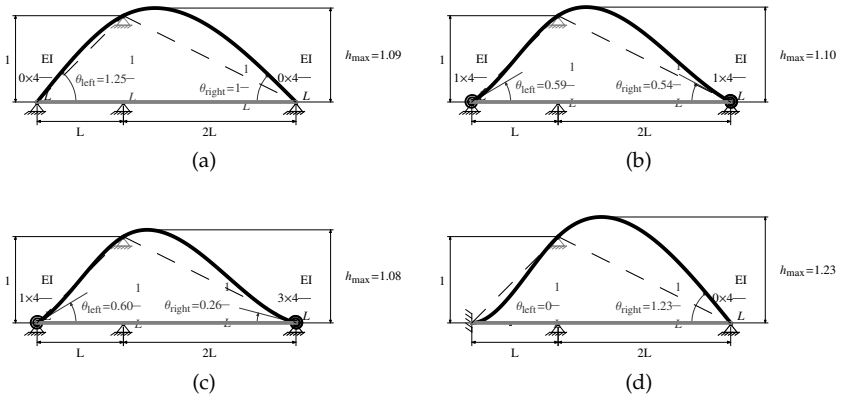
Figure 4.25. Influence lines for the vertical reaction at an internal support of a beam with rotary springs at both ends. In all cases the inner beam on the right is twice that on the left with various combinations of the rotary stiffness factors at each end shown.

In figures 4.25, the beams on the right are twice the length of those on the left. These figures shows the range of shapes obtained as the rotary stiffness factors change on either side. The largest deformation is obtained when the side nearest the inner support is fixed and the other side is hinged. Again, formula 4.6 may be used to estimate the end slopes and formula 4.7 may be used to estimate the slopes at either end.

4.3.3　Influence Line for Shear Forces in an Isolated Member

The second type of special loading we consider is that of a unit step jump in the displacement as shown in figure 4.26. As in other parts of this book, the passive response of the rest of the structure is modeled by equivalent rotary springs at the ends of the loaded member. For this type of loading, figure 4.22 shows the typical shape of the deformation. This deformation corresponds to the influence line for the shear force at the location of the jump. The influence line starts at zero at the left support and decreases monotonically to reach a minimum that is always greater or equal to negative one at the point of influence. This means the influence line from the left support till the point of influence is always negative. At the point of influence, the influence line jumps up by one and always reaches a positive value less or equal to one. Finally, to the right, the line is always positive and decreases monotonically from left to right to reach zero at the right support.
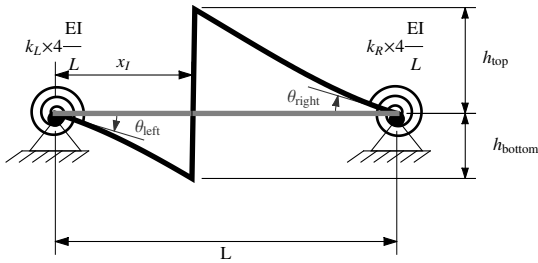
Figure 4.26. Influence lines for the shear force at a point with distance 'x_I' from the left support of a beam with rotary springs at both ends.

For the purposes of approximating the influence line, we need to identify the minimum and maximum values (*ie.* h_{bottom} and h_{top} in figure 4.22) and we also need to know the end slopes. The end slopes are needed in order to construct the influence lines of the attached members.

We start with the minimum and maximum values and these are exactly given by:

$$h_{\text{bottom}} = \frac{x_I}{L} + \frac{2\,(k_R + 2k_L k_R)}{3 + 4k_L + 4k_R + 4k_L k_R}\left(\frac{x_I}{L} - \frac{x_I^3}{L^3}\right)$$
$$- \frac{2\,(k_L + 2k_L k_R)}{3 + 4k_L + 4k_R + 4k_L k_R}\left(\left(1 - \tfrac{x_I}{L}\right) - \left(1 - \tfrac{x_I}{L}\right)^3\right) \qquad \text{(4.8a)}$$

$$h_{\text{top}} = 1 - h_{\text{bottom}} \qquad\qquad\qquad\qquad\qquad \text{(4.8b)}$$

where:

$h_{\textbf{bottom}}$ is the minimum value of the influence line and occurs slightly to the left of the influence point

$h_{\textbf{top}}$ is the max value of the influence line and occurs slightly to the right of the influence point

x_I is the distance of the point of influence from the left support

L is the length of the beam

k_L **and** k_R are the rotary stiffness factors on the left and right respectively (see figure 4.22)

Formula 4.8a is somewhat complicated but a significantly simpler yet sufficiently accurate approximate expression is currently unavailable. Note that there is a remarkably interesting feature to formula 4.8. Specifically, let 'x' be the coordinate of any point along the influence line with origin at the left support. If we take negative 'h_{bottom}' in formula 4.8a and replace 'x_I' by 'x' then we get the function describing the influence line from the left support until the point of influence. Similarly, if we take 'h_{top}' in formula 4.8b and replace 'x_I' by 'x' then we get the function describing the influence line from the point of influence to the right support. Note that the shapes of the influence lines before and after the point of influence are both independent of the location 'x_I' of that point and that this location 'x_I' only affects where the jump or discontinuity occurs. In particular, the slopes at the end supports are both independent of the location 'x_I' of the point of influence and depend only on the rotary stiffness factors. These end slopes are given exactly by:

$$\theta_{\text{left}} = \frac{3 + 6k_R}{3 + 4k_L + 4k_R + 4k_L k_R} \times \frac{1}{L} \qquad \text{(4.9a)}$$

$$\theta_{\text{right}} = \frac{3 + 6k_L}{3 + 4k_L + 4k_R + 4k_L k_R} \times \frac{1}{L} \qquad \text{(4.9b)}$$

where:

θ_{left} and θ_{right} are the slopes at the left and right ends respectively (see figure 4.22)

k_L and k_R are the rotary stiffness factors on the left and right respectively (see figure 4.22)

This independence of the shape of the influence line before and after the jump from the location of the point of influence is quite convenient but is unfortunately absent from the influence lines of those for the vertical reaction force at an internal support and for the bending moments.

In order to gain some familiarity with the shape of the influence line for a shear force in an isolated part, figures 4.27 and 4.28 provide some examples. In each of figures 4.27 and 4.28, we also show, as thick but light gray lines, the envelope of values for the maximum and the minimum of all influence lines at the given values of the rotary stiffness factors at the ends. In each of these figures and at the associated rotary stiffness factors, the influence line for the shear force may be obtained at any influence point by sketching along the lower envelope from the left support until the influence point, jumping to the upper envelope at the influence point and then sketching along the upper envelope until we reach the right support. Therefore, in each of these figures, the envelopes completely specify the influence line for shear forces at any location of the influence point on the beam but at the specified rotary stiffness factors. The solid lines are the influence line of the shear force at a particular influence point location.

In figures 4.27, the influence point is at the center of the beam. When both sides are hinged, the resulting shape is shown in figure 4.27a and correspond to the shape obtained for a statically determinate beam. The value of the minimum relative to the maximum value of the influence line depends on the relative rotary stiffness factors on either side. When the two sides have the same rotary stiffness factor then the absolute value of the minimum and maximum are the same as in the example shown in figure 4.27b. In general, the side with the higher stiffness will have a lower maximum or absolute value of the minimum on its side such as shown in figure 4.27c. However, the smallest relative value between maximum and absolute value of the minimum when the influence point is in the middle of the beam occurs when one side is fixed and the other hinged as in the example shown in figure 4.27d. In that case, the ratio of the smaller of the maximum or absolute value of minimum to the largest of the two equals about 0.31.
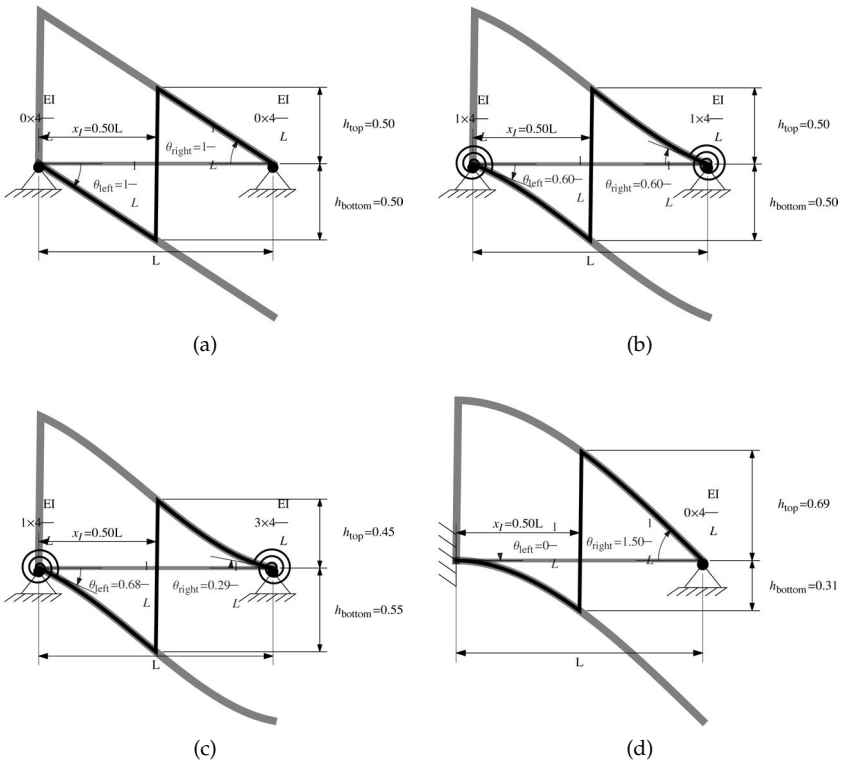
Figure 4.27. Influence lines (solid black lines) for the shear force in the middle of a beam with rotary springs at both ends. Examples having various combinations of the rotary stiffness factors at each end are shown. Even when one side is fixed and the other hinged, the value of the influence line at the jump on the side of the fixed end is still appreciable and equals about 0.31. Note that the slopes at either end of the beam scales or are multiples of $1/L$ where 'L' is the span of the beam while the maximum and minimum values are dimensionless.

In figures 4.28, we present influence lines for the shear force at influence points other than the center. These figures show a range of shapes obtained as the location of the influence point changes at fixed values of the rotary stiffness factors. The maximum of one is always reached when the influence point is at the left support as in figure 4.28d and the minimum of minus one is always reached when the influence point is at the right support. Note that because the rotary stiffness factors are held fixed in figures 4.28, the left and right slopes are always the same for any location of the influence point. This includes the cases when it is at the left support as in figure 4.28d and when it is at the right support.
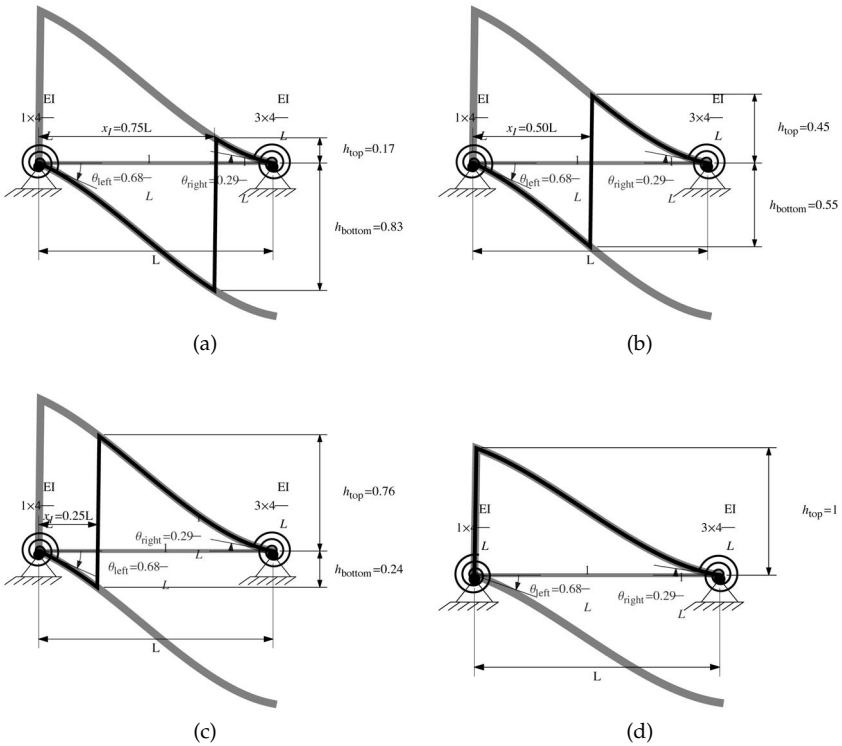
Figure 4.28. Influence lines (solid black lines) for the shear force at various locations in a beam with rotary springs at both ends. Examples having various combinations of the rotary stiffness factors at each end are shown. When the influence point is at a support, all the jump occurs on the side away from it as in figure (d). Also, the slope before and after the jump must match so that although the influence line of the shear is at the support, a non-zero slope will be enforced on the adjacent member. Finally, note that the slopes at either end of the beam are multiples of $1/L$ where 'L' is the span of the beam while the maximum and minimum values are dimensionless.

4.3.4   Influence Line for Bending Moments in An Isolated Member

The last type of special loading we consider is that of a unit change in slope or unit kink as shown in figures 4.29. As in other parts of this book, the passive response of the rest of the structure is modeled by equivalent rotary springs at the ends of the loaded member. For this type of loading, figure 4.29a shows one type of deformation and figures 4.29a and b show
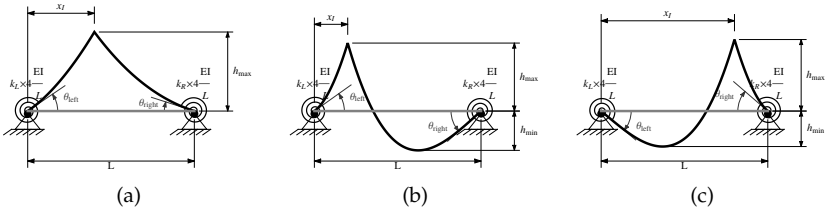
Figure 4.29. Influence lines for the bending moment at a point with distance 'x_I' from the left support of a beam with rotary springs at both ends. This influence line may have only positive values as in figure (a) or both positive and negative values as in figures (b) and (c).

another. In each case, these deformations correspond to the influence line for the bending moment at the location of the kink. Each of those shapes occurs under specific conditions which we will next discuss.

The first type of influence line of the bending moment is shown in figure 4.29a. The value is always positive and reaches a maximum at the location of the point of influence. This pattern of influence line for the bending moment always occurs when the location 'x_I' of the point of influence satisfies the following condition:

$$\frac{2k_L}{3+6k_L}L \le x_I \le \left(1 - \frac{2k_R}{3+6k_R}\right)L \tag{4.10}$$

$\Rightarrow$ influence line of bending moment has pattern of figure 4.29a.

where:

k_L **and** k_R are the rotary stiffness factors on the left and right respectively (see figure 4.29a)

L is the length of the span

x_I is the location of the point of influence relative to the left support as origin (see figure 4.29a)

The second type of influence line of the bending moment is shown in figures 4.29b and c. In that case, if the influence line is closer to the left support, the influence line starts at zero at the left, increases to a maximum at the point of influence then decreases to reach a minimum that has a negative value before increasing again to meet the right support at zero. The pattern is analogous when the influence point is closer to the right support and is shown in figure 4.29c. These patterns of influence

lines for the bending moment always occurs when the location 'x_I' of the point of influence satisfies either of the following conditions:

$$x_I \leq \frac{2k_L}{3+6k_L} L \qquad (4.11a)$$

$\qquad \Rightarrow \quad$ influence line of bending moment has pattern of figure 4.29b

$$x_I \geq \left(1 - \frac{2k_R}{3+6k_R}\right) L \qquad (4.11b)$$

$\qquad \Rightarrow \quad$ influence line of bending moment has pattern of figure 4.29c

For the purposes of approximating the influence line, we need to identify the minimum and maximum values (*ie.* h_{bottom} and h_{top} in figure 4.22), the location of the minimum value and we also need to know the end slopes. The end slopes are needed in order to construct the influence lines of the attached members. We start with the maximum with the exact result being given by:

$$
\begin{aligned}
h_{\max} = \frac{x_I}{L} &\left(1 - \frac{x_I}{L}\right) \\
&\times \Big((3 + 4k_R) + (6k_L - 2k_R + 8k_L k_R)(x_I/L) \\
&\quad - 2(k_L + k_R + 4k_L k_R)(x_I/L)^2 \Big) \frac{L}{z}
\end{aligned}
\qquad (4.12)
$$

where:

$$z = 3 + 4k_L + 4k_R + 4k_L k_R$$

$h_{\mathbf{max}}$ is the maximum value of the influence line and occurs at the influence point (see any of figures 4.29)

x_I is the distance of the point of influence from the left support

L is the length of the beam

k_L and k_R are the rotary stiffness factors on the left and right respectively (see any of figures 4.29)

Formula 4.12 is somewhat complicated but a significantly simpler yet sufficiently accurate approximate expression is currently unavailable. Of course, the formula reduces correctly to the solution for the maximum bending moment in a simply supported beam as a unit point force location varies from left to right. In fact, we can obtain simple upper and lower bounds on the maximum influence line value that correspond to the cases when the beam is simply supported and fixed-fixed respectively. The result is then:

$$2\left(\frac{x_I}{L}\right)^2 \left(1 - \frac{x_I}{L}\right)^2 L \leq h_{\max} \leq \frac{x_I}{L}\left(1 - \frac{x_I}{L}\right) L \qquad (4.13)$$

The expression for the minimum influence value is long and complicated, but fortunately, a simpler approximate expression may be specified as:

$$h_{\min} \approx \begin{cases} \frac{k_L}{1+k_L}\frac{(1+k_R)}{(5+7k_R)}\left(1 - \frac{(x_I/L)}{2k_L/(3+6k_L)}\right)^2 L & 0 \le x_I \le \frac{2k_L}{3+6k_L}L \\ \frac{k_R}{1+k_R}\frac{(1+k_L)}{(5+7k_L)}\left(1 - \frac{(1-(x_I/L))}{2k_R/(3+6k_R)}\right)^2 L & 1 - \frac{2k_R}{3+6k_R} \le x_I \le L \end{cases}$$

(4.14)

where:

$h_{\min}$ is the minimum value of the influence line (see figures 4.29b or c)

x_I is the distance of the point of influence from the left support

L is the length of the beam

k_L and k_R are the rotary stiffness factors on the left and right respectively (see any of figures 4.29)

Formula 4.14 is approximate and has a maximum absolute error of $0.01 \times L$ for all values of 'k_L,' 'k_R' and 'x_I.' This error is usually negligible for most cases as compared with the maximum of either the positive moment or the absolute value of the negative moment. The absolute value of the minimum increases as the influence point gets closer to a support and as the rotary stiffness factor of that support increases. A negative influence value corresponds to a negative bending moment in a beam with an applied point force on the beam. Such negative bending moment and associated negative curvature can only occur in statically indeterminate beams. Therefore, the influence lines for bending moments in statically indeterminate beams are distinguished from those of determinate ones by the possibility of having negative values within the beam containing the influence point. Of course, both statically determinate and indeterminate beams may have negative influence values outside the beam containing the influence point.

Associated with the minimum value of the influence line is the location of that minimum, this is approximately given by:

$$x_{\text{at min}}/L \approx \begin{cases} 1 - 3\frac{(1-s)}{(3-s)}\left(1 - 2f\frac{(1-s)}{(2-s)}\right) & 0 \le x_I \le \frac{2k_L}{3+6k_L}L \\ 3\frac{(1-s)}{(3-s)}\left(1 - 2f\frac{(1-s)}{(2-s)}\right) & 1 - \frac{2k_R}{3+6k_R} \le x_I \le L \end{cases}$$

(4.15)

with: $\quad s = \begin{cases} \frac{(x_I/L)}{2k_L/(3+6k_L)} & 0 \le x_I \le \frac{2k_L}{3+6k_L}L \\ \frac{1-(x_I/L)}{2k_R/(3+6k_R)} & 1 - \frac{2k_R}{3+6k_R} \le x_I \le L \end{cases}$

$$f = \begin{cases} \frac{0.42+0.33k_R}{1+k_R} & 0 \le x_I \le \frac{2k_L}{3+6k_L}L \\ \frac{0.42+0.33k_L}{1+k_L} & 1 - \frac{2k_R}{3+6k_R} \le x_I \le L \end{cases}$$

where:

$x_{\text{at min}}$ is the location of the minimum value of the influence line from the left support

x_I is the distance of the point of influence from the left support

L is the length of the beam

k_L and k_R are the rotary stiffness factors on the left and right respectively (see any of figures 4.29)

Note that formula 4.15 has absolute error less than $0.1 \times L$. Although this error is appreciable, it is sufficient for the purpose of approximately and manually sketching the shape of the influence lines.

The last result we need in order to approximately but quantitatively analyze influence lines for bending moments are expressions for the slopes at the ends of the isolated part. These are exactly given by:

$$\theta_{\text{left}} = \frac{(3+4k_R) - (3+6k_R)\,(x_I/L)}{3+4k_L+4k_R+4k_Lk_R} \tag{4.16a}$$

$$\theta_{\text{right}} = \frac{(3+4k_L) - (3+6k_L)\,(1-x_I/L)}{3+4k_L+4k_R+4k_Lk_R} \tag{4.16b}$$

where:

x_I is the distance of the point of influence from the left support

L is the length of the beam

θ_{left} and θ_{right} are the slopes at the left and right ends respectively (see figure 4.22)

k_L and k_R are the rotary stiffness factors on the left and right respectively (see figure 4.22)

Note that formulas 4.16 allows either slope to be both negative and positive. If we start with a beam having non-zero rotary stiffness factors at both ends and with the influence point in the middle of the beam then, if we consider another influence point sufficiently close to one of the supports, negative values in the influence line will appear and the slope at the support farthest from the influence point will switch sign.

In order to gain some familiarity with the shape of the influence line for a bending moment in an isolated part, figures 4.30 and 4.31 provide
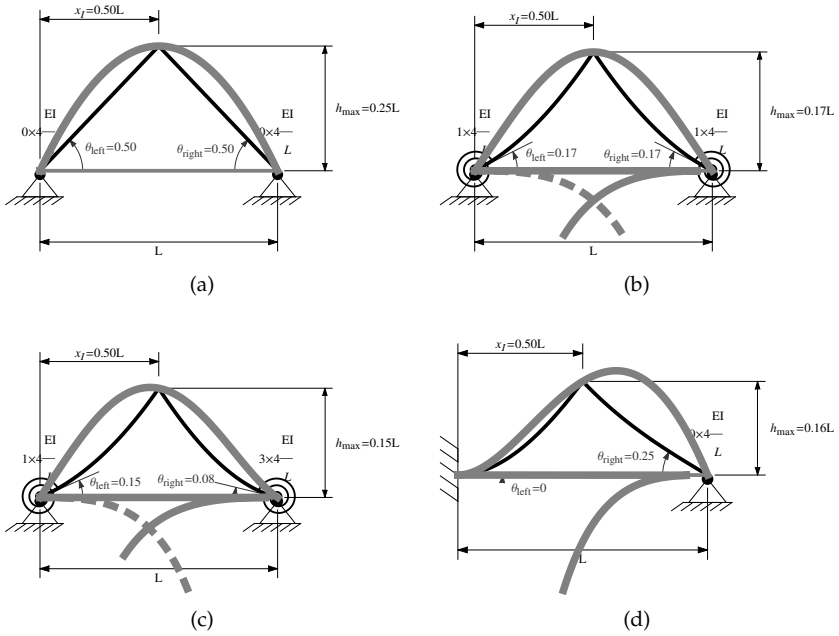
Figure 4.30. Influence lines (solid black lines) for the bending moment in the middle of a beam with rotary springs at both ends. Examples having various combinations of the rotary stiffness factors at each end are shown. Note that the slopes at either end of the beam are dimensionless while the maximum and minimum values are multiples of 'L' where 'L' is the span of the beam.

some examples. In each of figures 4.30 and 4.31, we also show, as thick but light gray lines, the envelope of values for the maximum and the minimum of all influence lines at the given values of the rotary stiffness factors at the ends. Note that in one case, that of the simply supported beam which is statically determinate, the minimum is always zero as is for example indicated in figure 4.30a by the lack of a lower negative envelope. In general, there are two separate branches to the envelopes of the negative minimum values. One is shown as a solid light gray line and occurs when the influence point is nearer to the left support which is opposite the side of the corresponding branch. The other branch is shown as a dashed light gray line and occurs when the influence point is nearer to the right support. Note that if the right support is a hinge, then we do not get negative values for the influence line when the influence point is near that right hinge and so the dashed light gray line will be missing as in figure 4.30d and in figure 4.31d. An equivalent condition
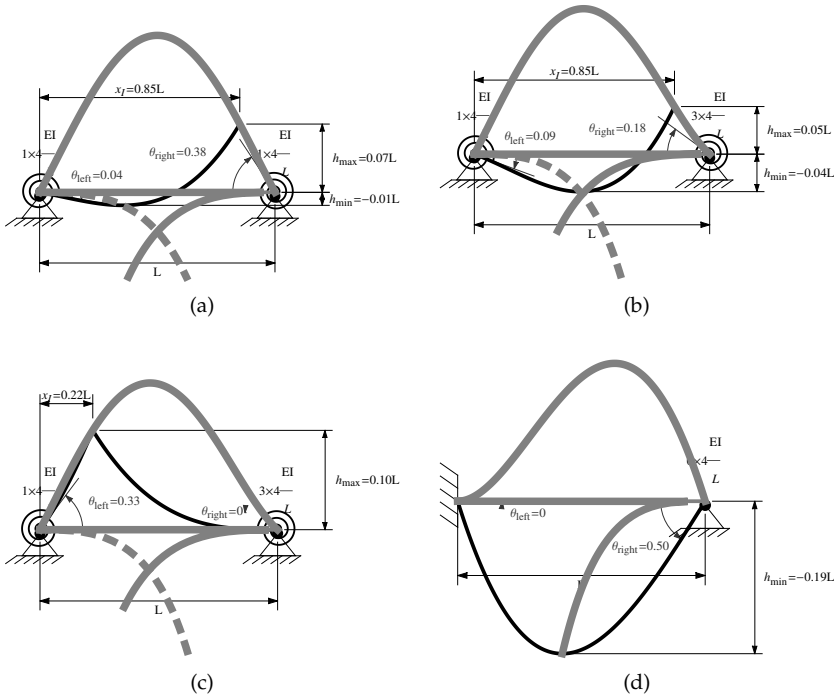
Figure 4.31. Influence lines (solid black lines) for the bending moment at various locations of a beam with rotary springs at both ends. Examples having various combinations of the rotary stiffness factors at each end are shown. Note that the slopes at either end of the beam are dimensionless while the maximum and minimum values are multiples of 'L' where 'L' is the span of the beam.

occurs when the left support is a hinge in which case the lower solid gray line will be missing indicating an absence of a negative minimum envelope when the influence point is near the left support.

Concerning the upper envelope, the influence line must always pass through one of those points since there are always positive values of the influence line. Furthermore, the maximum always occurs at the kink which is the location of the influence point. The interpretation is that for any beam with passive supports and loaded by a unit point force, the maximum bending moment always occurs at the location of the unit point force. Note that unlike the influence line for shear forces, the upper and lower envelopes generally match the influence line at only one (*ie.* the maximum) or two points (*ie.* maximum and minimum) rather than along whole segments. Finally, in all the figures for the influence

line for bending moments, the solid lines are the influence line of the bending moments at a particular influence point location.

In figures 4.30, the influence point is at the center of the beam. When both sides are hinged, the resulting shape is shown in figure 4.30a and correspond to the shape obtained for a statically determinate beam. In that case, the values of the envelope of the maximum values (*ie.* the light gray line with positive values in figure 4.30a) are also the upper bounds for the influence line for any influence line having the same span. For all the cases when the influence point is at the center, as the rotary stiffness factors increase, the maximum influence value decreases from $0.25L$ to $0.125L$ (*ie.* a total of 50% decrease). The largest decrease occurs when the rotary stiffness factors increase from zero to one on either side so that when both sides have stiffness factor of one, as in figure 4.30b, then the value of the influence line is about $0.17L$ (*ie.* 32% less than the simply supported case). Beyond a rotary stiffness factor of one, the change in maximum influence value decreases more gradually so that if we compare figure 4.30b and figure 4.30c, where the rotary stiffness factor on the right has increased from one to three with other parameters the same, the maximum influence value only changes from about $0.17L$ to $0.15L$ (*ie.* only by 12%). Finally, when the rotary stiffness factors on the ends are not symmetric, the envelope of maximum influence value always occurs closer to the end with the lower stiffness factor.

In figures 4.31, we present influence lines for the bending moment at influence points other than the center. Some observations concerning those examples are as follows:

- By comparing figures 4.31a and c, we note that the minimum decreases with an increase in the rotary stiffness factor nearest to the point of influence. Note that both influence lines in figures 4.31a and b achieve their maximum at some point on the light gray dashed line which is an envelope of minimum values when the influence point is closer to the right support.

- When the influence point is at exactly a boundary value in the conditions of formulas 4.11a and b, the influence line will be tangent to the horizontal at one side. For example, figure 4.31c shows the influence line for the bending moment when the influence line is at $0.222L$ which is at a boundary value in formula 4.11a. In that case, the influence line on the right is tangent to the horizontal and the slope is exactly zero at that end support. The implication is that a neighboring beam connected at the right end will have zero influence at the specified point of influence for any location of the unit point force on that beam. The reason is that the boundary values in formulas 4.11a and b correspond to an inflection point location in the beam with the influence point when

any load is applied to another beam attached on the right or on the left of it respectively.

- Finally, if we consider an influence point that is at exactly the left or at exactly the right support, then the influence values will all be negative as shown in example 4.31d where the influence point is exactly at the left support. In those cases, the minimum influence value will be the minimum value of either the left or the right lower envelope depending on whether the influence point is at the right or left support respectively. Also note that the slope at the end that is obtained by formula 4.16a and b when an influence point is right at a support is the slope of the neighboring member attached to that end rather than the slope of the influence line itself. For example, in figure 4.31d, the slope at the left support is identified to be zero based on formula 4.16a which is the slope of the fixed end rather than the slope of the influence line at that end.

4.3.5   Influence Line in a Transition Member for All Types

In the approach we present to obtain influence lines, we start by isolating the beam containing the influence point. When isolating that beam, we model the rest of the structure attached to either end by equivalent rotary springs. Once isolated, we sketch that beam's influence line based on the results presented in the previous sections. In addition, we obtain the slopes at either end of that isolated beam. Those slopes are then applied at the ends of the beams attached to that isolated beam which in turn may be attached to other beams. Therefore, each of the beams other than the one containing the influence point has basically the same configuration if it has no internal hinges. Those beams are unloaded but have a specified slope on one side and a passive structure attached to the other. This implies that they may be modeled as shown in figure 4.32 with an applied slope at one end which we call the near end and a rotary spring at the other end whcih we call the far end. Based on the Müller-Breslau principle if we determine the deformation of such a beam then this deformation corresponds to their influence line.

   The beam shown in figure 4.32 is fundamental in this book and has been analyzed and used several times in previous chapters. The current focus is to obtain the following pieces of information:

- The maximum displacement 'u_{max}' in terms of the applied slope 'θ_{near}' (see figure 4.32). Note that in previous studies, we applied a moment rather that a slope.
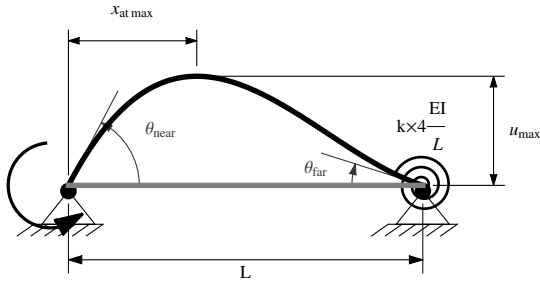
Figure 4.32. Transition member used to sketch influence lines of the members not containing the influence point.

- The approximate location '$x_{\text{at max}}$' of the maximum displacement. This has been extensively done in a previous chapter

- The slope at the far end 'θ_{far}' in terms of the applied or near end slope 'θ_{near}.'

First, we consider the slope at the far end which is exactly given by:

$$\theta_{\text{far}}/\theta_{\text{near}} = \frac{1}{2 + 2k} \tag{4.17}$$

where:

θ_{near} **and** θ_{far} are the slopes at the ends of the beam where 'θ_{near}' is considered as an applied slope (see figure 4.32)

k is the rotary stiffness factor at the far end (see figure 4.32)

Note that the ratio in equation 4.16 is a uniformly decreasing function of 'k' with the fastest decrease occuring between zero and one.

The next result is the maximum displacement 'u_{max}' and this is approximately given by:

$$u_{\text{max}} \approx \frac{0.19 + 0.15k}{1 + k} \theta_{\text{near}} L \tag{4.18}$$

where:

θ_{near} is the applied slope at one end of the beam (see figure 4.32)

k is the rotary stiffness factor at the far end (see figure 4.32)

L is the span or length of the beam (see figure 4.32)

We note that formula 4.18 has error less than 1.5% for any value of
'k' as compared with the exact result (see appendices). Also note that the
value of the maximum displacement varies monotonically from about
0.19 when the far end is a hinge to 0.15 when the far end is fixed. Finally,
the maximum displacement is always a multiple of the product of the
applied near slope 'θ_{near}' and the length of the beam 'L.'

Finally, the last result that is needed concerns the location of the max-
imum displacement and this is approximately given by:

$$x_{at\,max}/L \approx \frac{0.42 + 0.33k}{1 + k} \tag{4.19}$$

where:

$x_{at\,max}$ is the location of the maximum displacement (see figure 4.32)

k is the rotary stiffness factor at the far end (see figure 4.32)

L is the span or length of the beam (see figure 4.32)

We note that formula 4.19 has error less than 1% for any value of
'k' compared to the exact result (see appendices). Also note that the
value of the location of the maximum displacement varies monotonically
from about 0.42 when the far end is a hinge to 0.33 when the far end is
fixed.

The above simple results, and particularly formulas 4.17 and 4.18,
imply that the influence lines of statically indeterminate beams that are
free of internal hinges will be strikingly different in at least one fea-
ture. That feature is as follows: If we consider a statically indeterminate
beams with no internal hinges and where no span is longer than twice
the other then the maximum absolute value of the level of the influence
line in beams will decrease faster than some geometric progression as we
move consecutively away from the beam containing the influence point.
In statically determinate beams, such a feature is possible but generally
does not occur. The geometric decrease in the level of influence lines fol-
lows because the ratio between the far and near slope is always less than
half and the span ratios is less than two. Since the product of the slope
at the near end and the length of the span sets the maximum level of the
deformation in a beam, consecutive beams away from the one contain-
ing the influence point will have a decrease faster than some geometric
progression. Note that this decrease will generally be quite fast because
even when the rotary stiffness factor is one, formula 4.17 gives a ratio of
one quarter.

4.3.6 Examples of Sketching Influence Lines for Vertical Force Reactions

In this section, we will present examples of sketching the influence lines for vertical force reactions. The results in the figures shown are exact results and we will describe how the discussions and approximations developed in previous sections allow us to approximately sketch those influence lines. For simplicity, we will start with examples where all the spans are equal and have the same sectional properties as shown in figure 4.33. As specific examples, we will consider the influence line for the vertical reaction at A and for the vertical reaction at C. The rest of the cases shown in figure 4.33 may be similarly analyzed and are left as an exercise for the reader.

span	$x_{\text{at min}}$	h_{min}	$x_{\text{at max}}$	h_{max}
1	1	0	0	1
2	0.380	−0.079	1	0
3	0	0	0.377	0.021
4	0.333	−0.005	1	0
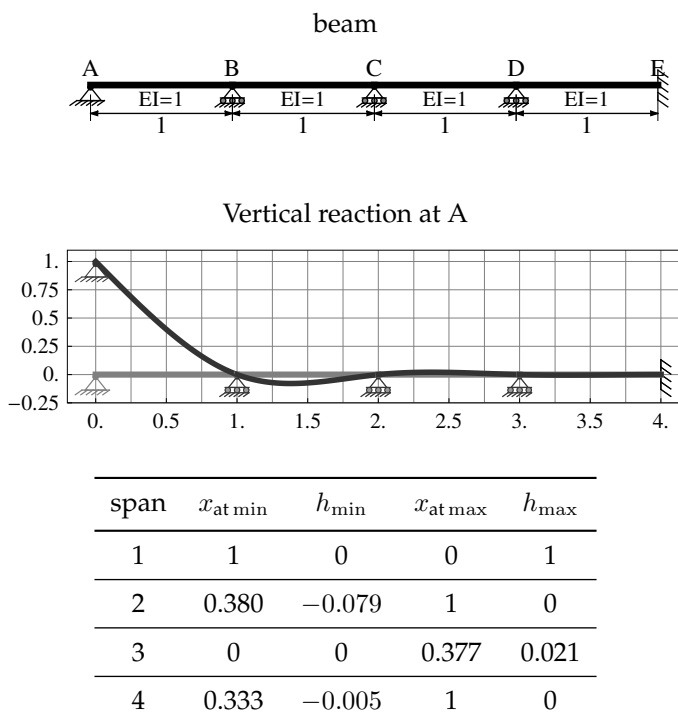
Figure 4.33. Influence lines for the vertical force reactions in a case where all beams have the same span and the same sectional properties. *(Continued below.)*

Vertical reaction at B
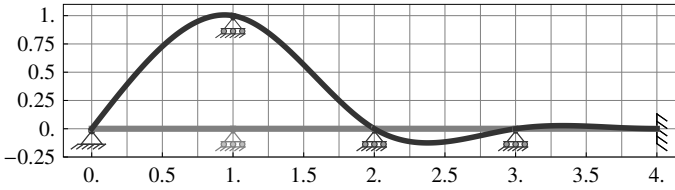
span	$x_{\text{at min}}$	$h_{\min}$	$x_{\text{at max}}$	$h_{\max}$
1	0	0	0.939	1.007
2	1	0	0	1
3	0.377	-0.125	1	0
4	0	0	0.333	0.027

Vertical reaction at C
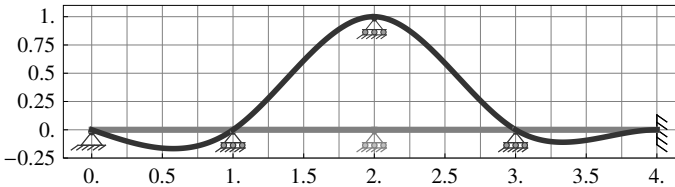
span	$x_{\text{at min}}$	$h_{\min}$	$x_{\text{at max}}$	$h_{\max}$
1	0.577	-0.167	1	0
2	0	0	0.993	1.000
3	1	0	0	1
4	0.333	-0.110	1	0

Figure 4.33. *(Continued from above and continued below.)*
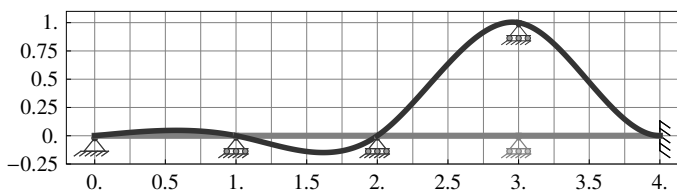
Vertical reaction at D

span	$x_{\text{at min}}$	$h_{\min}$	$x_{\text{at max}}$	$h_{\max}$
1	0	0	0.577	0.048
2	0.616	-0.149	1	0
3	0	0	0.956	1.005
4	1	0	0	1

Vertical reaction at E
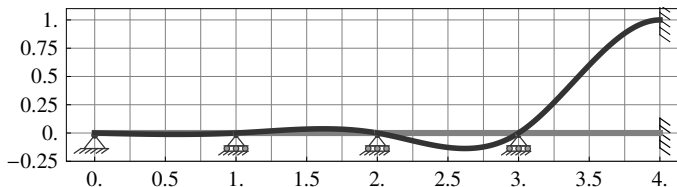
span	$x_{\text{at min}}$	$h_{\min}$	$x_{\text{at max}}$	$h_{\max}$
1	0.577	-0.012	1	0
2	0	0	0.616	0.037
3	0.619	-0.137	1	0
4	0	0	1	1

Figure 4.33. *(Continued from above.)* Influence lines for the vertical force reactions in a case where all beams have the same span and the same sectional properties.

Considering figure 4.33, we first describe how to approximately construct the influence line for the vertical reaction at A where there is a support at the end of the beam. For that influence line, we start by isolating member AB which is the member containing the influence point A. For that member AB, we estimate the rotary stiffness factor at B to be 1. At this point, we may sketch the shape of the influence line for member AB based on the patterns identified in figures 4.21. From the rotary stiffness at B, we may calculate an estimate of the slope at B using formula 4.5a which gives a slope of about 0.43. That slope is then applied on member BC so that the sketch of member BC must have the identical slope of 0.43 at B. Member BC is analyzed as a transition member with an applied slope of 0.43 at point B and a rotary spring at C for which we estimate the rotary stiffness factor to be 1. Using formula 4.18, we calculate the maximum influence to be 0.073 which has an error of about 7.6% compared with the exact result of 0.079 given in the table next to the influence line for the vertical reaction at A. Note that in that table, span 2 refers to the second member from the left which is member BC. Using formula 4.19, we calculate the location of that maximum influence to be 0.375 which has an error of about 1.32% compared with the exact result of 0.380. Based on these calculations, we can quantitatively sketch the influence line for member BC using figure 4.32 as a guide (also see chapter 1). Finally, using formula 4.17, we calculate the slope at C to be about 0.11. This slope is then applied on member CD which is again modeled as a transition member like the one shown in figure 4.32. Once we finish with member CD, we get the slope at D and sketch member DE in a similar manner which then completes the whole sketch of the influence line for the vertical reaction at A. This sketch includes relatively accurate approximations of maxima, minima and their locations.

Again considering figure 4.33, we next describe how to approximately construct the influence line for the vertical reaction at C where there is an internal support. For that influence line, we start by isolating the two beams BC and CD together with rotary springs at ends B and D. We estimate the stiffness factors at B and D to be 0.75 and 1 respectively. Based on the patterns identified in figures 4.24, we may approximately sketch the influence line in the segment between B and D. In that segment, we also determine that the maximum influence is about 1. Next we calculate the slopes at B and D using formula 4.7a and b which give values of 0.86 and 0.75 respectively. These slopes are then used as imposed values on transition members on the left and the right. For member AB on the left, the rotary stiffness factor is zero at A which using formula 4.18 gives a maximum value of $0.19 \times 0.86 \approx 0.163$. This compares well with the exact value of 0.167 which gives an error of only 2.5%. In regards to the location of the maximum, formula 4.19 gives a value of 0.42

from the location of the imposed slope which is point B or equivalently $1 - 0.42 = 0.57$ from point A. This value again compares well with the exact value of 0.577 corresponding to an error of only 1.21%. For member CD on the right of the isolated segment BCD, the rotary stiffness factor is infinity at D due to the fixed end. Applying a slope at D of 0.75 and using formulas 4.18 and 4.19, we get values of $0.15 \times 0.75 \approx 0.112$ and 0.33 for the maximum influence and location respectively. These again compare well with the exact values of 0.110 and 0.333 given for span 4 in the table next to the exact influence line.

Next we consider the beam shown in figure 4.34 where the spans are nonequal and the sectional properties are different. As specific examples, we will consider the influence line for the vertical reaction at E and for the vertical reaction at B. The rest of the cases may be similarly analyzed and are left as an exercise for the reader.

Considering figure 4.34, we first describe how to approximately construct the influence line for the vertical reaction at E where there is a support at the end of the beam. For that influence line, we start by isolating member DE which is the member containing the influence point E. For that member DE, we estimate the rotary stiffness factor at D to be $(1/1.5)/(0.8/0.75) \approx 0.625$. At this point, we may sketch the shape of the influence line for member DE based on the patterns identified in figures 4.22. From the rotary stiffness factor at D, we may calculate an estimate of the slope at using formula 4.5b which gives a slope of about 1.231. That slope is then applied on member DC so that the sketch of member DC must have the identical slope of 1.231 at D. Member DC is analyzed as a transition member with an applied slope of 1.231 at point D and a rotary spring at C for which we estimate the rotary stiffness factor to be $(0.8/0.75)/(1/1.5) \approx 1.6$. Using formula 4.18, we calculate the maximum influence to be 0.305 which has an error of about 4.1% compared with the exact result of 0.318 given in the table next to the influence line for the vertical reaction at D. Note that in that table, span 3 refers to the third member from the left which is member CD. Using formula 4.19, we calculate the location of that maximum influence to be 0.547 from the left support or $1.5 - 0.547 \approx 0.953$ from the left support C which has an error of about 0.95% compared with the exact result of 0.944. Based on these calculations, we can quantitatively sketch the influence line for member CD using figure 4.32 as a guide (also see chapter 1). Finally, using formula 4.17, we calculate the slope at C to be about 0.237. This slope is then applied on member CB which is again modeled as a transition member like the one shown in figure 4.32. Once we finish with member CB, we get the slope at D and sketch member AB in a similar manner which then completes the whole sketch of the influence line for the vertical reaction at E. This sketch includes

beam

Vertical reaction at A

span	$x_{at\ min}$	h_{min}	$x_{at\ max}$	h_{max}
1	1.250	0	0	1
2	0.292	−0.042	0.750	0
3	0		0.550	0.025
4	0.250	−0.002	0.750	0
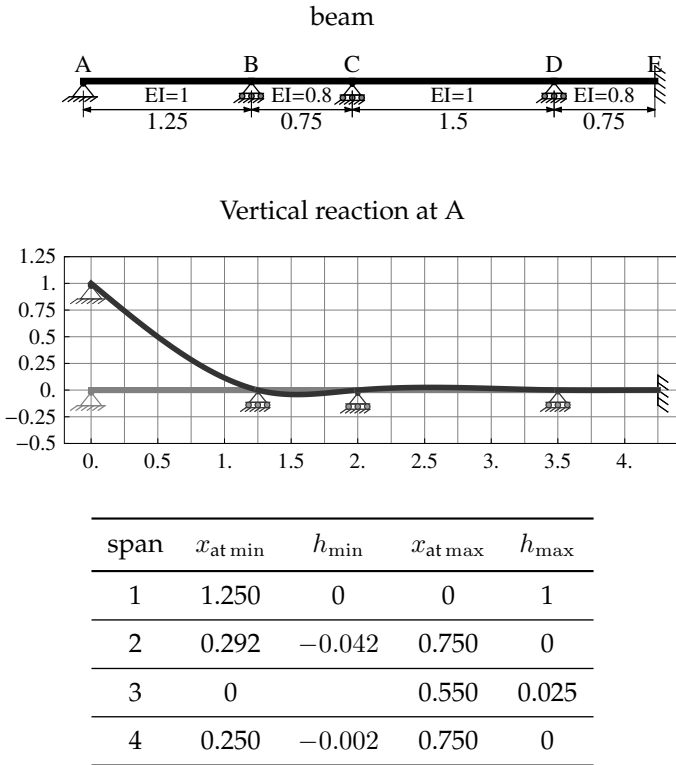
Figure 4.34. Influence lines for the vertical force reactions in a case where the beams have different span and different sectional properties. *(Continued below.)*

relatively accurate approximations of maxima, minima and their locations.

Again considering figure 4.34, we next describe how to approximately construct the influence line for the vertical reaction at B where there is an internal support. For that influence line, we start by isolating the two beams AB and BC together with a rotary springs at end C and a hinge at end A. We estimate the stiffness factor C to be 0.625. Based on the patterns identified in figures 4.25, we may approximately sketch the influence line in the segment between A and C. In that segment, we also determine that the maximum influence is about 1.053 which is very close to the exact value of 1.064 Next we calculate the slope C using formula 4.7b which gives a value of 0.977. This slope is then used as imposed value on the transition members on the right. For member CD on the right, the rotary stiffness factor is 1.6 at D which using formula 4.18

Vertical reaction at B
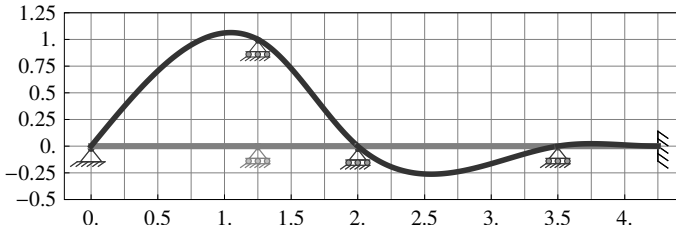
span	$x_{\text{at min}}$	h_{min}	$x_{\text{at max}}$	h_{max}
1	0	0	1.047	1.064
2	0.750	0	0	1
3	0.550	-0.262	1.500	0
4	0	0	0.250	0.023

Vertical reaction at C
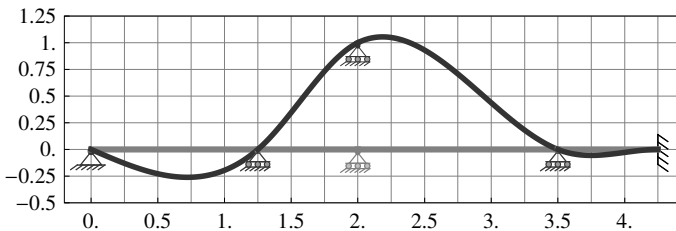
span	$x_{\text{at min}}$	h_{min}	$x_{\text{at max}}$	h_{max}
1	0.722	-0.261	1.250	0
2	0	0	0.750	1
3	1.500	0	0.187	1.055
4	0.250	-0.056	0.750	0

Figure 4.34. *(Continued from above and continued below.)*

Vertical reaction at D
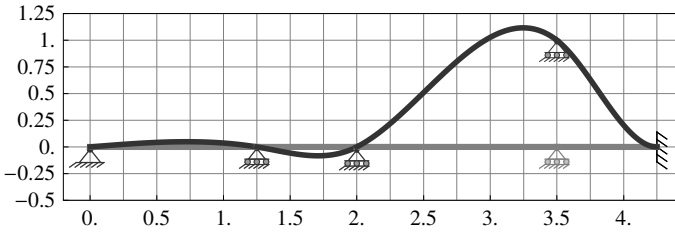
span	$x_{at\,min}$	h_{min}	$x_{at\,max}$	h_{max}
1	0	0	0.722	0.049
2	0.458	−0.083	0.750	0
3	0	0	1.248	1.116
4	0.750	0	0	1

Vertical reaction at E
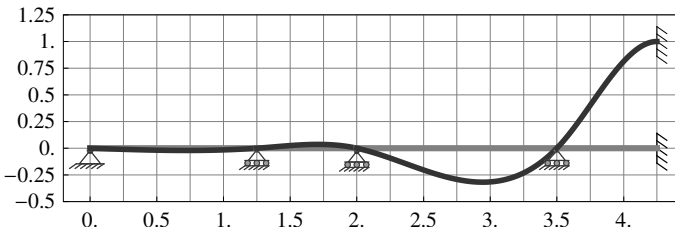
span	$x_{at\,min}$	h_{min}	$x_{at\,max}$	h_{max}
1	0.722	−0.021	1.250	0
2	0	0	0.458	0.036
3	0.944	−0.318	1.500	0
4	0	0	0.750	1

Figure 4.34. *(Continued from above.)* Influence lines for the vertical force re-actions in a case where the beams have different span and different sectional properties.

gives a maximum value of $0.977 * 1.5(0.19 + 0.15 * 1.6)/(1 + 1.6) \approx 0.242$. This compares well with the exact value of 0.262 which gives an error of 7.6%. In regards to the location of the maximum, formula 4.19 gives a value of 0.547 from the location of the imposed slope which is point C. This value again compares well with the exact value of 0.550 corresponding to an error of 0.55%. Next we use formula 4.17 to get the slope at D which gives a value of 0.188. This slope is then applied at D on member DE to sketch that member and to complete the influence line. This sketch of the influence line includes relatively accurate approximations of maxima, minima and their locations.

4.3.7 Examples of Sketching Influence Lines for Shear Forces

In this section, we will present examples of sketching the influence lines for shear forces. The results in the figures shown are exact results and we will describe how the discussions and approximations developed in previous sections allow us to approximately sketch those influence lines. For simplicity, we will start with examples where all the spans are equal and have the same sectional properties as shown in figure 4.35. As a specific example, we will consider the influence lines for the shear force at point D. The rest of the cases shown in figure 4.35 may be similarly analyzed and are left as an exercise for the reader.

Considering figure 4.35, we describe how to approximately construct the influence line for the shear force at D. For that influence line, we start by isolating member CE which is the member containing the influence point D. For that member CE, we estimate the rotary stiffness factors at C and E to be 0.75 and 1 respectively. Next, using formula 4.8a and b we calculate the values before and after the influence point D to be 0.514 and 0.486 respectively. These values have an error of 1.18% and 1.22% respectively compared with the exact result shown in a table near the corresponding figure for the influence line at span 2 which is member CE (*ie.* second span from the left). With these values and figures 4.27 and 4.28 as a guide, we can sketch the influence line for member CE. To proceed further, we calculate the slopes at C and E using formula 4.9a and b which give the values of 0.692 and 0.577 respectively. These slopes are then used as imposed values on transition members on the left and the right. For member AC on the left, the rotary stiffness factor is zero at A which using formula 4.18 gives a maximum value of $0.19 \times 0.692 \approx 0.131$ which is, to the specified precision, the exact result. The location of that maximum is calculated using formula 4.19 which gives a value of 0.42 from the location of the imposed slope which is point C or equivalently $1 - 0.42 = 0.57$ from point A. This value again compares well with the

beam

Shear force at B

span	$x_{\text{at min}}$	h_{min}	$x_{\text{at max}}$	h_{max}
1	0.300	-0.373	0.300	0.627
2	0.380	-0.079	1	0
3	0	0	0.377	0.021
4	0.333	-0.005	1	0
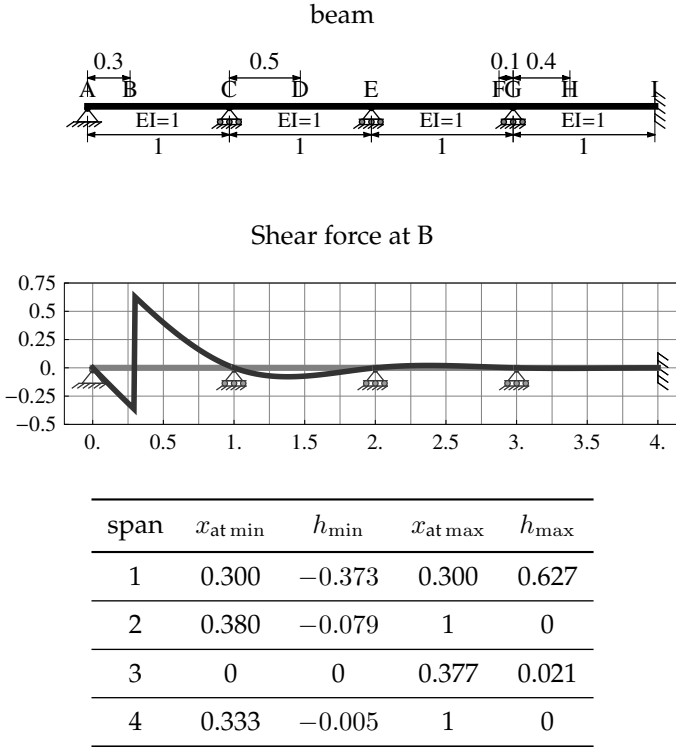
Figure 4.35. Influence lines for the shear forces in a case where all beams have the same span and the same sectional properties. *(Continued below.)*

exact value of 0.577 corresponding to an error of only 1.21%. With this information, we can then sketch the influence line for the member AC. Next we consider the member on the right of the isolated member CE which is member EG. Again we use the transition member shown in figure 4.32 with an applied slope obtained above as 0.577 at point E and we estimate the rotary stiffness factor at G to be 1. Using formulas 4.18 and 4.19, we obtain the maximum influence value and location to be 0.098 and 0.375 respectively which compare well with the exact results of 0.104 (*ie.* 5.8% error) and 0.377 (*ie.* 0.53% error) respectively. To finish with member EG, we obtain the slope at G using formula 4.17 which gives a value of about 0.14. Based on these calculations for member EG, we can quantitatively sketch its influence line using figure 4.32 as a guide (also see chapter 1). The influence line of the last member GI may be similarly sketched using the imposed slope of 0.14 at point G, figure 4.32 as

Shear force at D
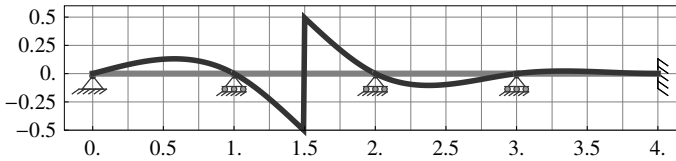
span	$x_{\text{at min}}$	$h_{\min}$	$x_{\text{at max}}$	$h_{\max}$
1	0	0	0.577	0.131
2	0.500	-0.508	0.500	0.492
3	0.377	-0.104	1	0
4	0	0	0.333	0.023

Shear force at F
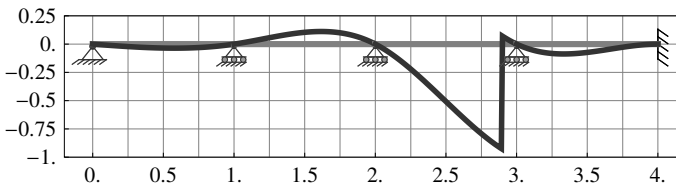
span	$x_{\text{at min}}$	$h_{\min}$	$x_{\text{at max}}$	$h_{\max}$
1	0.577	-0.036	1	0
2	0	0	0.616	0.111
3	0.900	-0.930	0.900	0.070
4	0.333	-0.087	1	0

Figure 4.35. *(Continued from above and continued below.)*

Shear force at H
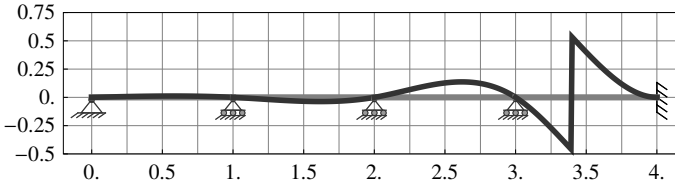
span	$x_{at\,min}$	h_{min}	$x_{at\,max}$	h_{max}
1	0	0	0.577	0.012
2	0.616	-0.037	1	0
3	0	0	0.619	0.137
4	0.400	-0.468	0.400	0.532

Shear force at I
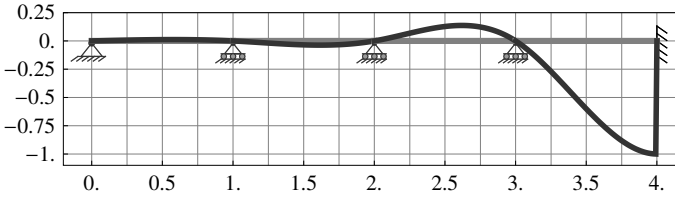
span	$x_{at\,min}$	h_{min}	$x_{at\,max}$	h_{max}
1	0	0	0.577	0.012
2	0.616	-0.037	1	0
3	0	0	0.619	0.137
4	1.000	-1.000	1	0

Figure 4.35. *(Continued from above.)* Influence lines for the shear forces in a case where all beams have the same span and the same sectional properties.

a guide with $k \to \infty$ and with the formulas associated with that figure. This then would complete the whole sketch of the influence line for the shear force at D. This sketch includes relatively accurate approximations of maxima, minima and their locations.

Next we consider the beam shown in figure 4.36 where the spans are nonequal and the sectional properties are different. As specific examples, we will consider the influence line for the shear forces at B+ and at F. The rest of the cases may be similarly analyzed and are left as an exercise for the reader.

Considering figure 4.36, we first describe how to approximately construct the influence line for the shear force at a point just to the right of point B which we refer to as point B+. For that influence line, we start by isolating member BC which is the member containing the influence point B+. For that member BC, we estimate the rotary stiffness factors

span	$x_{\text{at min}}$	h_{min}	$x_{\text{at max}}$	h_{max}
1	1.250	−1.000	1.250	0
2	0.292	−0.042	0.750	0
3	0	0	0.550	0.025
4	0.250	−0.002	0.750	0
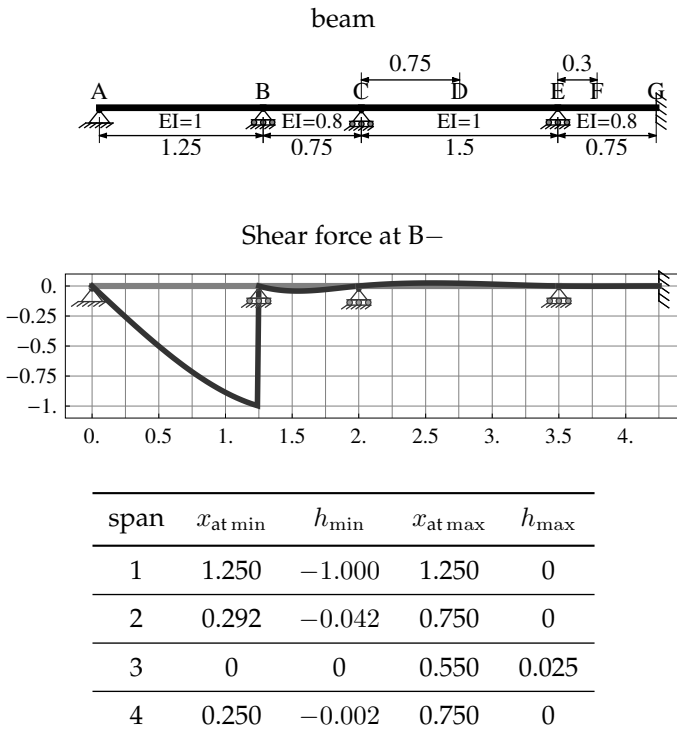
Figure 4.36. Influence lines for the shear forces in a case where the beams have different span and different sectional properties. *(Continued below.)*

Shear force at B+
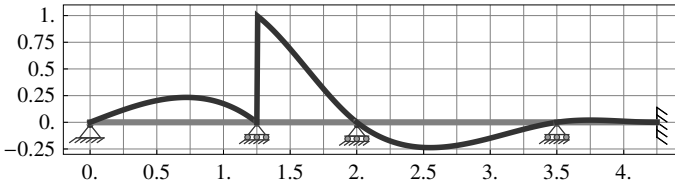
span	$x_{\text{at min}}$	h_{min}	$x_{\text{at max}}$	h_{max}
1	0	0	0.722	0.233
2	0	0	0.000	1.000
3	0.550	-0.237	1.500	0
4	0	0	0.250	0.021

Shear force at D
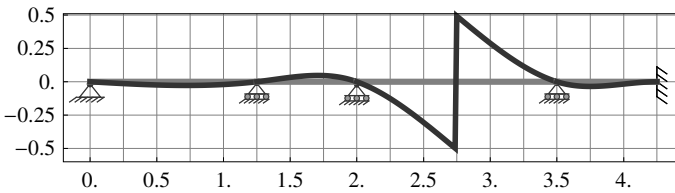
span	$x_{\text{at min}}$	h_{min}	$x_{\text{at max}}$	h_{max}
1	0.722	-0.028	1.250	0
2	0	0	0.458	0.047
3	0.750	-0.508	0.750	0.492
4	0.250	-0.035	0.750	0

Figure 4.36. *(Continued from above and continued below.)*

Shear force at F
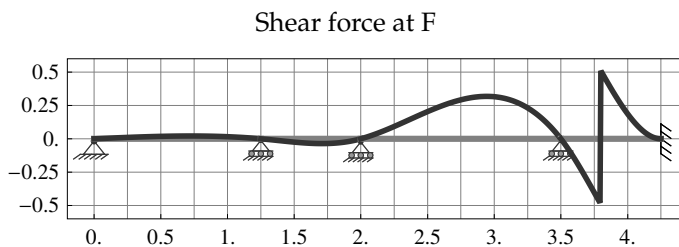
span	$x_{\text{at min}}$	h_{min}	$x_{\text{at max}}$	h_{max}
1	0	0	0.722	0.021
2	0.458	−0.036	0.750	0
3	0	0	0.944	0.318
4	0.300	−0.490	0.300	0.509
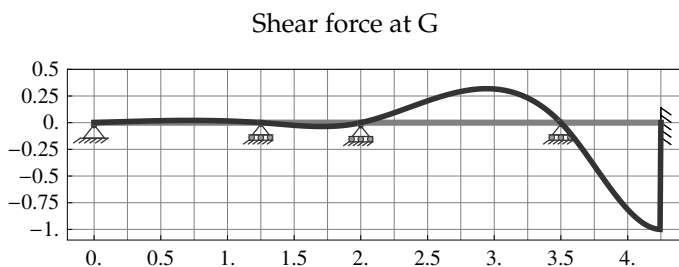
Shear force at G

span	$x_{\text{at min}}$	h_{min}	$x_{\text{at max}}$	h_{max}
1	0	0	0.722	0.021
2	0.458	−0.036	0.750	0
3	0	0	0.944	0.318
4	0.750	−1.000	0.750	0

Figure 4.36. *(Continued from above.)* Influence lines for the shear forces in a case where the beams have different span and different sectional properties.

at B and C to be 0.563 and 0.625 respectively. Next, either based on kinematic constraints or using formula 4.8a and b we identify the values before and after the influence point D to be 0 and 1 respectively which are the same as the exact results. With these values and figures 4.28d as a guide, we can sketch the influence line for member BC. From the estimates of the rotary stiffness factors at B and C, we may use formula 4.9a to calculate estimates of the slopes B and C which give 0.983 and 0.928 respectively. Those slopes are applied on the neighboring members AB and CD respectively using the transition model of figure 4.32. Starting with member AB, we have the rotary stiffness factor at the left equal zero because of the hinge at the end. Using formula 4.18 with the applied slope of 0.983 at B, we obtain the maximum influence value as 0.233 which is the exact result up to the precision of the calculations. As for the location of that maximum value, formula 4.19 gives a value of 0.525 from point B which is $(1.25 - 0.525) = 0.725$ from point A and is very close to the exact result of 0.722. At this point, we use the calculated values to sketch the influence line for member AB using figure 4.32 as a guide (also see chapter 1). Next we consider member CE as a transition member with an applied slope of 0.928 at C and a spring with rotary stiffness factor of 1.6 at E. Using formulas 4.18 and 4.19, we get the magnitude and location of the maximum influence value to be 0.230 and 0.547 respectively which are very close to the exact results of 0.237 (*ie.* about 2.5% error) and 0.550 (*ie.* about 0.55% error) respectively. With these values, member CE can be sketched using figure 4.32 as a guide (also see chapter 1). Considering member CE, we can also calculate the slope at E using 4.17 which gives a slope of 0.178 at point E. This slope is then imposed at point E of member EG with the model of figure 4.32 in order to calculate values and to sketch the influence line for member EG. This then completes the sketch for the whole influence line for the shear force at point B+ and includes relatively accurate approximations of maxima, minima and their locations.

Again considering figure 4.36, we next describe how to approximately construct the influence line for the shear force at F. For that influence line, we start by isolating member EG which is the member containing the influence point F. For that member EG, we estimate the rotary stiffness factor at the left to be 0.625 while that at the right is infinite due to the fixed end. Next we use formula 4.8a and b to calculate the values before and after the influence point F which we find to be 0.485 and 0.515 respectively. These values compare well with the exact values of 0.490 (*ie.* about 1.02% error) and 0.509 (*ie.* about 1.18% error) respectively. With these values and figures 4.27 and 4.28 as a guide, we can sketch the influence line for member EG. With the same isolated member EG, we may use formula 4.9a to calculate estimates of the slope at E which gives

a slope of 1.23. This slope is applied on the neighboring member CE at point E using the transition model of figure 4.32 and we estimate of the rotary spring factor at point C to be 1.6. Using formulas 4.18 and 4.19, we get the magnitude and location of the maximum influence value to be 0.305 and 0.547 from the right end (*ie.* 0.953 from the left end) respectively which are very close to the exact results of 0.318 (*ie.* about 4.1% error) and 0.944 (*ie.* about 0.95% error) respectively. Based on these calculations, we can quantitatively sketch the influence line for member CE using figure 4.32 as a guide (also see chapter 1). Finally, using formula 4.17, we calculate the slope at C to be about 0.237. This slope is then applied on member BC which is again modeled as a transition member like the one shown in figure 4.32. Once we finish with member BC, we get the slope at B and sketch member AB in a similar manner which then completes the whole sketch of the influence line for the shear force at F. This sketch includes relatively accurate approximations of maxima, minima and their locations.

4.3.8   Examples of Sketching Influence Lines for Bending Moments

In this section, we will present examples of sketching the influence lines for bending moments. The results in the figures shown are exact results and we will describe how the discussions and approximations developed in previous sections allow us to approximately sketch those influence lines. For simplicity, we will start with examples where all the spans are equal and have the same sectional properties as shown in figure 4.37. As a specific example, we will consider the influence lines for the bending moment at point F. The rest of the cases shown in figure 4.37 may be similarly analyzed and are left as an exercise for the reader.

Considering figure 4.37, we describe how to approximately construct the influence line for the shear force at F. For that influence line, we start by isolating member EG which is the member containing the influence point F. For that member EG, we estimate the rotary stiffness factors at E and G to be both equal to one. Next, using formula 4.12, we calculate the value of the maximum positive value which always occurs at the point of influence to be 0.048 which, up to the precision used, is the exact result. At this point, we have to determine the shape pattern of the influence line over that member. We may do that by checking each of formulas 4.10 and 4.11a and b where we find that condition 4.11b is true which implies that the pattern of deformation is that of figure 4.29c. This also means that we need to calculate the value and location of the minimum (*ie.* lowermost negative value). We do this using formulas 4.14 and 4.15 which give 0.025 and 0.475 respectively. We compare these values with the exact

beam

Bending moment at B

span	$x_{\text{at min}}$	h_{min}	$x_{\text{at max}}$	h_{max}
1	0	0	0.300	0.188
2	0.380	−0.024	1	0
3	0	0	0.377	0.006
4	0.333	−0.001	1	0
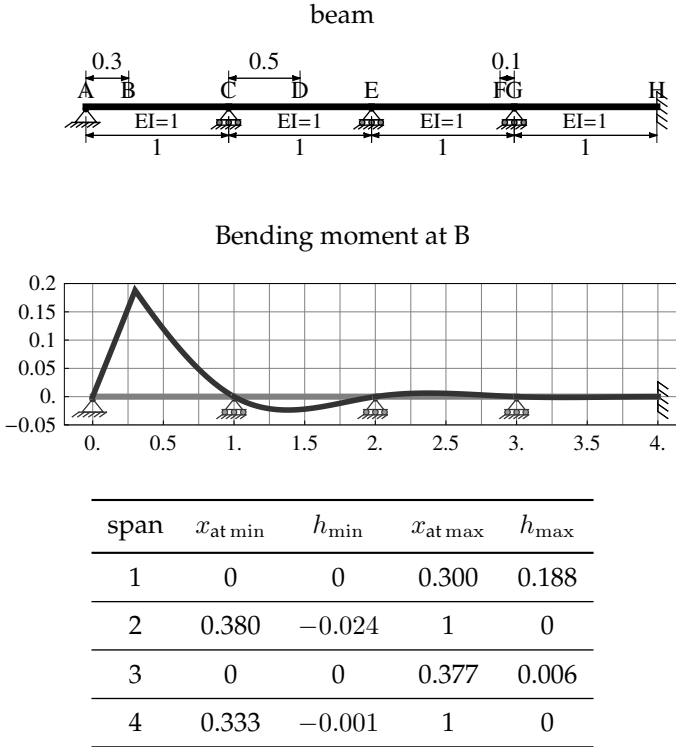
Figure 4.37. Influence lines for the bending moments in a case where all beams have the same span and the same sectional properties. *(Continued below.)*

results which are 0.035 (*ie.* about 28.6% error) and 0.467 (*ie.* about 1.71% error). While the error in the minimum value is appreciable, it is suffi-cient for an approximate analysis and the overall pattern of the influence line for member EG is still well-represented. At this point, we may sketch the influence line for member EG using the calculated values and either figure 4.29c or figure 4.31b as a guide. To proceed further, we calculate the slopes at E and G using formula 4.16a and b which give the values of 0.073 and 0.407 respectively. These slopes are then used as imposed values on transition members on the left and the right. For member GH on the right, the rotary stiffness factor is infinity at H because of the fixed end. Using formula 4.18 and 4.19 with the imposed slope of 0.407, we get a maximum value and location of 0.061 and 0.33 respectively which compare well with the exact results of 0.060 (*ie.* about 1.67% error) and 0.333 (*ie.* about 0.91% error) respectively. Based on these calculations for

Bending moment at D
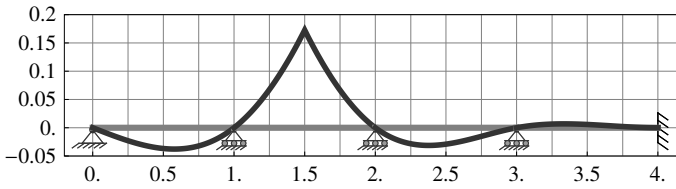
span	$x_{\text{at min}}$	h_{min}	$x_{\text{at max}}$	h_{max}
1	0.577	−0.038	1	0
2	0	0	0.500	0.173
3	0.377	−0.031	1	0
4	0	0	0.333	0.007

Bending moment at F
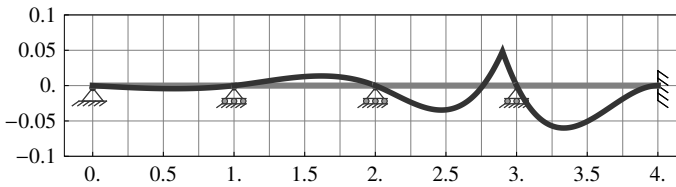
span	$x_{\text{at min}}$	h_{min}	$x_{\text{at max}}$	h_{max}
1	0.577	−0.004	1	0
2	0	0	0.616	0.014
3	0.467	−0.035	0.900	0.048
4	0.333	-0.060	1	0

Figure 4.37. *(Continued from above and continued below.)*

member GH, we can quantitatively sketch its influence line using fig-
ure 4.32 as a guide (also see chapter 1). For member CE on the left of
the member with the influence point, we have an imposed slope of 0.073
and we estimate the stiffness factor at point C to be 1. Using formula 4.18
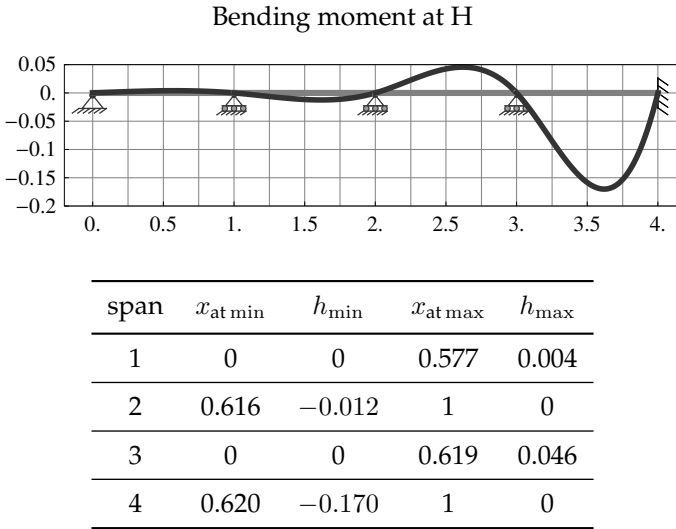
Bending moment at H

span	$x_{at\,min}$	h_{min}	$x_{at\,max}$	h_{max}
1	0	0	0.577	0.004
2	0.616	−0.012	1	0
3	0	0	0.619	0.046
4	0.620	−0.170	1	0

Figure 4.37. *(Continued from above.)* Influence lines for the bending moments in a case where all beams have the same span and the same sectional properties.

and 4.19 for member CE, we get a maximum value and location of 0.012 and 0.375 from the right (*ie.* 0.625 from the left) respectively which compare well with the exact results of 0.014 (*ie.* about 14.3% error) and 0.616 from the left (*ie.* about 1.46% error) respectively. Based on these calculations for member CE, we can quantitatively sketch its influence line using figure 4.32 as a guide (also see chapter 1). To finish with member CE, we obtain the slope at C using formula 4.17 which gives a value of about 0.018. This slope is imposed on member AC at point A and allows us to calculate basic values for member AC and to sketch its influence line. This then would complete the whole sketch of the influence line for the bending moment at F. This sketch includes relatively accurate approximations of maxima, minima and their locations.

Next we consider the beam shown in figure 4.38 where the spans are nonequal and the sectional properties are different. As specific examples, we will consider the influence line for the bending moments at B and at C. The rest of the cases may be similarly analyzed and are left as an exercise for the reader.

Considering figure 4.38, we first describe how to approximately construct the influence line for the bending moment at point B. Unlike the case for the influence line for the shear force, the influence lines for the points just before and just after point B are the same because the bending
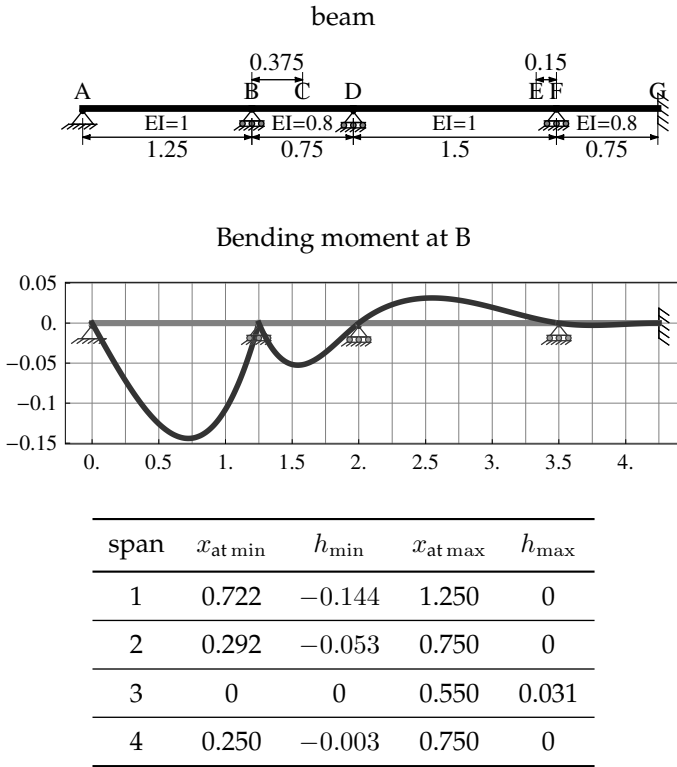
Figure 4.38. Influence lines for the bending moments in a case where the beams have different span and different sectional properties. *(Continued below.)*

moment unlike the shear force is continuous across an external hinge or roller support. For that influence line, we may start by isolating either member AB or member BD because they both contain the influence point B. In this discussion, we will start by isolating member AB and we estimate the rotary stiffness factor at point B to be $(0.8/0.75)/(1/1.25) \approx$ 1.33. The rotary stiffness factor at point A is zero due to the hinge support at the end of the whole beam. Using formula 4.12 or simply kinematic constraint, we determine the value of the maximum positive value to be zero since the influence point is right at the support. Also, by checking each of formulas 4.10 and 4.11a and b, we find that condition 4.11b is true which implies that the pattern of deformation is that of figure 4.29c. In fact, it is a limiting pattern of 4.29c when the maximum posiive value is zero such as in figure 4.31d but with the influence point at the right rather than on the left support. Therefore, to sketch the influence line of member AB, we must calculate the magnitude and location of the

Bending moment at C
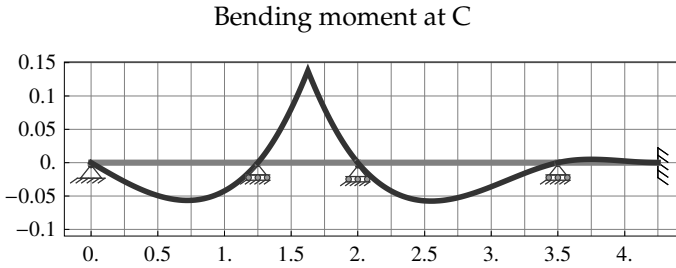
span	$x_{\text{at min}}$	h_{min}	$x_{\text{at max}}$	h_{max}
1	0.722	−0.057	1.250	0
2	0	0	0.375	0.138
3	0.550	−0.058	1.500	0
4	0	0	0.250	0.005
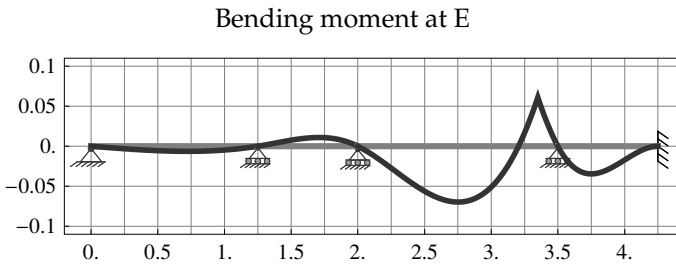
Bending moment at E

span	$x_{\text{at min}}$	h_{min}	$x_{\text{at max}}$	h_{max}
1	0.722	−0.006	1.250	0
2	0	0	0.458	0.011
3	0.753	−0.070	1.350	0.061
4	0.250	−0.035	0.750	0

Figure 4.38. *(Continued from above and continued below.)*
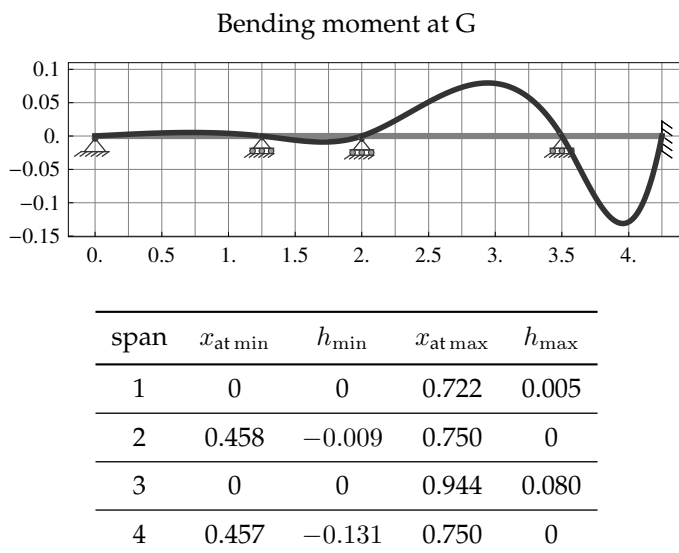
Bending moment at G

span	$x_{\text{at min}}$	h_{min}	$x_{\text{at max}}$	h_{max}
1	0	0	0.722	0.005
2	0.458	−0.009	0.750	0
3	0	0	0.944	0.080
4	0.457	−0.131	0.750	0

Figure 4.38. *(Continued from above.)* Influence lines for the bending moments in a case where the beams have different span and different sectional properties.

minimum over that member. Using formulas 4.14 and 4.15, we calculate those values to be 0.143 and 0.725 respectively. These values compare well with the exact results which are 0.144 (*ie.* about 0.69% error) and 0.722 (*ie.* about 0.42% error). At this point, we use the calculated values to sketch the influence line for member AB using figure 4.29c and figures 4.31 as a guide. To proceed further, we use formula 4.16b to calculate the slope at B to be 0.361. Note that there are two slopes at B due to the kink and that the calculated slope is to the right of point B which is the slope to be imposed on the member attached to the right of B. That member is BD which is modeled as a transition member with the rotary stiffness factor at D estimated as $(1/1.5)/(0.8/0.75) \approx 0.625$. With that value of stiffness factor and an imposed slope at B of 0.361, we use formulas 4.18 and 4.19 to get the magnitude and location of the maximum influence in member BD to be 0.047 and 0.289 respectively. These values are close to the exact results of 0.053 (*ie.* about 11.3% error) and 0.292 (*ie.* about 1.03% error) respectively. With these values, member BD can be sketched using figure 4.32 as a guide (also see chapter 1). Considering member BD, we can also calculate the slope at D using 4.17 which gives a slope of 0.111. This slope is then imposed at point D of member DF with the model of figure 4.32 in order to calculate values and to sketch the influence line for member DF. A similar procedure is again done for to

calculate basic values and to sketch the final member FG. This then completes the sketch for the whole influence line for the bending moment at B and includes relatively accurate approximations of maxima, minima and their locations.

Again considering figure 4.38, we next describe how to approximately construct the influence line for the bending moment at C. For that influence line, we start by isolating member BD which is the member containing the influence point C. For that member BD, we estimate the rotary stiffness factor at the left and right to be 0.75 and 0.625 respectively. Next, using formula 4.12, we calculate the value of the maximum positive value which always occurs at the point of influence to be 0.133 which compares well with the exact value of 0.138 (*ie.* about 3.6%). At this point, we have to determine the shape pattern of the influence line over that member. We may do that by checking each of formulas 4.10 and 4.11a and b where we find that condition 4.10 is true which implies that the pattern of deformation is that of figure 4.29a. This also means that there are no negative values and we can proceed to sketch the influence line over that member using figure 4.29a, figures 4.30 and figures 4.31 as a guide. To proceed further, we calculate the slopes at B and D using formula 4.16a and b which give the values of 0.205 and 0.217 respectively. These slopes are then used as imposed values on transition members on the left and the right. For member AB on the left, the rotary stiffness factor at B is zero because of the free hinged end. Using formula 4.18 and 4.19 with the imposed slope of 0.205, we get a maximum value and location of 0.049 and 0.525 from the right (*ie.* 0.725 from the left) respectively which compare well with the exact results of 0.057 (*ie.* about 14% error) and 0.722 (*ie.* about 0.42% error) respectively. Based on these calculations for member AB, we can quantitatively sketch its influence line using figure 4.32 as a guide (also see chapter1). For member DF on the left of the member with the influence point, we have an imposed slope of 0.217 and we estimate the stiffness factor at point F to be 1.6. Using formula 4.18 and 4.19 for member DF, we get a maximum value and location of 0.054 and 0.547 respectively which compare well with the exact results of 0.058 (*ie.* about 6.9% error) and 0.550 (*ie.* about 0.55% error) respectively. Based on these calculations for member CE, we can quantitatively sketch its influence line using figure 4.32 as a guide (also see chapter 1). To finish with member DF, we obtain the slope at C using formula 4.17 which gives a value of about 0.042. This slope is imposed on member FG at point F and allows us to calculate basic values for member FG and to sketch its influence line. This then would complete the whole sketch of the influence line for the bending moment at C. This sketch includes relatively accurate approximations of maxima, minima and their locations.

Appendix A

Beams—End-Moments and Inflection Points

A.1 Moment End-Loaded Beam
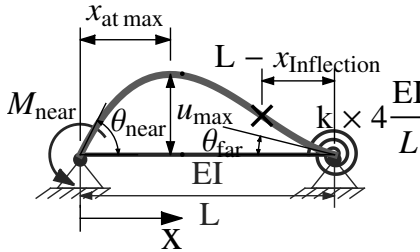
$$k_{\text{rotary spring stiffness at near}} = \frac{M_{\text{near}}}{\theta_{\text{near}}} = \frac{3 + 4k}{4 + 4k} \times 4 \times \frac{EI}{L}$$

$$\Leftrightarrow k_{\text{rotary stiffness factor at near}} = \frac{M_{\text{near}}}{4 \times \frac{EI}{L} \theta_{\text{near}}} = \frac{3 + 4k}{4 + 4k}$$

$$k_{\text{rotary spring stiffness at near}} = \frac{3\hat{x}_{\text{inflection}}}{6\hat{x}_{\text{inflection}} - 2}$$

$$\text{where:} \quad \hat{x}_{\text{inflection}} = \frac{x_{\text{inflection}}}{L} \quad (\text{for } 0 \leq \hat{x}_{\text{inflection}} \leq 1)$$

$$\text{carry-over-moment} = \frac{M_{\text{far}}}{M_{\text{near}}} = \frac{2k}{3 + 4k}$$

$$1 - \frac{x_{\text{inflection}}}{L} = \frac{2k}{3 + 6k}$$

$$\frac{\theta_{\text{far}}}{\theta_{\text{near}}} = \frac{1}{2+2k}$$

$$\frac{x_{\text{at max}}}{L} = \frac{3+4k-\sqrt{3+6k+4k^2}}{3+6k} \approx \frac{0.42+0.33k}{1+k}$$

$$\frac{EIu_{\text{max}}}{M_{\text{near}}L^2} = \frac{3\sqrt{3+6k+4k^2}+k(3+2k)\left(3+4k+2\sqrt{3+6k+4k^2}\right)}{27(1+2k)^2(3+4k)}$$

$$\frac{u_{\text{max}}}{\theta_{\text{near}}L} = \frac{3\sqrt{3+6k+4k^2}+k(3+2k)\left(3+4k+2\sqrt{3+6k+4k^2}\right)}{27(1+2k)^2(1+k)}$$

$$\approx \frac{0.19+0.15k}{1+k}$$

See table A.1.

Table A.1. Hinged Beam with Applied Moment at One End and Rotary Spring at Other.

k	$-\dfrac{M_{\text{far}}}{M_{\text{near}}}$	$\dfrac{M_{\text{near}}}{\theta_{\text{near}}4EI/L}$	$-\dfrac{\theta_{\text{far}}}{\theta_{\text{near}}}$	$1-\dfrac{x_{\text{infl}}}{L}$	$\dfrac{x_{\text{at max}}}{L}$	$\dfrac{u_{\text{max}}}{\theta_{\text{near}}L}$
0.000	0.000	0.750	0.500	0.000	0.423	0.192
0.500	0.200	0.833	0.333	0.167	0.392	0.176
0.750	0.250	0.857	0.286	0.200	0.384	0.172
1.000	0.286	0.875	0.250	0.222	0.377	0.168
1.500	0.333	0.900	0.200	0.250	0.368	0.164
2.000	0.364	0.917	0.167	0.267	0.362	0.161
3.000	0.400	0.938	0.125	0.286	0.355	0.158
4.000	0.421	0.950	0.100	0.296	0.350	0.156
∞	0.500	1.000	0.000	0.333	0.333	0.148

A.2   Uniformly Distributed Load

(a)   (b)   (c)
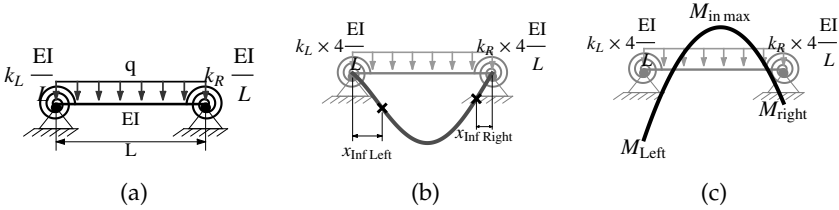
$$\frac{x_{\text{inf left}}}{L} = \frac{9 + 9k_R + 3k_L(5 + 4k_R)}{z}$$
$$- \frac{\sqrt{3}\sqrt{27(1+k_R)^2 + k_L^2(27 + 8k_R(5+2k_R)) + k_L(54 + 10k_R(9+4k_R))}}{z}$$
$$\approx \frac{0.92k_L}{3 + 4k_L} \qquad \text{where } z = 6\big(3 + 4k_R + 4k_L(1 + k_R)\big)$$

$$\frac{x_{\text{inf right}}}{L} = \frac{9 + 9k_R + 3k_L(5 + 4k_R)}{z}$$
$$+ \frac{\sqrt{3}\sqrt{27(1+k_R)^2 + k_L^2(27 + 8k_R(5+2k_R)) + k_L(54 + 10k_R(9+4k_R))}}{z}$$
$$\approx 1 - \frac{0.92k_R}{3 + 4k_R} \qquad \text{where } z = 6\big(3 + 4k_R + 4k_L(1 + k_R)\big)$$

$$\frac{M_{\text{left}}}{qL^2/8} = -\frac{4k_L(3 + 2k_R)}{9 + 12k_L + 12k_R + 12k_L\,k_R}$$

$$\frac{M_{\text{right}}}{qL^2/8} = -\frac{4(3 + 2k_L)k_R}{9 + 12k_L + 12k_R + 12k_L\,k_R}$$

$$\frac{M_{\text{in max}}}{qL^2/8} = \frac{27(1+k_R)^2 + k_L^2(27 + 8k_R(5+2k_R)) + k_L(54 + 10k_R(9+4k_R))}{3(3+4k_R+4k_L(1+k_R))^2}$$
$$\approx \left(1 - \frac{0.92k_L}{3 + 4k_L} - \frac{0.92k_R}{3 + 4k_R}\right)^2$$

$$EI \times \frac{\theta_{\text{near}}}{qL^3} = -\frac{6 + k_R}{144 + 48k_L + 48k_R + 12k_L\,k_R}$$
$$EI \times \frac{\theta_{\text{far}}}{qL^3} = \frac{6 + k_L}{144 + 48k_L + 48k_R + 12k_L\,k_R}$$

See tables A.2 through A.4.

Table A.2. Uniformly Loaded Beam: Symmetric Spring Resistance.

k	x_{Infl}/L at left	$1 - x_{\mathsf{Inf}}/L$ at right	$-M_{\mathsf{left}}/\frac{PL}{4}$	$-M_{\mathsf{right}}/\frac{PL}{4}$	$M_{\mathsf{in\ max}}/\frac{PL}{4}$
0.000	0.000	0.000	0.000	0.000	1.000
0.500	0.092	0.092	0.333	0.333	0.667
0.750	0.113	0.113	0.400	0.400	0.600
1.000	0.127	0.127	0.444	0.444	0.556
1.500	0.146	0.146	0.500	0.500	0.500
2.000	0.158	0.158	0.533	0.533	0.467
3.000	0.173	0.173	0.571	0.571	0.429
∞	0.211	0.211	0.667	0.667	0.333

Table A.3. Uniformly Loaded Beam: One End Hinged.

k	x_{Infl}/L at left	$1 - x_{\mathsf{Inf}}/L$ at right	$-M_{\mathsf{left}}/\frac{PL}{4}$	$-M_{\mathsf{right}}/\frac{PL}{4}$	$M_{\mathsf{in\ max}}/\frac{PL}{4}$
0.000	0.000	0.000	0.000	0.000	1.000
0.500	0.000	0.100	0.000	0.400	0.810
0.750	0.000	0.125	0.000	0.500	0.766
1.000	0.000	0.143	0.000	0.571	0.735
1.500	0.000	0.167	0.000	0.667	0.694
2.000	0.000	0.182	0.000	0.727	0.669
3.000	0.000	0.200	0.000	0.800	0.640
∞	0.000	0.250	0.000	1.000	0.563

Table A.4. Uniformly Loaded Beam: One End Fixed.
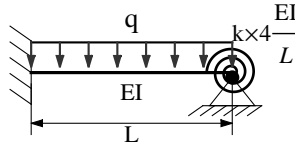
k	x_{Infl}/L at left	$1-x_{\text{Inf}}/L$ at right	$-M_{\text{left}}/\frac{PL}{4}$	$-M_{\text{right}}/\frac{PL}{4}$	$M_{\text{in max}}/\frac{PL}{4}$
0.000	0.250	0.000	1.000	0.000	0.563
0.500	0.240	0.073	0.889	0.222	0.472
0.750	0.236	0.094	0.857	0.286	0.449
1.000	0.234	0.109	0.833	0.333	0.432
1.500	0.230	0.130	0.800	0.400	0.410
2.000	0.227	0.144	0.778	0.444	0.396
3.000	0.223	0.161	0.750	0.500	0.379
∞	0.211	0.211	0.667	0.667	0.333

A.3   Point Force

(a)   (b)   (c)
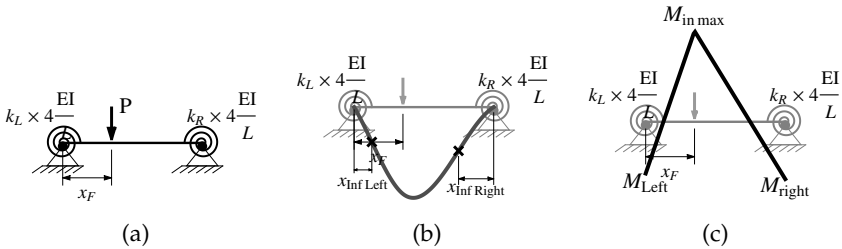
$$\hat{x}_F = x_F/L$$

$$\frac{x_{\text{inf left}}}{L} = \frac{2k_L\,\hat{x}_F\,(2+2k_R-(1+2k_R)\hat{x}_F)}{3+4k_L+4k_R+4k_L\,k_R+(4k_L-2k_R+4k_L\,k_R)\hat{x}_F-(2k_L+2k_R+8k_L\,k_R)\hat{x}_F^2}$$
$$\approx \frac{3k_L\,\hat{x}_F}{(2+4k_L)(1+\hat{x}_F)}$$

$$\frac{x_{\text{inf right}}}{L} = \frac{3+4k_R+(6k_L+8k_L\,k_R)\hat{x}_F-(2k_L+4k_L\,k_R)\hat{x}_F^2}{3+6k_R+(6k_L+12k_L\,k_R)\hat{x}_F-(2k_L+2k_R+8k_L\,k_R)\hat{x}_F^2}$$
$$\approx 1-\frac{3k_R(1-\hat{x}_F)}{(2+4k_R)(2-\hat{x}_F)}$$

$$\frac{M_{\text{left}}}{PL/4} = -\frac{8k_L(1-\hat{x}_F)\hat{x}_F(2+2k_R-(1+2k_R)\hat{x}_F)}{3+4k_L+4k_R+4k_L\,k_R}$$

$$\frac{M_{\text{right}}}{PL/4} = -\frac{8k_R(1-\hat{x}_F)\hat{x}_F(1+\hat{x}_F+2k_L\,\hat{x}_F)}{3+4k_L+4k_R+4k_L\,k_R}$$

$$\frac{M_{\text{in max}}}{PL/4} = \frac{4(1-\hat{x}_F)\hat{x}_F\left(3+4k_R+(6k_L-2k_R+8k_L\,k_R)\hat{x}_F-(2k_L+2k_R+8k_L\,k_R)\hat{x}_F^2\right)}{3+4k_L+4k_R+4k_L\,k_R}$$

$$EI \times \frac{\theta_{\text{near}}}{PL^2} = -\frac{(1-\hat{x}_F)\hat{x}_F(2+2k_R-(1+2k_R)\hat{x}_F)}{6+8k_L+8k_R+8k_L\,k_R}$$

$$EI \times \frac{\theta_{\text{far}}}{PL^2} = \frac{(1-\hat{x}_F)\hat{x}_F(1+\hat{x}_F+2k_L\,\hat{x}_F)}{6+8k_L+8k_R+8k_L\,k_R}$$

See tables A.5 through A.13.

Table A.5. Point Force on a Beam: Symmetric Spring Resistance.

k	x_{Infl}/L at left	$1-x_{\text{Inf}}/L$ at right	$-M_{\text{left}}/\frac{PL}{4}$	$-M_{\text{right}}/\frac{PL}{4}$	$M_{\text{in max}}/\frac{PL}{4}$
0.000	0.000	0.000	0.000	0.000	0.750
0.500	0.076	0.155	0.234	0.141	0.539
0.750	0.092	0.186	0.288	0.163	0.494
1.000	0.103	0.206	0.325	0.175	0.463
1.500	0.118	0.231	0.375	0.188	0.422
2.000	0.127	0.245	0.407	0.193	0.396
3.000	0.137	0.262	0.446	0.196	0.366
∞	0.167	0.300	0.563	0.188	0.281

Table A.6. Point Force on a Beam: Symmetric Spring Resistance.

k	x_{Infl}/L at left	$1 - x_{\text{Inf}}/L$ at right	$-M_{\text{left}}/\frac{PL}{4}$	$-M_{\text{right}}/\frac{PL}{4}$	$M_{\text{in max}}/\frac{PL}{4}$
0.000	0.000	0.000	0.000	0.000	1.000
0.500	0.125	0.125	0.250	0.250	0.750
0.750	0.150	0.150	0.300	0.300	0.700
1.000	0.167	0.167	0.333	0.333	0.667
1.500	0.188	0.188	0.375	0.375	0.625
2.000	0.200	0.200	0.400	0.400	0.600
3.000	0.214	0.214	0.429	0.429	0.571
∞	0.250	0.250	0.500	0.500	0.500

Table A.7. Point Force on a Beam: Symmetric Spring Resistance.
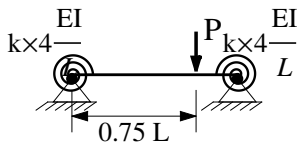
k	x_{Infl}/L at left	$1 - x_{\text{Inf}}/L$ at right	$-M_{\text{left}}/\frac{PL}{4}$	$-M_{\text{right}}/\frac{PL}{4}$	$M_{\text{in max}}/\frac{PL}{4}$
0.000	0.000	0.000	0.000	0.000	0.750
0.500	0.155	0.076	0.141	0.234	0.539
0.750	0.186	0.092	0.163	0.288	0.494
1.000	0.206	0.103	0.175	0.325	0.463
1.500	0.231	0.118	0.188	0.375	0.422
2.000	0.245	0.127	0.193	0.407	0.396
3.000	0.262	0.137	0.196	0.446	0.366
4.000	0.271	0.144	0.197	0.470	0.348
∞	0.300	0.167	0.188	0.563	0.281

Table A.8. Point Force on a Beam: One End Hinged.
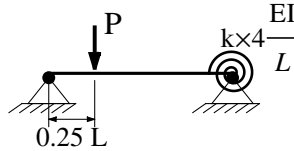
k	x_{Infl}/L at left	$1 - x_{Inf}/L$ at right	$-M_{left}/\frac{PL}{4}$	$-M_{right}/\frac{PL}{4}$	$M_{in\,max}/\frac{PL}{4}$
0.000	0.000	0.000	0.000	0.000	0.750
0.500	0.000	0.158	0.000	0.188	0.703
0.750	0.000	0.190	0.000	0.234	0.691
1.000	0.000	0.211	0.000	0.268	0.683
1.500	0.000	0.238	0.000	0.313	0.672
2.000	0.000	0.254	0.000	0.341	0.665
3.000	0.000	0.273	0.000	0.375	0.656
∞	0.000	0.319	0.000	0.469	0.633

Table A.9. Point Force on a Beam: One End Hinged.
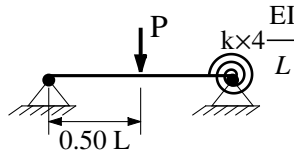
k	x_{Infl}/L at left	$1 - x_{Inf}/L$ at right	$-M_{left}/\frac{PL}{4}$	$-M_{right}/\frac{PL}{4}$	$M_{in\,max}/\frac{PL}{4}$
0.000	0.000	0.000	0.000	0.000	1.000
0.500	0.000	0.130	0.000	0.300	0.850
0.750	0.000	0.158	0.000	0.375	0.813
1.000	0.000	0.176	0.000	0.429	0.786
1.500	0.000	0.200	0.000	0.500	0.750
2.000	0.000	0.214	0.000	0.545	0.727
3.000	0.000	0.231	0.000	0.600	0.700
∞	0.000	0.273	0.000	0.750	0.625

Table A.10. Point Force on a Beam: One End Hinged.
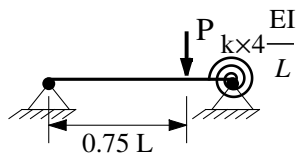
k	x_{Infl}/L at left	$1 - x_{Inf}/L$ at right	$-M_{left}/\frac{PL}{4}$	$-M_{right}/\frac{PL}{4}$	$M_{in\,max}/\frac{PL}{4}$
0.000	0.000	0.000	0.000	0.000	0.750
0.500	0.000	0.080	0.000	0.263	0.553
0.750	0.000	0.099	0.000	0.328	0.504
1.000	0.000	0.111	0.000	0.375	0.469
1.500	0.000	0.127	0.000	0.437	0.422
2.000	0.000	0.137	0.000	0.477	0.392
3.000	0.000	0.149	0.000	0.525	0.356
∞	0.000	0.179	0.000	0.656	0.258

Table A.11. Point Force on a Beam: One End Fixed.
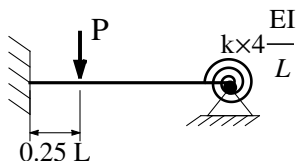
k	x_{Infl}/L at left	$1 - x_{Inf}/L$ at right	$-M_{left}/\frac{PL}{4}$	$-M_{right}/\frac{PL}{4}$	$M_{in\,max}/\frac{PL}{4}$
0.000	0.179	0.000	0.656	0.000	0.258
0.500	0.175	0.143	0.625	0.063	0.266
0.750	0.174	0.173	0.616	0.080	0.268
1.000	0.173	0.194	0.609	0.094	0.270
1.500	0.172	0.220	0.600	0.113	0.272
2.000	0.171	0.235	0.594	0.125	0.273
3.000	0.170	0.254	0.586	0.141	0.275
∞	0.167	0.300	0.562	0.188	0.281

Table A.12. Point Force on a Beam: One End Fixed.
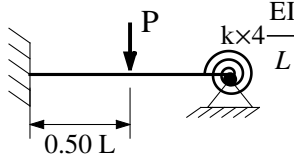
k	x_{Infl}/L at left	$1 - x_{\text{Inf}}/L$ at right	$-M_{\text{left}}/\frac{PL}{4}$	$-M_{\text{right}}/\frac{PL}{4}$	$M_{\text{in max}}/\frac{PL}{4}$
0.000	0.273	0.000	0.750	0.000	0.625
0.500	0.267	0.111	0.667	0.167	0.583
0.750	0.265	0.136	0.643	0.214	0.571
1.000	0.263	0.154	0.625	0.250	0.563
1.500	0.261	0.176	0.600	0.300	0.550
2.000	0.259	0.190	0.583	0.333	0.542
3.000	0.257	0.207	0.562	0.375	0.531
∞	0.250	0.250	0.500	0.500	0.500

Table A.13. Point Force on a Beam: One End Fixed.
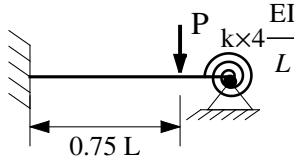
k	x_{Infl}/L at left	$1 - x_{\text{Inf}}/L$ at right	$-M_{\text{left}}/\frac{PL}{4}$	$-M_{\text{right}}/\frac{PL}{4}$	$M_{\text{in max}}/\frac{PL}{4}$
0.000	0.319	0.000	0.469	0.000	0.633
0.500	0.316	0.067	0.375	0.188	0.516
0.750	0.315	0.083	0.348	0.241	0.482
1.000	0.313	0.095	0.328	0.281	0.457
1.500	0.312	0.111	0.300	0.338	0.422
2.000	0.310	0.121	0.281	0.375	0.398
3.000	0.308	0.133	0.258	0.422	0.369
∞	0.300	0.167	0.187	0.563	0.281

Appendix B

Column—Shear Stiffness, End-Moments and Inflection Points

B.1 Cantilever
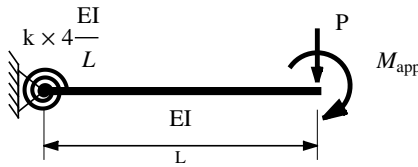
Deflection of a cantilever:

$$\delta = \left(\frac{1}{2} + \frac{1}{4k} \right) \frac{L^2}{EI} M_{\text{app}} + \left(\frac{1}{3} + \frac{1}{4k} \right) \frac{L^2}{EI} PL$$

Shear stiffness:

$$k_{\text{sh}} = \frac{4k}{\left((6k+3)\frac{M_{\text{app}}}{PL} + (4k+3) \right)} \frac{3EI}{L^3}$$

If $k = \infty$ (fixed support):

$$k_{\text{sh}} = \frac{4}{\left(6\frac{M_{\text{app}}}{PL} + 4 \right)} \frac{3EI}{L^3}$$

If $k = \infty$ (fixed support) and $M_{\text{app}} = 0$:

$$k_{\text{sh}} = \frac{3EI}{L^3}$$

B.2   Column for Single Story Building

hinge support   fixed support
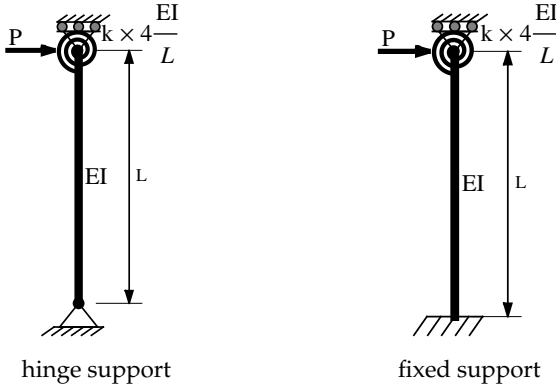
Shear stiffness:

$$k_{\text{sh}} = \begin{cases} \frac{4k}{(3+4k)} \frac{3EI}{L^3} & \text{(hinge support)} \\ \frac{(1+4k)}{(4+4k)} \frac{12EI}{L^3} & \text{(fixed support)} \\ 0 & \text{(roller support)} \end{cases}$$

Moment at top and bottom of column:

$$\begin{pmatrix} M_{\text{inner top}} \\ M_{\text{inner bottom}} \end{pmatrix} = \begin{pmatrix} \frac{2k}{1+4k} \\ -\frac{(1+2k)}{(1+4k)} \end{pmatrix} PL \quad \text{(fixed support)}$$

and

$$\begin{pmatrix} M_{\text{inner top}} \\ M_{\text{inner bottom}} \end{pmatrix} = \begin{pmatrix} 1 \\ 0 \end{pmatrix} PL \quad \text{(hinged support)}$$

Inflection point measured from the bottom:

$$x_I = \frac{(1+2k)}{(1+4k)} L \qquad \text{(fixed support)}$$

Note that in the above formulas, the inner bending moments $M_{\text{inner top}}$ and $M_{\text{inner bottom}}$ are considered to be positive when counterclockwise and clockwise respectively in conformance with standard conventions of bending moment diagrams.

Table of Results of Column with Hinge Support.

k	$k_{\text{shear}}/\left(EI/L^3\right)$
0	0.00
0.5	1.20
0.75	1.50
1	1.71
1.5	2.00
2	2.18
3	2.40
4	2.53
5	2.61
6	2.67
∞	3.00

Table of Results of Column with Fixed Support.

k	$k_{\text{shear}}/\left(EI/L^3\right)$	$M_{\text{bottom}}/(\text{PL})$	$M_{\text{top}}/(\text{PL})$	x_I/L
0	3.00	1.00	0.00	1.00
0.5	6.00	0.67	0.33	0.67
0.75	6.86	0.63	0.38	0.63
1	7.50	0.60	0.40	0.60
1.5	8.40	0.57	0.43	0.57
2	9.00	0.56	0.44	0.56
3	9.75	0.54	0.46	0.54
4	10.20	0.53	0.47	0.53
5	10.50	0.52	0.48	0.52
6	10.71	0.52	0.48	0.52
∞	12.00	0.50	0.50	0.50

B.3   Column for Multi-Story Building—First Floor
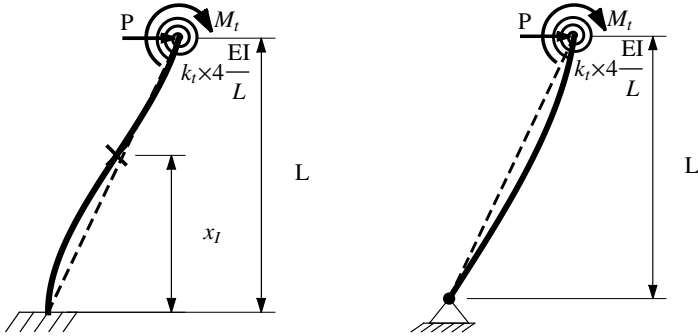
Shear stiffness:

$$k_{\text{sh}} = \begin{cases} \dfrac{1+4k_t}{(4+4k_t)+6(M_t/(PL))} \dfrac{12EI}{L^3} & \text{(fixed)} \\[2ex] \dfrac{4k_t}{(3+4k_t)+3(M_t/(PL))} \dfrac{3EI}{L^3} & \text{(hinge)} \end{cases}$$

Moment at top and bottom of column for fixed support:

$$\begin{pmatrix} M_{\text{inner top}} \\ M_{\text{inner bottom}} \end{pmatrix} = \begin{cases} \begin{pmatrix} +\frac{2k_t}{1+4k_t} \\ -\frac{1+2k_t}{1+4k_t} \end{pmatrix} PL + \begin{pmatrix} -\frac{1}{1+4k_t} \\ -\frac{1}{1+4k_t} \end{pmatrix} M_t & \text{(fixed support)} \\[3ex] \begin{pmatrix} 1 \\ 0 \end{pmatrix} PL & \text{(hinged support)} \end{cases}$$

Inflection point measured from the bottom (for fixed support):

$$x_I = \frac{(1+2k_t)+(M_t/(PL))}{(1+4k_t)} L \qquad \text{(on condition } 0 \leq x_I \leq L)$$

Note that in the above formulas, the applied moment M_t is considered positive when clockwise and the applied load P is considered positive when acting to the right. By contrast, the inner bending moments $M_{\text{inner top}}$ and $M_{\text{inner bottom}}$ are considered to be positive when counterclockwise and clockwise respectively in conformance with standard conventions of bending moment diagrams.

First Floor with Top Moment; Hinged Support; $k_{\text{sh}}/(3EI/L^3)$

$M_t/PL \downarrow$ $k_t \rightarrow$	0.	0.5	0.75	1	1.5	2	3	∞
-0.5	0.000	0.571	0.667	0.727	0.800	0.842	0.889	1.000
0	0.000	0.400	0.500	0.571	0.667	0.727	0.800	1.000
0.25	0.000	0.348	0.444	0.516	0.615	0.681	0.762	1.000
0.5	0.000	0.308	0.400	0.471	0.571	0.640	0.727	1.000
0.75	0.000	0.276	0.364	0.432	0.533	0.604	0.696	1.000
1	0.000	0.250	0.333	0.400	0.500	0.571	0.667	1.000
1.5	0.000	0.211	0.286	0.348	0.444	0.516	0.615	1.000
2	0.000	0.182	0.250	0.308	0.400	0.471	0.571	1.000

First Floor with Top Moment; Fixed Support; $k_{\text{sh}}/(12EI/L^3)$

$M_t/PL \downarrow$ $k_t \rightarrow$	0.	0.5	0.75	1	1.5	2	3	∞
-0.5	1.000	1.000	1.000	1.000	1.000	1.000	1.000	1.000
0	0.250	0.500	0.571	0.625	0.700	0.750	0.813	1.000
0.25	0.182	0.400	0.471	0.526	0.609	0.667	0.743	1.000
0.5	0.143	0.333	0.400	0.455	0.538	0.600	0.684	1.000
0.75	0.118	0.286	0.348	0.400	0.483	0.545	0.634	1.000
1	0.100	0.250	0.308	0.357	0.438	0.500	0.591	1.000
1.5	0.077	0.200	0.250	0.294	0.368	0.429	0.520	1.000
2	0.063	0.167	0.211	0.250	0.318	0.375	0.464	1.000

First Floor with Top Moment; Fixed Support; $(M_{\text{in }b}; M_{\text{in }t})/(PL)$

$M_t/PL \downarrow$ $k_t \rightarrow$	0.	0.75	1	2	3	∞
-0.5	$-0.500; 0.500$	$-0.500; 0.500$	$-0.500; 0.500$	$-0.500; 0.500$	$-0.500; 0.500$	$-0.500; 0.500$
0	$-1.000; 0.000$	$-0.625; 0.375$	$-0.600; 0.400$	$-0.556; 0.444$	$-0.538; 0.462$	$-0.500; 0.500$
0.25	$-1.250; -0.250$	$-0.688; 0.313$	$-0.650; 0.350$	$-0.583; 0.417$	$-0.558; 0.442$	$-0.500; 0.500$
0.5	$-1.500; -0.500$	$-0.750; 0.250$	$-0.700; 0.300$	$-0.611; 0.389$	$-0.577; 0.423$	$-0.500; 0.500$
0.75	$-1.750; -0.750$	$-0.813; 0.188$	$-0.750; 0.250$	$-0.639; 0.361$	$-0.596; 0.404$	$-0.500; 0.500$
1	$-2.000; -1.000$	$-0.875; 0.125$	$-0.800; 0.200$	$-0.667; 0.333$	$-0.615; 0.385$	$-0.500; 0.500$
1.5	$-2.500; -1.500$	$-1.000; 0.000$	$-0.900; 0.100$	$-0.722; 0.278$	$-0.654; 0.346$	$-0.500; 0.500$
2	$-3.000; -2.000$	$-1.125; -0.125$	$-1.000; 0.000$	$-0.778; 0.222$	$-0.692; 0.308$	$-0.500; 0.500$

Note: Inflection point is at $x_I/L = -M_{\text{in }b}$ from bottom subject to constraint ($0 \leq x_I \leq L$).

B.4   Column for Multi-Story Building—Top Floor (Top and Bottom Beams Similar)
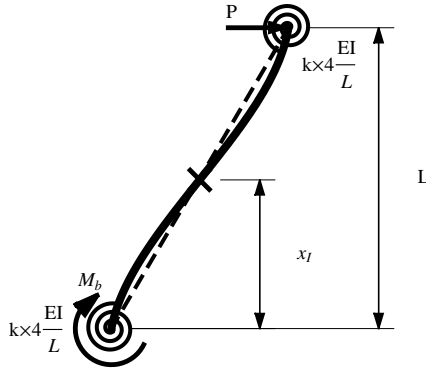
Shear stiffness:

$$k_{\text{sh}} = \frac{\left(2k + 4k^2\right)}{(3 + 8k + 4k^2) + 3(1 + 2k)(M_b/(PL)} \frac{12EI}{L^3}$$

Moment at top and bottom of column:

$$\begin{pmatrix} M_{\text{inner top}} \\ M_{\text{inner bottom}} \end{pmatrix} = \begin{pmatrix} +\frac{1}{2} \\ -\frac{1}{2} \end{pmatrix} PL + \begin{pmatrix} +\frac{1}{2+4k} \\ +\frac{1}{2+4k} \end{pmatrix} M_b$$

Inflection point measured from the bottom:

$$x_I = \tfrac{1}{2} - \frac{M_b/(PL)}{(2+4k)} L \quad \text{(on condition } 0 \leq x_I \leq L)$$

Note that in the above formulas, the applied moment M_b is considered positive when clockwise and the applied load P is considered positive when acting to the right. By contrast, the inner bending moments $M_{\text{inner top}}$ and $M_{\text{inner bottom}}$ are considered to be positive when counterclockwise and clockwise respectively in conformance with standard conventions of bending moment diagrams.

Top Floor with Bottom Moment; $k_{sh}/(12EI/L^3)$

$k \rightarrow$ $M_b/PL \downarrow$	0.	0.5	0.75	1	1.5	2	3	∞
−0.5	0.000	0.400	0.500	0.571	0.667	0.727	0.800	1.000
0	0.000	0.250	0.333	0.400	0.500	0.571	0.667	1.000
0.25	0.000	0.211	0.286	0.348	0.444	0.516	0.615	1.000
0.5	0.000	0.182	0.250	0.308	0.400	0.471	0.571	1.000
0.75	0.000	0.160	0.222	0.276	0.364	0.432	0.533	1.000
1	0.000	0.143	0.200	0.250	0.333	0.400	0.500	1.000
1.5	0.000	0.118	0.167	0.211	0.286	0.348	0.444	1.000
2	0.000	0.100	0.143	0.182	0.250	0.308	0.400	1.000

Top Floor with Bottom Moment; $(M_{in\,b}; M_{in\,t})/(PL)$

$k \rightarrow$ $M_b/PL \downarrow$	0.	0.75	1	2	3	∞
−0.5	−0.750; 0.250	−0.600; 0.400	−0.583; 0.417	−0.550; 0.450	−0.536; 0.464	−0.500; 0.500
0	−0.500; 0.500	−0.500; 0.500	−0.500; 0.500	−0.500; 0.500	−0.500; 0.500	−0.500; 0.500
0.25	−0.375; 0.625	−0.450; 0.550	−0.458; 0.542	−0.475; 0.525	−0.482; 0.518	−0.500; 0.500
0.5	−0.250; 0.750	−0.400; 0.600	−0.417; 0.583	−0.450; 0.550	−0.464; 0.536	−0.500; 0.500
0.75	−0.125; 0.875	−0.350; 0.650	−0.375; 0.625	−0.425; 0.575	−0.446; 0.554	−0.500; 0.500
1	0.000; 1.000	−0.300; 0.700	−0.333; 0.667	−0.400; 0.600	−0.429; 0.571	−0.500; 0.500
1.5	0.250; 1.250	−0.200; 0.800	−0.250; 0.750	−0.350; 0.650	−0.393; 0.607	−0.500; 0.500
2	0.500; 1.500	−0.100; 0.900	−0.167; 0.833	−0.300; 0.700	−0.357; 0.643	−0.500; 0.500

Note: Inflection point is at $x_I/L = -M_{in\,b}$ from bottom subject to constraint $(0 \le x_I \le L)$.

B.5 Column for Multi-Story Building—General Case
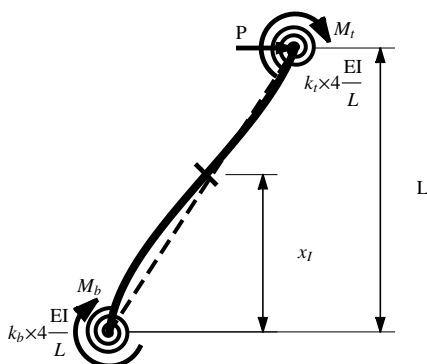
Shear stiffness:

$$k_{\text{sh}} = \frac{k_b+k_t+4k_bk_t}{(3+4k_b+4k_t+4k_bk_t)+3(1+2k_t)(M_b/(PL))+3(1+2k_b)(M_t/(PL))}\frac{12EI}{L^3}$$

Moment at top and bottom of column:

$$\begin{pmatrix} M_{\text{inner top}} \\ M_{\text{inner bottom}} \end{pmatrix} = \begin{pmatrix} +\frac{k_t+2k_bk_t}{k_b+k_t+4k_bk_t} \\ -\frac{k_b+2k_bk_t}{k_b+k_t+4k_bk_t} \end{pmatrix} PL + \begin{pmatrix} +\frac{k_t}{k_b+k_t+4k_bk_t} \\ +\frac{k_t}{k_b+k_t+4k_bk_t} \end{pmatrix} M_b$$

$$+ \begin{pmatrix} -\frac{k_b}{k_b+k_t+4k_bk_t} \\ -\frac{k_b}{k_b+k_t+4k_bk_t} \end{pmatrix} M_t$$

Inflection point measured from the bottom:

$$x_I = \frac{(k_b+2k_bk_t)-k_t(M_b/(PL))+k_b(M_t/(PL))}{(k_b+k_t+4k_bk_t)}L$$

$$(\text{on condition } 0 \leq x_I \leq L)$$

Note that in the above formulas, the applied moments M_t and M_b are considered positive when clockwise and the applied load P is considered positive when acting to the right. By contrast, the inner bending moments $M_{\text{inner top}}$ and $M_{\text{inner bottom}}$ are considered to be positive when counterclockwise and clockwise respectively in conformance with standard conventions of bending moment diagrams.

Appendix C

Beams—Deflections and Rotations

C.1 Displacements at Any Location
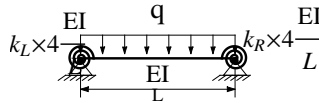
$$u_{\mathrm{UL}} = \frac{qL^4}{EI} \times \Big((6 + 4k_R)\, \hat{x} / \big(12\,(12 + 16k_L + 16k_R + 16k_L\, k_R) \big)$$

$$+ (6k_L + 4k_L k_R)\, \hat{x}^2 / \big(6\,(12 + 16k_L + 16k_R + 16k_L\, k_R) \big)$$

$$- (12 + 20k_L + 12k_R + 16k_L\, k_R)\, \hat{x}^3 / \big(12\,(12 + 16k_L + 16k_R + 16k_L\, k_R) \big)$$

$$+ \frac{\hat{x}^4}{24} \Big)$$
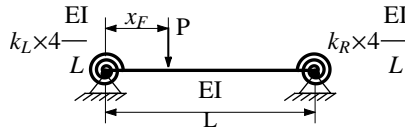
$$u_{\text{PF}} = \frac{PL^3}{EI} \times \begin{cases} \begin{aligned} &(\hat{x}\,(1-\hat{x}_F))\,/\,(18 + 24k_L + 24k_R + 24k_L\,k_R) \\ &\quad \big(\big(-(6+6k_R)\,\hat{x}_F + (3+6k_R)\,\hat{x}_F^2\big) \\ &\qquad +(-(12k_L + 12k_L\,k_R)\,\hat{x}_F \\ &\qquad\quad +(6k_L + 12k_L\,k_R)\,\hat{x}_F^2\big)\,\hat{x} \\ &\qquad +((3+4k_L + 4k_R + 4k_L\,k_R) \\ &\qquad\quad +(4k_L - 2k_R + 4k_L\,k_R)\,\hat{x}_F \\ &\qquad\quad -(2k_L + 2k_R + 8k_L\,k_R)\,\hat{x}_F^2\big)\,\hat{x}^2\big) \end{aligned} & 0 \le \hat{x} < \hat{x}_F \\[2em] \begin{aligned} &((1-\hat{x})\,\hat{x}_F)\,/\,(18 + 24k_L + 24k_R + 24k_L\,k_R) \\ &\quad \big((3+4k_L + 4k_R + 4k_L\,k_R)\,\hat{x}_F^2 \\ &\qquad +(-(6+6k_R)-(12k_L + 12k_L\,k_R)\,\hat{x}_F \\ &\qquad\quad +(4k_L - 2k_R + 4k_L\,k_R)\,\hat{x}_F^2\big)\,\hat{x} \\ &\qquad +((3+6k_R)(6k_L + 12k_L\,k_R)\,\hat{x}_F \\ &\qquad\quad -(2k_L + 2k_R + 8k_L\,k_R)\,\hat{x}_F^2\big)\,\hat{x}^2\big) \end{aligned} & \hat{x}_F \le \hat{x} \le 1 \end{cases}$$

$$u_M = \frac{ML^2}{EI} \times \begin{cases} \begin{aligned} &\hat{x}/\left(6 + 8k_L + 8k_R + 8k_L\,k_R\right) \\ &\quad ((-(2 + 2k_R) \\ &\qquad + (6 + 8k_R)\,\hat{x}_F - (3 + 6k_R)\,\hat{x}_F^2) \\ &\quad + (-(4k_L + 4k_L\,k_R) \\ &\qquad + (12k_L + 16k_L\,k_R)\,\hat{x}_F \\ &\qquad - (6k_L + 12k_L\,k_R)\,\hat{x}_F^2)\,\hat{x} \\ &\quad + (-(1 + 2k_R) - (4k_L + 8k_L\,k_R)\,\hat{x}_F \\ &\qquad - (2k_L + 2k_R + 8k_L\,k_R)\,\hat{x}_F^2)\,\hat{x}^2) \\ &(1 - \hat{x})/\left(6 + 8k_L + 8k_R + 8k_L\,k_R\right) \\ &\quad ((3 + 4k_L + 4k_R + 4k_L\,k_R)\,\hat{x}_F^2 \\ &\quad + (-(2 + 2k_R) - (8k_L + 8k_L\,k_R)\,\hat{x}_F \\ &\qquad + (4k_L - 2k_R + 4k_L\,k_R)\,\hat{x}_F^2)\,\hat{x} \\ &\quad + ((1 + 2k_R) + (4k_L + 8k_L\,k_R)\,\hat{x}_F \\ &\qquad - (2k_L + 2k_R + 8k_L\,k_R)\,\hat{x}_F^2)\,\hat{x}^2) \end{aligned} & \begin{aligned} &0 \le \hat{x} < \hat{x}_F \\[4em] &\hat{x}_F \le \hat{x} \le 1 \end{aligned} \end{cases}$$

Note:

- $\hat{x} = x/L$

- $\hat{x}_F = x_F/L$

C.2 Rotations at Any Location

$$\theta_{\text{UL}} = \frac{6+k_R}{z} + \frac{6k_L+k_L\,k_R}{z}\hat{x} - \frac{36+15k_L+9k_R+3k_L\,k_R}{z}\hat{x}^2$$

$$+ \frac{24+8k_L+8k_R+2k_L\,k_R}{1z}\hat{x}^3$$

$$z \;\; = 144 + 48k_L + 48k_R + 12k_L\,k_R$$

$$\theta_{\text{PF}} = \begin{cases} \dfrac{(2+2k_R)\hat{x}_F-(3+4k_R)\hat{x}_F^2+(1+2k_R)\hat{x}_F^3}{6+8k_L+8k_R+8k_L\,k_R} \\[4pt] \quad + \dfrac{(8k_L+8k_L\,k_R)\hat{x}_F-(12k_L+16k_L\,k_R)\hat{x}_F^2}{6+8k_L+8k_R+8k_L\,k_R}\hat{x} \\[4pt] \quad + \dfrac{(4k_L+8k_L\,k_R)\hat{x}_F^3}{6+8k_L+8k_R+8k_L\,k_R}\hat{x} \\[4pt] \quad + \dfrac{-(3+4k_L+4k_L\,k_R)+(3+6k_R)\hat{x}_F}{6+8k_L+8k_R+8k_L\,k_R} \\[4pt] \quad + \dfrac{(6k_L+12k_L\,k_R)\hat{x}_F^2-(2k_L+2k_R+8k_L\,k_R)\hat{x}_F^3}{6+8k_L+8k_R+8k_L\,k_R} \\[12pt] \dfrac{(2+2k_R)\hat{x}_F+(4k_L+4k_L\,k_R)\hat{x}_F^2+(1+2k_R)\hat{x}_F^3}{6+8k_L+8k_R+8k_L\,k_R} \\[4pt] \quad + \dfrac{-(6+8k_R)\hat{x}_F-(12k_L+16k_L\,k_R)\hat{x}_F^2}{6+8k_L+8k_R+8k_L\,k_R}\hat{x} \\[4pt] \quad + \dfrac{(4k_L+8k_L\,k_R)\hat{x}_F^3}{6+8k_L+8k_R+8k_L\,k_R}\hat{x} \\[4pt] \quad + \dfrac{(3+6k_R)\hat{x}_F+(6k_L+12k_L\,k_R)\hat{x}_F^2}{6+8k_L+8k_R+8k_L\,k_R}\hat{x}^2 \\[4pt] \quad - \dfrac{(2k_L+2k_R+8k_L\,k_R)\hat{x}_F^3}{6+8k_L+8k_R+8k_L\,k_R}\hat{x}^2 \end{cases} \begin{array}{l} \\ \\ \\ 0 \le \hat{x} \le \hat{x}_F \\ \\ \\ \\ \\ \\ \\ \hat{x}_F < \hat{x} \le 1 \\ \\ \\ \end{array}$$
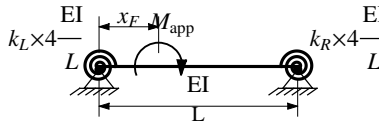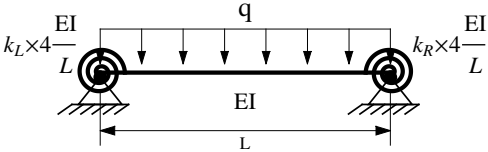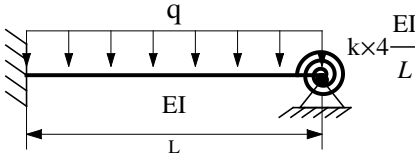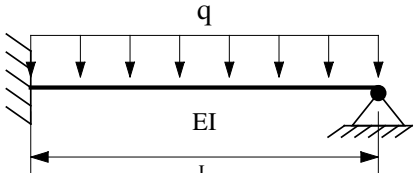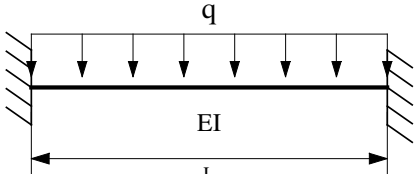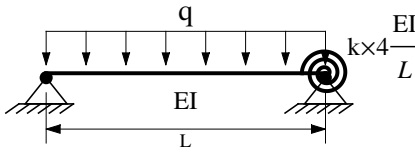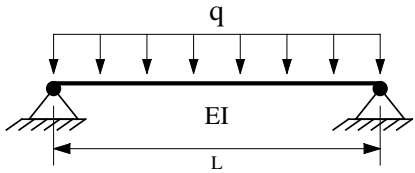
$$\theta_{\mathrm{PM}} = \begin{cases} \begin{aligned} & \frac{2+2k_R+(-6-8k_R)\hat{x}_F+(3+6k_R)\hat{x}_F^2}{6+8k_L+8k_R+8k_L\,k_R} \\ & + \frac{8k_L+8k_L\,k_R-(32k_L\,k_R+24k_L)\hat{x}_F}{6+8k_L+8k_R+8k_L\,k_R}\hat{x} \\ & + \frac{(12k_L+24k_L\,k_R)\hat{x}_F^2}{6+8k_L+8k_R+8k_L\,k_R}\hat{x} \\ & + \frac{(3+6k_R)+(12k_L+24k_L\,k_R)\hat{x}_F}{6+8k_L+8k_R+8k_L\,k_R}\hat{x}^2 \\ & - \frac{(24k_L\,k_R+6k_L+6k_R)\hat{x}_F^2}{6+8k_L+8k_R+8k_L\,k_R}\hat{x}^2 \end{aligned} & 0 \le \hat{x} \le \hat{x}_F \\[2em] \begin{aligned} & \frac{2+2k_R+(8k_L+8k_L\,k_R)\hat{x}_F+(3+6k_R)\hat{x}_F^2}{6+8k_L+8k_R+8k_L\,k_R} \\ & + \frac{-(8k_R+6)-(32k_L\,k_R+24k_L)\hat{x}_F}{6+8k_L+8k_R+8k_L\,k_R}\hat{x} \\ & + \frac{(12k_L+24k_L\,k_R)\hat{x}_F^2}{6+8k_L+8k_R+8k_L\,k_R}\hat{x} \\ & + \frac{(3+6k_R)+(12k_L+24k_L\,k_R)\hat{x}_F}{6+8k_L+8k_R+8k_L\,k_R}\hat{x}^2 \\ & - \frac{(24k_L\,k_R+6k_L+6k_R)\hat{x}_F^2}{6+8k_L+8k_R+8k_L\,k_R}\hat{x}^2 \end{aligned} & \hat{x}_F < \hat{x} \le 1 \end{cases}$$

Note:

- $\hat{x} = x/L$

- $\hat{x}_F = x_F/L$

- Rotations are clockwise when positive

C.3   Uniform Load—Mid Displacements

$k_L\times 4\dfrac{EI}{L}$ (beam with q, springs k_L, $k_R\times 4\dfrac{EI}{L}$, length L, EI)	$\delta_{\text{mid}} =$ $\dfrac{60+8k_L+8k_R+k_L\,k_R}{60+20k_L+20k_R+5k_L\,k_R}\dfrac{5}{384}\dfrac{qL^4}{EI}$
(fixed left, q, right spring $k\times 4\dfrac{EI}{L}$, length L, EI)	$\delta_{\text{mid}} = \dfrac{8+k}{20+5k}\dfrac{5}{384}\dfrac{qL^4}{EI}$
(fixed left, q, pin right, length L, EI)	$\delta_{\text{mid}} = \dfrac{2}{384}\dfrac{qL^4}{EI} = \dfrac{1}{192}\dfrac{qL^4}{EI}$
(fixed both ends, q, length L, EI)	$\delta_{\text{mid}} = \dfrac{1}{384}\dfrac{qL^4}{EI}$
(pin left, q, right spring $k\times 4\dfrac{EI}{L}$, length L, EI)	$\delta_{\text{mid}} = \dfrac{60+8k}{60+20k}\dfrac{5}{384}\dfrac{qL^4}{EI}$
(simply supported both ends, q, length L, EI)	$\delta_{\text{mid}} = \dfrac{5}{384}\dfrac{qL^4}{EI}$

Note:

- Maximum difference between mid displacement and maximum displacement is $\approx 3.84\%$ and occurs for fixed-hinge case

- Continuous beam with equal spacing and only one member loaded obtained with $k_L \approx k_R \approx 1$ for mid member or $k \approx 1$ for edge member

- Continuous beam with equal spacing and all members uniformly loaded obtained with fixed-fixed case

- Continuous beam with equal spacing and checker-board loading obtained with $k_L \approx k_R \approx 0.5$ for mid member or $k \approx 0.5$ for edge member

C.4   Point Force—Centrally Loaded— Mid Displacements

	$\delta_{\mathrm{mid}} =$ $\dfrac{12+7k_L+7k_R+4k_L\,k_R}{12+16k_L+16k_R+16k_L\,k_R}\dfrac{1}{48}\dfrac{PL^3}{EI}$
	$\delta_{\mathrm{mid}} = \dfrac{7+4k}{16+16k}\dfrac{1}{48}\dfrac{PL^3}{EI}$
	$\delta_{\mathrm{mid}} = \dfrac{7}{16}\dfrac{1}{48}\dfrac{PL^3}{EI} = \dfrac{7}{768}\dfrac{PL^3}{EI}$
	$\delta_{\mathrm{mid}} = \dfrac{1}{192}\dfrac{PL^3}{EI}$
	$\delta_{\mathrm{mid}} = \dfrac{12+7k}{12+16k}\dfrac{1}{48}\dfrac{PL^3}{EI}$
	$\delta_{\mathrm{mid}} = \dfrac{1}{48}\dfrac{PL^3}{EI}$

Note:

- Maximum difference between mid displacement and maximum displacement is $\approx 2.17\%$ and occurs for fixed-hinge case

- For same total load $(qL = P)$, we have:

    - fixed-fixed case of point load is 2 times that of distributed load
    - fixed-hinge case of point load is 1.75 times that of distributed load
    - hinge-hinge case of point load is 1.6 times that of distributed load

- Continuous beam with equal spacing and only one member loaded obtained with $k_L \approx k_R \approx 1$ for mid member or $k \approx 1$ for edge member

- Continuous beam with equal spacing and all members uniformly loaded obtained with fixed-fixed case

- Continuous beam with equal spacing and checker-board loading obtained with $k_L \approx k_R \approx 0.5$ for mid member or $k \approx 0.5$ for edge member

C.5   Point Force—Loaded Anywhere— Mid Displacements
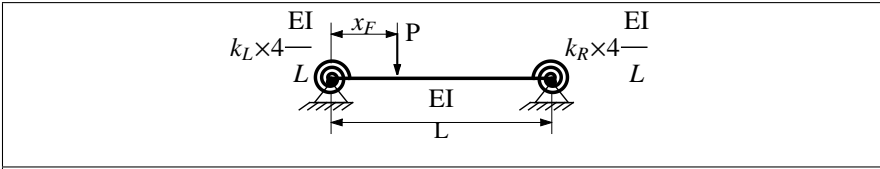
$\delta_{\text{at } x_{\overline{F}}}$ $16 \left(1 - \hat{x}_F\right)^2 \hat{x}_F^2$

$\times \left(\dfrac{3 + 3k_R + 4k_L\, \hat{x}_F - 2k_R\hat{x}_F + 4k_L\, k_R\hat{x}_F}{3 + 4k_L + 4k_R + 4k_L\, k_R} \right.$

$\left. + \dfrac{-k_L\, \hat{x}_F^2 - k_R\hat{x}_F^2 - 4k_L\, k_R\hat{x}_F^2}{3 + 4k_L + 4k_R + 4k_L\, k_R} \right)$

$\times \dfrac{1}{48} \dfrac{PL^3}{EI}$

$\delta_{\text{mid}} = \hat{x}_F$

$\times \left(\dfrac{(9 + 6k_R) + (18k_L + 12k_L\, k_R)\hat{x}_F}{(3 + 4k_L + 4k_R + 4k_L\, k_R)} \right.$

$\left. - \dfrac{(12 + 22k_L + 10k_R + 16k_L\, k_R)\hat{x}_F^2}{(3 + 4k_L + 4k_R + 4k_L\, k_R)} \right)$

$\times \dfrac{1}{48} \dfrac{PL^3}{EI}$ $0 \le \hat{x}_F \le 0.5$
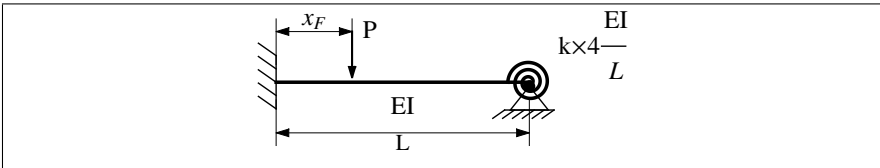
$\delta_{\text{at } x_F} = \dfrac{1}{1+k} 4 \left(1 - \hat{x}_F\right)^2 \hat{x}_F^3$

$\left(4 + 4k - \hat{x}_F - 4k\hat{x}_F\right) \dfrac{1}{48} \dfrac{PL^3}{EI}$

$\delta_{\text{mid}} = \dfrac{\hat{x}_F^2 (9 + 6k - 11\hat{x}_F - 8k\hat{x}_F)}{2(1+k)} \dfrac{1}{48} \dfrac{PL^3}{EI}$ $0 \le \hat{x}_F \le 0.5$
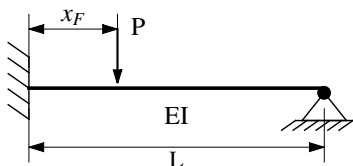
$$\delta_{\text{at } x_F} = 4\left(1 - \hat{x}_F\right)^2 \left(4 - \hat{x}_F\right) \hat{x}_F^3 \frac{1}{48} \frac{PL^3}{EI}$$

$$\delta_{\text{mid}} = \frac{1}{2}\hat{x}_F^2 (9 - 11\hat{x}_F) \frac{1}{48} \frac{PL^3}{EI} \qquad 0 \le \hat{x}_F \le 0.5$$
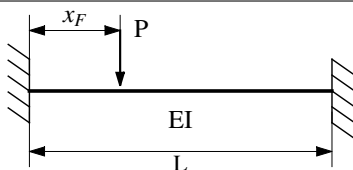
$$\delta_{\text{at } x_F} = 16(1 - \hat{x}_F)^3 \hat{x}_F^3 \frac{1}{48} \frac{PL^3}{EI}$$

$$\delta_{\text{mid}} = (3 - 4\hat{x}_F)\hat{x}_F^2 \frac{1}{48} \frac{PL^3}{EI} \qquad 0 \le \hat{x}_F \le 0.5$$
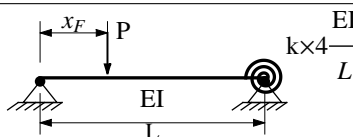
$$\delta_{\text{at } x_F} = \frac{1}{3+4k} 16 \left(1 - \hat{x}_F\right)^2$$
$$\hat{x}_F^2 \left(3 + 3k - 2k\hat{x}_F - k\hat{x}_F^2\right) \frac{1}{48} \frac{PL^3}{EI}$$

$$\delta_{\text{mid}} = \frac{\hat{x}_F \left(9 + 6k - 12\hat{x}_F^2 - 10k\hat{x}_F^2\right)}{3+4k} \frac{1}{48} \frac{PL^3}{EI} \qquad 0 \le \hat{x}_F \le 0.5$$
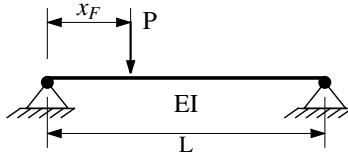
$$\delta_{\text{at } x_F} = 16(1 - \hat{x}_F)^2 \hat{x}_F^2 \frac{1}{48} \frac{PL^3}{EI}$$

$$\delta_{\text{mid}} = (3\hat{x}_F - 4\hat{x}_F^3) \frac{1}{48} \frac{PL^3}{EI} \qquad 0 \le \hat{x}_F \le 0.5$$

Note:

- $\hat{x}_F = x_F / L$

- Maximum difference between mid displacement and maximum displacement is $\approx 15.63\%$ and occurs for fixed-hinge case when the force is very close to the hinge. The maximum difference depends on the location of the point force but always occurs for the fixed-hinge case with the point force being closer to the hinge. The figure below shows the maximum relative error for those cases:
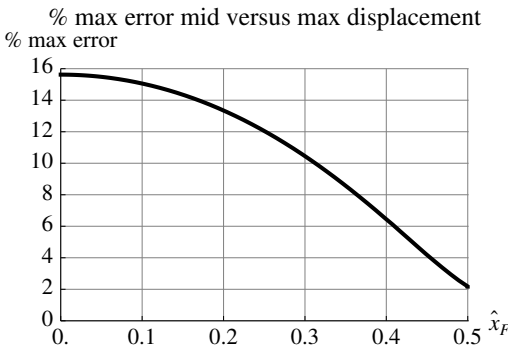
% max error mid versus max displacement

- Continuous beam with equal spacing and only one member loaded obtained with $k_L \approx k_R \approx 1$ for mid member or $k \approx 1$ for edge member

- Continuous beam with equal spacing and all members uniformly loaded obtained with fixed-fixed case

- Continuous beam with equal spacing and checker-board loading obtained with $k_L \approx k_R \approx 0.5$ for mid member or $k \approx 0.5$ for edge member

- For $\hat{x}_F > 1/2$, switch k_L with k_R and $\hat{x}_F$ with $(1 - \hat{x}_F)$

C.6 Point Moment—Loaded Anywhere— Mid Displacements
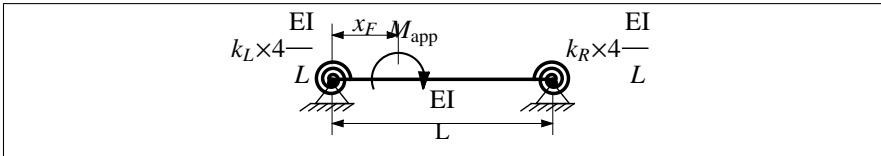
$$\delta_{\text{at } x_F} = 16 \left(1 - \hat{x}_F\right) \hat{x}_F$$
$$\times \left(\frac{1 + k_R - 2\hat{x}_F + 2k_L \,\hat{x}_F - 3k_R\hat{x}_F + 2k_L \, k_R\hat{x}_F}{3 + 4k_L + 4k_R + 4k_L \, k_R} \right.$$
$$\left. + \frac{-4k_L \,\hat{x}_F^2 + k_R\hat{x}_F^2 - 6K_L k_R \,\hat{x}_F 2k_L \,\hat{x}_F^4 + 4k_L \, k_R \,\hat{x}_F^3}{3 + 4k_L + 4k_R + 4k_L \, k_R} \right)$$
$$\times \frac{1}{16} \frac{ML^2}{EI}$$
$$\delta_{\overline{\text{mid}}} \left(\frac{3 + 2k_R + 12k_L\hat{x}_F + 8k_L \, k_R\hat{x}_F - 12\hat{x}_F^2}{3 + 4k_L + 4k_R + 4k_L \, k_R} \right.$$
$$\left. + \frac{-22k_L\hat{x}_F^2 - 10k_R\hat{x}_F^2 - 16k_L \, k_R \,\hat{x}_F^2}{3 + 4k_L + 4k_R + 4k_L \, k_R} \right)$$
$$\times \frac{1}{16} \frac{ML^2}{EI} \qquad\qquad 0 \le \hat{x}_F \le 0.5$$
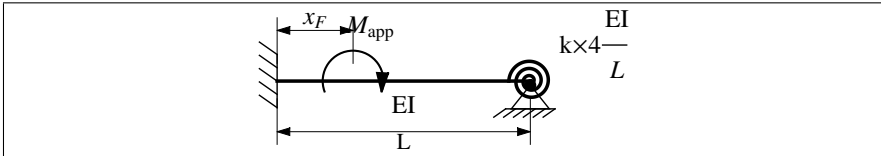
$$\delta_{\text{at } x_F} = 4 \left(1 - \hat{x}_F\right) \hat{x}_F^2$$
$$\times \frac{\left(2 + 2k - 4\hat{x}_F - 6k\hat{x}_F + \hat{x}_F^2 + 4k\hat{x}_F^2\right)}{1 + k}$$
$$\times \frac{1}{16} \frac{ML^3}{EI}$$
$$\delta_{\text{mid}} = \frac{(6_4 k - 11\hat{x}_F - 8k\hat{x}_F)\hat{x}_F}{2(1 + k)} \frac{1}{16} \frac{ML^3}{EI} \qquad 0 \le \hat{x}_F \le 0.5$$
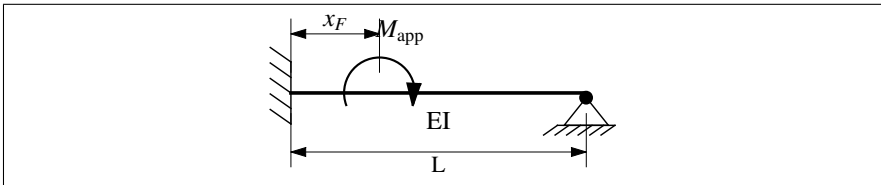
$$\delta_{\text{at } x_F} = 4 \left(1 - \hat{x}_F\right) \hat{x}_F^2 \left(2 - 4\hat{x}_F + \hat{x}_F^2\right) \frac{1}{16} \frac{ML^2}{EI}$$

$$\delta_{\text{mid}} = \frac{1}{2} \left(6 - 11\hat{x}_F\right) \hat{x}_F \frac{1}{16} \frac{ML^2}{EI} \qquad\qquad 0 \le \hat{x}_F \le 0.5$$
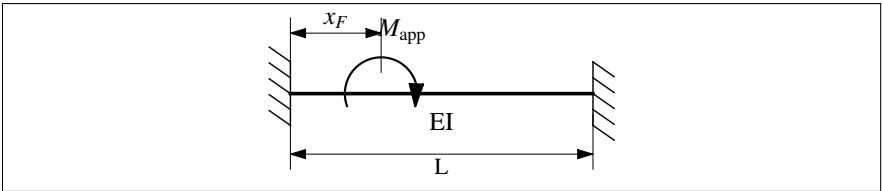
$$\delta_{\text{at } x_F} = 8\left(1 - \hat{x}_F\right)\hat{x}_F^2\left(1 - 3\hat{x}_F + 2\hat{x}_F^2\right)\frac{1}{16}\frac{ML^2}{EI}$$

$$\delta_{\text{mid}} = 2\left(1 - 2\hat{x}_F\right)\frac{1}{16}\frac{ML^2}{EI} \qquad\qquad 0 \le \hat{x}_F \le 0.5$$
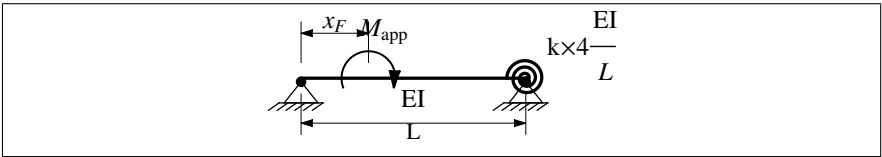
$$\delta_{\text{at } x_F} = \frac{16(1-\hat{x}_F)\hat{x}_F\left(1+k-2\hat{x}_F-3k\hat{x}_F+k\hat{x}_F^2+k\hat{x}_F^3\right)}{3+4k}$$
$$\times \frac{1}{16}\frac{ML^2}{EI}$$

$$\delta_{\text{mid}} = \frac{3+2k-12\hat{x}_F^2-10k\hat{x}_F^2}{3+4k}\frac{1}{16}\frac{ML^2}{EI} \qquad 0 \le \hat{x}_F \le 0.5$$
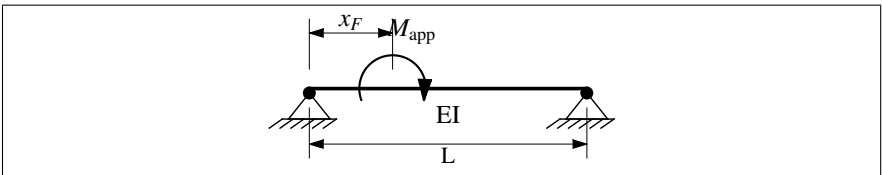
$$\delta_{\text{at } x_F} = \frac{16}{3}\left(1 - \hat{x}_F\right)\hat{x}_F\left(1 - 2\hat{x}_F\right)\frac{1}{16}\frac{ML^2}{EI}$$
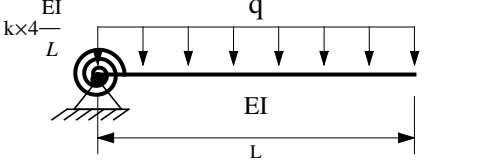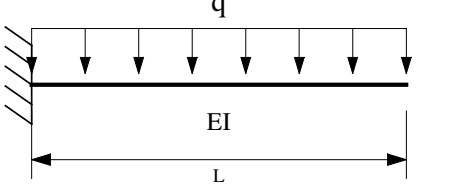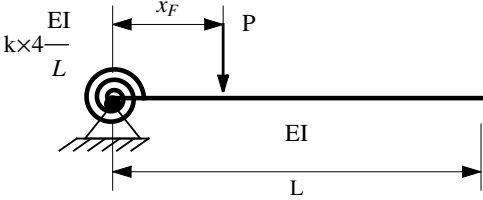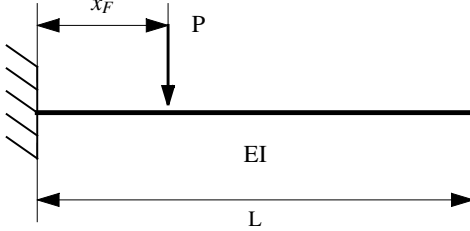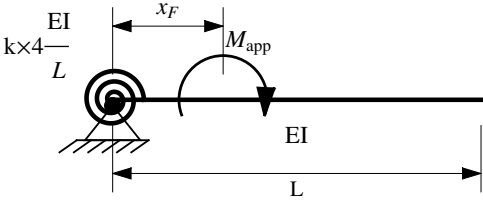
$$\delta_{\text{mid}} = \left(1 - 4\hat{x}_F\right)\frac{1}{16}\frac{ML^2}{EI} \qquad\qquad 0 \le \hat{x}_F \le 0.5$$

Note:

- $\hat{x}_F = x_F / L$

- In general, neither $\delta_{\text{at } x_F}$ nor δ_{mid} is the maximum deflection

- Continuous beam with equal spacing and only one member loaded obtained with $k_L \approx k_R \approx 1$ for mid member or $k \approx 1$ for edge member

- Continuous beam with equal spacing and all members uniformly loaded obtained with fixed-fixed case

- Continuous beam with equal spacing and checker-board loading obtained with $k_L \approx k_R \approx 0.5$ for mid member or $k \approx 0.5$ for edge member

- For $\hat{x}_F > 1/2$, switch k_L with k_R and $\hat{x}_F$ with $(1 - \hat{x}_F)$

C.7   Cantilever—Various Special Cases—Displacements

	$\delta_{\text{at tip}} = \left(\frac{1}{8} + \frac{1}{2k}\right)\frac{qL^4}{EI}$
	$\delta_{\text{at tip}} = \frac{1}{8}\frac{qL^4}{EI}$
	$\delta_{\text{at }x_F} = \left(\frac{3\hat{x}_F^3}{4k} + \hat{x}_F\right)\frac{1}{3}\frac{PL^3}{EI}$ $\delta_{\text{at tip}} = \left(\frac{3\hat{x}_F}{4k} + \frac{3-\hat{x}_F}{2}\right)\hat{x}_F^2\frac{1}{3}\frac{PL^3}{EI}$
	$\delta_{\text{at }x_F} = \hat{x}_F^3\frac{1}{3}\frac{PL^3}{EI}$ $\delta_{\text{at tip}} = \left(\frac{3-\hat{x}_F}{2}\right)\hat{x}_F^2\frac{1}{3}\frac{PL^3}{EI}$
	$\delta_{\text{at }x_F} = \left(\frac{\hat{x}_F}{2k} + \hat{x}_F^2\right)\frac{1}{2}\frac{M_{\text{app}}L^2}{EI}$ $\delta_{\text{at tip}} = \left(\frac{1}{2k} + (2 - \hat{x}_F)\,\hat{x}_F\right)$ $\times \frac{1}{2}\frac{M_{\text{app}}L^2}{EI}$
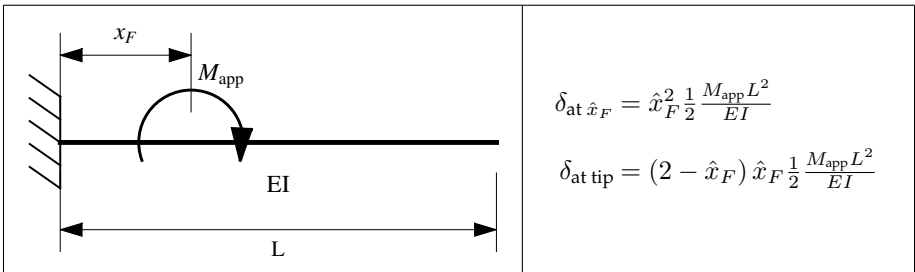
$$\delta_{\text{at } \hat{x}_F} = \hat{x}_F^2 \, \tfrac{1}{2} \, \frac{M_{\text{app}} L^2}{EI}$$

$$\delta_{\text{at tip}} = (2 - \hat{x}_F) \, \hat{x}_F \, \tfrac{1}{2} \, \frac{M_{\text{app}} L^2}{EI}$$

Note:

- $\hat{x}_F = x_F / L$

This page intentionally left blank

Appendix D

Useful Results for Influence Lines

D.1 Influence Lines for Vertical Force Reactions

(a)   (b)
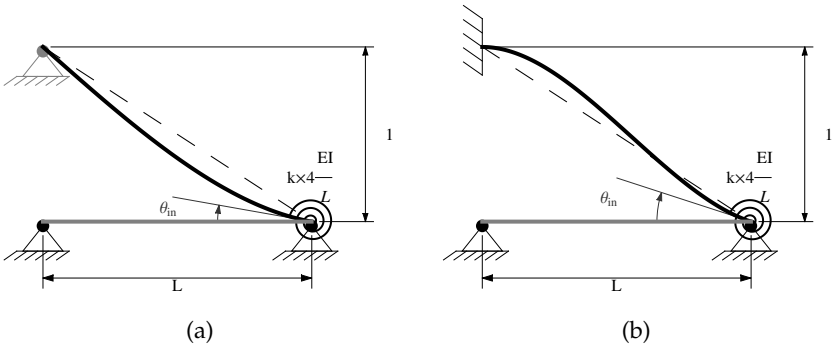
$$\theta_{in} = \begin{cases} \frac{3}{3+4k} \frac{1}{L} & \text{hinge or roller support at end} \\ \frac{3}{2+2k} \frac{1}{L} & \text{fixed support at end} \end{cases}$$
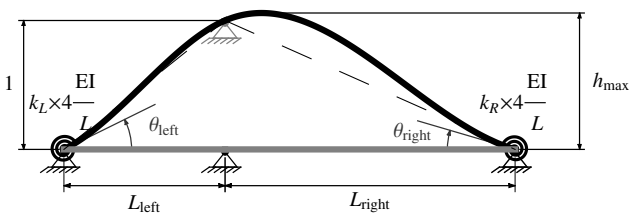
$$\theta_{\text{left}} \approx \frac{3}{4 + 4k_L} \left(\frac{1}{L_{\text{left}}} + \frac{1}{L_{\text{right}}} \right)$$

$$\theta_{\text{right}} \approx \frac{3}{4 + 4k_R} \left(\frac{1}{L_{\text{left}}} + \frac{1}{L_{\text{right}}} \right)$$

Note that formulas for the slopes above give a maximum possible error of 25% relative to the exact result when the ratio of the spans is between half and two (*ie.* neither span is longer than twice the other). If in addition the rotary stiffness factors on either side are larger than one then the maximum possible error is reduced to 10%.

Exact formula for the slopes at the ends above are given by:

$$\theta_{\text{left}} = \frac{3}{2} \left(\frac{1}{L_{\text{left}}} + \frac{1}{L_{\text{right}}} \right) \frac{\left(L_{\text{left}} + 2k_R L_{\text{left}} + 2\, L_{\text{right}} + 2k_R\, L_{\text{right}} \right)}{z}$$

$$\theta_{\text{right}} = \frac{3}{2} \left(\frac{1}{L_{\text{left}}} + \frac{1}{L_{\text{right}}} \right) \frac{\left(2\, L_{\text{left}} + 2k_L\, L_{\text{left}} + L_{\text{right}} + 2k_L\, L_{\text{right}} \right)}{z}$$

where:

$$z = 3\, L_{\text{left}} + 3k_L\, L_{\text{left}} + 4k_R\, L_{\text{left}} + 4k_L\, k_R L_{\text{left}}$$
$$+ 3\, L_{\text{right}} + 4k_L\, L_{\text{right}} + 3k_R\, L_{\text{right}} + 4k_L\, k_R\, L_{\text{right}}$$

Approximate expression for the maximum influence value is given by:

$$h_{\text{max}} \approx 1 + \frac{\left(1 - \left(L_{\text{right}} / L_{\text{left}} \right) \right)^2}{5 \left(L_{\text{right}} / L_{\text{left}} \right)}$$

Note that formula for h_{max} above gives a value always greater or equal to one, is symmetric with respect to L_{left} and L_{right} and gives a maximum error of 11% relative to the exact result when the ratio of the spans is between half and two (*ie.* neither span is longer than twice the other). Exact solution of h_{max} is available but is too long and complex to be useful except in computer implementations.

D.2   Influence Lines for Shear Forces
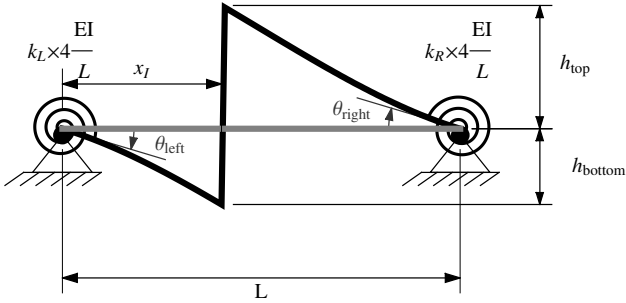
$$h_{\text{bottom}} = \frac{x_I}{L} + \frac{2\left(k_R + 2k_L\,k_R\right)}{3 + 4k_L + 4k_R + 4k_L\,k_R}\left(\frac{x_I}{L} - \frac{x_I^3}{L^3}\right)$$
$$- \frac{2\left(k_L + 2k_L\,k_R\right)}{3 + 4k_L + 4k_R + 4k_L\,k_R}\left(\left(1 - \tfrac{x_I}{L}\right) - \left(1 - \tfrac{x_I}{L}\right)^3\right)$$

$$h_{\text{top}} = 1 - h_{\text{bottom}}$$

$$\theta_{\text{left}} = \frac{3 + 6k_R}{3 + 4k_L + 4k_R + 4k_L\,k_R}$$

$$\theta_{\text{right}} = \frac{3 + 6k_L}{3 + 4k_L + 4k_R + 4k_L\,k_R}$$

D.3   Influence Lines for Bending Moments

(a)   (b)   (c)
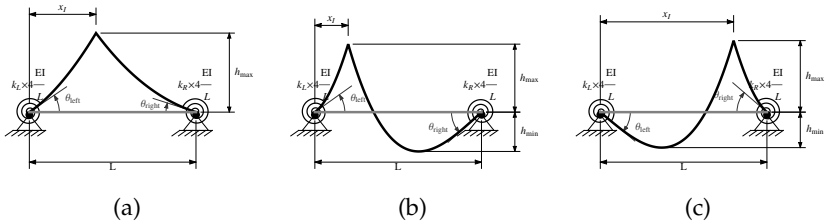
$$\frac{2k_L}{3+6k_L}L \le x_I \le \left(1 - \frac{2k_R}{3+6k_R}\right)L$$

$\Rightarrow$ influence line of bending moment has pattern of figure (a) above

$$x_I \le \frac{2k_L}{3+6k_L}L$$

$\Rightarrow$ influence line of bending moment has pattern of figure (b) above

$$x_I \ge \left(1 - \frac{2k_R}{3+6k_R}\right)L$$

$\Rightarrow$ influence line of bending moment has pattern of figure (c) above

$$h_{\max} = \frac{x_I}{L}\left(1 - \frac{x_I}{L}\right)$$
$$\left(\frac{(3+4k_R) + (6k_L - 2k_R + 8k_Lk_R)\,(x_I/L)}{z}\right.$$
$$\left. - \frac{2\,(k_L + k_R + 4k_Lk_R)\,(x_I/L)^2}{z}\right)L$$

where: $z = 3 + 4k_L + 4k_R + 4k_Lk_R$.

Bounds on the value of $h_{\max}$:

$$2\left(\frac{x_I}{L}\right)^2\left(1 - \frac{x_I}{L}\right)^2 L \le h_{\max} \le \frac{x_I}{L}\left(1 - \frac{x_I}{L}\right)L$$

$$h_{\min} \approx \begin{cases} \frac{k_L}{1+k_L}\frac{(1+k_R)}{(5+7k_R)}\left(1 - \frac{(x_I/L)}{2k_L/(3+6k_L)}\right)^2 L & 0 \le x_I \le \frac{2k_L}{3+6k_L}L \\ \frac{k_R}{1+k_R}\frac{(1+k_L)}{(5+7k_L)}\left(1 - \frac{(1-(x_I/L))}{2k_R/(3+6k_R)}\right)^2 L & 1 - \frac{2k_R}{3+6k_R} \le x_I \le L \end{cases}$$

Formula for $h_{\min}$ is approximate and has a maximum absolute error of $0.01 \times L$ for all values of 'k_L,' 'k_R' and 'x_I.'

$$x_{\text{at min}}/L \approx \begin{cases} 1 - 3\frac{(1-s)}{(3-s)}\left(1 - 2f\frac{(1-s)}{(2-s)}\right) & 0 \le x_I \le \frac{2k_L}{3+6k_L}L \\ 3\frac{(1-s)}{(3-s)}\left(1 - 2f\frac{(1-s)}{(2-s)}\right) & 1 - \frac{2k_R}{3+6k_R} \le x_I \le L \end{cases}$$

with:

$$
s = \begin{cases} \frac{(x_I/L)}{2k_L/(3+6k_L)} & 0 \le x_I \le \frac{2k_L}{3+6k_L}L \\ \frac{1-(x_I/L)}{2k_R/(3+6k_R)} & 1 - \frac{2k_R}{3+6k_R} \le x_I \le L \end{cases}
$$

$$
f = \begin{cases} \frac{0.42+0.33k_R}{1+k_R} & 0 \le x_I \le \frac{2k_L}{3+6k_L}L \\ \frac{0.42+0.33k_L}{1+k_L} & 1 - \frac{2k_R}{3+6k_R} \le x_I \le L \end{cases}
$$

Above formula for the location of the minimum has absolute error less than $0.1 \times L$.

$$
\theta_{\text{left}} = \frac{(3+4k_R) - (3+6k_R)(x_I/L)}{3+4k_L+4k_R+4k_L k_R}
$$

$$
\theta_{\text{right}} = \frac{(3+4k_L) - (3+6k_L)(1-x_I/L)}{3+4k_L+4k_R+4k_L k_R}
$$

D.4   Transition Member
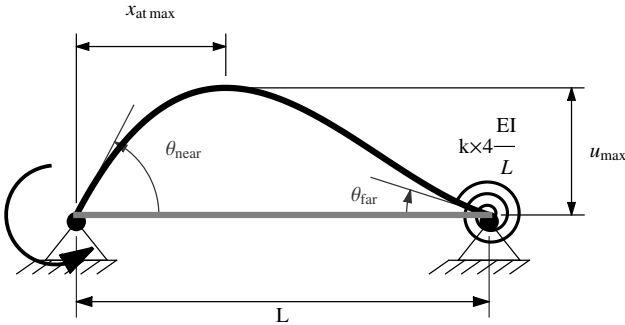
An exact expression for '$u_{\max}$' is given by:

$$
u_{\max} = \frac{3\sqrt{3+6k+4k^2} + k(3+2k)\left((3+4k)+2\sqrt{3+6k+4k^2}\right)}{27(1+k)(1+2k)^2}\theta_{\text{near}}L
$$

$$
u_{\max} \approx \frac{0.19+0.15k}{1+k}\theta_{\text{near}}L
$$

Approximate expression for the maximum displacement has error less than 1.5% for any value of 'k' as compared with the exact result.

$$
\frac{x_{\text{at max}}}{L} = \frac{3+4k - \sqrt{3+6k+4k^2}}{3+6k}
$$

$$
x_{\text{at max}}/L \approx \frac{0.42+0.33k}{1+k}
$$

Approximate expression of the location has error less than 1% for any value of 'k' compared to the exact result.

Note: The above results are available in a different appendix but selected results pertaining to influence lines are reproduced above.

Index

355